

# Mechanisms of Brain Ventricle Development

by

Laura Anne Lowery

B.S. Biology  
University of California San Diego, 2000

M.S. Biology  
University of California San Diego, 2001

Submitted to the Department of Biology  
in Partial Fulfillment of the Requirements for the Degree of

Doctor of Philosophy in Biology  
at the  
Massachusetts Institute of Technology

June 2008

© 2008 Laura Anne Lowery. All rights reserved.

The author hereby grants to MIT permission to reproduce and to distribute publicly  
paper and electronic copies of this thesis document in whole or in part.

Signature of Author.....  
Department of Biology  
May 2008

Certified by.....  
Hazel L. Sive  
Professor of Biology  
Associate Dean School of Science  
Thesis Supervisor

Accepted by.....  
Stephen P. Bell  
Professor of Biology  
Chairman, Graduate Student Committee



# Mechanisms of Brain Ventricle Formation

By  
Laura Anne Lowery

Submitted to the Department of Biology on April 2008 in Partial Fulfillment of the  
Requirements for the Degree of Doctor of Philosophy in Biology

## ABSTRACT

The brain ventricles are a conserved system of fluid-filled cavities within the brain that form during the earliest stages of brain development. Abnormal brain ventricle development has been correlated with neurodevelopmental disorders including hydrocephalus and schizophrenia. The mechanisms which regulate formation of the brain ventricles and the embryonic cerebrospinal fluid are poorly understood. Using the zebrafish, I initiated a study of brain ventricle development to define the genes required for this process. The zebrafish neural tube expands into the forebrain, midbrain, and hindbrain ventricles rapidly, over a four-hour window during mid-somitogenesis. In order to determine the genetic mechanisms that affect brain ventricle development, I studied 17 mutants previously-identified as having embryonic brain morphology defects and identified 3 additional brain ventricle mutants in a retroviral-insertion shelf-screen. Characterization of these mutants highlighted several processes involved in brain ventricle development, including cell proliferation, neuroepithelial shape changes (requiring epithelial integrity, cytoskeletal dynamics, and extracellular matrix function), embryonic cerebrospinal fluid secretion, and neuronal development. In particular, I investigated the role of the  $\text{Na}^+\text{K}^+\text{ATPase}$  alpha subunit, *Atp1a1*, in brain ventricle formation, elucidating novel roles for its function during brain development. This study was facilitated by the *snakehead* mutant, which has a mutation in the *atp1a1* gene and undergoes normal brain ventricle morphogenesis but lacks ventricle inflation. Analysis of the temporal and spatial requirements of *atp1a1* revealed an early requirement during formation, but not maintenance, of the neuroepithelium. I also demonstrated a later neuroepithelial requirement for *Atp1a1*-driven ion pumping that leads to brain ventricle inflation, likely by forming an osmotic gradient that drives fluid flow into the ventricle space. Moreover, I have discovered that the forebrain ventricle is particularly sensitive to  $\text{Na}^+\text{K}^+\text{ATPase}$  function, and reducing or increasing *Atp1a1* levels leads to a corresponding decrease or increase in ventricle size. Intriguingly, the  $\text{Na}^+\text{K}^+\text{ATPase}$  beta subunit *atp1b3a*, expressed in the forebrain and midbrain, is specifically required for their inflation, and thus may highlight a distinct regulatory mechanism for the forebrain and midbrain ventricles. In conclusion, my work has begun to define the complex mechanisms governing brain ventricle development, and I suggest that these mechanisms are conserved throughout the vertebrates.

Thesis Supervisor: Hazel L. Sive  
Title: Professor of Biology



Dedicated to my grandparents,  
Lester and Leah Sopkin



## Table of Contents

	<u>Page</u>
Abstract	3
Acknowledgements	9
Curriculum Vitae	11
Chapter 1	<b>Introduction – A Discussion of the Formation and Function of the Embryonic Brain Ventricles</b>
	13
	Introduction 15
	The Brain Ventricular System 16
	Brain Ventricle Abnormalities 18
	Formation of the Embryonic Brain Ventricles 20
	Mechanisms of Brain Ventricle Development 21
	Preview of Thesis 34
	Figures 35
	References 51
Chapter 2	<b>The zebrafish as a model for analyzing neural tube defects</b>
	63
	Introduction 65
	Zebrafish as a Model System 65
	Ontogeny of the Zebrafish Nervous System 67
	Zebrafish as a Model for Brain Ventricle Formation 75
	Lessons from Zebrafish Mutants 78
	Conclusion 82
	Table and Figures 83
	References 99
Chapter 3	<b>Characterization and Classification of 20 Zebrafish Brain Morphology Mutants</b>
	111
	Abstract 113
	Background 114
	Results and Discussion 115
	Conclusions 123
	Experimental Procedures 124
	Table and Figures 127
	References 141

Chapter 4	<b>Initial Formation of Zebrafish Brain Ventricles Occurs Independently of Circulation and Requires the <i>nagie oko</i> and <i>snakehead/atp1a1</i> Gene Products</b>	147
	Abstract	149
	Introduction	150
	Results	151
	Discussion	158
	Experimental Procedures	161
	Figures	167
	References	187
Chapter 5	<b>The Spatial and Temporal Requirements for Na<sup>+</sup>K<sup>+</sup>ATPase during Brain Ventricle Development</b>	193
	Abstract	195
	Introduction	196
	Results	197
	Discussion	204
	Experimental Procedures	207
	Tables and Figures	213
	References	233
Chapter 6	<b>Conclusions and Future Directions</b>	239
	Future studies of eCSF formation and function	241
	Na <sup>+</sup> K <sup>+</sup> ATPase function during brain development	246
	Cell proliferation and brain ventricle opening	248
	Table and Figures	249
	References	261
Appendix 1	<b><i>whitesnake/sfpq</i> is Required for Cell Survival and Neuronal Development in the Zebrafish</b>	265
	Abstract	266
	Introduction	267
	Results and Discussion	267
	Experimental Procedures	274
	Figures	279
	References	301
Appendix 2	<b>Formation of the midbrain-hindbrain boundary constriction requires laminin-dependent basal constriction</b>	305
	Abstract	306
	Introduction	307
	Results and Discussion	308
	Experimental Procedures	312
	Figures	315
	References	327



## Acknowledgments

I would like to thank all members of the Sive lab for their encouragement, support, and advice over the past six years. I am particularly thankful to the generosity of Elizabeth Wiellette, who taught me almost everything related to the zebrafish, Amanda Dickinson, who taught me microscopy, imaging, and Photoshop, and Jennifer Gutzman, my baymate and partner in zebrafish brain morphogenesis for the last three years. Jen Gutzman, in particular, has generously answered countless questions and has always been willing to give me needed feedback. Additionally, Jen Gutzman and Ellie Graeden provided significant support editing several thesis chapters. Furthermore, I could not have done my research without the fish husbandry provided by the Sive lab fish technician, Olivier Paugois. It was also a pleasure to mentor two MIT undergraduates, Jamie Rubin and Jenny Ruan, and I enjoyed teaching them as well as benefitted from their learning. The Sive Lab is fortunate to have the incredible Heather Ferguson as our administrative assistant, and I am quite appreciative of her work. Finally, I am indebted to my advisor, Hazel Sive. Without a doubt, I could not have chosen a better graduate advisor. She has been extraordinarily supportive, challenging, and understanding, changing depending on my own needs, and my success is in part a reflection of her outstanding abilities as my advisor. I will always be grateful for her infallible support.

I would also like to thank the current and past members of my thesis committee for their time, energy, and support: Martha Constantine-Paton, Richard Hynes, Paul Garrity, David Housman, and Michael Levin.

My research project could not have been possible without the great generosity of the zebrafish community. Over a dozen different labs provided me with zebrafish mutants to study and other useful reagents.

Additionally, I want to thank Duaa Mohammad for friendship and support throughout graduate school. She also read parts of this thesis and provided critiques.

Most importantly, I need to thank my family: my parents, who taught me that I have the ability to do anything and who have always believed in me; my in-laws Catherine and Burrell, who provided me with a special home and refuge during my time here at MIT; my son, Elliot, who has reminded me in an extreme way that there are more important things in life than work; and I am most thankful to my husband, Drew, who has brought me peace in times of chaos and has provided incredible support and partnership throughout graduate school and throughout our life together.



# Curriculum Vitae

# Laura Anne Lowery

former name: Laura Anne Hardaker

## Education

- Ph.D. Biology, Massachusetts Institute of Technology – 06/08
- M.S. Biology, University of California, San Diego – 03/01
- B.S. Biology, University of California, San Diego – 03/00, Cum Laude

## Research Experience

- 05/02 – 06/08, Doctoral thesis in lab of Dr. Hazel Sive, MIT/Whitehead Institute “Mechanisms of brain ventricle development”
- 04/99-06/01, Master’s thesis in lab of Dr. William R. Schafer, UC San Diego “Neuroendocrine regulation of egg-laying behavior in *C. elegans*”

## Teaching Experience

- Fall 04 – Spring 06: Whitehead High School Partnership Program
- Fall 04 – Spring 07: Undergraduate Research Mentor, MIT
- Spring 05: Graduate Teaching Assistant, 7.02: Undergrad Biology Lab, MIT
- Fall 02: Grad Teaching Assistant, 7.22: Undergrad Developmental Biology, MIT
- 11/00: Guest Lecturer for Undergraduate Biology class, University of San Diego
- Spring 00: Grad Teaching Assistant, BIBC 102: Undergrad Metabolic Biochemistry, UCSD
- Winter 00: Undergrad Teaching Assistant, BICD 100: Undergrad Genetics, UCSD
- Fall99: Undergrad Teaching Assistant, BIBC 102: Metabolic Biochemistry, UCSD

## Honors and Awards

- 05/05-05/08: Ruth L. Kirschstein NRSA Pre-doctoral Fellowship
- 06/05: Developmental Biology Gordon Conference Poster Award
- 09/04: Abraham J. Siegel Fellowship, Whitehead Institute
- 04/04: North East Society of Developmental Biology Poster Award
- 06/00: Revelle College Outstanding Academic and Leadership Excellence Award
- 06/99: Porter Beach Foundation Grant
- 1996-1999: Provost’s Honors, Revelle College, UCSD

## Presentations

- Selected talk, 6<sup>th</sup> International Meeting on Zebrafish Development and Genetics 07/04 “Investigation of Mechanisms Underlying Brain Ventricle Morphogenesis”
- Invited Talk, Whitehead Institute Forum 11/05

## Posters

- 4<sup>th</sup> European Zebrafish Genetics and Development Meeting 07/05 “The Genetic Mechanisms Underlying Zebrafish Brain Ventricle Morphogenesis”
- Developmental Biology Gordon Conference 06/05 “Brain Ventricle Morphogenesis in the Zebrafish” (selected for poster award)
- North East Society of Developmental Biology 04/04 “Brain Ventricle Morphogenesis in the Zebrafish” (selected for poster award)
- 13<sup>th</sup> International *C. elegans* Conference 06/01 “Serotonin modulates locomotory behavior and coordinates egg-laying and movement in *C. elegans*”
- West Coast *C. elegans* Conference 06/00 “Regulation of Egg-Laying by Sensory Cues”

## Publications

- **Lowery LA**, Rubin J, and Sive H. *wis/sfpq* is required for cell survival and neuronal development in the zebrafish, *Developmental Dynamics* 2007 May;236(5):1347-57. *Research paper*
- **Lowery LA** and Sive H. Formation of zebrafish brain ventricles occurs independently of circulation and requires the *nagie oko* and *snakehead/atp1a1a.1* gene products, *Development* 2005 May;132(9):2057-67. *Research paper*  
\*modified figures included in *Developmental Biology* textbook 7<sup>th</sup> edition, Gilbert
- Jo H,\* **Lowery LA**,\* Tropepe V, Sive H. The zebrafish as a model for analyzing neural tube defects. In “Neural Tube Defects: From Origin to Treatment” (ed. D.F. Wyszynski) Oxford University Press, 2005. *Review* \*these authors contributed equally
- **Lowery LA** and Sive H. Strategies of vertebrate neurulation and a re-evaluation of teleost neural tube formation, *Mech Development* 2004 Oct; 121(10):1189-97. *Review*
- **Hardaker LA**, Singer E, Kerr R, Zhou G, Schafer WR. Serotonin modulates locomotory behavior and coordinates egg-laying and movement in *Caenorhabditis elegans*. *J Neurobiology* 2001 Dec;49 (4):303-13. *Research paper*
- Waggoner LE, **Hardaker LA**, Golik S, and Schafer WR. Effect of a neuropeptide gene on behavioral states in *Caenorhabditis elegans* egg-laying. *Genetics* 2000, 154:1181-1192. *Research paper*

## Publications in preparation

- **Lowery LA**, De Rienzo G, Gutzman J, and Sive H. Classification and characterization of 17 zebrafish brain ventricle mutants. *Research paper*
- Gutzman JH, Graeden E, **Lowery LA**, Holley H, Sive H. Formation of the midbrain-hindbrain boundary constriction requires laminin-dependent basal constriction. *Research paper*
- **Lowery LA**, Ruan J and Sive H. The temporal and spatial requirements of Na K ATPase function during embryonic brain ventricle inflation. *Research paper*
- **Lowery LA** and Sive H. Formation and function of the embryonic brain ventricles. *Review*

# Chapter One

## **A Discussion of the Formation and Function of the Embryonic Brain Ventricles**

Contributions: I wrote this introductory chapter. Members of the Sive lab provided comments, critiques, and editing support.



## **INTRODUCTION**

The vertebrate brain has a characteristic and complex three-dimensional structure, whose development is not well understood. One highly conserved aspect of brain structure are the brain ventricles, a system of cerebrospinal fluid (CSF)-filled cavities within the brain (Fig. 1.1) (Davson and Segal 1996). While brain ventricle descriptions and proposed functions have existed for over two thousand years (reviewed in (Finger 1994)), our knowledge of the function and development of the brain ventricles is far from complete.

Abnormalities in brain ventricle structure and CSF regulation can lead to hydrocephaly, one of the most common birth defects (Zhang et al 2006), and abnormal brain ventricle size and structure have been correlated with a wide range of neurodevelopmental disorders including schizophrenia (Shenton et al 2001). Although the correlation between brain ventricle structure and brain function is unclear, brain ventricle abnormalities often arise during early stages of brain ventricle development (Gilmore et al 2001). Thus, discovering the mechanisms which regulate brain ventricle development may provide insights into the causes of neurodevelopmental disorders.

While adult brain ventricles have a complex shape, the embryonic brain begins as a straight tube, the lumen of which will form the brain ventricles (Fig. 1.2). During and after neurulation, the anterior neural tube dilates in three specific locations to form the future forebrain, midbrain, and hindbrain ventricles. This dilation pattern is highly conserved in all vertebrates. Until recently, the molecular mechanisms that regulate brain ventricle formation were essentially unknown. This has been due, in part, to lack of a genetic model in which early brain ventricle development could be observed. Furthermore, analysis of the formation and function of the embryonic CSF (eCSF) within the brain ventricles has been strikingly neglected, even though much evidence points to a critical role for eCSF during neural development (Miyan et al 2003).

In this introductory chapter, I will describe the current state of the field of embryonic brain ventricle development and function. First, I will describe the brain ventricular system, including abnormalities which can occur. Then, I will explain the morphological process by which the neural tube forms the embryonic brain ventricles. Finally, I will discuss the multiple mechanisms shown to affect brain ventricle development, including patterning of the neural tube, regulated cell proliferation, tissue morphogenesis, neuronal differentiation, and regulation of

eCSF formation. In the final section, I will also discuss possible functions of the eCSF within the embryonic brain ventricles.

## **THE BRAIN VENTRICULAR SYSTEM**

The brain ventricles, a highly conserved system of cavities within the brain that contain CSF and form a circulatory system throughout the brain (Cushing 1914; Milhorat et al 1971; Pollay and Curl 1967), were first described over two thousand years ago by the ancient Greek physician Herophilus (335-280 BC) (Tascioglu and Tascioglu 2005). In the adult human brain, there are four ventricles: two lateral ventricles within the cerebrum, a third ventricle within the diencephalon, and a fourth ventricle lying between the cerebellum and pons (Fig. 1.1) (Millen and Woollam 1962). The lateral ventricles are connected to the third ventricle by the foramen of Munroe, while the third and fourth ventricles are connected via the cerebral aqueduct. The fourth ventricle connects to the spinal cord canal and the subarachnoid space that envelops the brain.

Since their discovery, the function of the brain ventricles have been the subject of much debate. For over a thousand years, it was believed that higher mental functioning resided within the brain ventricles, although this was finally refuted during the Renaissance period (Finger 1994). While the ancient Greek physician Hippocrates (460-375 BC) first commented on “water” surrounding the brain, the anatomist Galen (130-200 AD) recognized that the fluid was located within the brain ventricles as well (Hajdu 2003). The discovery of CSF secretion is often attributed to Swedenborg (1688-1772) whose manuscript referred to CSF as a “highly gifted juice” that is secreted from the roof of the fourth ventricle, although the term “cerebrospinal fluid” was first coined by Magendie (Hajdu 2003).

CSF is produced mainly by the choroid plexuses, highly vascular undulating structures located within the ventricles (Fig. 1.1C) (Emerich et al 2005). It is assumed that a small amount of CSF is made by cells lining the ventricles, as well as from secretory circumventricular organs (Perez-Figares et al 2001; Vigh et al 2004). Total CSF volume in humans is roughly 140 ml, and of this, only about 23 ml is within the ventricles; the remainder surrounds the brain (Davson and Segal 1996). The choroid plexuses produce about 500 ml per day, suggesting that the fluid is exchanged 3-4 times per day (Davson and Segal 1996). CSF is believed to flow in a directional



manner through the ventricles (Fig. 1.1C) and then out into the subarachnoid space covering the brain outer surface where it is likely absorbed into the circulatory and lymphatic systems. This flow may be directed by pressure gradients produced by the one-way secretion and absorption as well as by uniformly-oriented beating cilia located on the ependymal epithelium that lines the ventricles (Nicholson 1999).

Numerous functions have been attributed to the brain ventricles and CSF. It was proposed by Magendie in the 1800s that the outside fluid cushions the brain, thus protecting it from injury (Hajdu 2003). In fact, this idea is one of the only proposed functions for which there has been general agreement for some time (Segal 2001). The CSF has also been called a “sink” for brain waste removal, as well as a source of nutrition for the brain (Segal 2001). Today, the currently accepted view is that CSF plays a role in controlling homeostatic, hormonal, and signaling mechanisms involved in brain function (Miyani et al 2003). For example, a circumventricular system of neurons sends dendrites and axons into the ventricular space to either sense or secrete neurotransmitters and other signals in the CSF (Vigh and Vigh-Teichmann 1998). Furthermore, there has been extensive work documenting that growth factors and other signals circulate within the CSF and have an effect on brain function (Chodobski and Szmydynger-Chodobska 2001; Emerich et al 2005). Finally, recent work has shown that cilia-mediated CSF flow in the lateral ventricles directs migration of developing neurons in the adult rat brain (Sawamoto et al 2006). Overall, these data indicate that the CSF within the brain ventricles plays more important and complex roles in brain function and development than previously appreciated.

## **BRAIN VENTRICLE ABNORMALITIES**

Abnormalities in brain ventricle structure and CSF regulation are some of the most common birth defects and can have severe consequences for brain function. These abnormalities include neural tube closure defects, hydrocephaly, and neurodevelopmental disorders.

### Cranial neural tube closure defects

During formation of the embryonic brain, the flat neural plate folds under and rolls into the neural tube. Neural tube defects arise when the process does not occur normally, often during closure of the neural tube. When the neural tube fails to close in the brain, the defect is called anencephaly. The brain ventricle system is abnormally open, eCSF can escape, and the brain is exposed to the outside environment. As a result, the brain region closest to the opening, usually the forebrain, does not form and exposed tissue degenerates (Moore 2006). Infants with anencephaly are either stillborn or die shortly after birth (Moore 2006).

### Hydrocephalus

Hydrocephalus is a neurological disorder characterized by an excess of CSF and dilation of the brain ventricles, and it is one of the most common birth defects, occurring in up to 1/300 births (Dirks 2004; Zhang et al 2006). It often results in severe disruption of brain development including decreased neurogenesis (Mashayekhi et al 2002). There are numerous possible origins and effects, depending on when hydrocephalus occurs during brain development. Late onset hydrocephaly (occurring in the adult) can cause intracranial pressure, damaging brain tissue that is already formed, whereas early onset hydrocephaly (in the fetus or infant) affects growth and development of the brain (Pourghasem et al 2001). Multiple genes have been implicated in human and mammalian models of hydrocephalus (Zhang et al 2006), but the underlying causal mechanisms have remained elusive. In approximately 40% of human cases, no specific cause for hydrocephaly can be identified. It has been suggested that hydrocephalus may result from too much CSF production, too little CSF absorption, impaired CSF flow, and/or abnormal brain shaping leading to blockages of narrow canals, especially the cerebral aqueduct (Pourghasem et al 2001; Ibanez-Tallon et al 2004; Zhang et al 2006). All of these cases would lead to excessive CSF within the brain ventricles and increased intracranial pressure. Interestingly, in cases of early onset hydrocephalus where shunts are used to relieve pressure prior to tissue damage, brain

development is still abnormal, suggesting that some aspect of CSF function is abnormal (McAllister and Chovan 1998; Mashayekhi et al 2002).

#### Neurodevelopmental disorders with altered brain ventricle structure

In addition to neural tube defects and hydrocephalus, a wide range of neurodevelopmental disorders have been correlated with more subtle abnormalities in brain ventricle size and shape. These disorders include schizophrenia, autism, idiopathic and syndromal mental retardation, fragile X syndrome, Down's syndrome, attention-deficit-hyperactivity disorder, and other learning disorders (Piven et al 1995; Reiss et al 1995; Castellanos et al 1996; Prassopoulos et al 1996; Frangou et al 1997; Sanderson et al 1999; Kurokawa et al 2000; Wright et al 2000; Gilmore et al 2001; Hardan et al 2001; Shenton et al 2001; Rehn and Rees 2005; Nopoulos et al 2007). Even mild ventricle enlargements are associated with developmental abnormalities, including motor and language delays in the first two years of life (Bromley et al 1991; Patel et al 1994; Bloom et al 1997; Whitaker et al 1997; Vergani et al 1998; Pulu et al 1999). In addition, ventricular enlargement is one of the earliest and most consistently reported structural brain abnormalities found in schizophrenia (Jeste et al 1982; Suddath et al 1990; Marsh et al 1994; Nelson et al 1998; Kurokawa et al 2000; Wright et al 2000; Malla et al 2002).

Although it is not obvious how brain ventricle abnormalities and these mental health disorders are correlated, in particular, whether loss of neural tissue leads to ventricle enlargement or whether ventricle enlargement is a proximal cause, clear possibilities for interplay between brain ventricle formation and brain function exist. For example, in many disorders, it has been demonstrated that brain ventricle abnormalities arise during early stages of brain ventricle development (Gilmore et al 2001; Malla et al 2002). Thus, further study of the mechanisms involved in brain ventricle formation may shed light on brain ventricle abnormalities and how to prevent them.

## **FORMATION OF THE EMBRYONIC BRAIN VENTRICLES**

In vertebrates, the embryonic brain originates from a columnar epithelium called the neural plate (Gray and Clemente 1985). In humans, the neural plate forms within the first few weeks of development, and by one month, undergoes neurulation, a morphogenetic process by which the neural plate changes shape to form the neural tube (O'Rahilly and Muller 1994). The anterior portion of the tube becomes the brain, and the posterior becomes the spinal cord. During and after neurulation, the anterior portion undergoes a series of bends, constrictions, and dilations to subdivide the brain into the future forebrain (prosencephalon, which splits into telencephalon and diencephalon), midbrain (mesencephalon), and hindbrain (rhombencephalon). These three brain regions have been called the primary embryonic “brain vesicles” (Fig. 1.2A) (Gray and Clemente 1985).

Inside the brain vesicles lie the embryonic brain ventricles (Fig. 1.2), which have stereotypic shape due to folding of the neuroepithelium. During the next few weeks of brain development, the ventricles undergo massive expansion, with ventricle volume increasing significantly faster than brain tissue growth (Bayer and Altman 2008). Upon reaching maximal ventricle-to-tissue ratio, the ratio then reduces as brain tissue growth out-paces ventricle expansion until the ventricles eventually assume the adult size and configuration (Fig. 1.2C). This occurs in a caudal to rostral direction, with hindbrain ventricle development leading and forebrain ventricle development trailing. The embryonic forebrain ventricle splits into the two lateral ventricles (inside the telencephalon, which forms the cerebrum) and the third ventricle (inside the diencephalon). The midbrain ventricle becomes the narrow cerebral aqueduct, and the hindbrain ventricle becomes the fourth ventricle (Fig. 1.2B,C) (Gray and Clemente 1985).

While the shape changes of the embryonic brain as it undergoes morphogenesis are well-documented, the molecular mechanisms which control this developmental process have not been well-studied. This has been due, in part, to difficulty in accessing and observing the brain at early developmental stages in most vertebrate systems. However, the structure of the early embryonic brain ventricles is highly conserved in all vertebrates, including the zebrafish (Fig. 1.3). My work, described in this thesis, establishes the zebrafish as a system to study early brain morphogenesis and formation of the embryonic brain ventricles.

## **MECHANISMS OF BRAIN VENTRICLE DEVELOPMENT**

In this section, I describe multiple mechanisms required for formation of the embryonic brain ventricles, based on my thesis work described in later chapters and incorporating research from other studies. These mechanisms include patterning of the neural tube, localized cell proliferation, tissue morphogenesis, neuronal differentiation, and regulation of the fluid within the brain ventricles.

### **Patterning of the Neural Tube**

Tissue-specific gene expression patterns provide tissue identity and positional information necessary for morphogenesis. Initial brain patterning occurs before and during neurulation such that by the neural tube stage, the embryonic brain tissue is subdivided into distinct gene expression domains (Fig. 1.4A) (Lumsden and Krumlauf 1996; Darnell 2005). Thus, brain ventricle formation takes place with neuroepithelial tissue that has already acquired initial anteroposterior and dorsoventral patterning, and patterning genes have crucial downstream roles in the regional morphogenesis of the brain (Rubenstein et al 1998). The precise positioning and distinct, stereotypical shapes of the ventricles within each brain region indicate that brain ventricle development is under direct or indirect control of brain patterning genes (Fig. 1.4B).

Several papers have discussed the roles of dorsoventral patterning genes and their direct influence on brain ventricle development (Tannahill et al 2005). One study has shown that the ventral neural signaling morphogen Sonic Hedgehog (Shh) is required for chick brain ventricle expansion (Britto et al 2002). Shh is secreted from the notochord, a rod-shaped structure underlying the neural tube. Separation of the notochord from the brain causes loss of ventral Shh brain expression and subsequent brain ventricle collapse (Britto et al 2002). Similarly, the homeodomain gene *hlx1*, expressed in a ventral midline longitudinal stripe in the rostral brain, is also required for zebrafish brain ventricle formation (Hjorth et al 2002). Finally, the patterning genes *zic1* and *zic4* (*zinc finger* homologs of *Drosophila odd-paired* genes) control zebrafish hindbrain ventricle opening by regulating fate specification in the dorsal hindbrain, and loss of function of these genes leads to specific hindbrain ventricle defects (Elsen et al 2008). Thus, without early establishment of tissue identity, the subsequent morphogenesis fails to occur.

## **Cell Proliferation**

His first suggested that differential growth could provide a morphogenetic force (His 1874), and in the last two decades, the connection between cell proliferation and tissue morphogenesis has gained significant support (Tuckett and Morriss-Kay 1985; Schoenwolf and Alvarez 1989; Sausedo et al 1997; Kahane and Kalcheim 1998). It has been suggested that brain ventricle shaping is simply a result of uneven cell proliferation, migration, and differentiation throughout the neural tube, determined by patterning mechanisms described above (Bergquist and Kallen 1953; Gray and Clemente 1985; Bayer and Altman 2008). For example, the telencephalic-specific transcription factor Bf-1 is required for proliferation of telencephalic neuroepithelial cells and is essential for normal morphogenesis of the telencephalon in the rat (Tao and Lai 1992; Xuan et al 1995). Another example is the *zic* family of genes. Whereas *zic2a* and *zic5* are required for cell proliferation in the midbrain, *zic1* and *zic4* are required for cell proliferation in the hindbrain, and loss of their functions lead to reduced midbrain and hindbrain ventricles, respectively, in the zebrafish (Nyholm et al 2007; Elsen et al 2008).

For several weeks after neural tube closure, the human embryonic brain consists mainly of proliferating neuroepithelial cells considered to be the earliest neural stem cells (Bayer and Altman 2008). As neural development proceeds, these cells give rise to differentiating post-mitotic daughter cells at various rates throughout the brain, which leave the proliferating zone and migrate to form the layers of the brain (Bayer and Altman 2008). The orientation of the cell division cleavage plane has an effect on brain shaping, as cells which divide parallel (planar) to the tube increase the length of the tube, whereas those that divide perpendicular increase the tube thickness. For instance, in the cerebral cortex of the ferret, planar mitoses account for most divisions, producing progeny that remain at the ventricle and continue to divide, whereas perpendicular mitoses result in one daughter cell migrating into the subventricular regions to differentiate (Chenn and McConnell 1995). Thus, cell proliferation can have an effect on the shaping of the brain, and each region of the brain may contain a genetic program for regulation of brain morphogenesis based on cell proliferation.

Consistent with this idea, in the embryonic chick brain, the boundaries between the forebrain and midbrain and between the two telencephalic ventricles in the forebrain are regions of post-mitotic cells, whereas the tissue surrounding the ventricles is highly proliferative (Kahane and Kalcheim 1998). Similarly, during initial brain ventricle formation in zebrafish, I observed that the midbrain-hindbrain boundary (MHB) has significantly less cell proliferation

compared to the midbrain and hindbrain surrounding it (Chapter 4), and this deficit may be one of the reasons that the MHB does not open into a ventricular space, or it may be evidence that CSF within the forming ventricles promotes cell proliferation.

However, regional cell proliferation is not the only mechanism directing brain ventricle morphogenesis, as I determined that pharmacologically blocking cell proliferation results in smaller but normally shaped brain ventricles (Chapter 4), consistent with previous studies showing that brain ventricle constrictions persist even when cell division is blocked (Kessel 1960; Harris and Hartenstein 1991). These data show that the formation and shaping of the brain ventricles is influenced by factors in addition to localized cell proliferation.

#### *A note on cell death*

Spatially-regulated cell death may also contribute to shaping of the brain, and it has been postulated that loss of certain cell populations allows brain tube bending (Glucksmann 1951; Kallen 1955). Programmed cell death has been recognized as a prominent event during formation of the vertebrate nervous system, contributing to neural tube closure (Geelen and Langman 1977), forebrain size and shape regulation (Haydar et al 1999), and control of cell numbers (Homma et al 1994; Thomaidou et al 1997). When cell death is perturbed, abnormalities in brain ventricle shape can result. For instance, blocking programmed cell death by gene ablation causes an overgrowth of brain tissue in mice, leading to obstructed brain ventricles (Kuida et al 1996). Conversely, mutations which cause too much cell death lead to a reduction in brain tissue and over-expansion of the brain ventricles (Keino et al 1994). However, I have not found evidence that localized cell death is involved in the initial bending and shaping of the brain ventricles (Chapter 4). Thus, while regulation of cell death may have some effect on later brain ventricle development, it does not appear to play a role in the initial shaping events.

## **Tissue Morphogenesis**

Tissue morphogenesis is the major mechanism, other than cell proliferation, that drives the shaping of the brain ventricles, and it is dependent on three processes: 1) formation and maintenance of the epithelium (requiring cell-adhesion junctions), 2) individual cell shape changes (requiring regulated cytoskeletal dynamics), and 3) epithelial anchoring and support (provided by the extracellular matrix bound to the epithelium by cell-matrix adhesions) (Fig. 1.5A-C). My thesis work has identified a number of genes required for tissue morphogenesis during brain ventricle development.

### *1) Formation and Maintenance of the Epithelium – Apical Junctions*

Brain ventricle morphogenesis requires an intact epithelium, defined as a sheet of cells interconnected by junctions, as the substrate for the shaping process (Fig. 1.5A-C). Thus, when cell junction proteins are not functional, neuroepithelial morphogenesis cannot occur normally. The resulting phenotype depends on the specific requirement for a protein during neuroepithelial formation and function (Fig. 1.5D-G). The mildest phenotype occurs in the zebrafish mutant *heart and soul*, which has a null mutation in the apical adherens junction component *prkci* (Chapter 3). In this mutant, junctions are present but normal brain ventricle shaping does not occur, suggesting that some other aspect of cell-cell coordination is missing (Fig. 1.5E). A more severe phenotype occurs in the *nagie oko* mutant, which has a mutation in the apical adherens junction component *mpp5* (Chapter 3,4). In *nagie oko* mutants, an intact neural tube forms but cell junctions are disorganized (Fig. 1.5F). The midline does not form or separate normally, leading to an absence of brain ventricles. Finally, the most severe case is when junctions do not form at all and the neuroepithelium falls apart (Fig. 1.5G). This occurs in the N-cadherin mutant, *parachute*, as N-cadherin is strictly required in the zebrafish neuroepithelium to connect the cells during neurulation. Neuroepithelial cells in the *parachute* mutant lack the adhesiveness required for neural tube structure, and they become rounded and form disorganized aggregates separated by large intercellular spaces (Lele et al 2002). As such, the tissue movement and cell shape-driven process of neurulation cannot occur (Hong and Brewster 2006). N-cadherin requirement specifically during brain ventricle morphogenesis has not been shown, but I speculate that it is required at all stages of neuroepithelial development, and in fact, many junction components shown to play a role in neurulation may also be necessary for epithelial coordination during brain ventricle shaping.



## 2) Individual Cell Shape Changes – Cytoskeletal Dynamics

Shaping of the neural tube to form the brain ventricles is at least partially driven by individual cell shape changes in specific locations of the brain. For example, it is likely that formation of wedge-shaped cells may be required to form the hinge-points on either side of the forebrain, midbrain, and hindbrain ventricles, as well as the sharp folding at the MHB (Fig. 1.5B,C). Formation of such wedge-shaped cells have been shown to drive the formation of numerous types of epithelial bends and folds, and this change in cell shape is usually driven by cytoskeletal rearrangements (Fristrom 1988; Lecuit and Lenne 2007). Furthermore, I identified one zebrafish brain ventricle mutant, *ppp1r12a*, which may have abnormal cytoskeletal regulation. The *ppp1r12a* gene encodes a homolog of mouse and human Mypt1 (myosin phosphatase target subunit 1), one of the subunits of myosin phosphatase and a key regulator of myosin activity. It is implicated in integrating signaling cascades for cytoskeletal remodeling and directly influencing cell contractility, cell morphology, and cell adhesion (Eto et al 2005; Xia et al 2005). Loss of Mypt1 in other systems leads to aberrant cytoskeletal and cell shape changes. Thus, it is likely that the brain ventricle defects seen in the *ppp1r12a* mutant (abnormal opening of the brain ventricles, Chapter 3 and Gutzman JH unpublished) are likely due to abnormal cytoskeletal dynamics.

## 3) Epithelial Anchoring and Support - Extracellular matrix

The extracellular matrix (ECM) has been shown to play a critical role in the epithelial morphogenesis of many different tissues (Gullberg and Ekblom 1995; Ashkenas et al 1996). Thus, it is not surprising that it is required for embryonic brain ventricle development as well. ECM components are required both outside and inside of the neural tube to provide structural support for the epithelium and newly-forming brain ventricles.

The outside of the neural tube epithelium is covered by a network of ECM called the basement membrane (Fig. 1.5A-C), and I have discovered that brain ventricle formation requires at least two basement membrane proteins, laminin and fibronectin. In zebrafish laminin mutants, the MHB constriction does not form, in addition to having other morphological abnormalities, whereas in a zebrafish fibronectin hypomorph, brain ventricle shape is normal but the ventricles do not expand (Chapter 3, Appendix 2). These defects are consistent with the known roles of ECM components in epithelial morphogenesis of other organs such as the heart, kidney, and lung

(Bernfield et al 1984; Miner and Yurchenco 2004; Trinh and Stainier 2004). In the case of the laminin mutant, we have shown that loss of laminin prevents cells at the MHB from undergoing columnar-to-wedge cell shape changes (Appendix 2: Gutzman et al, submitted), highlighting the importance of the extracellular matrix during tissue morphogenesis.

Extracellular matrix components reside inside the neural tube as well, at the apical surface of the neuroepithelium. Epithelial cells often secrete proteoglycans or other molecules at their apical surface to form specialised apical extracellular matrices (aECMs) that give apical epithelial support, assist in epithelial morphogenesis, or provide other specialized roles (Lane et al 1993; Bokel et al 2005; Moussian and Uv 2005). One well-studied example is the aECM of the *Drosophila* trachea tube, in which the aECM provides structural support to preserve the luminal space during tube development (Denholm and Skaer 2003). Similarly, the chick brain ventricles contain an aECM rich in chondroitin sulfate, hyaluronic acid, and other proteoglycans, which have been suggested to play a role in brain ventricle formation (Gato et al 1993; Ojeda and Piedra 2000). Proteoglycans have previously been shown to play a morphogenetic role in brain neurulation in the embryonic rat and chick, in particular by promoting neuroepithelial integrity and cell shape changes needed for brain tissue bending (Morriss-Kay and Crutch 1982; Schoenwolf and Fisher 1983; Tuckett and Morriss-Kay 1989; Yip et al 2002). Furthermore, proteoglycans have been implicated in the formation of various embryonic cavities, such as otic placode invagination and lens vesicle morphogenesis, by promoting the osmotic gradient to drive fluid secretion into the cavities (Moro-Balbas et al 2000; Gato et al 2001). The roles of proteoglycans in these other systems are likely similar to those utilized during brain ventricle morphogenesis.

### **Neuronal Differentiation/Transcription**

The decision that neuroepithelial daughter cells make, between migrating out of the ventricular zone in order to differentiate into neurons versus remaining neuroepithelial, has a profound effect on the shape of the brain (Bayer and Altman 2008). Thus, it follows that regulation of neuronal differentiation by transcription or other control mechanisms can have an effect on brain ventricle shaping. Consistent with this idea, I have discovered two zebrafish mutants, *otter* and *whitesnake*, that lack function of the transcription factors *med12* (*mediator of RNA polymerase II transcription, subunit 12 homolog*) and *sfpq* (*splicing factor proline glutamine rich*), respectively, show abnormalities in brain tissue shaping and brain ventricle

structure (Fig. 1.6) (Chapter 3, Appendix 1). In both mutants, the brain ventricles do not open normally. Loss of *med12* has an early effect, showing a mutant phenotype from the beginning stages of brain ventricle opening, whereas loss of *sfpq* does not affect early brain shaping but has a noticeable phenotype during brain ventricle expansion. The roles that *med12* and *sfpq* play specifically in brain ventricle development are unclear. However, in addition to brain ventricle defects, both *otter* and *whitesnake* mutants also show loss of specific neuronal classes (Chapter 3, Appendix 1), and thus it is possible that *med12* and *sfpq* are directly involved in regulation of neuronal differentiation. Interestingly, polymorphisms of the *med12* gene in humans are associated with an increased risk for schizophrenia (Philibert et al 2007), a disorder which is correlated with abnormal brain structure and increased ventricle size (Antonova et al 2004; Crespo-Facorro et al 2007).

### **Brain Ventricle Fluid Regulation and Function**

An additional vital component in the formation of the brain ventricles is the presence of fluid (eCSF) within the ventricles. Regulation of eCSF formation is not well-understood, but it includes mechanisms within the neuroepithelium as well as outside the neuroepithelium. Moreover, significant evidence suggests that intraluminal pressure created by eCSF, in addition to growth factors within the fluid, may play crucial roles during brain development (Miyan et al 2003).

#### *1) eCSF has a complex protein composition, formed from neural and non-neural sources*

eCSF has a complex protein composition which differs substantially from adult CSF. While adult CSF has only trace amounts of protein, with detectable levels usually indicating infection, damage, or other pathology (Davson and Segal 1996), eCSF is a protein-rich fluid whose composition changes during different developmental stages and also between ventricles (Parada et al 2005; Parada et al 2006; Zappaterra et al 2007). Recent proteomic analysis studies of human, rat, mouse, and chick eCSF have identified approximately 200 different proteins, including signaling and growth factors, extracellular matrix proteins, transport and carrier proteins, enzymes and proteases (Parada et al 2005; Parada et al 2006; Zappaterra et al 2007), demonstrating that eCSF is a heterogeneous mixture of many classes of proteins with varying functions.

Just as eCSF protein composition differs from that of adult, the process of its formation is different as well. Adult CSF is formed mainly by the choroid plexuses located in each of the ventricles, and many of the mechanisms that regulate adult CSF production have been identified (Speake et al 2001; Brown et al 2004; Praetorius 2007). However, substantial embryonic brain ventricle expansion concurrent with eCSF production occurs several weeks prior to choroid plexus formation in humans (Bayer and Altman 2008). Thus, central questions regarding eCSF include: where does early eCSF come from, how is it regulated, and what is the functional relevance of its composition?

## *2) Neuroepithelial sources of eCSF*

The source of eCSF has not been confirmed, although evidence suggests that it is produced, at least in part, by the neuroepithelium. Weiss first reported that the neuroepithelial tissue is secretory, based on experiments using hanging-drop cultures of neuroepithelial fragments (Weiss 1934). Additionally, secretory vesicles are present at the neuroepithelial apical surface (Gato et al 1993). Thus, because neuroepithelial tissue is thought to be secretory, it is presumed that eCSF secretion occurs as the neural tube elongates and enlarges at the anterior end to form the fluid-filled brain ventricles (Miyani et al 2003). Considering that eCSF is surrounded by neuroepithelial tissue completely, it follows that a major source of the fluid is the neuroepithelium itself.

My research has shown that eCSF formation is an active process that requires  $\text{Na}^+ \text{K}^+$  ATPase ion pumping within the neuroepithelium (Chapter 5). Formation of the fluid and concurrent inflation of the brain ventricles requires the activity of the Atp1a1 ion pump, and it is thought that this pump forms the osmotic gradient required for fluid movement into the ventricular spaces, mediated at least in part through aquaporin channels (Brown et al 2004; Lehmann et al 2004). Additionally, proteoglycans in the eCSF are secreted by the neuroepithelium and have also been shown to osmotically regulate fluid movement into the embryonic brain ventricles (Gato et al 1993; Alonso et al 1998). The proteoglycans are located homogeneously throughout the brain ventricle cavities from the earliest stages of brain ventricle development (Gato et al 1993), and perturbing proteoglycan synthesis results in changes in brain ventricle size in chick and rat embryos (Alonso et al 1998; Alonso et al 1999). Proteoglycans have been proposed to be fundamental molecules in the regulation of water content in numerous biological tissues, as small variations in concentration lead to large changes in osmotic capacity

(Alonso et al 1998). Thus, it is likely that both  $\text{Na}^+ \text{K}^+$  ATPase ion pumping and proteoglycan secretion serve to form and regulate the osmotic gradient that drives fluid secretion into the ventricles (Fig. 1.7).

### *3) Non-neuroepithelial sources of eCSF*

It has been suggested that eCSF also has non-neuroepithelial inputs (Gato et al 2004), and one confirmed source is the blood plasma. Circulation and blood vasculature clearly play a role in eCSF pressure maintenance. For example, reducing hydrostatic pressure in the vascular system leads to reduced brain ventricle expansion in the chick (Li and Desmond 1991), and my studies show that circulation is necessary for normal brain ventricle expansion in the zebrafish (Chapter 4). However, it is important to note that the embryonic brain ventricles initially form and begin expansion prior to heartbeat and circulation. The choroid plexuses, which secrete CSF, form only later in embryonic brain ventricle development. Once they form, active and passive transport moves solutes and water from blood vessels within the choroid plexus tissue to the eCSF (Dziegielewska et al 2001). Thus, while initial brain shaping is not dependent on circulation, circulation plays an important role in later eCSF production and embryonic brain ventricle expansion (Chapter 4).

Additionally, Parada et al claims that some of the gene products identified in chick eCSF are not produced by the neuroepithelium, but by other structures such as the embryonic liver or from yolk storage (Parada et al 2006). One study suggests that the eCSF factor Fgf2 has a non-neuroepithelial source and is actively transported through the neuroepithelium into the brain ventricles (Martin et al 2006). While these studies are not conclusive, it is certainly possible that the neuroepithelium acts as a conduit for the regulated transport of factors from outside the brain (Fig. 1.7).

### *4) The role of fluid pressure during brain ventricle development*

Classic studies in chick embryos have suggested that intraluminal pressure resulting from the accumulation of fluid inside the brain ventricles is necessary for normal brain ventricle expansion and continued neural development. It was first demonstrated in 1958 that intubation of the chick embryonic hindbrain ventricle results in a collapse of the ventricle (Coulombre and Coulombre 1958). This was followed by demonstration that brain ventricle expansion requires a

certain level of intraluminal pressure (Jelinek and Pexieder 1970; Pexieder and Jelinek 1970). Desmond and colleagues further investigated the requirement of the eCSF for brain cavity expansion in a series of publications. They showed that eCSF drainage in both chick and mice leads to a reduction of brain tissue growth, brain tissue folding into the ventricles, reduced brain expansion to only a fifth of its normal size, and 50% fewer neuroepithelial cells than in control embryos (Desmond and Jacobson 1977; Desmond 1985; Inagaki et al 1997). Additionally, they observed a 50-fold increase in intraluminal pressure during brain ventricle expansion, and artificially increasing pressure with a saline solution leads to a greater amount of mitosis (Desmond et al 2005). In sum, Desmond and colleagues suggest that pressure within the brain, combined with differences in resistance of the brain wall and surrounding tissues to eCSF pressure, leads to normal brain enlargement and brain shaping, and that the brain is blown up like a balloon (Desmond and Jacobson 1977; Desmond et al 2005).

While the mechanisms which form and regulate eCSF remain poorly understood, these studies suggest that fluid pressure within the brain ventricles plays a hydromechanical role in brain ventricle expansion and brain development (Fig. 1.7). This is consistent with the development of other organ systems such as the heart, where blood flow through the heart modifies the morphology of the heart atrial and ventricular lumens (Berdougo et al 2003), the flow of blood through the ventricles stimulates valve morphogenesis (Hove et al 2003), and in tissue culture, where cell stretching increases cell proliferation (Liu et al 1992; Tanner et al 1995).

##### *5) Factors in the eCSF are required for neuroepithelial proliferation and brain development*

While the hydromechanical role of eCSF may be important, there is significant recent data which suggest that factors within the eCSF are also required for brain development. First, it is notable that proximity to eCSF appears to be essential for most neuroepithelial cell divisions (Fig. 1.7). During early brain development, neuroepithelial cell proliferation occurs almost exclusively at the ventricular surface, in contact with eCSF (Sauer 1936). Moreover, there is a striking spatial and temporal correlation between brain ventricular size and the amount of neuronal cell proliferation which subsequently occurs within that region (Bayer and Altman 2008). Although certain neuronal progenitors do undergo mitosis away from the ventricles (such as the external germinal layer of the cerebellum (Altman and Bayer 1982)), these cells are fate-restricted and late-generated, and thus, contact with the eCSF and the factors contained in it may

be a prerequisite for the production of the early, pluripotent neuroepithelial cells that generate most neurons (Bayer and Altman 2008).

Several studies have demonstrated that drainage of eCSF leads to significantly reduced cell proliferation and increased apoptosis in the developing chick brain (Desmond and Jacobson 1977; Desmond 1985; Mashayekhi and Salehi 2006; Salehi and Mashayekhi 2006). Additionally, immunodepleting the ventricles of Fgf2, a component of eCSF which is known to play an important role in the regulation of neurogenesis, also reduces cell proliferation by 50% (Tao et al 1997; Panchision and McKay 2002; Martin et al 2006). Similarly, in the human cranial neural tube defect anencephaly, whereby failure of neural tube closure allows escape of eCSF, there is reduced neuronal development and brain tissue degeneration (Moore 2006).

Just as eCSF appears to be required for brain growth *in vivo*, it can also promote neuroepithelial stem cell growth in culture. Cultures of chick and rat embryonic brain cells are not able to survive, replicate, or undergo neurogenesis alone, but addition of eCSF to the cultures promotes neuroepithelial cell survival and induces proliferation and neurogenesis (Gato et al 2005; Miyan et al 2006). Moreover, cells behave differently depending on the embryonic age of eCSF, suggesting that components within the eCSF regulate neurogenesis in a developmental-stage-dependent manner (Miyan et al 2006).

In addition to promoting cell proliferation, there is evidence that eCSF collaborates with other signaling centers to regulate gene expression. For example, Parada and colleagues have shown that explants of chick midbrain tissue cultured with basal medium do not express midbrain-specific genes such as *otx2* and *fgf8*. However, when cultured with eCSF-supplemented medium, the tissues maintain normal gene expression patterns (Parada et al 2005).

Interestingly, abnormal factors within eCSF may be directly responsible for the brain defects which occur in some cases of hydrocephalus, contrary to the currently accepted view that brain defects result from increased pressure. As noted earlier, hydrocephalus is a disorder characterized by an excess of CSF and dilation of the brain ventricles. While normal eCSF promotes cell proliferation, eCSF obtained from the enlarged ventricles of the hydrocephalic rat model actually inhibits cell proliferation in culture (Owen-Lynch et al 2003). Furthermore, abnormalities in the eCSF protein content, including reduced proteoglycans, are detectable prior to any morphological brain defects (Pourghasem et al 2001). Finally, while cortical cells in the hydrocephalic rat do not divide, they proliferate normally once they are removed from the *in vivo* environment and cultured *in vitro* with wild-type eCSF (Owen-Lynch et al 2003). These

results all suggest that abnormal regulation of eCSF factors, rather than increased fluid pressure, may be an underlying cause of hydrocephalus-related brain damage.

Investigation of the functional roles of eCSF has gained recent attention as a promising avenue of neurodevelopment research and may play a critical role in the success of neural stem cell technology (Cottingham 2007; Zappaterra et al 2007). Central to understanding the function of eCSF is to determine how eCSF is produced and regulated. Future studies will likely uncover further insights into eCSF formation, regulation, and its role in brain development, as eCSF may hold the key to how the process of neuronal development is coordinated in the normal brain and how it is perturbed in many neurodevelopmental abnormalities.



### **Coordination between mechanisms responsible for brain ventricle development**

To summarize, multiple mechanisms required for embryonic brain ventricle development include patterning of the neural tube, localized cell proliferation, tissue morphogenesis, neuronal differentiation, and fluid formation (Fig. 1.8). These mechanisms are not controlled independently, as there is considerable amount of coordination between them.

At the top of the hierarchy is neural tube patterning, which confers cell identity and position and drives all subsequent brain ventricle developmental processes.

Fluid formation is required for normal cell proliferation and, either directly or indirectly, neuronal differentiation, as shown by the requirement of eCSF for neuronal development. This effect of the fluid within the brain ventricles is consistent with studies demonstrating the role of fluid pressure and flow in the epithelial morphogenesis in other systems, as discussed earlier in the case of heart morphogenesis.

Cell proliferation has a direct effect on neuronal differentiation, since each neuroepithelial cell makes the decision between continuing to proliferate versus differentiating. The balance between the two outcomes affects the shape of the brain ventricles and the potential for further brain development. Furthermore, when neuroepithelial cells make the decision to differentiate into neurons, they migrate out of the epithelium and undergo distinct changes in cell morphology. Finally, cell proliferation also influences tissue morphogenesis, as alterations in cell cycle and cell proliferation can generate forces that drive cellular movements and changes in cell shape (Kahane and Kalcheim 1998).

Together, these five mechanisms transform the straight neuroepithelial tube into the highly conserved brain ventricular structures present during the brain development of all vertebrates.

## **PREVIEW OF THESIS**

In chapter 1, I have presented an introduction to the formation and function of the embryonic brain ventricular system.

In chapter 2, I present my considerations in choosing zebrafish as a model for analyzing the brain morphogenetic processes of neurulation and brain ventricle development.

In chapter 3, I describe the characterization and classification of 20 brain morphology mutants, all of which have various defects in embryonic brain ventricle structure.

In chapter 4, I characterize normal brain ventricle formation in the zebrafish and examine in detail the phenotypes of two severe brain ventricle mutants, *nagie oko* and *snakehead*, and I show that *snakehead* corresponds to the Na<sup>+</sup> K<sup>+</sup> ATPase gene *atp1a1*.

In chapter 5, I further elucidate the temporal and spatial requirements for Na<sup>+</sup> K<sup>+</sup> ATPase function during brain ventricle development and embryonic CSF formation.

In chapter 6, I summarize my current model of the mechanisms which regulate brain ventricle development, and I discuss future studies and unanswered questions.

Appendix 1 presents a study of the *whitesnake* mutant, which shows later brain ventricle abnormalities, and I demonstrate that *sfpq*, mutated in the *whitesnake* mutant, is required for cell survival and neuronal differentiation.

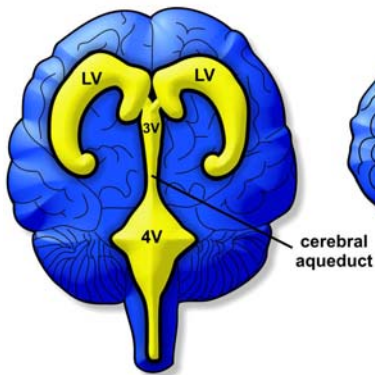
Appendix 2 reveals that one aspect of brain morphogenesis, formation of the constriction between the midbrain and hindbrain, requires laminin-dependent cell shape changes.

**Figure 1.1 Adult human brain ventricles.**

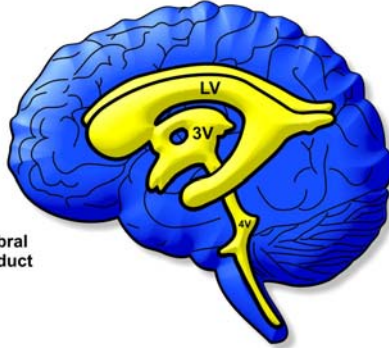
A and B: blue represents brain tissue and yellow shows brain ventricles. C: choroid plexuses are in red, blue arrows designate direction of CSF flow.

LV lateral ventricle, 3V third ventricle, 4V fourth ventricle.

**A Anterior View**



**B Lateral View**



**C Lateral View with Choroid Plexuses**

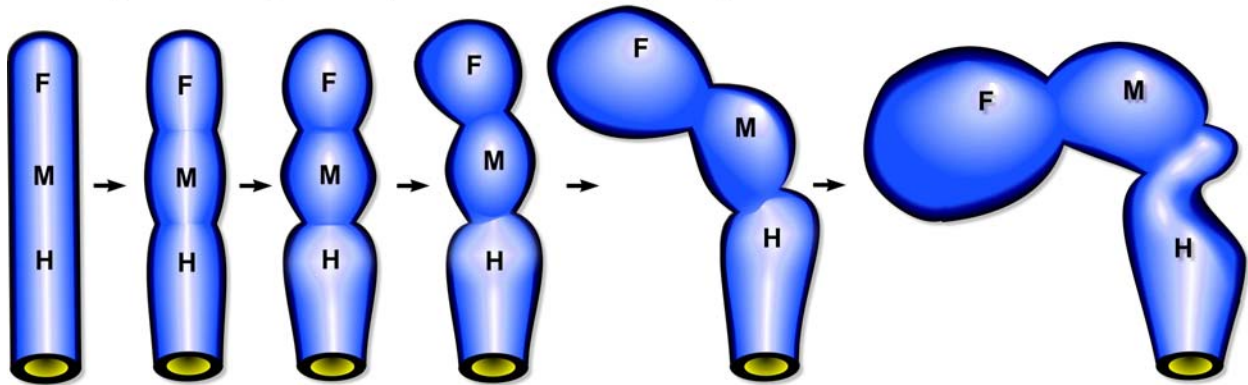




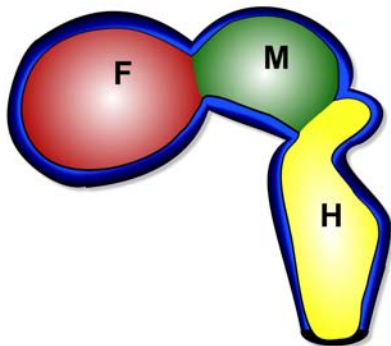
**Figure 1.2 Cartoon schematic of vertebrate embryonic brain development.**

A: Lateral views of the neural tube as it undergoes early embryonic brain morphogenesis to form the primary brain vesicles. B: Lateral section through the brain vesicles to show the brain ventricles within. C: Anterior view of adult brain ventricles. In B and C, colors correspond to the same ventricle regions in the embryo and adult. Not to scale. F forebrain, M midbrain, H hindbrain, LV lateral ventricle, 3V third ventricle, 4V fourth ventricle.

**A Steps of Early Embryonic Brain Morphogenesis**



**B Early Embryonic Brain Ventricles**



**C Adult Brain Ventricles**

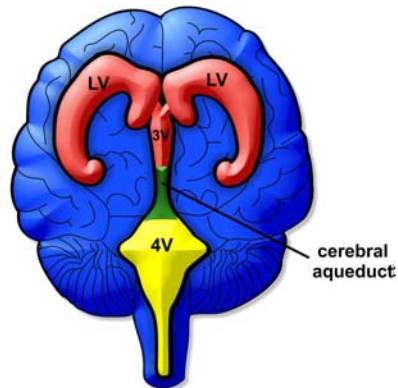




**Figure 1.3 Conservation of embryonic brain ventricle structure.**

Tracings of embryonic brain ventricles at similar corresponding stages in development, all lateral views. A: Human embryo brain ventricles, stage 17 (approximately 43 days post fertilization), traced from <http://virtualhumanembryo.lsuhscc.edu/videos/JHUmorph.htm>. B: Rat embryo brain ventricles, stage E14 (14 days post fertilization), from (Altman and Bayer 1995); C: Chick embryo brain ventricles, stage 16 (approximately 2.5 days post fertilization), from (Pacheco et al 1986); D: Zebrafish embryo brain ventricles, 24 hours post fertilization. F forebrain ventricle, M midbrain ventricle, H hindbrain ventricle.

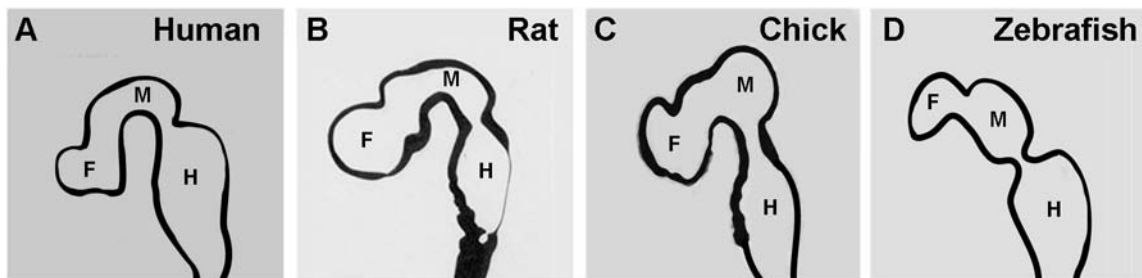


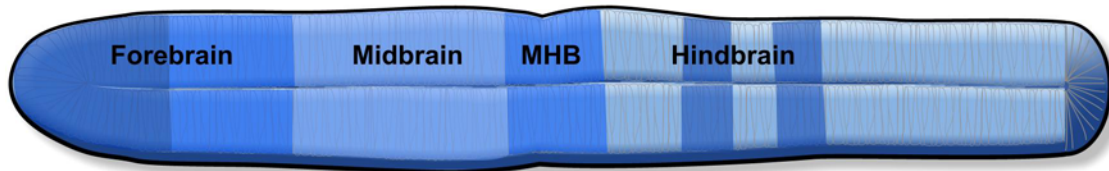




**Figure 1.4 Patterning of the neural tube is required for brain ventricle development.**

A: At the neural tube stage, distinct brain regions are already specified. Different shades of blue designate specific gene expression patterns. B: Gene expression patterns correspond to stereotypical shape changes in the opening brain ventricles. F forebrain ventricle, M midbrain ventricle, H hindbrain ventricle, MHB midbrain-hindbrain boundary.

**A Patterned brain, closed neural tube**



**B Patterned brain, open brain ventricles**

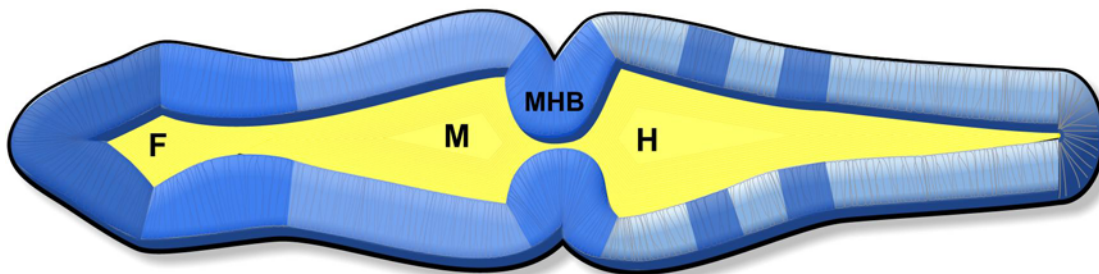




**Figure 1.5 Tissue morphogenesis during brain ventricle development.**

A-C: Tissue morphogenesis requires maintenance of the epithelium by apical junctions (red), cytoskeletal-induced cell shape changes (example: apical constriction at lateral hinge-points of forebrain, midbrain, hindbrain, marked with asterisks), and structural support by extracellular matrix (purple). D-G: Cartoons of transverse sections of midbrain ventricle depicting range of phenotypes observed when epithelium is not maintained and coordinated. F forebrain ventricle, M midbrain ventricle, H hindbrain ventricle, MHB midbrain-hindbrain boundary.

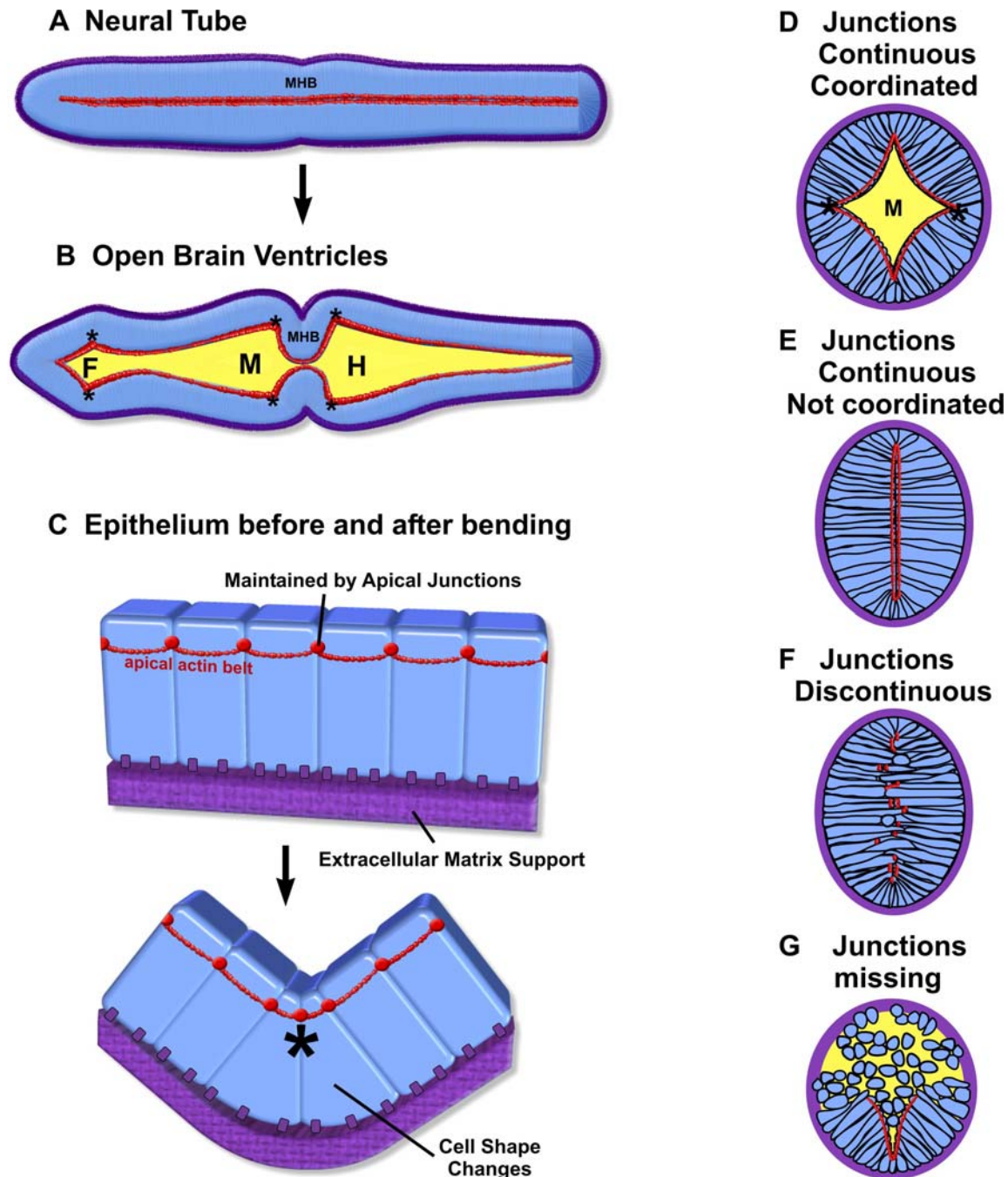




**Figure 1.6 Brain ventricle development is abnormal in *otter* and *whitesnake* mutants.**

These mutants have mutations in transcription factors *med12* and *sfpq*, respectively, and both are also required for neuronal differentiation. A: Dorsal view of wild-type zebrafish embryo at 28 hpf after ventricle injection with fluorescent-dextran. B,C: Ventricles of mutants are reduced in size.

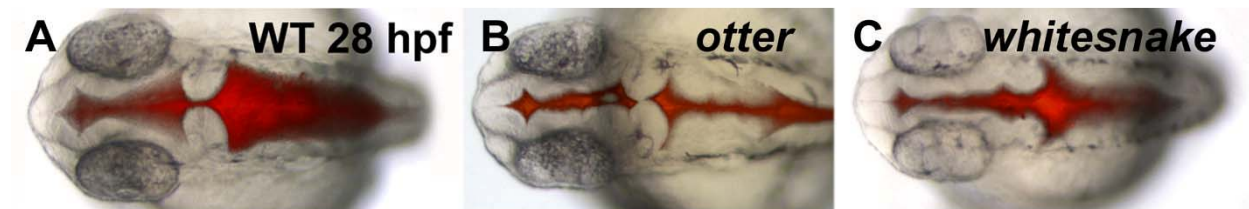




**Figure 1.7 eCSF formation contributes to brain ventricle formation.**

Neuroepithelial sources of eCSF include ion pumping and proteoglycan secretion. These form the osmotic gradient that drives fluid secretion into the ventricles, at least in part through aquaporin channels. Additionally, both fluid pressure and growth factors within the eCSF are proposed to stimulate neuroepithelial cell proliferation. Non-neural sources include transport of serum factors from the blood vasculature (after circulation begins later in brain ventricle development) as well as possibly other embryonic sources. Not drawn to scale. Cells and molecules are enlarged for detail. PG: proteoglycans, AQ: aquaporin

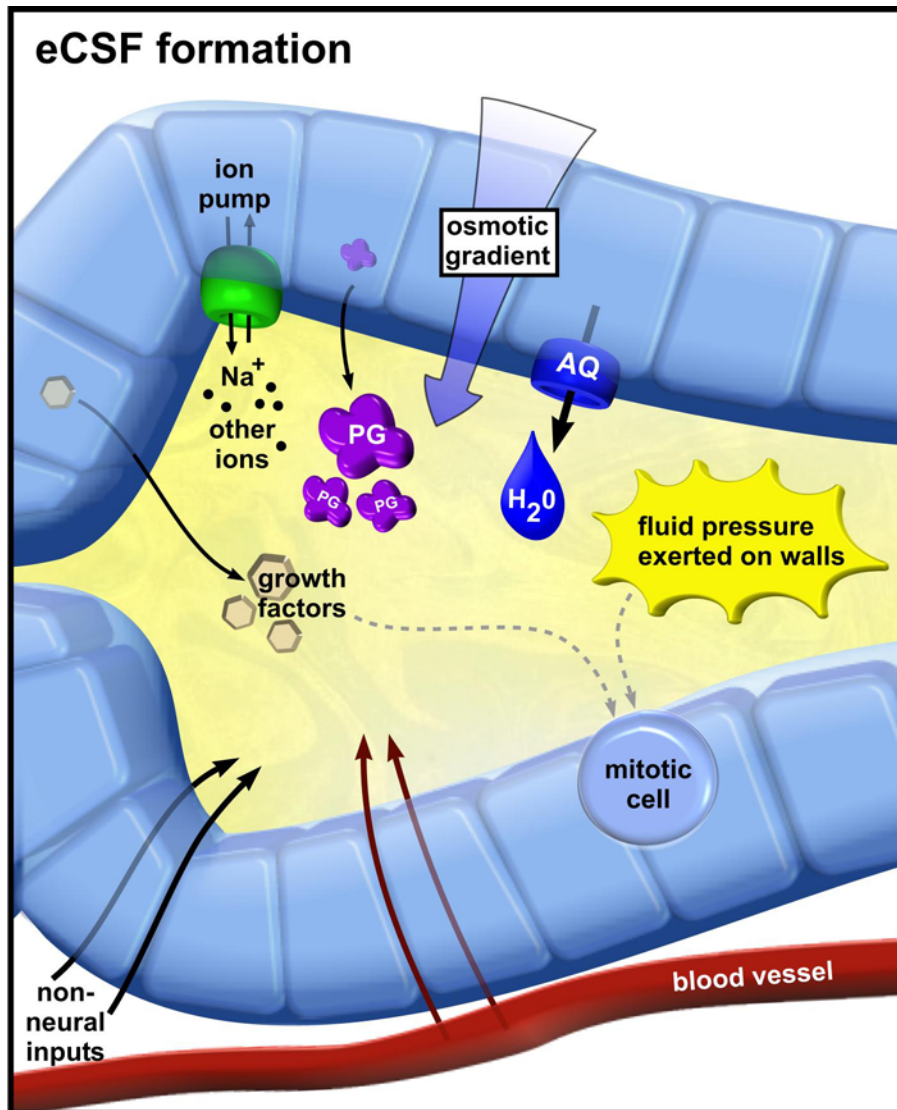
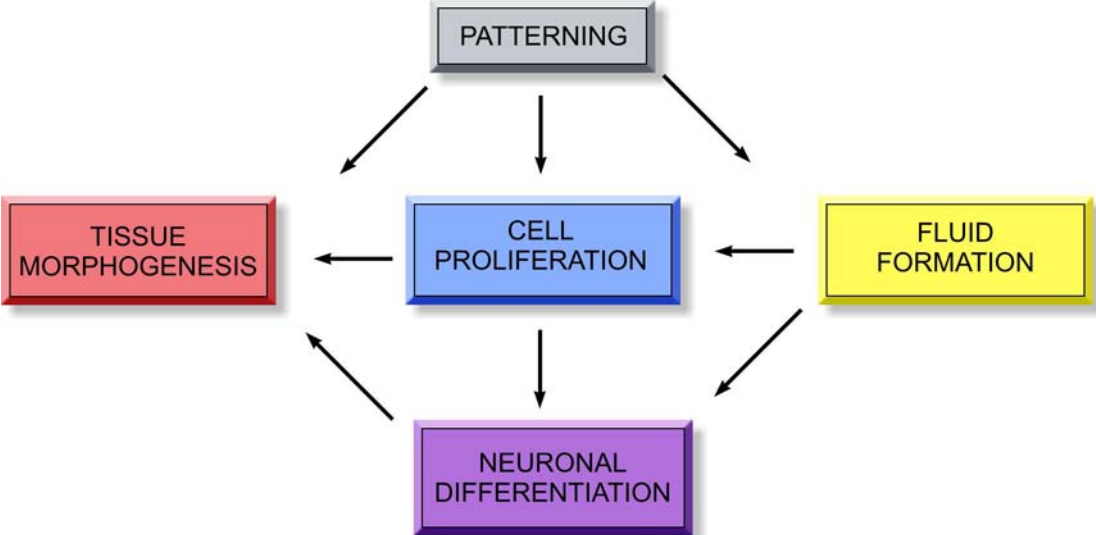






**Figure 1.8** Flow-chart depicting the coordination between mechanisms that regulate brain ventricle formation.





## References

- Alonso, M. I., A. Gato, J. A. Moro and E. Barbosa (1998). Disruption of proteoglycans in neural tube fluid by beta-D-xyloside alters brain enlargement in chick embryos. *Anat Rec* 252(4): 499-508.
- Alonso, M. I., A. Gato, J. A. Moro, P. Martin and E. Barbosa (1999). Involvement of sulfated proteoglycans in embryonic brain expansion at earliest stages of development in rat embryos. *Cells Tissues Organs* 165(1): 1-9.
- Altman, J. and S. A. Bayer (1982). Morphological development of the rat cerebellum and some of its mechanisms. *The Cerebellum: New Vistas*. S. L. Palay and V. Chan-Palay. Berlin, Springer-Verlag: 8-49.
- Altman, J. and S. A. Bayer (1995). Atlas of prenatal rat brain development. Boca Raton, Fla., CRC Press.
- Antonova, E., T. Sharma, R. Morris and V. Kumari (2004). The relationship between brain structure and neurocognition in schizophrenia: a selective review. *Schizophr Res* 70(2-3): 117-45.
- Ashkenas, J., J. Muschler and M. J. Bissell (1996). The extracellular matrix in epithelial biology: shared molecules and common themes in distant phyla. *Dev Biol* 180(2): 433-44.
- Bayer, S. A. and J. Altman (2008). The human brain during the early first trimester. Boca Raton, Fla.; London, CRC.
- Berdougo, E., H. Coleman, D. H. Lee, D. Y. Stainier and D. Yelon (2003). Mutation of weak atrium/atrial myosin heavy chain disrupts atrial function and influences ventricular morphogenesis in zebrafish. *Development* 130(24): 6121-9.
- Bergquist, H. and B. Kallen (1953). On the development of neuromeres to migration areas in the vertebrate cerebral tube. *Acta Anat (Basel)* 18(1): 65-73.
- Bernfield, M., S. D. Banerjee, J. E. Koda and A. C. Rapraeger (1984). Remodelling of the basement membrane: morphogenesis and maturation. *Ciba Found Symp* 108: 179-96.
- Bloom, S. L., D. D. Bloom, C. DellaNebbia, L. B. Martin, M. J. Lucas and D. M. Twickler (1997). The developmental outcome of children with antenatal mild isolated ventriculomegaly. *Obstet Gynecol* 90(1): 93-7.
- Bokel, C., A. Prokop and N. H. Brown (2005). Papillote and Piopio: Drosophila ZP-domain proteins required for cell adhesion to the apical extracellular matrix and microtubule organization. *J Cell Sci* 118(Pt 3): 633-42.
- Britto, J., D. Tannahill and R. Keynes (2002). A critical role for sonic hedgehog signaling in the early expansion of the developing brain. *Nat Neurosci* 5(2): 103-10.

- Bromley, B., F. D. Frigoletto, Jr. and B. R. Benacerraf (1991). Mild fetal lateral cerebral ventriculomegaly: clinical course and outcome. *Am J Obstet Gynecol* 164(3): 863-7.
- Brown, P. D., S. L. Davies, T. Speake and I. D. Millar (2004). Molecular mechanisms of cerebrospinal fluid production. *Neuroscience* 129(4): 957-70.
- Castellanos, F. X., J. N. Giedd, W. L. Marsh, S. D. Hamburger, A. C. Vaituzis, D. P. Dickstein, S. E. Sarfatti, Y. C. Vauss, J. W. Snell, N. Lange, D. Kaysen, A. L. Krain, G. F. Ritchie, J. C. Rajapakse and J. L. Rapoport (1996). Quantitative brain magnetic resonance imaging in attention-deficit hyperactivity disorder. *Arch Gen Psychiatry* 53(7): 607-16.
- Chenn, A. and S. K. McConnell (1995). Cleavage orientation and the asymmetric inheritance of Notch1 immunoreactivity in mammalian neurogenesis. *Cell* 82(4): 631-41.
- Chodobski, A. and J. Szmydynger-Chodobska (2001). Choroid plexus: target for polypeptides and site of their synthesis. *Microsc Res Tech* 52(1): 65-82.
- Cottingham, K. (2007). The complex composition of embryonic CSF. *J Proteome Res* 6(9): 3366.
- Coulombre, A. J. and J. L. Coulombre (1958). The role of mechanical factors in the brain morphogenesis. *Anat Rec* 130: 289-90.
- Crespo-Facorro, B., L. Barbadillo, J. M. Pelayo-Teran and J. M. Rodriguez-Sanchez (2007). Neuropsychological functioning and brain structure in schizophrenia. *Int Rev Psychiatry* 19(4): 325-36.
- Darnell, D. K. (2005). Anteroposterior and Dorsoventral Patterning. *Developmental Neurobiology* 4th Edition. M. Jacobson. New York, Kluwer Academic/Plenum Publishers.
- Davson, H. and M. B. Segal (1996). *Physiology of the CSF and blood-brain barriers*. Boca Raton, CRC Press.
- Denholm, B. and H. Skaer (2003). Tubulogenesis: a role for the apical extracellular matrix? *Curr Biol* 13(23): R909-11.
- Desmond, M. E. (1985). Reduced number of brain cells in so-called neural overgrowth. *Anat Rec* 212(2): 195-8.
- Desmond, M. E. and A. G. Jacobson (1977). Embryonic brain enlargement requires cerebrospinal fluid pressure. *Dev Biol* 57(1): 188-98.
- Desmond, M. E., M. L. Levitan and A. R. Haas (2005). Internal luminal pressure during early chick embryonic brain growth: descriptive and empirical observations. *Anat Rec A Discov Mol Cell Evol Biol* 285(2): 737-47.
- Dirks, P. (2004). Genetics of Hydrocephalus. *Pediatric Hydrocephalus*. G. Cinalli, W. J. Maixner and C. Sainte-Rose. Milano, Springer-Verlag: 1-18.

- Dziegielewska, K. M., J. Ek, M. D. Habgood and N. R. Saunders (2001). Development of the choroid plexus. *Microsc Res Tech* 52(1): 5-20.
- Elsen, G. E., L. Y. Choi, K. J. Millen, Y. Grinblat and V. E. Prince (2008). *Zic1* and *Zic4* regulate zebrafish roof plate specification and hindbrain ventricle morphogenesis. *Dev Biol* 314(2): 376-92.
- Emerich, D. F., S. J. Skinner, C. V. Borlongan, A. V. Vasconcellos and C. G. Thanos (2005). The choroid plexus in the rise, fall and repair of the brain. *Bioessays* 27(3): 262-74.
- Eto, M., J. A. Kirkbride and D. L. Brautigan (2005). Assembly of MYPT1 with protein phosphatase-1 in fibroblasts redirects localization and reorganizes the actin cytoskeleton. *Cell Motil Cytoskeleton* 62(2): 100-9.
- Finger, S. (1994). *Origins of neuroscience : a history of explorations into brain function*. New York, Oxford University Press.
- Frangou, S., E. Aylward, A. Warren, T. Sharma, P. Barta and G. Pearlson (1997). Small planum temporale volume in Down's syndrome: a volumetric MRI study. *Am J Psychiatry* 154(10): 1424-9.
- Fristrom, D. (1988). The cellular basis of epithelial morphogenesis. A review. *Tissue Cell* 20(5): 645-90.
- Gato, A., C. Martin, M. I. Alonso, C. Martinez-Alvarez and J. A. Moro (2001). Chondroitin sulphate proteoglycan is involved in lens vesicle morphogenesis in chick embryos. *Exp Eye Res* 73(4): 469-78.
- Gato, A., P. Martin, M. I. Alonso, C. Martin, M. A. Pulgar and J. A. Moro (2004). Analysis of cerebro-spinal fluid protein composition in early developmental stages in chick embryos. *J Exp Zool A Comp Exp Biol* 301(4): 280-9.
- Gato, A., J. A. Moro, M. I. Alonso, D. Bueno, A. De La Mano and C. Martin (2005). Embryonic cerebrospinal fluid regulates neuroepithelial survival, proliferation, and neurogenesis in chick embryos. *Anat Rec A Discov Mol Cell Evol Biol* 284(1): 475-84.
- Gato, A., J. A. Moro, M. I. Alonso, J. F. Pastor, J. J. Represa and E. Barbosa (1993). Chondroitin sulphate proteoglycan and embryonic brain enlargement in the chick. *Anat Embryol (Berl)* 188(1): 101-6.
- Geelen, J. A. and J. Langman (1977). Closure of the neural tube in the cephalic region of the mouse embryo. *Anat Rec* 189(4): 625-40.
- Gilmore, J. H., J. J. van Tol, H. Lewis Streicher, K. Williamson, S. B. Cohen, R. S. Greenwood, H. C. Charles, M. A. Kliewer, J. K. Whitt, S. G. Silva, B. S. Hertzberg and N. C. Chescheir (2001). Outcome in children with fetal mild ventriculomegaly: a case series. *Schizophr Res* 48(2-3): 219-26.
- Glucksmann, A. (1951). Cell deaths in normal vertebrate ontogeny. *Biol Rev* 26: 59-86.

- Gray, H. and C. D. Clemente (1985). *Anatomy of the human body*. Philadelphia, Lea & Febiger.
- Gullberg, D. and P. Ekblom (1995). Extracellular matrix and its receptors during development. *Int J Dev Biol* 39(5): 845-54.
- Hajdu, S. I. (2003). A note from history: discovery of the cerebrospinal fluid. *Ann Clin Lab Sci* 33(3): 334-6.
- Hardan, A. Y., N. J. Minshew, M. Mallikarjunn and M. S. Keshavan (2001). Brain volume in autism. *J Child Neurol* 16(6): 421-4.
- Harris, W. A. and V. Hartenstein (1991). Neuronal determination without cell division in *Xenopus* embryos. *Neuron* 6(4): 499-515.
- Haydar, T. F., C. Y. Kuan, R. A. Flavell and P. Rakic (1999). The role of cell death in regulating the size and shape of the mammalian forebrain. *Cereb Cortex* 9(6): 621-6.
- His, H. (1874). *Unsere körperform und das physiologische problem ihrer entstehung*. Translated Our body form and the physiological problem of their emergence. Leipzig, Vogel.
- Hjorth, J. T., R. M. Connor and B. Key (2002). Role of *hlx1* in zebrafish brain morphogenesis. *Int J Dev Biol* 46(4): 583-96.
- Homma, S., H. Yaginuma and R. W. Oppenheim (1994). Programmed cell death during the earliest stages of spinal cord development in the chick embryo: a possible means of early phenotypic selection. *J Comp Neurol* 345(3): 377-95.
- Hong, E. and R. Brewster (2006). N-cadherin is required for the polarized cell behaviors that drive neurulation in the zebrafish. *Development* 133(19): 3895-905.
- Hove, J. R., R. W. Koster, A. S. Forouhar, G. Acevedo-Bolton, S. E. Fraser and M. Gharib (2003). Intracardiac fluid forces are an essential epigenetic factor for embryonic cardiogenesis. *Nature* 421(6919): 172-7.
- Ibanez-Tallon, I., A. Pagenstecher, M. Fliegauf, H. Olbrich, A. Kispert, U. P. Ketelsen, A. North, N. Heintz and H. Omran (2004). Dysfunction of axonemal dynein heavy chain *Mdnah5* inhibits ependymal flow and reveals a novel mechanism for hydrocephalus formation. *Hum Mol Genet* 13(18): 2133-41.
- Inagaki, T., G. C. Schoenwolf and M. L. Walker (1997). Experimental model: change in the posterior fossa with surgically induced spina bifida aperta in mouse. *Pediatr Neurosurg* 26(4): 185-9.
- Jelinek, R. and T. Pexieder (1970). Pressure of the CSF and the morphogenesis of the CNS. I. Chick embryo. *Folia Morphol (Praha)* 18(2): 102-10.
- Jeste, D. V., J. E. Kleinman, S. G. Potkin, D. J. Luchins and D. R. Weinberger (1982). Ex uno multi: subtyping the schizophrenic syndrome. *Biol Psychiatry* 17(2): 199-222.

- Kahane, N. and C. Kalcheim (1998). Identification of early postmitotic cells in distinct embryonic sites and their possible roles in morphogenesis. *Cell Tissue Res* 294(2): 297-307.
- Kallen, B. (1955). Cell degeneration during normal ontogenesis of the rabbit brain. *J Anat* 89: 153-161.
- Keino, H., S. Masaki, Y. Kawarada and I. Naruse (1994). Apoptotic degeneration in the arhinencephalic brain of the mouse mutant Pdn/Pdn. *Brain Res Dev Brain Res* 78(2): 161-8.
- Kessel, R. G. (1960). The role of cell division in gastrulation of *Fundulus heteroclitus*. *Exp Cell Res* 20: 277-82.
- Kuida, K., T. S. Zheng, S. Na, C. Kuan, D. Yang, H. Karasuyama, P. Rakic and R. A. Flavell (1996). Decreased apoptosis in the brain and premature lethality in CPP32-deficient mice. *Nature* 384(6607): 368-72.
- Kurokawa, K., K. Nakamura, T. Sumiyoshi, H. Hagino, T. Yotsutsuji, I. Yamashita, M. Suzuki, M. Matsui and M. Kurachi (2000). Ventricular enlargement in schizophrenia spectrum patients with prodromal symptoms of obsessive-compulsive disorder. *Psychiatry Res* 99(2): 83-91.
- Lane, M. C., M. A. Koehl, F. Wilt and R. Keller (1993). A role for regulated secretion of apical extracellular matrix during epithelial invagination in the sea urchin. *Development* 117(3): 1049-60.
- Lecuit, T. and P. F. Lenne (2007). Cell surface mechanics and the control of cell shape, tissue patterns and morphogenesis. *Nat Rev Mol Cell Biol* 8(8): 633-44.
- Lehmann, G. L., S. A. Gradilone and R. A. Marinelli (2004). Aquaporin water channels in central nervous system. *Curr Neurovasc Res* 1(4): 293-303.
- Lele, Z., A. Folchert, M. Concha, G. J. Rauch, R. Geisler, F. Rosa, S. W. Wilson, M. Hammerschmidt and L. Bally-Cuif (2002). parachute/n-cadherin is required for morphogenesis and maintained integrity of the zebrafish neural tube. *Development* 129(14): 3281-94.
- Li, X. Y. and M. E. Desmond (1991). Modulation of Na<sup>+</sup>/K<sup>+</sup>ATPase pumps in the heart of the chick embryo influences brain expansion. *Soc Neurosci Abstr* 17: 21.16.
- Liu, M., S. J. Skinner, J. Xu, R. N. Han, A. K. Tanswell and M. Post (1992). Stimulation of fetal rat lung cell proliferation in vitro by mechanical stretch. *Am J Physiol* 263(3 Pt 1): L376-83.
- Lumsden, A. and R. Krumlauf (1996). Patterning the vertebrate neuraxis. *Science* 274(5290): 1109-15.

- Magendie, F. (1842). Recherches physiologique et clinique sur le liquide céphalorachidien ou cerebrospinal. Paris, Mequignon-Marvis.
- Malla, A. K., C. Mittal, M. Lee, D. J. Scholten, L. Assis and R. M. Norman (2002). Computed tomography of the brain morphology of patients with first-episode schizophrenic psychosis. *J Psychiatry Neurosci* 27(5): 350-8.
- Marsh, L., R. L. Suddath, N. Higgins and D. R. Weinberger (1994). Medial temporal lobe structures in schizophrenia: relationship of size to duration of illness. *Schizophr Res* 11(3): 225-38.
- Martin, C., D. Bueno, M. I. Alonso, J. A. Moro, S. Callejo, C. Parada, P. Martin, E. Carnicero and A. Gato (2006). FGF2 plays a key role in embryonic cerebrospinal fluid trophic properties over chick embryo neuroepithelial stem cells. *Dev Biol* 297(2): 402-16.
- Mashayekhi, F., C. E. Draper, C. M. Bannister, M. Pourghasem, P. J. Owen-Lynch and J. A. Miyan (2002). Deficient cortical development in the hydrocephalic Texas (H-Tx) rat: a role for CSF. *Brain* 125(Pt 8): 1859-74.
- Mashayekhi, F. and Z. Salehi (2006). The importance of cerebrospinal fluid on neural cell proliferation in developing chick cerebral cortex. *Eur J Neurol* 13(3): 266-72.
- McAllister, J. P., 2nd and P. Chovan (1998). Neonatal hydrocephalus. Mechanisms and consequences. *Neurosurg Clin N Am* 9(1): 73-93.
- Millen, J. W. and D. H. M. Woollam (1962). *The Anatomy of the Cerebrospinal Fluid*. London, Oxford University Press.
- Miner, J. H. and P. D. Yurchenco (2004). Laminin functions in tissue morphogenesis. *Annu Rev Cell Dev Biol* 20: 255-84.
- Miyan, J. A., M. Nabiyouni and M. Zendah (2003). Development of the brain: a vital role for cerebrospinal fluid. *Can J Physiol Pharmacol* 81(4): 317-28.
- Miyan, J. A., M. Zendah, F. Mashayekhi and P. J. Owen-Lynch (2006). Cerebrospinal fluid supports viability and proliferation of cortical cells in vitro, mirroring in vivo development. *Cerebrospinal Fluid Res* 3: 2.
- Moore, C. A. (2006). *Classification of Neural Tube Defects*. Neural tube defects : from origin to treatment. D. F. Wyszynski. Oxford ; New York, NY, Oxford University Press.
- Moro-Balbas, J. A., A. Gato, M. I. Alonso, P. Martin and A. de la Mano (2000). Basal lamina heparan sulphate proteoglycan is involved in otic placode invagination in chick embryos. *Anat Embryol (Berl)* 202(4): 333-43.
- Morriss-Kay, G. M. and B. Crutch (1982). Culture of rat embryos with beta-D-xyloside: evidence of a role for proteoglycans in neurulation. *J Anat* 134(Pt 3): 491-506.



- Moussian, B. and A. E. Uv (2005). An ancient control of epithelial barrier formation and wound healing. *Bioessays* 27(10): 987-90.
- Nelson, M. D., A. J. Saykin, L. A. Flashman and H. J. Riordan (1998). Hippocampal volume reduction in schizophrenia as assessed by magnetic resonance imaging: a meta-analytic study. *Arch Gen Psychiatry* 55(5): 433-40.
- Nicholson, C. (1999). Signals that go with the flow. *Trends Neurosci* 22(4): 143-5.
- Nopoulos, P., L. Richman, N. C. Andreasen, J. C. Murray and B. Schutte (2007). Abnormal brain structure in adults with Van der Woude syndrome. *Clin Genet* 71(6): 511-7.
- Nyholm, M. K., S. F. Wu, R. I. Dorsky and Y. Grinblat (2007). The zebrafish *zic2a-zic5* gene pair acts downstream of canonical Wnt signaling to control cell proliferation in the developing tectum. *Development* 134(4): 735-46.
- Ojeda, J. L. and S. Piedra (2000). Evidence of a new transitory extracellular structure within the developing rhombencephalic cavity. An ultrastructural and immunoelectron-microscopic study in the chick. *Anat Embryol (Berl)* 202(3): 257-64.
- O'Rahilly, R. and F. Muller (1994). Neurulation in the normal human embryo. *Ciba Found Symp* 181: 70-82; discussion 82-9.
- Owen-Lynch, P. J., C. E. Draper, F. Mashayekhi, C. M. Bannister and J. A. Miyan (2003). Defective cell cycle control underlies abnormal cortical development in the hydrocephalic Texas rat. *Brain* 126(Pt 3): 623-31.
- Pacheco, M. A., R. W. Marks, G. C. Schoenwolf and M. E. Desmond (1986). Quantification of the initial phases of rapid brain enlargement in the chick embryo. *Am J Anat* 175(4): 403-11.
- Panchision, D. M. and R. D. McKay (2002). The control of neural stem cells by morphogenic signals. *Curr Opin Genet Dev* 12(4): 478-87.
- Parada, C., A. Gato, M. Aparicio and D. Bueno (2006). Proteome analysis of chick embryonic cerebrospinal fluid. *Proteomics* 6(1): 312-20.
- Parada, C., A. Gato and D. Bueno (2005). Mammalian embryonic cerebrospinal fluid proteome has greater apolipoprotein and enzyme pattern complexity than the avian proteome. *J Proteome Res* 4(6): 2420-8.
- Parada, C., C. Martin, M. I. Alonso, J. A. Moro, D. Bueno and A. Gato (2005). Embryonic cerebrospinal fluid collaborates with the isthmic organizer to regulate mesencephalic gene expression. *J Neurosci Res* 82(3): 333-45.
- Patel, M. D., A. L. Filly, D. R. Hersh and R. B. Goldstein (1994). Isolated mild fetal cerebral ventriculomegaly: clinical course and outcome. *Radiology* 192(3): 759-64.

- Perez-Figares, J. M., A. J. Jimenez and E. M. Rodriguez (2001). Subcommissural organ, cerebrospinal fluid circulation, and hydrocephalus. *Microsc Res Tech* 52(5): 591-607.
- Pexieder, T. and R. Jelinek (1970). Pressure of the CSF and the morphogenesis of the CNS. II. Pressure necessary for normal development of brain vesicles. *Folia Morphol (Praha)* 18(2): 181-92.
- Philibert, R. A., P. Bohle, D. Secret, J. Deaderick, H. Sandhu, R. Crowe and D. W. Black (2007). The association of the HOPA(12bp) polymorphism with schizophrenia in the NIMH genetics initiative for schizophrenia sample. *Am J Med Genet B Neuropsychiatr Genet* 144(6): 743-7.
- Pilu, G., P. Falco, S. Gabrielli, A. Perolo, F. Sandri and L. Bovicelli (1999). The clinical significance of fetal isolated cerebral borderline ventriculomegaly: report of 31 cases and review of the literature. *Ultrasound Obstet Gynecol* 14(5): 320-6.
- Piven, J., S. Arndt, J. Bailey, S. Haverkamp, N. C. Andreasen and P. Palmer (1995). An MRI study of brain size in autism. *Am J Psychiatry* 152(8): 1145-9.
- Pourghasem, M., F. Mashayekhi, C. M. Bannister and J. Miyan (2001). Changes in the CSF fluid pathways in the developing rat fetus with early onset hydrocephalus. *Eur J Pediatr Surg* 11 Suppl 1: S10-3.
- Praetorius, J. (2007). Water and solute secretion by the choroid plexus. *Pflugers Arch* 454(1): 1-18.
- Prassopoulos, P., D. Cavouras and S. Golfopoulos (1996). Developmental changes in the posterior cranial fossa of children studied by CT. *Neuroradiology* 38(1): 80-3.
- Rehn, A. E. and S. M. Rees (2005). Investigating the neurodevelopmental hypothesis of schizophrenia. *Clin Exp Pharmacol Physiol* 32(9): 687-96.
- Reiss, A. L., M. T. Abrams, R. Greenlaw, L. Freund and M. B. Denckla (1995). Neurodevelopmental effects of the FMR-1 full mutation in humans. *Nat Med* 1(2): 159-67.
- Rubenstein, J. L., K. Shimamura, S. Martinez and L. Puelles (1998). Regionalization of the prosencephalic neural plate. *Annu Rev Neurosci* 21: 445-77.
- Salehi, Z. and F. Mashayekhi (2006). The role of cerebrospinal fluid on neural cell survival in the developing chick cerebral cortex: an in vivo study. *Eur J Neurol* 13(7): 760-4.
- Sanderson, T. L., J. J. Best, G. A. Doody, D. G. Owens and E. C. Johnstone (1999). Neuroanatomy of comorbid schizophrenia and learning disability: a controlled study. *Lancet* 354(9193): 1867-71.
- Sauer, F. C. (1936). The interkinetic migration of embryonic epithelial nuclei. *J Morphology* 60: 1-11.

- Sausedo, R. A., J. L. Smith and G. C. Schoenwolf (1997). Role of nonrandomly oriented cell division in shaping and bending of the neural plate. *J Comp Neurol* 381(4): 473-88.
- Sawamoto, K., H. Wichterle, O. Gonzalez-Perez, J. A. Cholfín, M. Yamada, N. Spassky, N. S. Murcia, J. M. Garcia-Verdugo, O. Marin, J. L. Rubenstein, M. Tessier-Lavigne, H. Okano and A. Alvarez-Buylla (2006). New neurons follow the flow of cerebrospinal fluid in the adult brain. *Science* 311(5761): 629-32.
- Schoenwolf, G. C. and I. S. Alvarez (1989). Roles of neuroepithelial cell rearrangement and division in shaping of the avian neural plate. *Development* 106(3): 427-39.
- Schoenwolf, G. C. and M. Fisher (1983). Analysis of the effects of *Streptomyces hyaluronidase* on formation of the neural tube. *J Embryol Exp Morphol* 73: 1-15.
- Segal, M. B. (2001). Transport of nutrients across the choroid plexus. *Microsc Res Tech* 52(1): 38-48.
- Shenton, M. E., C. C. Dickey, M. Frumin and R. W. McCarley (2001). A review of MRI findings in schizophrenia. *Schizophr Res* 49(1-2): 1-52.
- Speake, T., C. Whitwell, H. Kajita, A. Majid and P. D. Brown (2001). Mechanisms of CSF secretion by the choroid plexus. *Microsc Res Tech* 52(1): 49-59.
- Suddath, R. L., G. W. Christison, E. F. Torrey, M. F. Casanova and D. R. Weinberger (1990). Anatomical abnormalities in the brains of monozygotic twins discordant for schizophrenia. *N Engl J Med* 322(12): 789-94.
- Tannahill, D., L. W. Harris and R. Keynes (2005). Role of morphogens in brain growth. *J Neurobiol* 64(4): 367-75.
- Tanner, G. A., P. F. McQuillan, M. R. Maxwell, J. K. Keck and J. A. McAteer (1995). An in vitro test of the cell stretch-proliferation hypothesis of renal cyst enlargement. *J Am Soc Nephrol* 6(4): 1230-41.
- Tao, W. and E. Lai (1992). Telencephalon-restricted expression of BF-1, a new member of the HNF-3/fork head gene family, in the developing rat brain. *Neuron* 8(5): 957-66.
- Tao, Y., I. B. Black and E. DiCicco-Bloom (1997). In vivo neurogenesis is inhibited by neutralizing antibodies to basic fibroblast growth factor. *J Neurobiol* 33(3): 289-96.
- Tascioglu, A. O. and A. B. Tascioglu (2005). Ventricular anatomy: illustrations and concepts from antiquity to Renaissance. *Neuroanatomy* 4: 57-83.
- Thomaidou, D., M. C. Mione, J. F. Cavanagh and J. G. Parnavelas (1997). Apoptosis and its relation to the cell cycle in the developing cerebral cortex. *J Neurosci* 17(3): 1075-85.
- Trinh, L. A. and D. Y. Stainier (2004). Fibronectin regulates epithelial organization during myocardial migration in zebrafish. *Dev Cell* 6(3): 371-82.

- Tuckett, F. and G. M. Morriss-Kay (1985). The kinetic behaviour of the cranial neural epithelium during neurulation in the rat. *J Embryol Exp Morphol* 85: 111-9.
- Tuckett, F. and G. M. Morriss-Kay (1989). Heparitinase treatment of rat embryos during cranial neurulation. *Anat Embryol (Berl)* 180(4): 393-400.
- Vergani, P., A. Locatelli, N. Strobelt, M. Cavallone, P. Ceruti, G. Paterlini and A. Ghidini (1998). Clinical outcome of mild fetal ventriculomegaly. *Am J Obstet Gynecol* 178(2): 218-22.
- Vigh, B., M. J. Manzano e Silva, C. L. Frank, C. Vincze, S. J. Czirok, A. Szabo, A. Lukats and A. Szel (2004). The system of cerebrospinal fluid-contacting neurons. Its supposed role in the nonsynaptic signal transmission of the brain. *Histol Histopathol* 19(2): 607-28.
- Vigh, B. and I. Vigh-Teichmann (1998). Actual problems of the cerebrospinal fluid-contacting neurons. *Microsc Res Tech* 41(1): 57-83.
- Weiss, P. (1934). Secretory activity of the inner layer of the embryonic midbrain of the chick as revealed by tissue culture. *Anat Record* 58: 299-302.
- Whitaker, A. H., R. Van Rossem, J. F. Feldman, I. S. Schonfeld, J. A. Pinto-Martin, C. Tore, D. Shaffer and N. Paneth (1997). Psychiatric outcomes in low-birth-weight children at age 6 years: relation to neonatal cranial ultrasound abnormalities. *Arch Gen Psychiatry* 54(9): 847-56.
- Wright, I. C., S. Rabe-Hesketh, P. W. Woodruff, A. S. David, R. M. Murray and E. T. Bullmore (2000). Meta-analysis of regional brain volumes in schizophrenia. *Am J Psychiatry* 157(1): 16-25.
- Xia, D., J. T. Stull and K. E. Kamm (2005). Myosin phosphatase targeting subunit 1 affects cell migration by regulating myosin phosphorylation and actin assembly. *Exp Cell Res* 304(2): 506-17.
- Xuan, S., C. A. Baptista, G. Balas, W. Tao, V. C. Soares and E. Lai (1995). Winged helix transcription factor BF-1 is essential for the development of the cerebral hemispheres. *Neuron* 14(6): 1141-52.
- Yip, G. W., P. Ferretti and A. J. Copp (2002). Heparan sulphate proteoglycans and spinal neurulation in the mouse embryo. *Development* 129(9): 2109-19.
- Zappaterra, M. D., S. N. Lisgo, S. Lindsay, S. P. Gygi, C. A. Walsh and B. A. Ballif (2007). A comparative proteomic analysis of human and rat embryonic cerebrospinal fluid. *J Proteome Res* 6(9): 3537-48.
- Zhang, J., M. A. Williams and D. Rigamonti (2006). Genetics of human hydrocephalus. *J Neurol* 253(10): 1255-66.





# Chapter Two

## **The zebrafish as a model for analyzing neural tube defects**

### Portions Published As:

Laura Anne Lowery and Hazel Sive. Strategies of vertebrate neurulation and a re-evaluation of teleost neural tube formation. *Mech Development* 121(10), 2004.

Hakryul Jo\*, Laura Anne Lowery\*, Vincent Tropepe, and Hazel Sive. The zebrafish as a model for analyzing neural tube defects. In “Neural Tube Defects: From Origin to Treatment” (ed. D.F. Wyszynski) Oxford University Press, 2005. \*authors contributed equally, listed alphabetically

### Contributions:

VT wrote the sub-sections comparing adult zebrafish and human brain structure and describing the methods used in zebrafish research, and made Figure 2.1. HJ wrote the section on zebrafish neural tube defect mutants. LAL wrote all the sections related to neurulation and brain ventricle formation, and LAL made Figures 2.2 to 2.6. Together, HJ and LAL co-wrote all remaining sections and compiled Table 2.1. HS edited the manuscript.





## **INTRODUCTION**

In this review, we consider whether the zebrafish, *Danio rerio*, is a useful model system for uncovering the genetic and molecular basis for human neural tube defects (NTDs) and conclude that the zebrafish is an excellent NTD model. This conclusion is based on the similarities in development and structure of the human and zebrafish brain. It is also based on characteristics of the zebrafish as a model, including the accessibility of early embryos, and the ability to use both powerful genetic and molecular techniques to analyze the zebrafish nervous system.

Neural tube defects per se refer to incorrect formation of the neural tube – the precursor to the central nervous system. However, it is often not possible to determine whether neurological defects result from abnormalities in the specific morphogenetic processes by which the neural tube forms, or from other distinct processes that occur prior to neural tube formation (e.g. neural induction) or in the early stages after the tube has formed. We therefore define NTDs more broadly to include any abnormality of early nervous system formation. Most NTDs manifest at birth, however late onset neurological abnormalities may have their origins in early defects of the nervous system, and we include these in our definition.

## **ZEBRAFISH AS A MODEL SYSTEM**

The zebrafish boasts an impressive record for providing insight into mechanisms that control vertebrate patterning, organogenesis, physiology and behavior. Consequently, advancements in these areas of basic research have made a great impact on our understanding of human biology and medicine. In the next sections we provide a general overview of the zebrafish as an experimental model. We outline the many genetic, molecular and embryological techniques available to study this organism.

### **Basic features of zebrafish biology**

Several basic aspects of zebrafish biology make this organism an attractive genetic and molecular experimental model, particularly in the field of neural development. Fertilization of zebrafish eggs is external, which allows all embryonic stages to be easily observed. Zebrafish have a relatively short generation time of 3 months and clutch sizes from a single mating pair range between 100 and 200 embryos (Streisinger et al 1981; Kimmel 1989). Development is rapid, allowing rapid assays- for example the neural plate is present by 6-7 hours post-

fertilization (hpf) and the first neurons form by 16 hpf. An important feature of zebrafish embryos is their optical transparency, resulting from the sequestration of yolk granules into a single, giant yolk cell. Thus, easily accessible, transparent embryos offer an unprecedented advantage for visualizing molecular and cellular processes in live embryos. Furthermore, since zebrafish adults grow to an average size of only 3-4 cm, a rather large number of fish can be housed in a relatively small area and therefore the infrastructure and maintenance costs required for housing large numbers of animals for screening for morphological or behavioral mutants is far less than equivalent assays in mouse.

### **Genetic, molecular and embryological methods in zebrafish research**

Experiments using zebrafish have proven to be very useful for studying fundamental embryological processes, including morphogenesis, lineage specification (what cells will become), timing of commitment (when cells decide to assume a certain fate) and the mechanism by which cell fate is acquired. As a consequence of embryonic transparency, the fate of individual cells across a broad range of developmental stages can be clearly resolved *in vivo* by labeling cells with lineage tracers, such as fluorescent dyes. In addition, the external development of zebrafish embryos allows various embryological assays, including transplant and explant experiments (the latter developed in our lab) (Woo and Fraser 1997; Grinblat et al 1999), to determine the cell fate and the timing of tissue-specific inductive interactions.

Furthermore, assays have been developed to perform molecular “gain of function” experiments to determine what a gene can do, and “loss of function” experiments to determine what it normally does. For example, microinjection of synthetic mRNA (Hyatt and Ekker 1999) can be used during early embryogenesis in gain of function assays and to place genes in genetic pathways. More recently, chemically modified oligonucleotides (morpholinos), which target nascent mRNA and block translation, have been used in loss of function assays to ablate the function of specific genes, particularly early during development (Nasevicius and Ekker 2000).

The attractive biological and economical aspects of zebrafish inspired the first large-scale chemical mutagenesis screens in a vertebrate species (Driever et al 1996; Haffter et al 1996) resulting in approximately 2000 mutations in developmental genes affecting a wide range of tissues. Subsequent approaches have included viral insertional mutagenesis screens for developmental genes in diploid embryos (Amsterdam et al 1999), for neural pattern formation genes in haploid gynogenotes (Wiellette et al 2001), and for cocaine sensitivity based on

behavioral phenotypes (Darland and Dowling 2001). Although reverse genetics techniques (gene knock-outs) have not been established, an alternative approach (termed target-selected gene inactivation) to isolating fish with a desired gene mutation has been described (Wienholds et al 2002).

Together, these and other screens have generated thousands of mutant fish with a wide range of morphological, physiological and behavioral phenotypes, and many of which have been shown to recapitulate various human genetic and pathological conditions (for review see Barut and Zon 2000; Dodd et al 2000). Therefore, studying these mutants is likely to uncover the key aspects of pathogenic processes of complex human disorders, such as NTDs.

## **ONTOGENY OF THE ZEBRAFISH NERVOUS SYSTEM**

Specializations in brain structure and function exist between vertebrates with distinct adaptations to specific environments. Despite these differences, however, the development and organization of the nervous system as a whole is highly conserved among all vertebrates (Fig. 2.1). In the next sections we discuss formation of the neural tube and brain ventricles (Fig. 2.2), including a comparison between zebrafish and mammalian systems. We then compare zebrafish brain structure and function, highlighting the many similar organizational features that are shared with the mammalian brain. This discussion provides a conceptual foundation for our claim that the zebrafish is an excellent model of human brain ontogeny and neural tube defects.

### **Similar mechanisms underlying zebrafish and mammalian neural tube formation**

During the formation of the vertebrate nervous system, the initial neuroectoderm must form a tube that will become the future brain and spinal cord. This process is called neurulation. Later, the initial neural tube expands in several places to form the brain ventricles. There are many possible events during neurulation that could be perturbed, leading to neural tube defects of varying severities.

The vertebrate neural tube develops by two distinct mechanisms. Anteriorly, in the brain and future trunk (cervicothoracic) region, “primary neurulation” occurs, where an epithelial sheet rolls or bends into a tube. Posteriorly, in the future lumbar and tail region, the neural tube forms by “secondary neurulation,” where a mesenchymal cell population condenses to form a solid rod that undergoes transformation to an epithelial tube. Teleost neurulation has been described as different from that of other vertebrates. This is principally because the teleost trunk

neural tube initially forms a solid rod (the neural keel) that later develops a lumen. This process has also been termed “secondary neurulation.” However, this description is not accurate since the teleost neural tube derives from an epithelial sheet that folds. This best fits the description of primary neurulation. It has also been suggested that teleost neurulation is primitive, however, both primary and secondary neurulation are found in groups with a more ancient origin than the teleosts. The similarity between neurulation in teleosts and other vertebrates indicates that this group includes viable models (such as the zebrafish) for understanding human neural tube development.

### **The neural tube forms by joining two distinct tubes that form by different mechanisms**

The vertebrate neural tube forms from two tubes that develop independently, by distinct morphogenetic and molecular processes. An anterior (or primary) tube extends from the brain to the cervicothoracic region, and a more posterior tube develops later in the lumbar and tail region (Fig. 2.3A). The anterior tube forms via “primary neurulation” from an epithelial cell sheet (the neural plate) (Colas and Schoenwolf 2001). In contrast, the posterior tube forms from the tail bud via “secondary neurulation” in which there is a transformation of a solid rod of mesenchymal cells to an epithelial tube (Criley 1969; Griffith et al 1992). Key to the distinction between primary and secondary neurulation is the definition of epithelial and mesenchymal cell populations. We define epithelial tissues as an organized and contiguous sheet of cells held together by junctional complexes, while we define mesenchymal tissue as a loosely associated group of cells.

For both the primary and secondary neural tubes, closure of the tube does not occur synchronously along the anteroposterior axis, but generally progresses from anterior to posterior. Furthermore, the precise position to which the anterior tube extends is variable in different organisms, and a region of transition between anterior and posterior neural tubes is often apparent. For example, in chick, there is an overlap region where primary neurulation occurs more dorsally and secondary neurulation more ventrally within the same neural tube. Thus, in this region, there are two neural tubes that eventually coalesce into a single tube (Schoenwolf and Delongo 1980). As will be discussed in the following sections, primary and secondary neurulation involve distinct morphogenetic and molecular mechanisms.

## Primary neurulation

The key characteristic of primary neurulation is that it occurs from a preexisting epithelial substrate, which folds, rolls, or bends into a tube. The term “primary” refers to the tissues involved in this process as derived from the three germ layers of “primary body development” (Holmdahl 1932, see Nakao and Ishizawa 1984). Neurulation of the anterior neural tube has been carefully described in frog, chick, mouse, and rabbit (Davidson and Keller 1999; Morriss-Kay et al 1994; Peeters et al 1998; Smith and Schoenwolf 1991), and while slightly different in each of these animals, the basic steps which are specific to primary neurulation are conserved in all these species (Fig. 2.4). These include columnarization of the ectoderm to form the neural plate, thickening of the edges of the neural plate to form the neural folds, convergent extension of the neural plate that assists bending to form the neural groove and also elongates the future neural tube, and closure of the groove to form the neural tube (Fig. 2.3B) (Colas and Schoenwolf 2001).

While primary neurulation always starts with an epithelial substrate and ends with a tube, some of the steps involved can be quite variable between vertebrates and within one species at different levels of the anterior neural tube (Fig. 2.4). This variability is apparent at the point when an “open” neural tube has formed, that is, one that is partially rolled up but where the folds have not yet fused. In order to form the open neural tube, there can be a smooth rolling of the epithelium (Fig. 2.4A). This occurs in the brain of the frog *Xenopus* and also in part of the mouse spinal cord. Another strategy to form the open neural tube is a bending of the epithelium at defined “hinge points,” where cells become wedge shaped (Fig. 2.4B,C). Even in a single species it has been shown that the neural plate folds or rolls differently depending on anteroposterior location and developmental stage (Shum and Copp 1996). For example, in mouse, at the 12 somite stage in the region of the posterior neuropore, one median acute bend or “hinge point” is apparent, with the two sides of the neural plate elevating and simply folding up, leaving a slit-like lumen. Later, at the 20 somite stage, in the posterior neuropore region, there are two additional dorsolateral hinge points. Finally, at the 29 somite stage, the neuroepithelium at the posterior neuropore region rolls into a round tube, with no obvious hinge points (Shum and Copp 1996). Similarly, in the chick, along the length of the anterior neural tube, a median hinge point is located in the ventral midline (overlying the notochord), while in the brain region, two additional dorsolateral hinge points develop. As a result of the different movements involved in

tube closure, the appearance of the initial neural tube cavity can be quite variable (Fig. 2.4). The lumen of the chick brain is large and diamond shaped, whereas in the spinal cord region, it is slit-like (Smith and Schoenwolf 1991). In *Xenopus*, the lumen of the spinal cord is initially occluded, and subsequently opens from ventral to dorsal (Davidson and Keller 1999). Finally, the open neural tube may not have a medial opening but may be a solid rod of cells, the neural “keel” (Fig. 2.4D). This is apparent in *Xenopus* (Davidson and Keller 1999), and, as will be discussed below, in the teleosts. Despite these variations, the underlying morphogenetic movements involved in the reshaping of the neuroepithelium are thought to be conserved.

A large number of candidate genes and molecules have been implicated in defects of primary neurulation and include those that regulate cell adhesion and cytoskeletal dynamics (see reviews Copp et al 2003; and Colas and Schoenwolf 2001). Although it is not yet clear whether these candidate genes directly affect the neural tube or act more indirectly, recent studies have begun to address the molecular mechanisms involved. For example, the actin binding protein Shroom regulates apical constriction and is required for hinge point formation during neural tube closure in *Xenopus* (Haigo et al 2003). The adhesion signaling molecule p190 RhoGAP may also play a role in neural fold closure, for its loss disrupts the apical constriction of neuroepithelial cells (Brouns et al 2000). The non-canonical Wnt pathway plays a key role in the convergent extension movements of the neural plate (Wallingford and Harland 2002; Wiggan and Hamel 2002). Mutation of the cell membrane signaling molecule ephrin A5 prevents the fusion of the neural folds at the dorsal midline, but does not effect their elevation or apposition (Holmberg et al 2000). Moreover, a wide variety of teratogenic agents disrupt cranial but not cervicothoracic primary neural tube closure, showing that primary neurulation may not be regulated uniformly along the neural tube (Copp et al 1990; Shum and Copp 1996).

### **Secondary neurulation**

In contrast to primary neurulation, the term “secondary neurulation” refers to the “secondary body development” that occurs in vertebrates, in which the posterior or tail region of the organism develops from tissue of the undifferentiated tail bud after more anterior regions have developed (Griffith et al 1992; Holmdahl 1932, see Nakao and Ishizawa 1984; Schoenwolf and Delongo 1980). The unifying concept underlying secondary neurulation is that the posterior neural tube derives from a mesenchymal population of cells, rather than an epithelial population as in primary neurulation. These mesenchymal cells coalesce into a rod (the medullary cord) that

transforms to an epithelium (the presumptive neuroepithelium) and a lumen develops to form a tube. Thus, during secondary neurulation, there is no epithelial neural plate intermediary equivalent to the case in primary neurulation (Fig. 2.3B).

As in primary neurulation, there are a number of variations to secondary neurulation in different species or in the same species at different stages (Fig. 2.5). In mouse, after medullary cord formation, the secondary neural tube forms by two mechanisms. In day 9.5-10 embryos, the entire mesenchymal region undergoing neurulation becomes epithelial, with later appearance of a lumen (Fig. 2.5A). In older embryos (day 11-12), only the dorsal part of the medullary cord becomes an epithelium initially- the medullary “plate” (Fig. 2.5B). Mesenchymal cells are recruited from the edges of the plate and added to the epithelium to eventually form a tube (Schoenwolf 1984). In chick, formation of the medullary cord is followed by a separation into two cell populations: the central cells remain mesenchymal, while the peripheral cells become epithelial (Fig. 2.5C). Cavitation occurs at the boundaries between these two populations, where small cavities of varied size and shape form and coalesce into a single, central lumen (Catala et al 1995; Schoenwolf and Delongo 1980).

It is likely that the molecular mechanisms underlying secondary neurulation are distinct from those involved in primary neurulation, however few candidate genes implicated in secondary neurulation have been identified. One example of a candidate gene is N-CAM. Whereas the form of N-CAM with a low sialic acid content has been implicated in primary neurulation, the highly sialated form has been suggested to be important for the mesenchymal to epithelial transition of secondary neurulation (Griffith et al 1992; Sunshine et al 1987). The secreted protein, midkine, has been implicated in the mesenchymal to epithelial transition during formation of the chick secondary neural tube (Griffith 1997). Mesenchymal to epithelial transitions also occur during formation of other hollow structures. For example, in the early mouse embryo, this process transforms the solid embryonic ectoderm into the columnar epithelium surrounding the proamniotic cavity. BMP signaling plays a role in this conversion process (Coucouvanis and Martin 1995; Coucouvanis and Martin 1999) and it is plausible that the molecular mechanisms underlying formation of a proamniotic cavity and secondary neural tube are conserved.

## **Mechanism of zebrafish trunk neurulation**

Descriptions of teleost neurulation have been confusing. This is primarily because in the brain and trunk region, the zebrafish neurectoderm first forms a solid rod, the neural keel, and only later forms a tube with a lumen (Fig. 2.4D). Initially, the neural keel was thought to be a mass of mesenchymal cells, and neurulation therefore equivalent to the secondary process that occurs in the tailbud of most animal groups (von Kupffer 1890, see Reichenbach et al 1990). More careful examination using several model systems, including the zebrafish, showed that this is not correct (Geldmacher-Voss et al 2003; Kingsbury 1932; Miyayama and Fujimoto 1977; Reichenbach et al 1990; Strahle and Blader 1994). However, teleost neurulation has continued to be termed secondary (Geldmacher-Voss et al 2003; Handrigan 2003; Kimmel et al 1995; Papan and Campos-Ortega 1994). Given the variations of primary and secondary neurulation in other groups, we re-evaluated the literature and the mechanism of teleost neurulation.

In the zebrafish, which we consider as a teleost model, only the spinal cord (anterior trunk region) has been carefully examined (Fig. 2.6). Several studies have analyzed zebrafish neurulation using fate mapping, time-course serial sectioning, and confocal time-lapse imaging of neurulation movements *in vivo* (Geldmacher-Voss et al 2003; Kimmel et al 1994; Papan and Campos-Ortega 1994; Papan and Campos-Ortega 1999; Schmitz et al 1993). We consider the events of zebrafish neurulation in developmental order, and highlight aspects of this process that have led to its designation as different from that of neurulation in other vertebrates.

As in other vertebrates, an early step in zebrafish neurulation is formation of the neural plate. It is not clear whether cells in the zebrafish neural plate are connected by tight junctions, as expected for an epithelium. Indeed, the zebrafish neural plate does not show polarized expression of ZO-1, a molecule that can be associated with tight junctions and/or adherens junctions, but is not an unequivocal epithelial marker (Geldmacher-Voss et al 2003; Aaku-Saraste et al 1996). Expression of occludin, which does always indicate the presence of tight junctions, and is present in the neuroepithelium of other vertebrate embryos undergoing neurulation (Aaku-Saraste et al 1996), has not been analyzed in zebrafish. However, morphologically the zebrafish neural plate is clearly an epithelium in the sense of being a cohesive sheet of cells which moves in an ordered manner. In particular, the lateral edges of the neural plate thicken and neural plate cells appear to “sink” and form the neural keel, which is a solid mass or rod of cells (Schmitz et al 1993). Recent data show that even at the neural keel



stage, the midline is distinct (Geldmacher-Voss et al 2003), with a pseudostratified columnar epithelium on either side. Subsequently, the lumen of the neural tube opens, beginning ventrally and moving dorsally (Schmitz et al 1993). The initial epithelial nature of the zebrafish neural plate suggests that zebrafish trunk neurulation occurs by a primary neurulation mode. It has been argued that there is no obvious “rolling up” of the zebrafish neural plate, for there is no obvious elevation of neural folds, and instead the neural plate seems to sink down into the embryo. However, fate mapping indicates that the movements of the neural plate are equivalent in teleosts and other vertebrates, where initial mediolateral cell position corresponds to later dorsoventral position in the neural tube (Fig. 2.6) (Papan and Campos-Ortega 1994). Even more convincingly, confocal time-lapse imaging *in vivo* shows a clear rolling of the neural plate, characteristic of primary neurulation (Geldmacher-Voss et al 2003). Consistently, in the teleost *Chiclasoma nigrofasciatum*, a dorsal median neural groove is visible once the covering enveloping layer is removed from the embryo (Reichenbach et al 1990). Thus, both the initial cell type and cell movements of the zebrafish are characteristic of primary neurulation.

Another phenomenon that has suggested teleost neurulation is unusual is the ability of daughter cells to cross the midline of the zebrafish neural keel, prior to lumen formation. Some cells have been shown to cross the midline of the *Xenopus* and chick neural tubes soon after closure (Collazo et al 1993; Schoenwolf 2003), although not at the frequency which occurs in zebrafish (Geldmacher-Voss et al 2003). The ability of cells to cross the midline and the reorganization of the neural keel cells as the lumen opens raises the question of whether neural keel cells have mesenchymal character that allows them to move relative to one another. Although cells can cross the midline, the midline is always apparent, emphasizing that the neural keel is not simply a mass of disorganized mesenchymal cells. The distinction between mesenchymal and epithelial cells is fluid as these tissue states are interconvertible. However, rather than being discrete states, epithelial and mesenchymal tissues may form a continuum of cell states, where epithelial cell populations may have some mesenchymal character, and vice versa. This may be particularly true where an epithelium is undergoing cell rearrangement. For example, in the *Xenopus* neural tube during convergent extension, the epithelium transiently consists of bipolar protrusive cells that appear much more “mesenchymal” than epithelial (Davidson and Keller 1999). Similarly, in the zebrafish neural keel, the neuroepithelium may comprise cells less tightly associated than some epithelia but much more organized than a typical mesenchymal tissue.

Perhaps the major point of confusion with regard to teleost neurulation is the opening of a lumen in the neural keel after formation of this solid tube. This is the phenomenon that has led to the designation of teleost trunk neurulation as secondary (Kimmel et al 1995; Papan and Campos-Ortega 1994). However, this is not an accurate use of the term “secondary neurulation,” since the initial substrate for the trunk neural tube is epithelial and not mesenchymal. Lumen formation after initial primary neurulation is not a teleost-specific phenomenon, and in both chick and *Xenopus*, the trunk spinal cord is initially occluded, with a lumen developing after neural tube closure. Indeed, the developing *Xenopus* spinal cord appears similar to the zebrafish neural keel (Davidson and Keller 1999). Although it has not yet been investigated, it is likely that true secondary neurulation occurs in the tailbud region of the zebrafish as in other vertebrates.

In conclusion, assessment of the literature has allowed us to understand the range of variation that is found in primary neurulation. This assessment in combination with experiments in the zebrafish strongly suggests that in the trunk region of zebrafish, the neural tube forms by a primary neurulation mechanism.

### **Evolutionary considerations: is zebrafish neurulation primitive?**

The distinction between primary and secondary neurulation is particularly apparent in the stages that bracket formation of the neural tube. For example, prior to neural tube formation, primary neurulation utilizes a flat neural plate whereas secondary neurulation begins with a mesenchymal population of cells which condense. These early stages may best serve as comparisons for evolutionary conservation. As discussed above, details of the precise movements in different vertebrates show a variety of solutions to the problem of changing the sheet of neural plate cells into a tube, and these details may be less helpful in evolutionary comparisons.

Previous descriptions of zebrafish trunk neurulation have suggested that this process is more primitive than neurulation in “higher” vertebrates. This does not appear to be true, since organisms from more primitive lineages clearly undergo both primary and secondary neurulation. For example, the sturgeon, from a more ancient lineage than zebrafish, generates the neural tube by a direct folding of neural plate epithelium (Ginsburg and Dettlaff 1991). The myxinoids (hagfish) and elasmobranches (sharks and rays), from even more primitive lineages, use primary neurulation in the brain and spinal cord region and secondary neurulation in the tail

(Nakao and Ishizawa 1984). Amphioxus and ascidians (both protochordates) roll up an epithelial neural plate (Conklin 1932; Holland et al 1996; Swalla 1993), characteristic of primary neurulation.

Thus, evolutionarily, teleosts are flanked by more ancient and more modern lineages that employ primary neurulation anteriorly and secondary neurulation posteriorly. This is consistent with conclusions that teleost trunk neurulation should be described as primary.

## **ZEBRAFISH AS A MODEL FOR BRAIN VENTRICLE FORMATION**

After neurulation is complete, the anterior region of the neural tube dilates in three specific locations to form the future forebrain, midbrain, and hindbrain ventricles (Fig. 2.2). During this process, the neural tube tissue must undergo proper morphogenesis to result in the positionally-correct three-dimensional structure, which is thought to be necessary for normal brain function.

Like neurulation defects, defects in brain ventricle formation can have drastic effects on brain development and survival. Hydrocephaly, a defect in which increased cerebrospinal fluid and pressure within the brain leads to large increases in the brain ventricle space, is one of the most common brain ventricle defects in humans, and it can lead to death without treatment (Machado et al 1991). Chiari malformation is a developmental defect in which part of the cerebellum protrudes into the spinal canal, due to abnormal neurulation and subsequent ventricular abnormalities. This can lead to compression of the cerebellum and other regions, and a variety of neurological defects and nervous system damage can result (McLone and Knepper 1989). In addition, a number of mental health disorders such as autism and schizophrenia display brain ventricle abnormalities (Hardan et al 2001; Kurokawa et al 2000). Although it is unknown whether the ventricular defects are primary or secondary to the mental health disorders, it is clear that more needs to be learned regarding how brain ventricle development is controlled at the genetic and molecular level. This has been difficult due to lack of a good model system for studying brain ventricle morphogenesis.

Morphologically, brain ventricle development is highly conserved in all vertebrates from fish to humans. In previous mutagenesis screens, zebrafish mutants in brain ventricle formation were identified (Jiang et al 1996; Schier et al 1996). We have initiated a project to analyze brain ventricle formation using these and newly defined mutant lines (Table 2.1). This is likely to

uncover mechanisms by which defects in ventricle formation arise, and provide a means to interpret human neural tube defects that involve brain ventricle abnormalities.

### **Conserved structure of the adult zebrafish and human brain**

The conservation of overall adult brain structure in zebrafish, humans and other vertebrates is also apparent after neural tube closure. As the simple neural tube structure takes shape and begins to grow, it forms a series of transverse bulges and constrictions giving rise to a segmented appearance, which in zebrafish occurs at ~ 16 hours post-fertilization (Kimmel et al 1995). Collectively, the segments are called neuromeres. This neuroanatomical topography was recognized in several vertebrate species well over a century ago, and today remains as one of the most striking examples of conserved morphology in the developing vertebrate brain. Interestingly, pioneering studies in zebrafish were, in part, the first studies to demonstrate more convincingly that in the hindbrain and spinal cord, a serially repeated pattern of restricted neurogenesis existed (Eisen et al 1986; Metcalfe et al 1986; Hanneman et al 1988; Trevarrow et al 1990). Analyses of early differentiation and axonogenesis (Chitnis and Kuwada 1990; Wilson et al 1990; Ross et al 1992), cell proliferation (Wullimann and Puelles 1999) and early regionalized gene expression patterns (Hauptmann and Gerster 2000; Hauptmann et al 2002a) have firmly established that the formation of the zebrafish forebrain, midbrain and hindbrain follow the principles of the neuromeric model (reviewed in Puelles 1995; Rubenstein et al 1998). Thus, the neuromeric organization of the neural tube defines the fundamental subdivisions of the embryonic brain in all vertebrates and prefigures the major functional subdivisions of the adult brain (Fig. 2.1).

### **Functional conservation of the zebrafish nervous system**

There are differences in neuroanatomy between teleosts and mammals. Perhaps the most obvious difference is that the teleost telencephalon is rather small relative to the rest of the brain and lacks the characteristic structure of the cerebral cortex, with its highly folded appearance (resulting in the formation of gyri and sulci). Clearly, these specializations that are found in mammals reflect the specializations in the function of the telencephalon, especially in humans. Despite these differences, all teleosts retain the basic neural circuitry for sensory and motor functions that are characteristic of a vertebrate nervous system.

Zebrafish possess all of the classical sense modalities (vision, olfaction, taste, tactile, balance and hearing) and their sensory pathways share an overall homology with humans. For example, axons of sensory neurons expressing the same odorant receptor in the nasal epithelium project to a common glomerulus in the olfactory bulb (Byrd et al 1996), a phenomenon that occurs in the mammalian primary olfactory pathway (Mombaerts 2001). Similar to the mammalian olfactory system, neurons in the olfactory bulb project to secondary and tertiary targets in the telencephalon and diencephalon (Wullimann 1998). In the visual system, the topographical projection of the retinotectal pathway for visual processing is highly conserved among all vertebrates. Interestingly, second order motion perception, which in humans involves processing of relatively complex visual information in the visual cortex, can be observed in larval zebrafish, suggesting that higher-level cortical-like visual processing capacities are similarly inherent in teleosts (Orger et al 2000). Although the neuroanatomical substrates for this complex behavior are currently unresolved, the ability to test this behavior in the zebrafish may facilitate the discovery of novel genetic pathways that are involved in mediating the function of this visual related cognitive process. With some exceptions, the descending motor and premotor pathways in the teleostean brain are conserved with that of mammals, including the reticulospinal, rubrospinal and vestibulospinal projections, as well as the projections from the midbrain tectum and cerebellum to brainstem targets (Butler and Hodos 1996).

Evidence for neuroanatomical and functional homology of integrative brain regions, such as the cerebellum, tectum and telencephalon, between teleosts and other vertebrates offers a broader perspective of the evolution of cognitive processing. For example, spatial memory in mammals is critically dependent on the hippocampus (Eichenbaum et al 1999), a structure that is developmentally derived from the medial part of the dorsal telencephalon (the medial pallium). In mammals, the central lumen of the telencephalic neural tube expands to form the lateral ventricles as the dorsal part of the neural tube bulges out in a process of evagination. However, in teleosts the telencephalon is everted such that the roof of the neural tube over the telencephalic central lumen thins and elongates causing the dorsal part of the tube on each side to bend back on itself. Thus, the lateral pallium of teleosts appears to be structurally homologous to the mammalian hippocampus – medial pallium (Butler 2000; Rodríguez et al 2002a). Although the theory of simple eversion accounting for the peculiar anatomy of the teleostean telencephalon is still controversial (Bradford 1995), evidence from goldfish (a cyprinid cousin to the zebrafish) suggests that lesions of the lateral pallium do in fact selectively impair spatial

memory representations, like hippocampal lesions in mammals (Rodríguez et al 2002b). This is a striking example of functional conservation between the brains of teleosts and mammals despite a rather distinct process of telencephalic morphogenesis.

These observations indicate that the neural circuitry and function of the teleost and mammalian nervous system are highly conserved. Thus, identifying the molecular and cellular determinants that govern the formation of the nervous system in zebrafish will provide us with a fundamental understanding of human brain formation, and the mechanisms by which NTDs have devastating consequences on nervous system function (see Tropepe and Sive 2003).

## **LESSONS FROM ZEBRAFISH MUTANTS**

The formation of neural tube is a complex cellular process subjected to perturbation by many genetic components, thus any defects at the cellular level, including aberrant cell death, proliferation, differentiation, migration, and adhesion during neurulation may result in NTDs. Various studies in animal models, mouse knockouts in particular, have proven useful for revealing the critical steps and providing candidate genes for human NTDs. However, these mouse models have three major obstacles that discourage systematic investigations for identifying the genetic and cellular pathways underlying human NTDs. First, in most cases, the precise molecular mechanisms by which the loss of a particular gene function leads to NTDs are not known. Second, the intrauterine development of mouse embryos prevents analysis of the developmental time course of NTDs. Third, many NTDs may be caused by mutations in multiple genes (Colas and Schoenwolf 2001; Harris and Juriloff 1997; Juriloff and Harris 2000), and their phenotypic characterization may therefore require compound genetic analyses, such as identification of genetic modifiers. A relatively small litter size and expensive housing costs make it difficult to carry out such analyses in mouse. In the next sections, we discuss the advantages of using zebrafish as a complementary genetic model system to study NTDs. We first discuss results of zebrafish mutant screens that have yielded brain mutants, highlighting those that may include NTD candidates. We then discuss feasible experimental strategies in zebrafish that could help elucidate the molecular mechanisms underlying human NTDs.

### **Zebrafish mutants that include some with putative NTDs**

Forward genetic screens in zebrafish have yielded a large number of mutants reflecting the key aspects of various developmental problems. In Table 2.1, we list zebrafish mutants

defective in brain morphology and neural function. We group these mutants into several categories according to cellular function of the corresponding genes. These categories include mutants defective in major signaling pathways and those that alter cell polarity and adhesion, neuroectoderm specification and patterning, development of the neural crest and neurogenesis. Importantly, some of these mutants encode zebrafish orthologs of mouse NTD genes allowing phenotypes to be compared between species (Table 2.1). Many other zebrafish mutants with putative NTDs have been isolated, for which the corresponding gene has not been identified (Schier et al 1996; Schilling et al 1996).

One interesting example that lends itself to comparison is the mouse *loop-tail* mutant, which corresponds to a homolog of *Drosophila* Strabismus (Kibar et al 2001a; Kibar et al 2001b; Wolff and Rubin 1998), a PDZ domain transmembrane protein involved in the planar cell polarity (PCP) pathway. The *loop-tail* mutant exhibits craniorachischisis, a failure of neural tube closure from midbrain to lower spinal cord. However, the mechanisms by which loss of gene function gives rise to neural tube defects has not been investigated, partly due to relatively inaccessible nature of mouse embryos. Recently, the zebrafish *trilobite* mutant has been cloned and the gene encodes a fish ortholog of this protein (Jessen et al 2002). In contrast to mouse, analysis of the fish mutant was relatively simple, and by employing cell transplantation coupled with time-lapse imaging, has revealed the mechanism by which the *trilobite* gene product controls cell shape changes and movements during gastrulation and neuronal migration (Jessen et al 2002).

Further emphasizing the importance of the PCP pathway in vertebrate neurulation, disruption of mouse orthologs of other fly PCP components also lead to neural tube defects. Furthermore, genetic interactions between these components have been shown (Curtin et al 2003; Hamblet et al 2002; Kibar et al 2001b; Montcouquiol et al 2003; Murdoch et al 2003). Similarly, zebrafish mutants defective in PCP components produce varying degrees of brain and craniofacial defects (Heisenberg et al 2000; Jessen et al 2002; Rauch et al 1997; Topczewski et al 2001), and these phenotypes are enhanced by inhibition of other PCP components (Carreira-Barbosa et al 2003; Topczewski et al 2001).

Another appealing attribute of zebrafish is the ability to isolate multiple mutant alleles, allowing detailed analyses of gene dosage and structure-function relationships leading to brain phenotypes. For example, the zebrafish *foggy* encodes transcription elongation factor Spt5, and three alleles (*m806*, *sk8*, and *s30*) have been reported (Guo et al 2000; Keegan et al 2002). The *m806* allele contains a mis-sense mutation (V1012D), still leaving significant aspects of Spt5

function, whereas both the *sk8* and *s30* alleles are thought to be null. The differences in nature of molecular lesion correlate with the phenotypic strength of mutant alleles: m806 exhibits neurogenesis defects without significant abnormalities in brain shape (Guo et al 2000) whereas both *sk8* and *s30* manifest some degrees of the altered brain morphology (Keegan et al 2002). In a striking example, 12 alleles of zebrafish *grumpy* and 19 alleles of zebrafish *sleepy* mutants have been isolated, encoding laminin beta 1 and gamma 1, respectively, components of basal laminae (see <http://zfin.org>).

Relative inexpensive maintenance of zebrafish mutant stocks and a large clutch size facilitate compound genetic analyses to determine genetic interactions (i.e. epistatic, synergistic, or antagonistic relationships) between NTD genes. For example, the zebrafish *knypek*, encoding a heparan sulfate proteoglycan, shows craniofacial defects with no cyclopic phenotype (Topczewski et al 2001). Double mutants of *knypek* and *silberlick*, which encodes wnt 11 (that is involved in PCP signaling (Heisenberg et al 2000)), manifests strong cyclopic phenotypes, identifying Kny as a component of PCP pathway. Such analyses can either be performed by making "classical" double mutants or by using reverse genetics tools, such as antisense morpholino oligomers.

Epithelial cells display apical-basal cell polarization, by a mechanism conserved between vertebrates and invertebrates. In fly, localization of apical determinants, such as Crumb, is controlled by Scribble (Bilder and Perrimon 2000). A mouse ortholog of fly Scribble is a component of PCP (Montcouquiol et al 2003), indicating a direct link between apical-basal polarization and PCP pathways. The zebrafish mutants in apical-basal polarity have been isolated and include *nagie oko*, *heart and soul*, and *parachute (glass onion)* (Horne-Badovinac et al 2001; Lele et al 2002; Malicki et al 2003; Peterson et al 2001; Wei and Malicki 2002a). These mutants exhibit a certain degree of neural tube defects, suggesting that genetic components involved in apical-basal cell polarity are candidates for NTDs and phenotypic analyses of these mutants may provide new insights into cellular defects of NTDs.

### **Strategies to study neural tube defects in zebrafish**

What experimental strategies in zebrafish would help better understand the molecular etiology of human NTDs? First, a "candidate" gene approach can be employed in the zebrafish, where function of genes correlating with human NTD candidates is analyzed in the fish. Reverse genetic approaches will be very useful in this regard, as it is possible to generate partial loss of



function phenotypes that may correspond to the situation in the human NTD. Partial loss of function phenotypes can be generated by injecting varying amounts of antisense morpholino or via target-selected gene inactivation (Wienholds et al 2002; Wienholds et al 2003), which allows isolation of multiple alleles of a single gene that may display different severity. Multiple alleles will also facilitate structure/function analysis of a given protein.

NTD phenotypes could be due either to direct effects of a given gene on the neural tube or to secondary effects of its early function. In situ hybridization and immunocytochemistry to determine where the protein is expressed is clearly essential. However, for ubiquitously expressed gene products, asking when the gene product is required will help narrow down the target of the gene. Temporally controlled expression can be effected using a heat-shock-inducible promoter driving the gene of interest, allowing its controlled expression in a mutant line and assaying for rescue of the phenotype (Halloran et al 2000; Yeo et al 2001). Another mechanism to address the target of a gene product is to ask where this is required. Spatially restricted expression is possible using tissue-specific promoters and deriving lines of such fish that can be used to attempt rescue mutant lines.

Second, a forward genetics approach (random mutagenesis) will lead to identification of potential NTD genes in a relatively unbiased manner. Several forward genetic screens have yielded mutants affecting the brain morphology and neural function (Table 2.1), however a directed screen for mutants displaying NTDs has not been performed. Such a screen will be extremely useful in expanding the collection of potential NTD risk genes in human. Some NTDs may be caused by mutations in multiple genes, perhaps in association with environmental factors. Mutation in one NTD risk gene therefore may not cause an obvious phenotype. A crucial issue is then how to define genes that must act in concert with others to cause a NTD. One promising avenue is the use of genetic modifier screens. These would start with a weak allele of a locus that gives a NTD when null. Forward genetic approaches could then be used to isolate other genes that strengthen or further weaken the phenotype.

Another approach with potential therapeutic ramifications, uses small molecules of defined or unknown specificity could be applied to mutant embryos, in an effort to strengthen or weaken the phenotype. Such an approach has been taken with wild-type zebrafish embryos (Peterson et al 2000). For example, in zebrafish *heart and soul* mutant, neuroepithelial polarity is disrupted due to loss of  $\alpha$ PKC lambda. A chemical inhibitor of this kinase has been identified and shown to cause has phenotypes in wild-type embryos (Peterson et al 2001). Since  $\alpha$ PKC

lambda is a good candidate for NTD, genetic screens could be designed to look for suppressors (or enhancers) of the chemical inhibitor. This chemical approach could not only be used to define pathways that alter the NTD phenotype, but could provide potential therapeutic agents that may abrogate neonatal NTD phenotypes.

## **CONCLUSION**

In summary, we have discussed the utility of the zebrafish as a model for identifying and analyzing genes that cause human neural tube defects. Multiple zebrafish mutants that give NTDs have already been isolated and some show similar defects to the mouse model. The powerful forward and reverse genetic approaches available in the zebrafish make this a highly promising model for clarifying the mechanisms underlying human NTDs.

**Table 2.1**

<b>Mutant</b>	<b>Gene</b>	<b>Function/Phenotype (Reference)</b>
<b><u>Planar cell polarity pathway</u></b>		
<i>knypek</i>	<i>kny</i>	heparan sulfate proteoglycan, craniofacial defects (Topczewski et al 2001)
<i>trilobite(a)</i>	<i>vangl2</i>	transmembrane protein, associated with PCP, NTD in mouse (loop tail) knockout (Jessen et al 2002; Kibar et al 2001a)
<i>pipe tail</i>	<i>wnt5a</i>	impaired development of head skeleton (Rauch et al 1997)
<i>silberblick</i>	<i>wnt11</i>	cyclopia and midline defects in the head (Heisenberg et al 2000)
<b><u>Cell polarity and adhesion</u></b>		
<i>grumpy</i>	<i>lamb1</i>	laminin beta 1, notochord and brain defects (Parsons et al 2002)
<i>heart and soul</i>	<i>aPKC λ</i>	defects in the polarized epithelia of the retina/neural tube (Horne-Badovinac et al 2001; Peterson et al 2001)
<i>nagie oko</i>	<i>mpp5</i>	MAGUK, abnormal brain, retinal cell patterning defects (Wei and Malicki 2002b)
<i>parachute/ glass onion</i>	<i>cdh2</i>	cell adhesion, defects in neural tube and eye (Lele et al 2002; Malicki et al 2003)
<i>sleepy</i>	<i>lamc1</i>	laminin gamma 1, irregular brain shape (Parsons et al 2002)
<b><u>Hedgehog signaling</u></b>		
<i>detour</i>	<i>gli1</i>	zinc finger TF, defects in ventral neuroectoderm (Karlstrom et al 2003)
<i>slow muscle omitted</i>	<i>smoothened</i>	lateral floor plate and subpopulation of hypothalamic cells (Varga et al 2001)
<i>sonic you<sup>(a)</sup></i>	<i>shh</i>	motorneuron axons and ganglion cells, NTD in mouse knockout (Harris and Juriloff 1997; Schauerte et al 1998)
<i>you too</i>	<i>gli2</i>	zinc finger TF, midline development, retinal axon guidance, ectopic lens, interfere with hh signaling (Karlstrom et al 2003)

**Table 2.1 Continued**

<b>Mutant</b>	<b>Gene</b>	<b>Function/Phenotype (Reference)</b>
<b><u>Nodal signaling</u></b>		
<i>bonnie and clyde</i>	<i>mixer</i>	paired-class homeodomain TF, abnormal brain shape (Kikuchi et al 2000)
<i>cyclops</i>	<i>ndr2</i>	nodal related 2, ventral midline patterning (Rebagliati et al 1998; Sampath et al 1998)
<i>schmalspur</i>	<i>foxh1/fast1</i>	winged-helix transcription factor, prechordal plate and ventral neuroectoderm (Pogoda et al 2000; Sirotkin et al 2000)
<i>squint</i>	<i>ndr1</i>	nodal related 1, mild eye cyclopia (Feldman et al 1998)
<i>one eyed pinhead</i>	<i>oep</i>	EGF-CFC member and a co-receptor for nodal, cyclopia, mutation in human holoprosencephaly (Zhang et al 1998)
<b><u>Neuroectoderm specification and patterning</u></b>		
<i>acerebellar</i>	<i>fgf8</i>	defects in MHB and cerebellum (Reifers et al 1998)
<i>bozozok</i>	<i>dharma</i>	homeodomain TF, loss of neural fate anterior to MHB (Fekany et al 1999)
<i>chokh</i>	<i>rx3</i>	homeodomain TF, loss of eye (Loosli et al 2003)
<i>dino</i>	<i>chordin</i>	BMP antagonist, reduced brain size (Schulte-Merker et al 1997)
<i>headless</i>	<i>tcf3</i>	truncation of forebrain structures (Kim et al 2000)
<i>lazarus</i>	<i>pbx</i>	segmental patterning of hindbrain and anterior trunk (Popperl et al 2000)
<i>masterblind</i> <sup>(a)</sup>	<i>axin1</i>	reduced eye and forebrain, NTD in mouse knockout (Heisenberg et al 2001; Zeng et al 1997)
<i>neckless</i> <sup>(a)</sup>	<i>aldh1a2</i>	retinaldehydehydrogenase type 2, defects in neural tube and paraxial mesoderm, NTD in mouse knockout (Begemann et al 2001; Niederreither et al 1999)

**Table 2.1 Continued**

<b>Mutant</b>	<b>Gene</b>	<b>Function/Phenotype (Reference)</b>
<i>no isthmus</i>	<i>pax2.1</i>	no MHB, dorsal and ventral midbrain are abnormal (Brand et al 1996)
<i>snailhouse</i>	<i>bmp7</i>	expansion of neuroectoderm (Dick et al 2000; Schmid et al 2000)
<i>somitabun</i> <sup>(a)</sup>	<i>smad5</i>	expansion of neuroectoderm, NTD in mouse knockout (Chang et al 1999; Hild et al 1999)
<i>spiel ohne grenzen</i>	<i>pou2</i>	POU-domain transcription factor, MHB midbrain size and patterning of hind brain (Hauptmann et al 2002b; Reim and Brand 2002)
<i>swirl</i>	<i>bmp2b</i>	expansion of neuroectoderm (Kishimoto et al 1997)
<i>too few</i>	<i>fez1</i>	zinc finger transcription factor, defects in hypothalamic DA and 5HT neurons (Levkowitz et al 2003)
<i>valentino</i>	<i>val</i>	bZip transcription factor, required for r5 and 6, defects in inner ear (Moens et al 1998)
<b><u>Neural crest</u></b>		
<i>lock jaw / mont blanc</i> <sup>(a)</sup>	<i>tfap2a</i>	hind brain and sympathetic noradrenergic neurons, neural crest development, NTD in knockout (Harris and Juriloff 1997; Holzschuh et al 2003; Knight et al 2003)
<i>van gogh</i>	<i>tbx1</i>	T-box gene, pharyngeal mesoderm, neural crest derived cartilages, Di George syndrome (Piotrowski et al 2003)
<b><u>Neurogenesis</u></b>		
<i>foggy</i>	<i>spt5</i>	transcription elongation factor, reduction of DA neurons and surplus of 5ht neurons, notochord defects (Guo et al 2000)
<i>mind bomb</i>	<i>mib</i>	ring ubiquitin ligase, Notch signaling, excessive neuronal differentiation (Itoh et al 2003)

**Table 2.1 Continued**

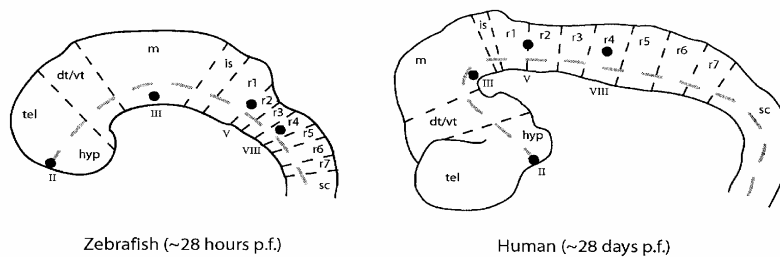
<b>Mutant</b>	<b>Gene</b>	<b>Function/Phenotype (Reference)</b>
<i>pandora</i>	<i>spt6</i>	transcription elongation factor, defects in brain ventricle, eye and ear (Keegan et al 2002)
<b><u>Subtle neural function</u></b>		
<i>ache</i>	<i>ache</i>	acetylcholinesterase; muscle fiber formation and innervation, primary sensory neurons death (Behra et al 2002)
<i>astray</i>	<i>robo2</i>	roundabout homolog 2, defects in axon pathfinding (Fricke et al 2001)
<i>lakritz</i>	<i>ath5</i>	basic helix-loop-helix transcription factor, retinal ganglion cell determination (Kay et al 2001)
<i>mariner</i>	<i>myosin 7a</i>	hair bundles, Usher 1B syndrome (Ernest et al 2000)
<i>nicotinic</i>	<i>chrna1</i>	cholinergic receptor nicotinic alpha polypeptide 1, receptor nonmotile, no clustering of acetylcholine receptors (Sepich et al 1998)
<i>no optokientic response f</i>	<i>gnat2</i>	G protein alpha transducing activity polypeptide 2 defects in cone photoreceptor, mutation in human achromatopsia (color blindness) (Brockerhoff et al 2003)
<i>soulless</i>	<i>phox2a</i>	homeodomain transcription factor, reduction in locus coeruleus noradrenergic neurons (Guo et al 1999)
<i>twich once</i>	<i>rapsyn</i>	inhibition of formation of acetylcholine receptor clusters, reduced synaptic strength (Ono et al 2002)
<i>young</i>	<i>smarca4</i>	chromatin remodeling complex, retinal cell differentiation (Gregg et al 2003)

(a) indicates zebrafish mutants carrying mutations in zebrafish orthologs of mouse NTD genes (Juriloff and Harris 2000)

**Figure 2.1 Brain development and structure is conserved between zebrafish and humans**

The overall organization of the many parts of the vertebrate brain is similar among all vertebrates. (A) Here we provide a schematic representation of an embryonic and adult zebrafish brain and compare it to a schematic of the human embryonic and adult brain (anterior to the left, dorsal to the top). The figure depicts the segmental (neuromeric) organization of the embryonic brain highlighting only a few of the proposed subdivisions (separated by black dashed lines). As a reference point, the boundary between the main alar (dorsal) and basal (ventral) subdivision of the brain and spinal cord is shown as a grey dashed line and the location of four cranial nerve primordia are depicted as black dots (II, optic nerve; III, oculomotor nerve; V, trigeminal nerve; VIII, octaval or vestibulocochlear nerve). (B) Despite the numerous morphological changes that occur during the course of development and the eventual size differences in a number of regions, the adult zebrafish and human brain share similar features. tel, telencephalon; hyp, hypothalamus; dt/vt, dorsal thalamus/ventral thalamus; m, midbrain; is, isthmus; r1-r7, rhombomeres 1-7; sc, spinal cord; ce, cerebellum (a derivative of the dorsal r1); h, hindbrain (the combined derivative of r2-r7).

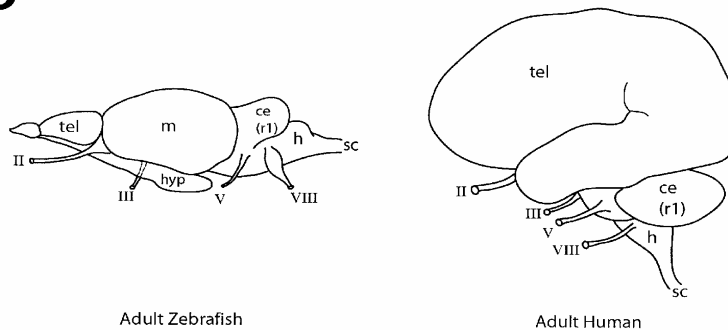
**A**



Zebrafish (~28 hours p.f.)

Human (~28 days p.f.)

**B**



Adult Zebrafish

Adult Human





### Figure 2.2 Steps in Early Brain Development

The first step of brain development is neural determination, in which cells of the neural plate make the decision to form neural tissue, but do not yet differentiate as neurons. The neural plate then undergoes neurulation, in which the epithelial neural plate rolls or bends to form the closed neural tube. During and after neural tube closure, the anterior portion of the tube dilates in three specific locations to form the future forebrain, midbrain, and hindbrain ventricles, which later undergo rapid expansion. ep = eye primordium.

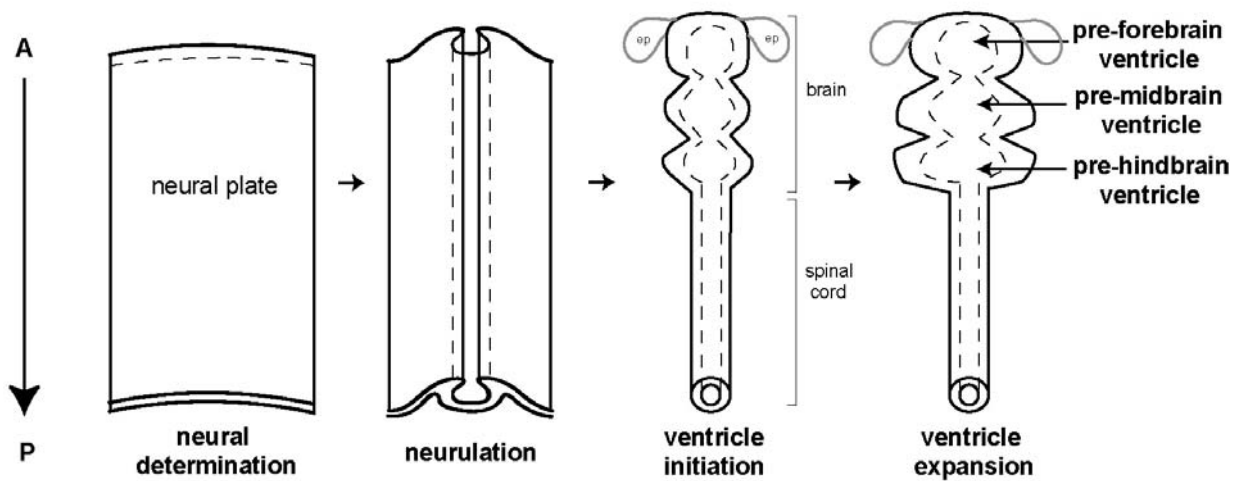




**Figure 2.3 The neural tube forms by two different mechanisms along the anteroposterior axis**

**A.** Level of the neural tube at which primary and secondary neurulation occur. In a transition zone near the junction of primary and secondary tubes, a mix of the mechanisms may be present.

**B.** Comparison of primary and secondary neurulation. a: primary neurulation involves columnarization of an existing epithelium, and then rolling or folding the epithelium (blue). b: secondary neurulation is characterized by condensation of mesenchyme (brown) to form a rod, which then undergoes an epithelial transition to form the neural tube.

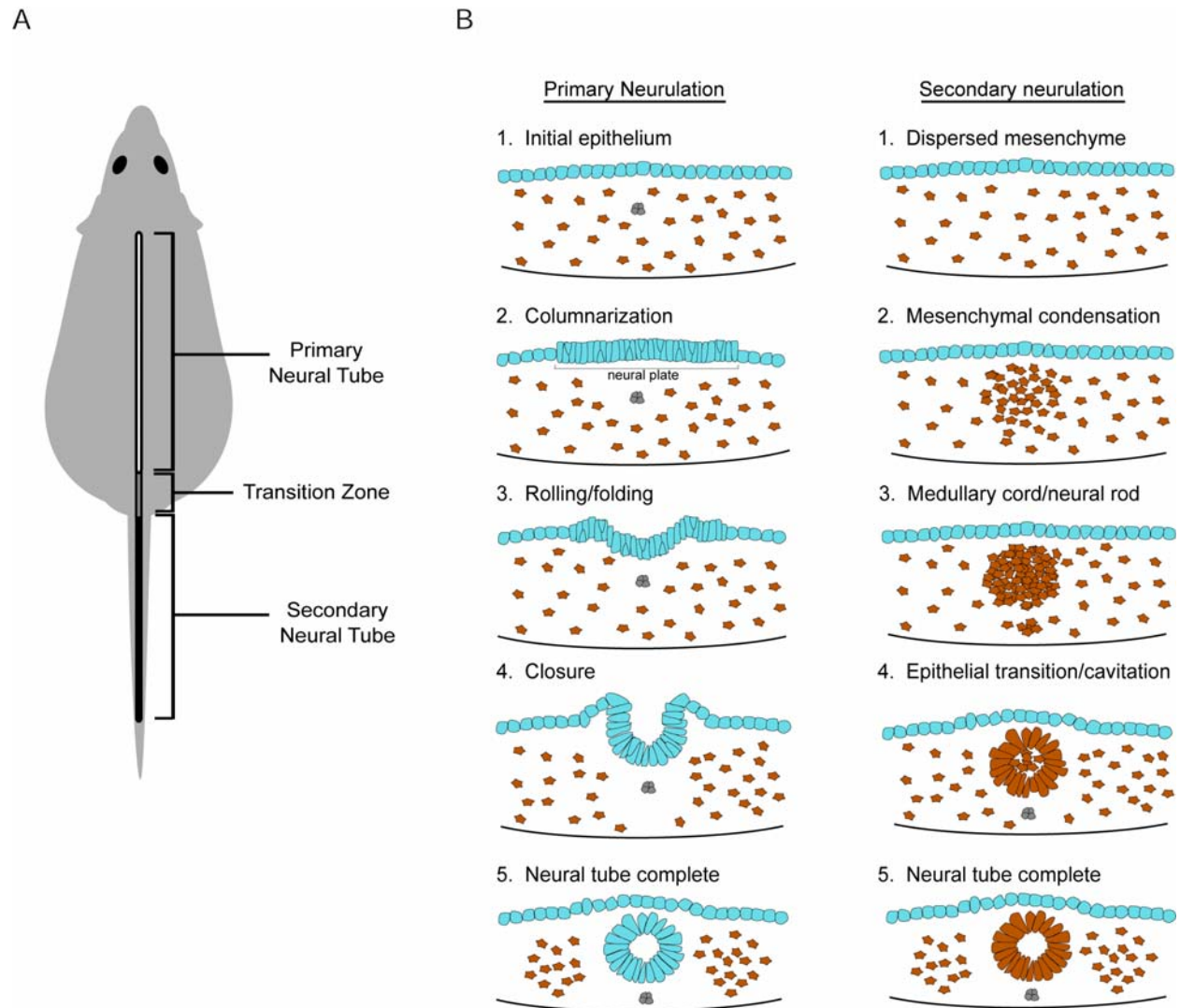




### Figure 2.4 Variations of primary neurulation

The neural tube is shown at the open stage (top row) and after initial closure (bottom row) (see also Fig. 2.3). The initial flat neuroepithelium may roll smoothly into a tube (a), bend sharply at one (b) or more (c) hinge points, or form a solid rod of cells (d). See text for details.

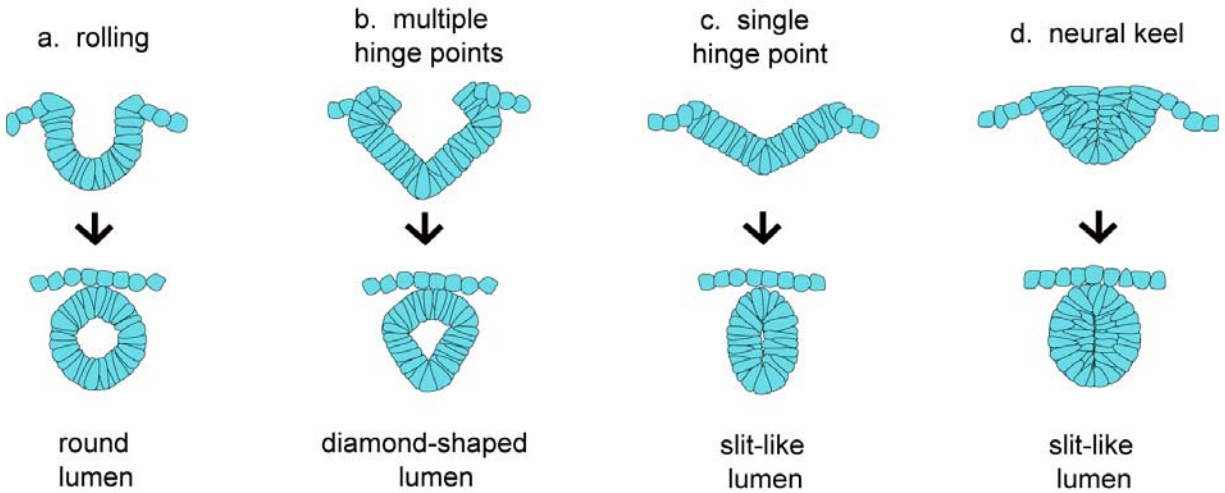
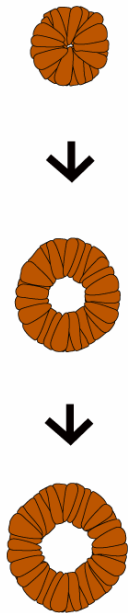




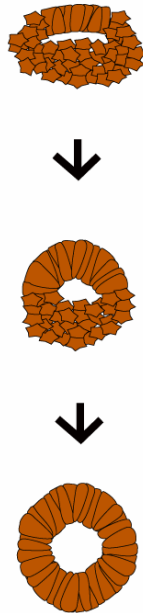
### Figure 2.5 Variations of secondary neurulation

The neural tube is shown subsequent to condensation of the starting mesenchyme into the medullary cord (see also Fig. 2.3). In one variation (a) a solid mass of epithelium (the medullary rosette) expands to form a lumen. (b) A medullary plate comprises an epithelium abutting mesenchyme with a space between. The epithelium expands to replace the mesenchyme with concomitant lumen expansion. (c) The medullary cord may form an epithelium at its edges while mesenchyme remains centrally. A lumen forms by expansion of spaces between the epithelium and mesenchyme and by loss of the mesenchyme. See text for details.

a. mouse  
medullary "rosette"



b. mouse  
medullary "plate"



c. chick

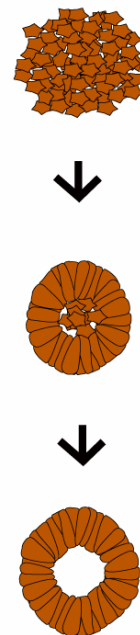
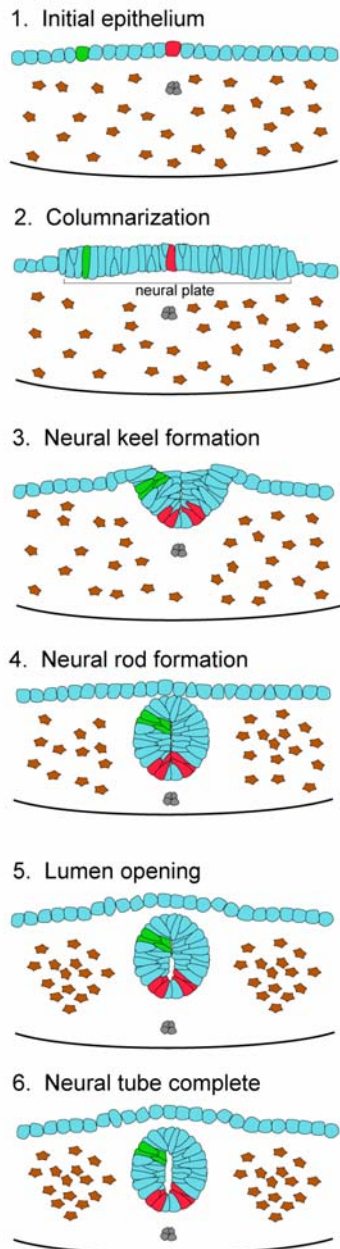






### Figure 2.6 Zebrafish trunk neurulation

An initial epithelium columnarizes to form the neural plate, which then forms a solid neural keel and solid tube. The midline of the tube becomes distinct and a lumen opens from ventral to dorsal. Neural plate cells lineage labeled prior to neural keel formation (red and green) maintain their relative positions during neural tube formation, indicating that cells form the keel by cryptic rolling or folding. The derivation of the zebrafish neural tube from an epithelium and the cell movements involved are typical of primary neurulation.





## References

- Aaku-Saraste E, Hellwig A and Huttner, WB (1996). Loss of occludin and functional tight junctions, but not ZO-1, during neural tube closure--remodeling of the neuroepithelium prior to neurogenesis. *Dev Biol* 180:664-79.
- Amsterdam A, Burgess S, Golling G, Chen W, Sun Z, Townsend K, Farrington S, et al. (1999). A large-scale insertional mutagenesis screen in zebrafish. *Genes Dev* 13:2713-2724.
- Barut BA and Zon LI (2000). Realizing the potential of zebrafish as a model for human disease. *Physiol. Genomics* 2:49-51.
- Begemann G, Schilling TF, Rauch GJ, Geisler R and Ingham PW (2001). The zebrafish neckless mutation reveals a requirement for raldh2 in mesodermal signals that pattern the hindbrain. *Development* 128:3081-94.
- Behra M, Cousin X, Bertrand C, Vonesch JL, Biellmann D, Chatonnet A and Strahle U (2002). Acetylcholinesterase is required for neuronal and muscular development in the zebrafish embryo. *Nat Neurosci* 5:111-8.
- Bilder D and Perrimon N (2000). Localization of apical epithelial determinants by the basolateral PDZ protein Scribble. *Nature* 403:676-80.
- Bradford MR Jr (1995). Comparative aspects of forebrain organization in the ray-finned fishes: touchstones or not? *Brain Behav Evol* 46:259-274.
- Brand M, Heisenberg CP, Jiang YJ, Beuchle D, Lun K, Furutani-Seiki M, Granato M et al. (1996). Mutations in zebrafish genes affecting the formation of the boundary between midbrain and hindbrain. *Development* 123:179-90.
- Brockerhoff SE, Rieke F, Matthews HR, Taylor MR, Kennedy B, Ankoudinova I, Niemi GA et al. (2003). Light stimulates a transducin-independent increase of cytoplasmic Ca<sup>2+</sup> and suppression of current in cones from the zebrafish mutant *nof*. *J Neurosci* 23:470-80.
- Brouns MR, Matheson SF, Hu KQ, Delalle I, Caviness VS, Silver J, Bronson RT and Settleman J (2000). The adhesion signaling molecule p190 RhoGAP is required for morphogenetic processes in neural development. *Development* 127: 4891-903.
- Butler AB, Hodos W (1996). *Comparative vertebrate neuroanatomy. Evolution and adaptation.* Wiley-Liss, New York.
- Butler, AB (2000). Topography and topology of the teleost telencephalon: a paradox resolved. *Neurosci Lett* 293:95-98.
- Byrd CA, Jones JT, Quattro JM, Rogers ME, Brunjes PC and Vogt RG (1996). Ontogeny of odorant receptor gene expression in zebrafish, *Danio rerio*. *J Neurobiol* 29:445-458.

- Carreira-Barbosa F, Concha ML, Takeuchi M, Ueno N, Wilson SW and Tada M (2003). Prickle 1 regulates cell movements during gastrulation and neuronal migration in zebrafish. *Development* 130:4037-46.
- Catala M, Teillet MA and Le Douarin NM (1995). Organization and development of the tail bud analyzed with the quail-chick chimera system. *Mech Dev* 51:51-65.
- Chang H, Huylebroeck D, Verschueren K, Guo Q, Matzuk MM and Zwijsen A (1999). Smad5 knockout mice die at mid-gestation due to multiple embryonic and extraembryonic defects. *Development* 126:1631-42.
- Chitnis AB and Kuwada JY (1990). Axonogenesis in the brain of zebrafish embryos. *J Neurosci* 10:1892-1905.
- Colas JF and Schoenwolf GC (2001). Towards a cellular and molecular understanding of neurulation. *Dev Dyn* 221:117-45.
- Collazo A, Bronner-Fraser M and Fraser SE (1993). Vital dye labelling of *Xenopus laevis* trunk neural crest reveals multipotency and novel pathways of migration. *Development* 118:363-76.
- Conklin EG (1932). The embryology of amphioxus. *Journal of Morphology* 54:69-151.
- Copp AJ, Brook FA, Estibeiro JP, Shum AS and Cockroft DL (1990). The embryonic development of mammalian neural tube defects. *Prog Neurobiol* 35: 363-403.
- Copp AJ, Greene ND and Murdoch JN (2003). The genetic basis of mammalian neurulation. *Nat Rev Genet* 4:784-93.
- Coucouvani E and Martin GR (1995). Signals for death and survival: a two-step mechanism for cavitation in the vertebrate embryo. *Cell* 83:279-87.
- Coucouvani E and Martin GR (1999). BMP signaling plays a role in visceral endoderm differentiation and cavitation in the early mouse embryo. *Development* 126:535-46.
- Criley BB (1969). Analysis of embryonic sources and mechanisms of development of posterior levels of chick neural tubes. *J Morphol* 128:465-501.
- Curtin JA, Quint E, Tsipouri V, Arkell RM, Cattanch B, Copp AJ, Henderson DJ et al. (2003). Mutation of *Celsr1* disrupts planar polarity of inner ear hair cells and causes severe neural tube defects in the mouse. *Curr Biol* 13:1129-33.
- Darland T and Dowling JE (2001). Behavioral screening for cocaine sensitivity in mutagenized zebrafish. *Proc Natl Acad Sci USA* 98:11691-11696.
- Davidson LA and Keller RE (1999). Neural tube closure in *Xenopus laevis* involves medial migration, directed protrusive activity, cell intercalation and convergent extension. *Development* 126:4547-56.

- Dick A, Hild M, Bauer H, Imai Y, Maifeld H, Schier AF, Talbot WS et al. (2000). Essential role of Bmp7 (snailhouse) and its prodomain in dorsoventral patterning of the zebrafish embryo. *Gene* 127:343-54.
- Dodd A, Curtis PM, Williams LC and Love DR (2000). Zebrafish: bridging the gap between development and disease. *Hum. Mol. Genet.* 9:2443-2449.
- Driever W, Solnica-Krezel L, Schier AF, Neuhaus SCF, Malicki J, Stemple DL, Stainier DYR, et al. (1996). A genetic screen for mutations affecting embryogenesis in zebrafish. *Development* 123:37-46.
- Eichenbaum H, Dudchenko P, Wood E, Shapiro M and Tanila H (1999). The hippocampus, memory, and place cells: Is it spatial memory or a memory space? *Neuron* 23:209-226.
- Eisen JS, Myers PZ and Westerfield M (1986). Pathway selection by growth cones of identified motoneurons in live zebra fish embryos. *Nature* 320:269-71.
- Ernest S, Rauch GJ, Haffter P, Geisler R, Petit C and Nicolson T (2000). Mariner is defective in myosin VIIA: a zebrafish model for human hereditary deafness. *Hum Mol Genet* 9:2189-96.
- Fekany K, Yamanaka Y, Leung T, Sirotkin HI, Topczewski J, Gates MA, Hibi M et al. (1999). The zebrafish bozozok locus encodes Dharma, a homeodomain protein essential for induction of gastrula organizer and dorsoanterior embryonic structures. *Development* 126:1427-38.
- Feldman B, Gates MA, Egan ES, Dougan ST, Rennebeck G, Sirotkin HI, Schier AF et al. (1998). Zebrafish organizer development and germ-layer formation require nodal-related signals. *Nature* 395:181-5.
- Fricke C, Lee JS, Geiger-Rudolph S, Bonhoeffer F and Chien CB (2001). astray, a zebrafish roundabout homolog required for retinal axon guidance. *Science* 292:507-10.
- Geldmacher-Voss B, Reugels AM, Pauls S and Campos-Ortega JA (2003). A 90 degrees rotation of the mitotic spindle changes the orientation of mitoses of zebrafish neuroepithelial cells. *Development* 130:3767-80.
- Ginsburg A and Dettlaff TA (1991). The Russian sturgeon *Acipenser guldenstadti*. In Vassetzky, S.G. (ed.), *Animal species for development studies*, Consultants Bureau, New York, Vol. 2, pp. 15-66.
- Gregg RG, Willer GB, Fadool JM, Dowling JE and Link BA (2003). Positional cloning of the young mutation identifies an essential role for the Brahma chromatin remodeling complex in mediating retinal cell differentiation. *Proc Natl Acad Sci USA* 100:6535-40.

- Griffith CM, Wiley MJ and Sanders EJ (1992). The vertebrate tail bud: three germ layers from one tissue. *Anat Embryol (Berl)* 185:101-13.
- Griffith, M. (1997). Midkine and secondary neurulation. *Teratology* 55:213-23.
- Grinblat Y, Lane ME, Sagerström C and Sive H (1999). Analysis of zebrafish development using explant culture assays. In: Detrich HW, Westerfield M, Zon LI (eds). *Methods in Cell Biology*. Vol 59. *The Zebrafish: Biology*. Academic Press, Boston, pp 128-156.
- Guo S, Brush J, Teraoka H, Goddard A, Wilson SW, Mullins MC and Rosenthal A (1999). Development of noradrenergic neurons in the zebrafish hindbrain requires BMP, FGF8, and the homeodomain protein *soulless/Phox2a*. *Neuron* 24:555-66.
- Guo S, Yamaguchi Y, Schilbach S, Wada T, Lee J, Goddard A, French D et al. (2000). A regulator of transcriptional elongation controls vertebrate neuronal development. *Nature* 408:366-9.
- Haffter P, Granato M, Brand M, Mullins MC, Hammerschmidt M, Kane DA, Odenthal J, van Eeden FJM, Jiang YJ, Heisenberg CP, Kelsh RN, Furutani-Seiki M, Vogelsang E, Beuchle D, Schach U, Fabian C and Nüsslein-Volhard C (1996). The identification of genes with unique and essential functions in the development of the zebrafish, *Danio rerio*. *Development* 123:1-36.
- Haigo SL, Hildebrand JD, Harland RM and Wallingford JB (2003). *Shroom* induces apical constriction and is required for hinge point formation during neural tube closure. *Curr Biol* 13:2125-37.
- Halloran MC, Sato-Maeda M, Warren JT, Su F, Lele Z, Krone PH, Kuwada JY et al. (2000). Laser-induced gene expression in specific cells of transgenic zebrafish. *Development* 127:1953-60.
- Hamblet NS, Lijam N, Ruiz-Lozano P, Wang J, Yang Y, Luo Z, Mei L et al. (2002). *Dishevelled 2* is essential for cardiac outflow tract development, somite segmentation and neural tube closure. *Development* 129:5827-38.
- Handrigan GR (2003). *Concordia discors*: duality in the origin of the vertebrate tail. *J Anat* 202:255-67.
- Hanneman E, Trevarrow B, Metcalfe WK, Kimmel CB and Westerfield M (1988). Segmental pattern of development of the hindbrain and spinal cord of the zebrafish embryo. *Development* 103:49-58.
- Hardan AY, Minshew NJ, Mallikarjunn M and Keshavan MS (2001). Brain volume in autism. *J Child Neurol* 16:421-4.
- Harris MJ and Juriloff DM (1997). Genetic landmarks for defects in mouse neural tube closure. *Teratology* 56:177-87.

- Hauptmann G and Gerster T (2000). Regulatory gene expression patterns reveal transverse and longitudinal subdivisions of the embryonic zebrafish forebrain. *Mech Dev* 91:105-118.
- Hauptmann G, Söll I and Gerster T (2002a). The early embryonic zebrafish forebrain is subdivided into molecularly distinct transverse and longitudinal domains. *Brain Res Bull* 57:371-375.
- Hauptmann G, Belting HG, Wolke U, Lunde K, Soll I, Abdelilah-Seyfried S, Prince V et al. (2002b). *spiel ohne grenzen/pou2* is required for zebrafish hindbrain segmentation. *Development* 129:1645-55.
- Heisenberg CP, Tada M, Rauch GJ, Saude L, Concha ML, Geisler R, Stemple DL et al. (2000). Silberblick/Wnt11 mediates convergent extension movements during zebrafish gastrulation. *Nature* 405:76-81.
- Heisenberg CP, Houart C, Take-Uchi M, Rauch GJ, Young N, Coutinho P, Masai I, Caneparo L, Concha ML, Geisler R, Dale TC, Wilson SW and Stemple DL (2001). A mutation in the Gsk3-binding domain of zebrafish Masterblind/Axin1 leads to a fate transformation of telencephalon and eyes to diencephalon. *Genes Dev* 15:1427-34.
- Hild M, Dick A, Rauch GJ, Meier A, Bouwmeester T, Haffter P and Hammerschmidt M (1999). The *smad5* mutation *somitabun* blocks Bmp2b signaling during early dorsoventral patterning of the zebrafish embryo. *Development* 126:2149-59.
- Holland ND, Panganiban G, Henyey EL and Holland LZ (1996). Sequence and developmental expression of *AmphiDll*, an amphioxus *Distal-less* gene transcribed in the ectoderm, epidermis and nervous system: insights into evolution of craniate forebrain and neural crest. *Development* 122:2911-20.
- Holmberg J, Clarke DL and Frisen J (2000). Regulation of repulsion versus adhesion by different splice forms of an Eph receptor. *Nature* 408:203-6.
- Holmdahl D (1932). Die zweifache Bildungsweise des zentralen Nervensystems bei den Wirbeltieren. Eine formgeschichtliche und materialgeschichtliche Analyse. *Wilhelm Roux' Arch Entwicklungsmech Org* 129:206-54.
- Holzschuh J, Barrallo-Gimeno A, Ettl AK, Durr K, Knapik EW and Driever W (2003). Noradrenergic neurons in the zebrafish hindbrain are induced by retinoic acid and require *tfap2a* for expression of the neurotransmitter phenotype. *Development* 130:5741-54.
- Horne-Badovinac S, Lin D, Waldron S, Schwarz M, Mbamalu G, Pawson T, Jan Y, Stainier DY and Abdelilah-Seyfried S (2001). Positional cloning of heart and soul reveals multiple roles for PKC lambda in zebrafish organogenesis. *Curr Biol* 11:1492-502.
- Hyatt TM and Ekker SC (1999). Vectors and techniques for ectopic gene expression in zebrafish. In: Detrich HW, Westerfield M, Zon LI (eds). *Methods in Cell Biology*. Vol 59. *The Zebrafish: Biology*. Academic Press, Boston, pp 117-126.

- Itoh M, Kim CH, Palardy G, Oda T, Jiang YJ, Maust D, Yeo SY et al. (2003). Mind bomb is a ubiquitin ligase that is essential for efficient activation of Notch signaling by Delta. *Dev Cell* 4:67-82.
- Jessen JR, Topczewski J, Bingham S, Sepich DS, Marlow F, Chandrasekhar A and Solnica-Krezel L (2002). Zebrafish trilobite identifies new roles for Strabismus in gastrulation and neuronal movements. *Nat Cell Biol* 4:610-5.
- Jiang YJ, Brand M, Heisenberg CP, Beuchle D, Furutani-Seiki M, Kelsh RN, Warga RM, Granato M, Haffter P, Hammerschmidt M, Kane DA, Mullins MC, Odenthal J, van Eeden FJ and Nusslein-Volhard C (1996). Mutations affecting neurogenesis and brain morphology in the zebrafish, *Danio rerio*. *Development* 123:205-16.
- Juriloff DM and Harris MJ (2000). Mouse models for neural tube closure defects. *Hum Mol Genet* 9:993-1000.
- Karlstrom RO, Tyurina OV, Kawakami A, Nishioka N, Talbot WS, Sasaki H and Schier AF (2003). Genetic analysis of zebrafish *gli1* and *gli2* reveals divergent requirements for gli genes in vertebrate development. *Development* 130:1549-64.
- Kay JN, Finger-Baier KC, Roeser T, Staub W and Baier H (2001). Retinal ganglion cell genesis requires lakritz, a Zebrafish atonal Homolog. *Neuron* 30:725-36.
- Keegan BR, Feldman JL, Lee DH, Koos DS, Ho RK, Stainier DY and Yelon D (2002). The elongation factors Pandora/Spt6 and Foggy/Spt5 promote transcription in the zebrafish embryo. *Development* 129:1623-32.
- Kibar Z, Underhill DA, Canonne-Hergaux F, Gauthier S, Justice MJ and Gros P (2001a). Identification of a new chemically induced allele (Lp(m1Jus)) at the loop-tail locus: morphology, histology, and genetic mapping. *Genomics* 72:331-7.
- Kibar Z, Vogan KJ, Groulx N, Justice MJ, Underhill DA and Gros P (2001b). Ltap, a mammalian homolog of *Drosophila* Strabismus/Van Gogh, is altered in the mouse neural tube mutant Loop-tail. *Nat Genet* 28:251-5.
- Kikuchi Y, Trinh LA, Reiter JF, Alexander J, Yelon D and Stainier DY (2000). The zebrafish *bonnie* and *clyde* gene encodes a Mix family homeodomain protein that regulates the generation of endodermal precursors. *Genes Dev* 14:1279-89.
- Kim CH, Oda T, Itoh M, Jiang D, Artinger KB, Chandrasekharappa SC, Driever W et al. (2000). Repressor activity of Headless/Tcf3 is essential for vertebrate head formation. *Nature* 407:913-6.
- Kimmel CB (1989). Genetics and early development of zebrafish. *Trends Genet* 5:283-288.



- Kimmel CB, Warga RM and Kane DA (1994). Cell cycles and clonal strings during formation of the zebrafish central nervous system. *Development* 120:265-76.
- Kimmel CB, Ballard WW, Kimmel SR, Ullmann B and Schilling TF (1995). Stages of embryonic development of the zebrafish. *Dev Dyn* 203:253-310.
- Kingsbury BF (1932). The "law" of cephalocaudal differential growth in its application to the nervous system. *J Comp Neurol* 56:431-63.
- Kishimoto Y, Lee KH, Zon L, Hammerschmidt M and Schulte-Merker S (1997). The molecular nature of zebrafish swirl: BMP2 function is essential during early dorsoventral patterning. *Development* 124:4457-66.
- Knight RD, Nair S, Nelson SS, Afshar A, Javidan Y, Geisler R, Rauch GJ and Schilling TF (2003). lockjaw encodes a zebrafish tfap2a required for early neural crest development. *Development* 130:5755-68.
- Kurokawa K, Nakamura K, Sumiyoshi T, Hagino H, Yotsutsuji T, Yamashita I, Suzuki M et al. (2000). Ventricular enlargement in schizophrenia spectrum patients with prodromal symptoms of obsessive-compulsive disorder. *Psychiatry Res* 99:83-91.
- Lele Z, Folchert A, Concha M, Rauch GJ, Geisler R, Rosa F, Wilson SW, Hammerschmidt M and Bally-Cuif L (2002). parachute/n-cadherin is required for morphogenesis and maintained integrity of the zebrafish neural tube. *Development* 129:3281-94.
- Levkowitz G, Zeller J, Sirotkin HI, French D, Schilbach S, Hashimoto H, Hibi M, Talbot WS and Rosenthal A (2003). Zinc finger protein too few controls the development of monoaminergic neurons. *Nat Neurosci* 6:28-33.
- Loosli F, Staub W, Finger-Baier KC, Ober EA, Verkade H, Wittbrodt J and Baier H (2003). Loss of eyes in zebrafish caused by mutation of chokh/rx3. *EMBO Rep* 4:894-9.
- Machado HR, Martelli N, Assirati Junior JA and Colli BO (1991). Infantile hydrocephalus: brain sonography as an effective tool for diagnosis and follow-up. *Childs Nerv Syst* 7:205-10.
- Malicki J, Jo H and Pujic Z (2003). Zebrafish N-cadherin, encoded by the glass onion locus, plays an essential role in retinal patterning. *Dev Biol* 259:95-108.
- McLone DG and Knepper PA (1989). The cause of Chiari II malformation: a unified theory. *Pediatr Neurosci* 15:1-12.
- Metcalfe WK, Mendelson B and Kimmel CB (1986). Segmental homologies among reticulospinal neurons in the hindbrain of the zebrafish larva. *J Comp Neurol* 251:147-159.
- Miyayama Y and Fujimoto T (1977). Fine morphological study of neural tube formation in the teleost, *Oryzias latipes*. *Okajimas Folia Anat Jpn* 54:97-120.

- Moens CB, Cordes SP, Giorgianni MW, Barsh GS and Kimmel CB (1998). Equivalence in the genetic control of hindbrain segmentation in fish and mouse. *Development* 125:381-91.
- Mombaerts P (2001). How smell develops. *Nat Neurosci* 4 Suppl:1192-1198.
- Montcouquiol M, Rachel RA, Lanford PJ, Copeland NG, Jenkins NA and Kelley MW (2003). Identification of *Vangl2* and *Scrb1* as planar polarity genes in mammals. *Nature* 423:173-7.
- Morriss-Kay G, Wood H and Chen WH (1994). Normal neurulation in mammals. *Ciba Found Symp* 181:51-63; discussion 63-9.
- Murdoch JN, Henderson DJ, Doudney K, Gaston-Massuet C, Phillips HM, Paternotte C, Arkell R et al. (2003). Disruption of *scribble* (*Scrb1*) causes severe neural tube defects in the circletail mouse. *Hum Mol Genet* 12:87-98.
- Nakao T and Ishizawa A (1984). Light- and electron-microscopic observations of the tail bud of the larval lamprey (*Lampetra japonica*), with special reference to neural tube formation. *Am J Anat* 170:55-71.
- Nasevicius A and Ekker SC (2000). Effective targeted gene 'knockdown' in zebrafish. *Nat Genet* 26:216-20.
- Niederreither K, Subbarayan V, Dolle P and Chambon P (1999). Embryonic retinoic acid synthesis is essential for early mouse post-implantation development. *Nat Genet* 21:444-8.
- Ono F, Shcherbatko A, Higashijima S, Mandel G and Brehm P (2002). The Zebrafish motility mutant twitch once reveals new roles for rapsyn in synaptic function. *J Neurosci* 22:6491-8.
- Orger MB, Smear MC, Anstis SM and Baier H (2000). Perception of Fourier and non-Fourier motion by larval zebrafish. *Nat Neurosci* 3:1128-1133.
- Papan C and Campos-Ortega JA (1994). On the formation of the neural keel and neural tube in the zebrafish *Danio* (*Brachydanio rerio*). *Roux's Arch Dev Biol* 203:178-86.
- Papan C and Campos-Ortega JA (1999). Region-specific cell clones in the developing spinal cord of the zebrafish. *Dev Genes Evol* 209:135-44.
- Parsons MJ, Pollard SM, Saude L, Feldman B, Coutinho P, Hirst EM and Stemple DL (2002). Zebrafish mutants identify an essential role for laminins in notochord formation. *Development* 129:3137-46.
- Peeters MC, Viebahn C, Hekking JW and van Straaten HW (1998). Neurulation in the rabbit embryo. *Anat Embryol (Berl)* 197:167-75.

- Peterson RT, Link BA, Dowling JE and Schreiber SL (2000). Small molecule developmental screens reveal the logic and timing of vertebrate development. *Proc Natl Acad Sci U S A* 97:12965-9.
- Peterson RT, Mably JD, Chen JN and Fishman MC (2001). Convergence of distinct pathways to heart patterning revealed by the small molecule concentramide and the mutation heart-and-soul. *Curr Biol* 11:1481-91.
- Piotrowski T, Ahn DG, Schilling TF, Nair S, Ruvinsky I, Geisler R, Rauch GJ et al. (2003). The zebrafish van gogh mutation disrupts *tbx1*, which is involved in the DiGeorge deletion syndrome in humans. *Development* 130:5043-52.
- Pogoda HM, Solnica-Krezel L, Driever W and Meyer D (2000). The zebrafish forkhead transcription factor FoxH1/Fast1 is a modulator of nodal signaling required for organizer formation. *Curr Biol* 10:1041-9.
- Popperl H, Rikhof H, Chang H, Haffter P, Kimmel CB and Moens CB (2000). *lazarus* is a novel *pbx* gene that globally mediates *hox* gene function in zebrafish. *Mol Cell* 6:255-67.
- Puelles L (1995). A segmental morphological paradigm for understanding vertebrate forebrains. *Brain Behav Evol* 46:319-337.
- Rauch GJ, Hammerschmidt M, Blader P, Schauerte HE, Strahle U, Ingham PW, McMahon AP et al. (1997). *Wnt5* is required for tail formation in the zebrafish embryo. *Cold Spring Harb Symp Quant Biol* 62:227-34.
- Rebagliati MR, Toyama R, Haffter P and Dawid IB (1998). *cyclops* encodes a nodal-related factor involved in midline signaling. *Proc Natl Acad Sci USA* 95:9932-7.
- Reichenbach A, Schaaf P and Schneider H (1990). Primary neurulation in teleosts--evidence for epithelial genesis of central nervous tissue as in other vertebrates. *J Hirnforsch* 31:153-8.
- Reifers F, Bohli H, Walsh EC, Crossley PH, Stainier DY and Brand M (1998). *Fgf8* is mutated in zebrafish acerebellar (*ace*) mutants and is required for maintenance of midbrain-hindbrain boundary development and somitogenesis. *Development* 125:2381-95.
- Reim G and Brand M (2002). *Spiel-ohne-grenzen/pou2* mediates regional competence to respond to *Fgf8* during zebrafish early neural development. *Development* 129:917-33.
- Rodríguez F, López JC, Vargas JP, Broglio C, Gómez Y and Salas C (2002a). Spatial memory and hippocampal pallium through vertebrate evolution: Insights from reptiles and teleost fish. *Brain Res Bull* 57:499-503.
- Rodríguez F, López JC, Vargas JP, Gómez Y, Broglio C and Salas C (2002b). Conservation of spatial memory function in the pallial forebrain of reptiles and ray-finned fishes. *J Neurosci* 22:2894-2903.

- Ross LS, Parrett T and Easter SS Jr (1992). Axonogenesis and morphogenesis in the embryonic zebrafish brain. *J Neurosci* 12:467-482.
- Rubenstein JLR, Shimamura K, Martinez S and Puelles L (1998). Regionalization of the prosencephalic neural plate. *Annu Rev Neurosci* 21:445-477.
- Sampath K, Rubenstein AL, Cheng AM, Liang JO, Fekany K, Solnica-Krezel L, Korzh V et al. (1998). Induction of the zebrafish ventral brain and floorplate requires cyclops/nodal signalling. *Nature* 395:185-9.
- Schauerte HE, van Eeden FJ, Fricke C, Odenthal J, Strahle U and Haffter P (1998). Sonic hedgehog is not required for the induction of medial floor plate cells in the zebrafish. *Development* 125:2983-93.
- Schier AF, Neuhauss SC, Harvey M, Malicki J, Solnica-Krezel L, Stainier DY, Zwartkruis F, Abdelilah S, Stemple DL, Rangini Z, Yang H and Driever W (1996). Mutations affecting the development of the embryonic zebrafish brain. *Development* 123:165-78.
- Schilling TF, Piotrowski T, Grandel H, Brand M, Heisenberg CP, Jiang YJ, Beuchle D et al. (1996). Jaw and branchial arch mutants in zebrafish I: branchial arches. *Development* 123:329-44.
- Schmid B, Furthauer M, Connors SA, Trout J, Thisse B, Thisse C and Mullins MC (2000). Equivalent genetic roles for *bmp7/snailhouse* and *bmp2b/swirl* in dorsoventral pattern formation. *Development* 127:957-67.
- Schmitz B, Papan C and Campos-Ortega JA (1993). Neurulation in the anterior trunk region of the zebrafish *Brachydanio rerio*. *Roux's Arch Dev Biol* 202:250-59.
- Schoenwolf GC and Delongo, J. (1980) Ultrastructure of secondary neurulation in the chick embryo. *Am J Anat* 158:43-63.
- Schoenwolf GC (1984). Histological and ultrastructural studies of secondary neurulation in mouse embryos. *Am J Anat* 169:361-76.
- Schoenwolf GC (2003) personal communication.
- Schulte-Merker S, Lee KJ, McMahon AP and Hammerschmidt M (1997). The zebrafish organizer requires *chordino*. *Nature* 387:862-3.
- Sepich DS, Wegner J, O'Shea S and Westerfield M (1998). An altered intron inhibits synthesis of the acetylcholine receptor alpha-subunit in the paralyzed zebrafish mutant *nic1*. *Genetics* 148:361-72.
- Shum AS and Copp AJ (1996). Regional differences in morphogenesis of the neuroepithelium suggest multiple mechanisms of spinal neurulation in the mouse. *Anat Embryol (Berl)* 194:65-73.

- Smith JL and Schoenwolf GC (1991). Further evidence of extrinsic forces in bending of the neural plate. *J Comp Neurol* 307:225-36.
- Sirotkin HI, Gates MA, Kelly PD, Schier AF and Talbot WS (2000). Fast1 is required for the development of dorsal axial structures in zebrafish. *Curr Biol* 10:1051-4.
- Strahle U and Blader P (1994). Early neurogenesis in the zebrafish embryo. *Faseb J* 8: 692-8.
- Streisinger G, Walker C, Dower N, Knauber D and Singer F (1981). Production of clones of homozygous diploid zebra fish (*Brachydanio rerio*). *Nature* 291:293-296.
- Sunshine, J., Balak, K., Rutishauser, U. and Jacobson, M. (1987). Changes in neural cell adhesion molecule (NCAM) structure during vertebrate neural development. *Proc Natl Acad Sci U S A* 84:5986-90.
- Swalla BJ (1993). Mechanisms of gastrulation and tail formation in ascidians. *Microsc Res Tech* 26:274-84.
- Topczewski J, Sepich DS, Myers DC, Walker C, Amores A, Lele Z, Hammerschmidt M et al. (2001). The zebrafish glypican knypek controls cell polarity during gastrulation movements of convergent extension. *Dev Cell* 1:251-64.
- Trevarrow B, Marks DL and Kimmel CB (1990). Organization of hindbrain segments in the zebrafish embryo. *Neuron* 4:669-679.
- Tropepe V and Sive HL (2003). Can zebrafish be used as a model to study the neurodevelopmental causes of autism? *Genes Brain Behav* 2:268-81.
- Varga ZM, Amores A, Lewis KE, Yan YL, Postlethwait JH, Eisen JS and Westerfield M (2001). Zebrafish smoothed functions in ventral neural tube specification and axon tract formation. *Development* 128:3497-509.
- von Kupffer C (1890). Die Entwicklung von *Petromyzon Planeri*. *Arch mikrosk Anat* 35.
- Wallingford JB and Harland RM (2002). Neural tube closure requires Dishevelled-dependent convergent extension of the midline. *Development* 129:5815-25.
- Wei, X. and Malicki, J. (2002). *nagie oko*, encoding a MAGUK-family protein, is essential for cellular patterning of the retina. *Nat Genet* 31:150-7.
- Wiellette E, Grinblat Y, Austen M, Hopkins N and Sive H (2001). An insertional screen for identification of genes required for neural induction and patterning in the zebrafish. *FASB J* 15:A1071.
- Wienholds E, Schulte-Merker S, Walderich B and Plasterk RH (2002). Target-selected inactivation of the zebrafish *rag1* gene. *Science* 297:99-102.

- Wienholds E, van Eeden F, Kusters M, Mudde J, Plasterk RH and Cuppen E (2003). Efficient target-selected mutagenesis in zebrafish. *Genome Res* 13:2700-7.
- Wiggan O and Hamel PA (2002). Pax3 regulates morphogenetic cell behavior in vitro coincident with activation of a PCP/non-canonical Wnt-signaling cascade. *J Cell Sci* 115:531-41.
- Wilson SW, Ross LS, Parrett T and Easter SS Jr (1990). The development of a simple scaffold of axon tracts in the brain of the embryonic zebrafish, *Brachydanio rerio*. *Development* 108:121-145.
- Wolff T and Rubin GM (1998). Strabismus, a novel gene that regulates tissue polarity and cell fate decisions in *Drosophila*. *Development* 125:1149-59.
- Woo K and Fraser SE (1997). Specification of the zebrafish nervous system by nonaxial signals. *Science* 277:254-257.
- Wullimann MF (1998). The central nervous system. In: Evans DH (ed). *The Physiology of Fishes* (Second edition). CRC Press LLC, New York, pp. 245-281.
- Wullimann MF and Puelles L (1999). Postembryonic neural proliferation in the zebrafish forebrain and its relationship to prosomeric domains. *Anat Embryol* 329:329-348.
- Yeo SY, Little MH, Yamada T, Miyashita T, Halloran MC, Kuwada JY, Huh TL et al. (2001). Overexpression of a slit homologue impairs convergent extension of the mesoderm and causes cyclopia in embryonic zebrafish. *Dev Biol* 230:1-17.
- Zeng L, Fagotto F, Zhang T, Hsu W, Vasicek TJ, Perry WL 3<sup>rd</sup>, Lee JJ, Tilghman SM, Gumbiner BM and Costantini F (1997). The mouse Fused locus encodes Axin, an inhibitor of the Wnt signaling pathway that regulates embryonic axis formation. *Cell* 90:181-92.
- Zhang J, Talbot WS and Schier AF (1998). Positional cloning identifies zebrafish one-eyed pinhead as a permissive EGF-related ligand required during gastrulation. *Cell* 92:241-51.

## Chapter Three

# Characterization and classification of 20 zebrafish brain morphology mutants

Expanded and Adapted From:

Laura Anne Lowery, Gianluca De Rienzo, Jennifer H. Gutzman, and Hazel Sive.  
Characterization and classification of zebrafish brain morphology mutants.  
In preparation for submission.

## Contributions:

LAL helped design the study, collected and categorized the mutants, performed the shelf-screen of the Hopkins lab retroviral insertion mutants, performed the brain ventricle imaging of 27 figure panels, compiled all figures, and wrote the manuscript. GD carried out the immunohistochemistry and *in situ* hybridization experiments, and participated in the brain ventricle imaging for 9 panels. JHG participated in the brain ventricle imaging for 7 panels. HS participated in the conception and design of the study and edited the manuscript.





## **Abstract**

The mechanisms by which the vertebrate brain achieves its three-dimensional structure are clearly complex, requiring the functions of many genes. Using the zebrafish as a model, we have begun to define genes required for brain morphogenesis, including brain ventricle formation, by studying 17 mutants previously identified as having embryonic brain morphology defects and identifying 3 additional brain morphology mutants in a shelf-screen of retroviral insertion mutants. We report the phenotypic characterization of these 20 mutants at several time-points using brain ventricle injection and imaging and immunohistochemistry with neuronal markers. These mutants can be broadly classified into two groups, one affecting initial brain shaping and the other affecting later brain ventricle expansion. Within these two classes, mutants can be further subdivided based on the specific brain phenotypes. This study defines several functions that are required for brain morphogenesis. During initial brain shaping, these include midline separation (requiring epithelial junction formation and maintenance, cell proliferation, and cell shape changes), ventricle inflation (requiring ion pumping), midbrain-hindbrain boundary constriction (requiring basement membrane), and a requirement for transcriptional regulation. Later brain ventricle expansion requires cardiovascular circulation, the extracellular matrix, and transcription/splicing-dependent events. We suggest that these processes are likely to be used during brain morphogenesis throughout the vertebrates.

## Background

Organ function is dependent not only on proper tissue specification, but also on the three-dimensional organization of those tissues, directed by morphogenetic processes. In vertebrates, the embryonic brain originates from a simple columnar epithelium that forms a tube which will become the brain and spinal cord (Gray and Clemente 1985). Brain morphogenesis occurs as the anterior neural tube undergoes a series of bends and constrictions to subdivide the brain into the future forebrain, midbrain, and hindbrain that allow it to pack into the skull. The first morphogenetic event is formation of a constriction at the midbrain-hindbrain boundary (Lowery and Sive 2004; Lowery and Sive 2005). Another key event in brain morphogenesis is the opening of the brain ventricles, cavities inside the brain which contain cerebrospinal fluid (Lowery and Sive 2005). Correct brain structure is intimately connected to normal brain function, as abnormalities in brain structure during development are correlated with a wide range of neurodevelopmental disorders (Kurokawa et al 2000; Gilmore et al 2001; Hardan et al 2001; Rehn and Rees 2005; Nopoulos et al 2007).

Brain morphogenesis requires the function of many genes, but these have generally not been well-characterized. The zebrafish is an ideal model system for these studies, since brain morphogenesis can be live-imaged at single cell resolution, and mutants defective in brain morphogenesis can be identified. Furthermore, the early structure of the zebrafish brain is very similar to that of other vertebrates, including chicken, rat and human, further indicating that this is a useful model system (Tropepe and Sive 2003; Lowery and Sive 2004; Jo et al 2005). In order to identify the genetic mechanisms that regulate brain morphogenesis, we have examined 20 zebrafish brain mutants previously suggested to have abnormal embryonic brain morphology or newly identified in a shelf-screen for brain morphology phenotypes (Jiang et al 1996; Schier et al 1996; Amsterdam et al 2004). Seventeen of these mutants were identified in two large-scale mutagenesis screens (Jiang et al 1996; Schier et al 1996). Together, Schier et al. and Jiang et al. identified 33 mutants with various embryonic brain morphology defects, 23 of which were described as having defects in embryonic brain ventricle morphology but their specific brain ventricle phenotypes were not reported. Through the generous sharing of the zebrafish community, we established 17 of these lines in our lab. Additionally, we conducted a shelf-screen of 300 retroviral insertion mutants (Amsterdam et al 2004), identifying three mutants with brain ventricle phenotypes. In this report, we describe the brain phenotypes of all 20 of these

mutants, including three mutants, *nagie oko*, *snakehead*, and *whitesnake*, on which we have previously published (Lowery and Sive 2005; Lowery et al 2007) (see Chapter 4 and Appendix 1). Based on these data, we classify these mutants and describe some of the processes required for normal brain morphogenesis.

## Results and Discussion

### *Mutants can be classified based on brain morphology and timing of phenotype onset*

We have suggested that early brain morphogenesis in zebrafish occurs in two phases (Lowery and Sive 2005)(see Chapter 4). The first phase, occurring between 17 hours post fertilization (hpf) and 24 hpf, includes the shaping of the brain epithelium, as the straight neural tube undergoes regionally-specific bends and also opens to form the brain ventricles (Lowery and Sive 2005). During the second phase, which occurs between 24 and 36 hpf, along with the onset of heartbeat and circulation, the brain shape changes minimally, but both the amount of brain tissue and the volume of the brain ventricles increase substantially (Lowery and Sive 2005; Mueller and Wullimann 2005; Bayer and Altman 2007).

In order to examine the phenotypes of brain morphology mutants, we first analyzed initial brain morphogenesis of each mutant between 17 hpf and 36 hpf using brightfield microscopy (Table 3.1; data not shown). One criterion for calling each mutant a “brain morphology” mutant is that it makes a healthy neural tube with no visible necrosis through at least 20 hpf (not shown), implying that earlier stages of neural development, including neurulation, are normal. While numerous mutants in the shelf-screen exhibited brain phenotypes, almost all of them were accompanied by significant visible necrosis, and thus all of these were excluded from further analysis. From the shelf-screen of retroviral insertion mutants, three mutants (*mib*, *fbxo5*, and *ppp1r12a*) showed abnormal brain morphology but no visible necrosis, and thus we used these mutants for further studies.

We observed that the abnormal brain phenotypes of 17 mutants are obvious by 20-21 hpf, indicating that initial brain shaping and opening were perturbed. The remaining three mutants (*vip*, *nat*, *wis*) appear to have wild-type brain morphology until 28 hpf, at which point brain morphology defects become apparent, indicating that these mutants are defective in brain expansion (Table 3.1).

Brain morphogenesis occurs on neuroepithelium that has already acquired initial anteroposterior and dorsoventral pattern. We therefore wondered whether any early brain phenotypes result from patterning defects. Although Schier et al. 1996 and Jiang et al. 1996 reported that expression of various patterning markers is normal in brain morphology mutants, we extended analysis of patterning using *in situ* hybridization for the anteroposterior markers *krox20* and *pax2a*, and the dorsoventral patterning markers *shh* and *zic1*. No obvious abnormalities are obvious, although we cannot exclude subtle perturbations (data not shown).

All 17 early mutants appear to have brain ventricles of reduced size by brightfield microscopy. For these mutants, we augmented our analyses at two time-points by injecting a fluorescent dye into the brain cavity to highlight the brain ventricular space (Lowery and Sive 2005). From this assay, the 17 early mutants can be separated into 4 phenotypic classes, as detailed below.

***Initial brain shaping – Class 1 - “Midline separation” defects (nok, moe, ome, has, mib, fbxo5, ppp1r12a, zon, atl)***

One group of mutants shows defects during the event we have termed “midline separation”. After neurulation in zebrafish, the neural tube is closed but shows a distinct midline (Lowery and Sive 2004). The tube subsequently opens at the midline, leaving the ventricular space centrally (that is filled with fluid) (Fig. 3.1A). Brain ventricle injections show that midline separation is perturbed in nine mutants analyzed (Fig. 3.1B-T). In these mutants, the hindbrain tube does not open uniformly. In several of these mutants, opening of the forebrain and midbrain is also perturbed. At 22 hpf, either the sides of the brain do not open at all (as throughout in *nok*, Fig. 3.1B, and in forebrain and midbrain of *zon*, Fig. 3.1N), or there are localized regions where the hindbrain tube does not separate at the midline (arrows, Fig. 3.1C-E, K-O). These phenotypes persist through at least 36 hpf, although there is a range of severity (Fig. 3.1G-J, P-T).

Four of the mutants in this group correspond to mutations in genes previously implicated in epithelial polarity and junction formation. The most severe midline separation mutant is *nagie oko* (*nok*), which has a mutation in the *mpp5* gene encoding a MAGUK protein localized to apical junction complexes (Wei and Malicki 2002). This mutant has an almost straight brain tube with no or little brain opening at 24 hpf (Fig. 3.1B). When dye is injected into the midline

where the hindbrain ventricle normally opens, the dye does not diffuse into other areas of the brain, suggesting that the brain tube is stuck shut (Fig. 3.1B). This defect persists through 36 hpf (Fig. 3.1G). We have previously observed in histological sections that *nok* mutants have a disorganized epithelium with no continuous midline, although there are small, intermittent regions with a midline present (Lowery and Sive 2005). We suggest that these obstructions in the midline most likely correspond to locations where the brain tube is stuck shut.

Three mutants, *mosaic eyes (moe)*, *oko meduzy (ome)* and *heart and soul (has)*, which have mutations in the *erythrocyte membrane protein band 4.1 like 5 (epb4115)*, *crumbs homolog 2 (crb2)* and *protein kinase C iota (prkci)* genes, respectively (Horne-Badovinac et al 2001; Jensen and Westerfield 2004; Omori and Malicki 2006), display similar brain phenotypes. All three have disrupted hindbrain opening, with several small openings instead of one large opening at 22 hpf (Fig. 3.1C-E) and persisting through 36 hpf (Fig. 3.1H-J), and *moe* has disrupted forebrain and midbrain opening as well (Fig. 3.1C,H). A hypomorphic allele of *nok*, *wi83* (Wiellette et al 2004; Lowery and Sive 2005), shows a less severe midline separation phenotype than the null mutant (not shown), but it is still more severe than the null *ome* and *has* phenotypes, but not the *moe* phenotype (Horne-Badovinac et al 2001; Wei and Malicki 2002; Omori and Malicki 2006). However, loss of function of Mpp5, Epb4115, Crb2a, or Prkci results in similar phenotypes in other organ systems, such as abnormal junction formation in the retina and abnormal heart tube morphogenesis (Yelon et al 1999; Horne-Badovinac et al 2001; Wei and Malicki 2002; Omori and Malicki 2006; Rohr et al 2006). The Mpp5, Epb4115, Crb2a, and Prkci proteins co-localize at the apical surface of neuroepithelia and control apical junction formation and epithelial apicobasal polarity (Horne-Badovinac et al 2001; Hsu et al 2006; Omori and Malicki 2006), although the mechanisms underlying brain phenotypes in these mutants have not yet been thoroughly explained. While the adherens and tight junctions of the *nok* mutant are abnormal (Lowery and Sive 2005), the junctions in the brain epithelium of *ome* and *has* mutants appear normal (Horne-Badovinac et al 2001; Omori and Malicki 2006), and thus it is unclear what is leading to the midline separation defect.

How do apical junction complex proteins regulate brain morphogenesis? In the case of the *nok* mutant, the neural tube midline is defective immediately after neurulation (Lowery and Sive 2005), suggesting that Mpp5 may be required prior to neural tube closure, for normal epithelial integrity, apicobasal polarity, and formation of a midline corresponding to a plane of

cell separation. Without a midline, the neural tube cannot open properly. In the case of *ome* and *has*, the neural tube does open in places, suggesting that the midline forms normally. However, apical junction regulation is likely required to coordinate the epithelium and allow it to change shape. For example, during gut tube formation, *has* often shows multiple small lumens rather than one large one, due to a lack of apical clustering of adherens junctions (Horne-Badovinac et al 2001). Further investigation will be required to determine the precise mechanisms that are disrupted in each mutant and how these regulate midline separation.

Finally, five additional mutants, *mindbomb* (*mib*), *fbxo5* (*fbxo5*), *ppp1r12a* (*ppp1r12a*), *zonderzon* (*zon*), and *atlantis* (*atl*), also show midline separation defects (Fig. 3.1K-T). Three of these (*mib*, *fbxo5*, and *ppp1r12a*) were identified in the shelf-screen of retroviral insertion mutants as having specific brain morphology defects, and this is the first report of any brain phenotype for *fbxo5* and *ppp1r12a*.

The *mib* mutant, which has a retroviral insertion mutation in the E3 ubiquitin ligase *mindbomb* required for Delta/Notch signaling (Itoh et al 2003), has a severe midline separation defect in the hindbrain by 30 hpf (Fig. 3.1P), although the phenotype at 24 hpf is not as obvious (Fig. 3.1K). Unlike the other mutants reported in this study, the brain phenotype of *mib* has been previously characterized and is relatively well-understood. Due to absence of Notch signaling in the hindbrain, an overproduction of early differentiating neurons occurs, accompanied by a loss of neuroepithelial cells (Bingham et al 2003). Loss of midline neuroepithelial cells leads to disrupted ventral midline patterning, and the abnormally differentiating neurons cluster and fuse across the midline (Bingham et al 2003) leading to the midline separation defects seen in Fig. 3.1P. This demonstrates the importance of both patterning and neuroepithelial maintenance during brain morphogenesis and highlights that abnormal brain ventricle development can occur when neuronal development is perturbed.

The *fbxo5* mutant has a retroviral insertion mutation in the *F-box protein 5* gene, the zebrafish homolog to the mitotic regulator Emi1 (Reimann et al 2001). In addition to midline separation defects (Fig. 3.1L,Q), we have observed that *fbxo5* mutants display significantly reduced cell proliferation, no body growth, and increased cell size (data not shown). However, it is unclear exactly how cell proliferation and midline separation are coordinated. Perhaps there is not enough tissue for brain ventricle opening, or cells may need to be actively cycling to respond

to morphogenetic cues. Further analysis will be needed to understand the underlying morphogenetic cause of the phenotype.

The last mutant identified in the shelf-screen is *ppp1r12a* (Amsterdam et al 2004), which shows the midline separation defect at both 24 and 30 hpf (Fig. 3.1M,R). This mutant has a retroviral insertion mutation in the myosin regulatory light chain phosphatase, *protein phosphatase 1 regulatory inhibitor subunit 12a*, homolog of mouse and human MYPT1 (myosin phosphatase target subunit 1). Mypt1 is one of the subunits of myosin phosphatase, is a key regulator of myosin activity, and is implicated in integrating signaling cascades for cytoskeletal remodeling and directly influencing cell contractility, cell morphology, and adhesion (Eto et al 2005; Xia et al 2005). We hypothesize that the midline separation defect observed is a result of aberrant cytoskeletal and cell shape changes that have been shown to occur with loss of Mypt1 in other systems (Eto et al 2000; Mizuno et al 2002; Tan et al 2003).

The mutations corresponding to *zon* and *atl* have not been identified. While the *zon* midline separation defect can be severe at 24 hpf (Fig. 3.1N) and sometimes persists through 36 hpf (Fig. 3.1S), the expressivity is variable. The *atl* mutant, however, consistently shows a mild midline separation defect, with at least one point of contact at the midline within the hindbrain between 24 and 30 hpf (Fig. 3.1O,T arrows). This mutant is the least severe of the group, and in some, the brain appears wild-type by 36 hpf. The *atl* mutant is also the only mutant described in this paper in which some homozygous mutants are viable. Further analysis of *zon* and *atl* and identification of their corresponding genes will be required to understand the underlying cause of the midline separation phenotype.

One question we have considered is the relationship between early brain morphology and neuronal development and function. In particular, do any of these midline separation mutants also display neuronal abnormalities? We examined several axon tracts in the early embryo, looking at the early axon scaffolds in the forebrain and midbrain at 36 hpf, which can be visualized with an antibody to acetylated tubulin (Chitnis and Kuwada 1990), at the reticulospinal neurons in the hindbrain at 36 hpf with an antibody to neurofilament M (Pleasure et al 1989), and at commissural neurons in the hindbrain at 30 hpf with the zn8 antibody (Trevarrow et al 1990). Within most of the mutants in this class, all neuronal tracts appear normal, although *zon* shows reticulospinal neuron defects with reduced expressivity (not shown), *mib* is already known to have abnormal axonal development (Bingham et al 2003; Riley et al

2004), and the *fbxo5* and *ppp1r12a* mutants have not been analyzed at this time. The data from the other five mutants suggest that the midline separation defects in these mutants and formation of the early axon scaffold are under independent control.

### ***Initial brain shaping – Class 2 - Inflation defect (snk)***

The *snakehead* (*snk*) mutant lacks visible brain ventricles at 22 hpf by brightfield microscopy (Fig. 3.2B). By 30 hpf, however, small ventricles are visible by dye injection (Fig. 3.2D), and at this stage, *snk* brain morphology is similar to wild type, although the brain tissue and all three ventricles are smaller than normal (Fig. 3.2D). *snk* corresponds to a mutation in the *atp1a1* gene, encoding a Na<sup>+</sup>K<sup>+</sup> ATPase alpha subunit (Lowery and Sive 2005). This pump is likely required for embryonic CSF secretion by creating an ionic gradient across the membrane, that results in water flow into the luminal space (Lowery and Sive 2005). It is likely that the absence of fluid inside the brain ventricles leads to the *snk* brain phenotype, indicating that normal brain morphogenesis requires inflation of the brain ventricles with fluid (Lowery and Sive 2005). At the stages analyzed, we detected no obvious abnormalities in the neuronal populations examined (Table 3.1 and data not shown).

### ***Initial brain shaping – Class 3 - Midbrain-hindbrain boundary and ventricle defects (sly, gup)***

In two mutants, *sleepy* (*sly*) and *grumpy* (*gup*), the acute basally-located epithelial constriction that normally occurs by 22 hpf at the midbrain-hindbrain boundary (MHB) does not form (Fig. 3.3B,C). Furthermore, all brain ventricles are reduced in size compared to wild type (Fig. 3.3B,C), although by 36 hpf, MHB shape and hindbrain ventricle size are partially recovered (Fig. 3.3E,F). The *sly* and *gup* loci both encode components of the extracellular matrix proteins, *laminin gamma1* and *laminin beta1*, respectively. These genes have previously been shown to play a number of roles during zebrafish developmental processes including notochord differentiation (Parsons et al 2002), retina morphogenesis (Biehlmaier et al 2007), blood vessel formation (Pollard et al 2006), and retinotectal axon pathfinding (Karlstrom et al 1996). As laminin in the basement membrane outlines the brain epithelium (data not shown), we hypothesize that loss of laminin in the basement membrane results in the inability to form the MHB constriction and undergo additional brain shaping processes.



Consistent with the previously reported role of laminin during axon guidance, we observed that the hindbrain reticulospinal neurons are disrupted in both mutants (Fig. 3.3H,I), as are the commissural neurons (Fig. 3.3K,L). Although the early axon scaffolds in the forebrain and midbrain are disorganized in the *sly* mutant (Fig. 3.3N), they are virtually indistinguishable from wild type in the *gup* mutant, suggesting that *gup/lamb1* function is not essential for axonogenesis (Fig. 3.3O). It is possible that the axon defects of the *sly* and *gup* mutants are functionally distinct from the brain morphology defect.

#### **Initial brain shaping – Class 4 - Reduced ventricle size (*ful*, *lnf*, *ott*, *log*, *esa*)**

Another class of mutants, including *otter* (*ott*), *fullbrain* (*ful*), *landfill* (*lnf*), *logelei* (*log*), and *eraserhead* (*esa*), exhibit reduced brain ventricle size and occasional misshapen midbrain tissue at 22 and 36 hpf, although the midlines of these mutants appear to separate normally (which distinguishes these mutants from Class 1 above) and there are no other significant phenotypic abnormalities of brain morphology (Fig. 3.4A-L). The brain phenotypes of *ott*, *ful*, *lnf*, and *log* are very similar, although at 22 hpf, *ott* ventricles are generally the most reduced in size, and the *log* ventricles are the least reduced, relative to wild type (Fig. 3.4D,E). The *esa* phenotype, while similar to the others in ventricle size reduction, is more variable (Fig. 3.4F,L) and is occasionally accompanied by additional brain and body phenotypes which do not occur elsewhere in the group. These abnormalities include gastrulation defects (data not shown), which sometimes result in a twisting of the brain tissue (not shown).

Since the phenotypes of *ott*, *ful*, *lnf*, and *log* appear similar, complementation crosses were performed between them. While a note added in the proof of (Schier et al 1996) specified that *logelei* does not complement *ott*, we did not find this to be the case. Three individual crosses of *log* and *ott* heterozygote carriers resulted in 100% wild-type embryos (n=154), demonstrating that *log* and *ott* do complement each other genetically. Crosses of all other mutant combinations also showed genetic complementation, indicating that each of these corresponds to a distinct locus.

We observed that the brain phenotypes of this mutant class resembled that of the mutants *motionless* (Guo et al 1999) and *kohtalo* (Hong et al 2005), which both have mutations in *med12*, a subunit of the mediator complex (Hong et al 2005; Wang et al 2006). A complementation cross between *mot* and *ott* resulted in 14 mutants (21%) and 54 wild-types (79%), suggesting that *ott* and *mot* are allelic, although the specific mutation in the *ott* mutant has not yet been reported.

What role does the mediator complex play during development, and what could be responsible for the *ott* brain morphology phenotype? The mediator complex is a multi-protein complex that regulates transcription by acting as a bridge between DNA-binding transcription factors and RNA polymerase II (Conaway et al 2005). Several mediator subunits, including *med12*, possess gene-specific activity (Yoda et al 2005; Rau et al 2006; Loncle et al 2007), and *med12* has been shown to interact with beta-catenin and transduce Wnt signaling (Kim et al 2006). In the zebrafish *med12* mutant, the morphogenesis of many organ systems are affected as tissue extension, cell movements, and generation of tissue architecture are all disrupted in various tissues (Hong et al 2005). Interestingly, polymorphisms of the *med12* gene in humans are associated with an increased risk for schizophrenia (Philibert et al 2007), a disorder which is correlated with abnormal brain structure and increased ventricle size (Antonova et al 2004; Crespo-Facorro et al 2007).

Zebrafish mutants deficient in *med12* display specific neuronal defects, though not all neurons are affected (Guo et al 1999; Wang et al 2006). We find that *lnf*, *ful*, and *ott* all show strong defects in the hindbrain axons, with reticulospinal and commissural neurons reduced or missing (Fig. 3.4N-P,T-V), although the early axon scaffolds in the forebrain and midbrain look normal (not shown). The *log* mutant has reduced commissural neurons (Fig. 3.4W) but all others appear normal (Fig. 3.4Q and not shown). The *esa* mutant phenotype is different than the others in that the reticulospinal and commissural neurons appear normal (Fig. 3.4R,X), but the axons in the forebrain and midbrain are severely (but variably) affected, having a “feathered” appearance (Fig. 3.4Z).

### ***Later brain expansion mutants***

In addition to the 13 early brain shape mutants described above, three of the brain morphology mutants, *viper* (*vip*), *natter* (*nat*), and *whitesnake* (*wis*), show only later defects in brain morphology. All three display completely normal brain ventricles at 22 hpf (data not shown), although by 28 hpf, it is apparent that the dorsoventral height of the hindbrain ventricle is reduced (Fig. 3.5B,C,D, bars). All three also lack heartbeat and circulation. It was previously shown that circulation is required for later brain expansion (Schier et al 1996; Lowery and Sive 2005), and thus, it is possible that the brain defects of these mutants are secondary to a lack of circulation. As the *vip* mutant, corresponding to an unknown mutation, shows no other phenotypes other than reduced brain ventricle height and lack of heartbeat/circulation, and as the

brain phenotype is similar to that of the *silent heart* mutant corresponding to a cardiac-specific troponin (Lowery and Sive 2005), it is quite possible that the brain phenotype of this mutant is solely due to lack of circulation.

Conversely, the *nat* brain defect is more severe than the *vip* phenotype (compare Fig. 3.5B and C), and it is likely that the brain phenotype of this mutant is due to brain-specific effects as well as lack of circulation. The *nat* mutant corresponds to the fibronectin gene *fn1*, a component of the extracellular matrix (ECM), indicating that the ECM is essential for normal brain ventricle expansion, consistent with the requirement for laminin function (class 3 mutants, Fig. 3.3) for initial brain shaping. However, the phenotypes of the laminin mutants *sly* and *gup* are different from *nat* and appear earlier. This indicates that not all ECM components are required at the same time or that the maternal contribution of fibronectin persists longer than that of laminin proteins.

The *wis* mutant has abnormalities in other aspects of embryonic brain morphology (not shown, (Lowery et al 2007)) in addition to the reduction in brain ventricle height (Fig. 3.5D), and further analysis of this mutant and its corresponding gene, *sfpq*, is described elsewhere (Lowery et al 2007). This mutant has defects in neural development, accompanied by increased cell death (Lowery et al 2007), and these abnormalities may later result in abnormal brain morphology.

## Conclusions

Analysis of these brain morphology mutants has allowed us to define several steps and corresponding gene functions required for brain morphogenesis (Fig. 3.6). Processes involved in initial brain shaping include midline separation, brain lumen inflation, midbrain-hindbrain boundary formation, and other mechanisms affecting brain morphology at these early stages. Midline separation requires the function of epithelial integrity and junction components, *mpp5*, *epb4115*, *prcki*, and *crb2*, Notch ubiquitin ligase *mindbomb*, cell proliferation regulator *fbxo5*, and cell shape-affecting myosin regulator molecule *ppp1r121a*. Brain lumen inflation requires the Na<sup>+</sup> K<sup>+</sup> ATPase, *atp1a1*. Midbrain-hindbrain boundary formation requires the extracellular matrix protein laminin, specifically the *lamc1* and *lamb1* genes which encode the gamma and beta chains, respectively, components of the laminin heterotrimer. The transcription regulator

*med12*, which can affect early neuronal development (Guo et al 1999; Wang et al 2006), also has an effect on early brain morphology. Later brain ventricle expansion requires the extracellular matrix protein fibronectin in order to maintain normal ventricle height, as well as the splicing/transcription factor *sfpq*, which contributes to normal brain morphology. There are certainly many more genes whose function is required for brain morphogenesis, but that did not present in the mutant set we examined. This may be because the mutant set was not large enough or because earlier phenotypes obscured a later brain morphogenesis phenotype.

In conclusion, this detailed phenotypic characterization of 20 zebrafish brain mutants has enabled us to determine some of the various processes that are required for early brain morphogenesis. We suggest that these processes and their underlying mechanisms are conserved throughout the vertebrates.

## Experimental Procedures

### Fish lines and maintenance

*Danio rerio* fish were raised and bred according to standard methods (Westerfield 1995). Embryos were kept at 28.5°C and staged as described previously (Kimmel et al 1995). Times of development are expressed as hours post-fertilization (hpf).

Lines used were: *snk*<sup>to273a</sup>, *atl*<sup>tc234b</sup>, *ott*<sup>ta76b</sup>, *wis*<sup>tr241</sup>, *vip*<sup>tw212e</sup> (Jiang et al 1996), *nok*<sup>m227</sup>, *has*<sup>m567</sup>, *ome*<sup>m98</sup> (Malicki et al 1996), *moe*<sup>b781</sup> (Jensen and Westerfield 2004), *zon*<sup>m163</sup>, *ful*<sup>m133</sup>, *lnf*<sup>m551</sup>, *log*<sup>m673</sup>, *esa*<sup>m725</sup>, *sly*<sup>m86</sup> (Schier et al 1996), *mib*<sup>hi904</sup>, *fbxo5*<sup>hi2648</sup>, *ppp1r12a*<sup>hi2653</sup>, *gup*<sup>hi1113B</sup> (Amsterdam et al 2004), *nat*<sup>tl43c</sup> (Trinh and Stainier 2004), *mot*<sup>mot\_m807</sup> (Guo et al 1999). As *mot* and *ott* are allelic, these two alleles were used interchangeably in our mutant analysis.

### Brain ventricle imaging

Brain ventricle imaging was performed as described previously (Lowery and Sive 2005). Briefly, embryos were anesthetized in 0.1 mg/ml Tricaine (Sigma) dissolved in embryo medium prior to hindbrain ventricle microinjection with 2-10 nl dextran conjugated to Rhodamine (5% in 0.2 mol/l KCl, Sigma), and then embryos were imaged by light and fluorescence microscopy with a Leica dissecting microscope, using a KT Spot Digital Camera (RT KE Diagnostic Instruments). Images were superimposed in Photoshop 6 (Adobe).

## **Immunohistochemistry**

Whole-mount immunostaining was carried out using mouse anti-acetylated alpha tubulin (Sigma, 1:1000), mouse anti-neurofilament RM044 (Zymed #13-0500, 1:50), and mouse anti-zn8 (Developmental Studies Hybridoma Bank, 1:20). Goat anti-mouse Alexa Fluor 488 (Molecular Probes, 1:500) was used as a secondary antibody.

For labeling with acetylated tubulin and RM044 antibodies, dechorionated 36 hpf embryos were fixed in 2% trichloroacetic acid for 3 hours at room temperature, washed in PBS, permeabilized in 0.5 % Triton X in PBS and blocked in 0.5 % Triton X, 10% normal goat serum, 0.1% BSA in PBS for 3 hours, prior to incubation in antibody. Brains were flat-mounted in glycerol and imaged with confocal microscopy.

For labeling with zn8 antibody, dechorionated 30 hpf embryos were fixed in 4% paraformaldehyde overnight at 4 degrees, then rinsed in phosphate buffer and permeabilized in 0.5 % Triton X in phosphate buffer. Blocking was done for 4 hours at room temperature in 0.5 % Triton X, 10% normal goat serum, 0.1% BSA in phosphate buffer. Brains were flat-mounted in glycerol and imaged with confocal microscope.

To block pigmentation, embryos were incubated in 0.2mM 1-phenyl-2-thiourea in embryo media beginning at 22 hpf.

## **In situ hybridization**

RNA probes containing digoxigenin-11-UTP were synthesized from linearized plasmid DNA for *pax2.1* (Krauss et al 1991), *krox20* (Oxtoby and Jowett 1993), *zic1* (Grinblat et al 1998), and *shh* (Krauss et al 1993) as described (Harland 1991). Standard methods for hybridization and for single color labeling were used as described elsewhere (Sagerstrom et al 1996). After staining, embryos were fixed in 4% paraformaldehyde overnight at 4 degrees C and washed in PBS prior to mounting in glycerol and imaging with a Nikon compound microscope.

## **Acknowledgements**

We thank members of the Sive Lab for helpful comments and Olivier Paugois for fish husbandry. Many thanks to the Nusslein-Volhard lab for providing us with the *snk*, *atl*, *wis*, *vip*, and *ott* mutants, the Zebrafish International Resource Center for the *zon*, *ful*, *log*, *esa*, and *lnf* mutants, the Malicki lab for *nok*, *has*, and *ome*, the Zon lab for *sly*, Adam Amsterdam and the

Hopkins lab for allowing us to screen through their collection of retroviral insertion mutants and specifically for providing us with *gup*, *fbxo5*, *ppp1r12a*, and *mib*, the Jensen lab for *moe*, and the Stainier lab for *nat*. The zn8 antibody developed by B. Trevarrow was obtained from the Developmental Studies Hybridoma Bank developed under the auspices of the NICHD and maintained by the University of Iowa, Department of Biogoical Sciences, Iowa City, IA 52242. This work was conducted utilizing the W.M. Keck Foundation Biological Imaging Facility at the Whitehead Institute. The Zebrafish International Resource Center is supported by grant #RR12546 from the NIH-NCRR. This work was supported by NIH MH70926 and MH59942 to HLS, NIH NRSA pre-doctoral fellowship and Abraham J. Siegel Fellowship at the Whitehead Institute to LAL, MIT/CSBi/Merck postdoctoral fellowship to JHG.

**Table 3.1 – New Classifications of Brain Morphology Mutants**

Brain Phenotype	Locus <sup>allele</sup>	Gene	Gene Function	Brain phenotype Onset <sup>a</sup>	Neuronal Abnormalities <sup>b</sup>			Reference
					fb <sup>c</sup>	hb <sup>d</sup>	co <sup>e</sup>	
<b>Initial Shaping and Inflation</b>								
Midline separation defect	<i>nok</i> <sup>m227</sup>	<i>mpp5</i>	Junctions/epithelium	20 hpf				(Schier et al 1996; Wei and Malicki 2002)
	<i>moe</i> <sup>b781</sup>	<i>epb4115</i>	Junctions/epithelium	20 hpf				(Jensen and Westerfield 2004)
	<i>has</i> <sup>m567</sup>	<i>prkci</i>	Junctions/epithelium	21 hpf				(Schier et al 1996; Horne-Badovinac et al 2001)
	<i>ome</i> <sup>m98</sup>	<i>crb2</i>	Junctions/epithelium	21 hpf				(Schier et al 1996; Omori and Malicki 2006)
	<i>mib</i> <sup>h1904</sup>	<i>mib</i>	Delta/Notch signaling	21 hpf	ND	hb <sup>f</sup>	Co <sup>f</sup>	(Itoh et al 2003; Amsterdam et al 2004)
	<i>fbxo5</i> <sup>h1264B</sup>	<i>fbxo5</i>	Cell proliferation	20 hpf	ND	ND	ND	(Amsterdam et al 2004)
	<i>ppp1r12a</i>	<i>ppp1r12a</i>	Myosin regulator	20 hpf	ND	ND	ND	(Amsterdam et al 2004)
	<i>zon</i> <sup>m163</sup>	ND	ND	20 hpf		hb		(Schier et al 1996)
	<i>atl</i> <sup>h234b</sup>	ND	ND	21 hpf				(Jiang et al 1996)
Lumen inflation defect	<i>snk</i> <sup>h273a</sup>	<i>atp1a1</i>	NaK ATPase	19 hpf				(Jiang et al 1996; Schier et al 1996; Lowery and Sive 2005)
MHB abnormal	<i>sly</i> <sup>m86</sup>	<i>lamc1</i>	Extracellular matrix	21 hpf	fb	hb	Co	(Jiang et al 1996; Schier et al 1996; Parsons et al 2002)
	<i>gup</i> <sup>h1113B</sup>	<i>lamb1</i>	Extracellular matrix	21 hpf		hb	Co	(Jiang et al 1996; Schier et al 1996; Parsons et al 2002)
Reduced ventricles	<i>ott</i> <sup>h1a76b</sup>	<i>med12</i>	Transcription	20 hpf		hb	Co	(Jiang et al 1996; Wang et al 2006)
	<i>ful</i> <sup>m133</sup>	ND	ND	20 hpf		hb	Co	(Jiang et al 1996; Schier et al 1996)
	<i>lnf</i> <sup>m551</sup>	ND	ND	20 hpf		hb	Co	(Schier et al 1996)
	<i>log</i> <sup>m673</sup>	ND	ND	20 hpf		hb <sup>g</sup>	Co	(Schier et al 1996)
	<i>esa</i> <sup>m725</sup>	ND	ND	20 hpf	fb <sup>h</sup>			(Schier et al 1996)
<b>Later Brain Ventricle Expansion</b>								
Reduced ventricle height	<i>vip</i> <sup>h212e</sup>	ND	ND <sup>i</sup>	28 hpf	ND	ND	ND	(Jiang et al 1996)
	<i>nat</i> <sup>h143c</sup>	<i>fn1</i>	Extracellular matrix	28 hpf	ND	ND	ND	(Jiang et al 1996; Trinh and Stainier 2004)
Abnormal morphology	<i>wis</i> <sup>h241</sup>	<i>sfpq</i>	Splicing/transcription	28 hpf		hb <sup>j</sup>	ND	(Schier et al 1996; Lowery et al 2007)

### Table 3.1 Continued

<sup>a</sup> Other embryonic phenotypes may be visible earlier

<sup>b</sup> It is noted when obvious neuronal abnormalities are detected by whole mount immunohistochemistry. Cells left blank indicate no abnormalities are detected, although there may be subtle defects which are not apparent.

<sup>c</sup> Axon scaffolds in the forebrain are labeled with acetylated tubulin antibody at 36 hpf.

<sup>d</sup> Reticulospinal neurons in the hindbrain are labeled with RM044 antibody at 36 hpf.

<sup>e</sup> Commissural neurons in the hindbrain are labeled with zn8 antibody at 30 hpf.

<sup>f</sup> Described in (Bingham et al 2003; Riley et al 2004).

<sup>g</sup> The reticulospinal neurons of *log* were usually similar to wild-type, as shown in Fig. 3.3Q, but there were occasional missing neurons at low frequency (10-20%), with phenotypes similar to the other mutants in this group

<sup>h</sup> The phenotype of *esa* mutants were quite variable, ranging from severely disrupted axon scaffolds to wild-type-like scaffolds.

<sup>i</sup> As the only obvious mutant phenotype other than reduced ventricle height is lack of heartbeat, we speculate that the *vip* gene is important for some aspect of heart development and function.

<sup>j</sup> Many reticulospinal neurons of *wis* were absent, as shown in Lowery et al 2007.

ND = not determined; MHB = midbrain-hindbrain boundary



**Figure 3.1 Brain ventricle injections of *midline separation defect* class (class 1, described in the text).**

Dorsal views of living, anesthetized embryos are shown, anterior to right, at 22 hpf (A-E, K-O) and 32-36 hpf (F-J, P-T) with brightfield microscopy. Ventricles are injected with Rhodamine-dextran, except in G. Compared to WT (A, F), the left and right sides of the brain tube do not open uniformly in the midline separation mutants (B-E, G-J, K-O, P-T). In *nok* (B,G) and *moe* (C,H), dye injected into the hindbrain ventricle does not move. In the mutants (C,H) *moe*, (D,I) *ome*, (E,J) *has*, (K,P) *mib*, (L,Q) *fbxo5*, (M,R) *ppp1r12a*, (N,S) *zon*, (O,T) *atl*, there are regions where the tube opens separated by places where the sides appear to be touching (arrows). The ventricles of WT are labeled for comparison. F: forebrain ventricle, M: midbrain ventricle, H: hindbrain ventricle.

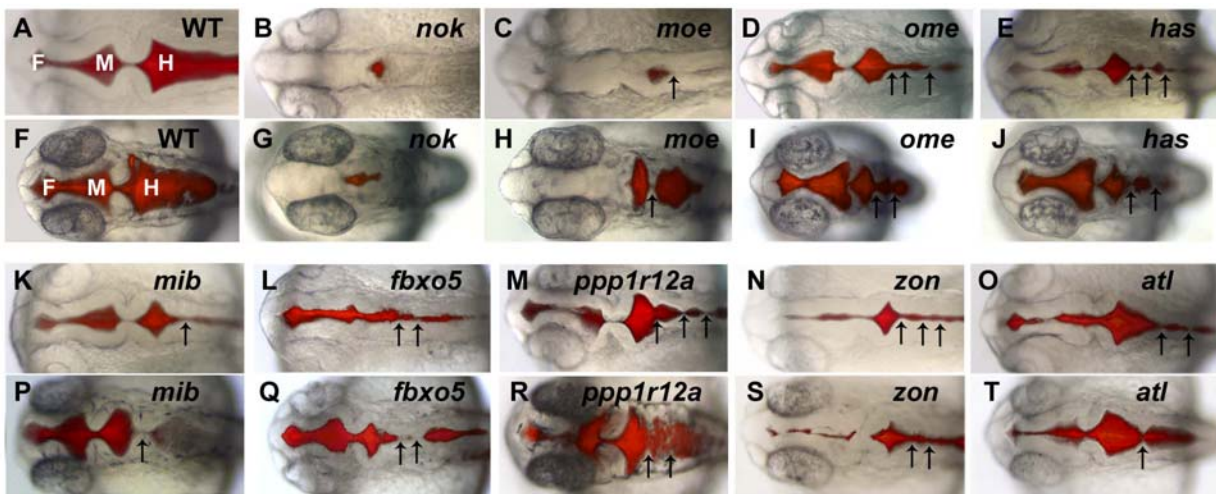




**Figure 3.2 Brain images of *brain inflation defect* class (class 2, described in the text).** Dorsal views of living, anesthetized embryos are shown, anterior to right, at 22 hpf (A,B) and 30 hpf (C,D) with brightfield microscopy. Ventricles are injected with Rhodamine-dextran, except in B. While the *snk* mutant at 22 hpf (B) has no visible ventricles, by 30 hpf (D), there are small ventricles in which dye can be injected, showing smaller but relatively normal shaping compared to wild type (A,C).

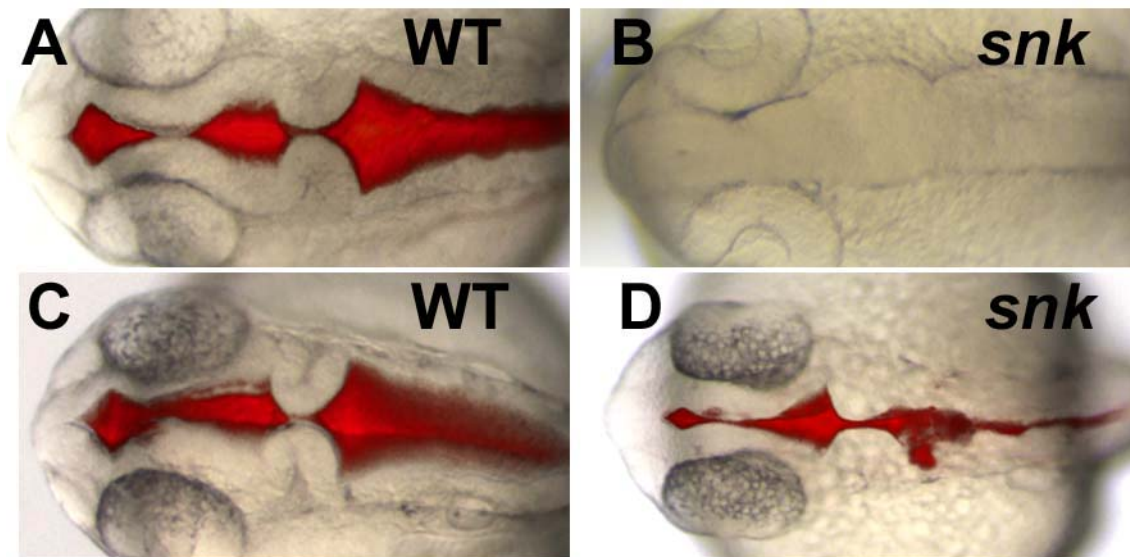




**Figure 3.3 Brain ventricle injections and neuronal antibody labelings for *MHB morphology defect* class.**

Dorsal views of living, anesthetized embryos are shown, anterior to right, at 22 hpf (A-C) and 36 hpf (D-F) with brightfield microscopy. Ventricles are injected with Rhodamine-dextran. At 22 hpf, both *sly* and *gup* (B,C) show an abnormal midbrain-hindbrain boundary. By 36 hpf, the *sly* and *gup* (E,F) boundary region has mostly recovered compared to WT (D), although the forebrain and midbrain ventricles are not as large as in WT. The ventricles of WT are labeled for comparison. F: forebrain ventricle, M: midbrain ventricle, H: hindbrain ventricle. (G-I) Dorsal views of 36 hpf hindbrain flatmounts, anterior is to the top, after labeling with the RMO44 Ab (reticulospinal neurons) shows disruption in axon pathfinding in both *sly* (H) and *gup* (I), compared to wild type (G). (J-L) Dorsal views of 30 hpf hindbrain flatmounts, anterior is to the top, after labeling with the zn8 Ab (hindbrain commissural neurons) shows reduced commissures and disruption in axon pathfinding in both *sly* (H) and *gup* (I), compared to wild type (G). (M-O) Lateral views of 36 hpf forebrain and midbrain flatmounts, anterior is to the left, dorsal is to the top, after labeling with acetylated tubulin Ab, which identifies the early axon scaffolds, shows that *sly* axonal pathfinding is disrupted (N), although *gup* (O) looks similar to wild type (M).

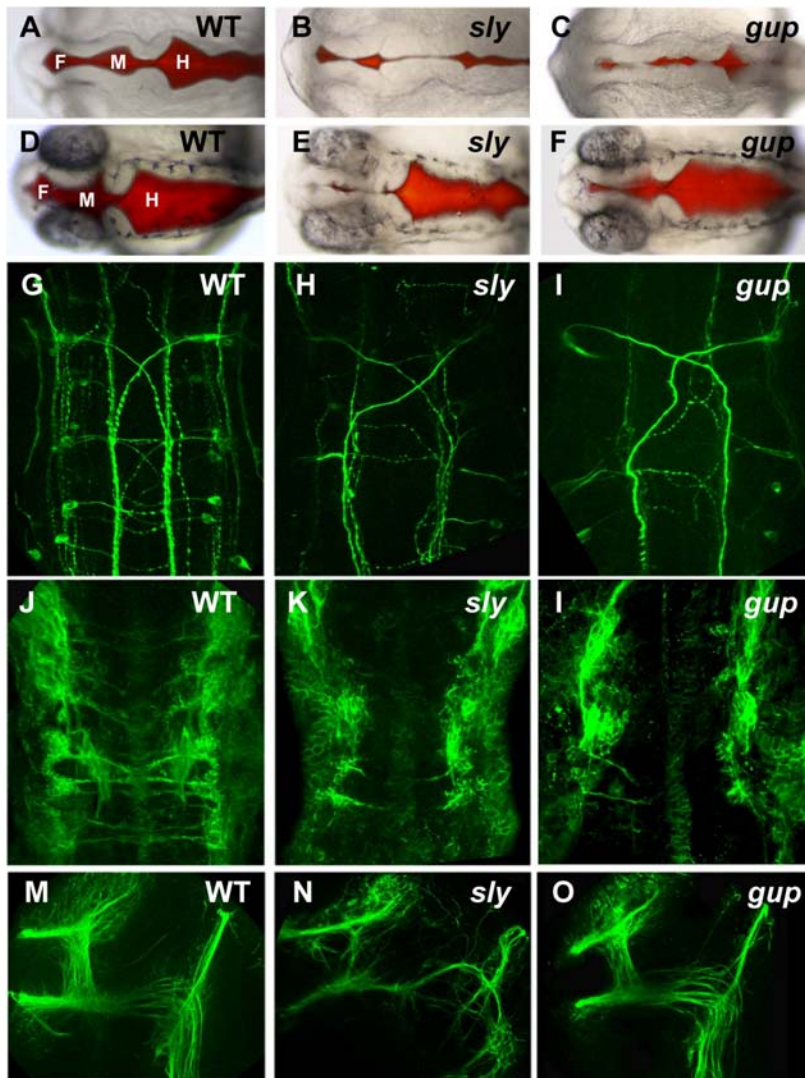




**Figure 3.4 Brain ventricle injections and antibody labelings for *reduced ventricle size* class.** Dorsal views of living, anesthetized embryos are shown, anterior to right, at 22 hpf (A-F) and 36 hpf (G-L) with brightfield microscopy. Ventricles are injected with Rhodamine-dextran. The brain ventricles of *lnf* (B,H), *ful* (C,I), *ott* (D,J), *log* (E,K), and *esa* (F,L) are all similarly reduced compared to wild type (A,G). (M-R) Dorsal views of 36 hpf hindbrain flatmounts, anterior is to the top, after labeling with the RMO44 Ab (reticulospinal neurons) shows reduced number of cell bodies and axons in *lnf* (N), *ful* (O), *ott* (P), and *log* (Q), compared to wild type (M), although *esa* (R) appears similar to wild type (M). (S-X) Dorsal views of 30 hpf hindbrain flatmounts, anterior is to the top, after labeling with the zn8 Ab (hindbrain commissural neurons) shows various levels of reduced commissures in *lnf* (T), *ful* (U), *ott* (V), and *log* (W), although *esa* (X) is indistinguishable from wild type (S). (Y,Z) Lateral views of 36 hpf forebrain and midbrain flatmounts, anterior is to the left, dorsal is to the top, after labeling with acetylated tubulin Ab, which identifies the early axon scaffolds, shows that *esa* axonal pathfinding is severely disrupted, with the axons having a “feathered” appearance rather than fasciculating normally (Z), compared to wild type (Y).

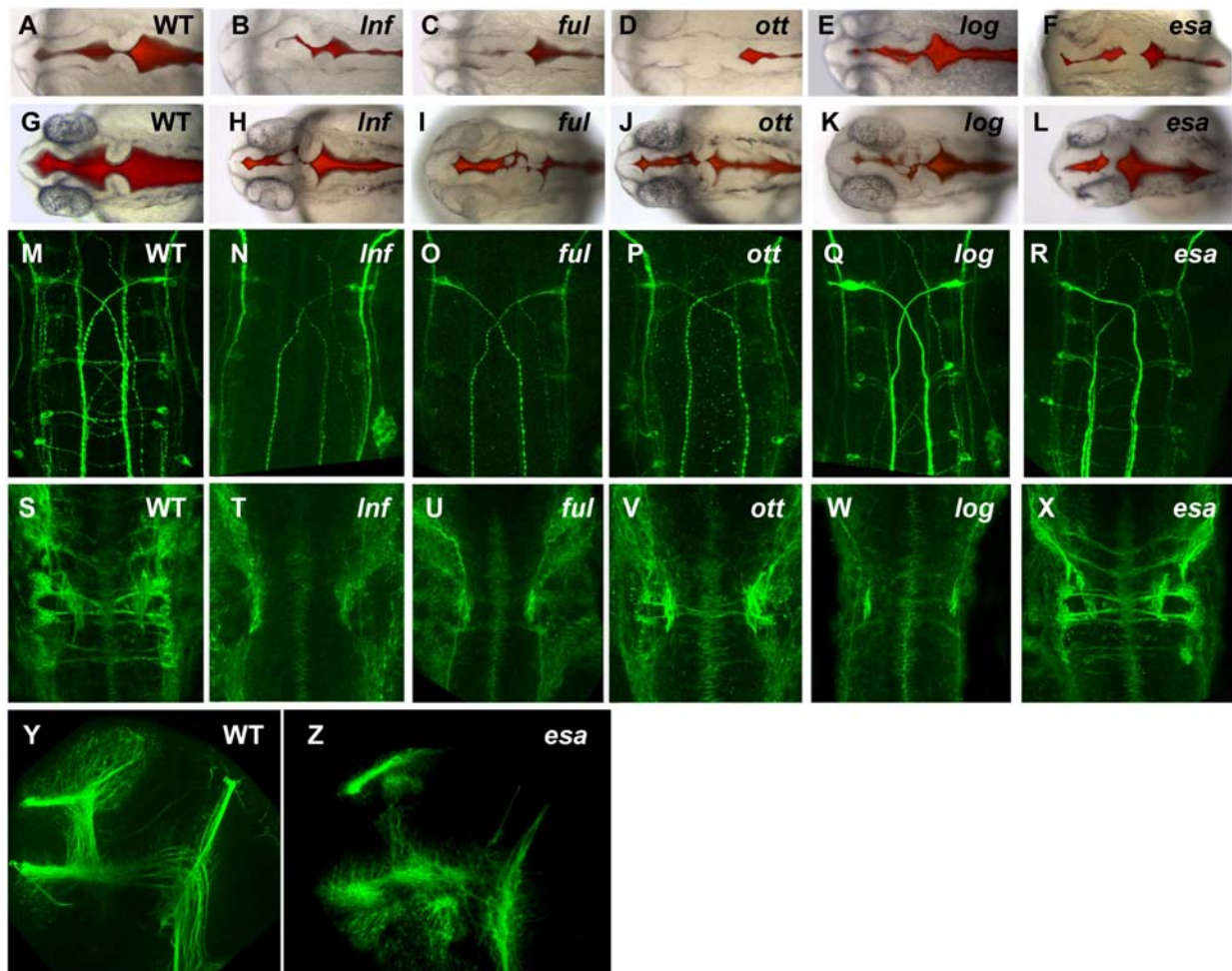






**Figure 3.5 Later brain ventricle expansion class.**

Lateral views of living, anesthetized embryos are shown, anterior to right, at 28 hpf, with brightfield microscopy. The *vip* mutant shows reduced hindbrain ventricle height (B, red bracket) compared to wild type (A). The *nat* mutant shows more severe brain ventricle height reduction (C, red bracket). The *wis* mutant also shows significantly reduced hindbrain ventricle height (D, red bracket), in addition to reduced pigmentation and other brain morphology abnormalities not shown in this figure.

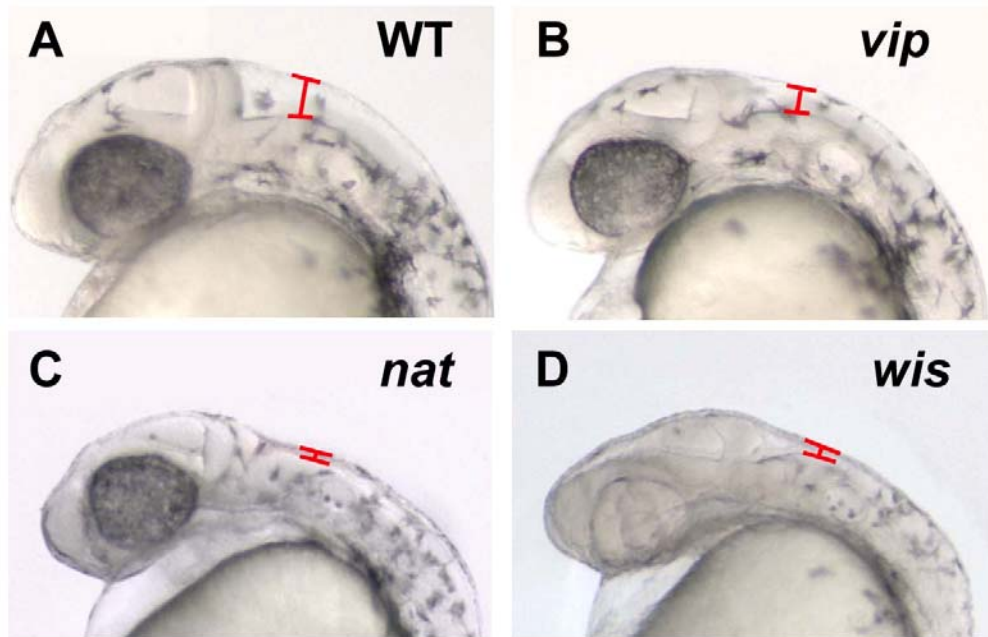
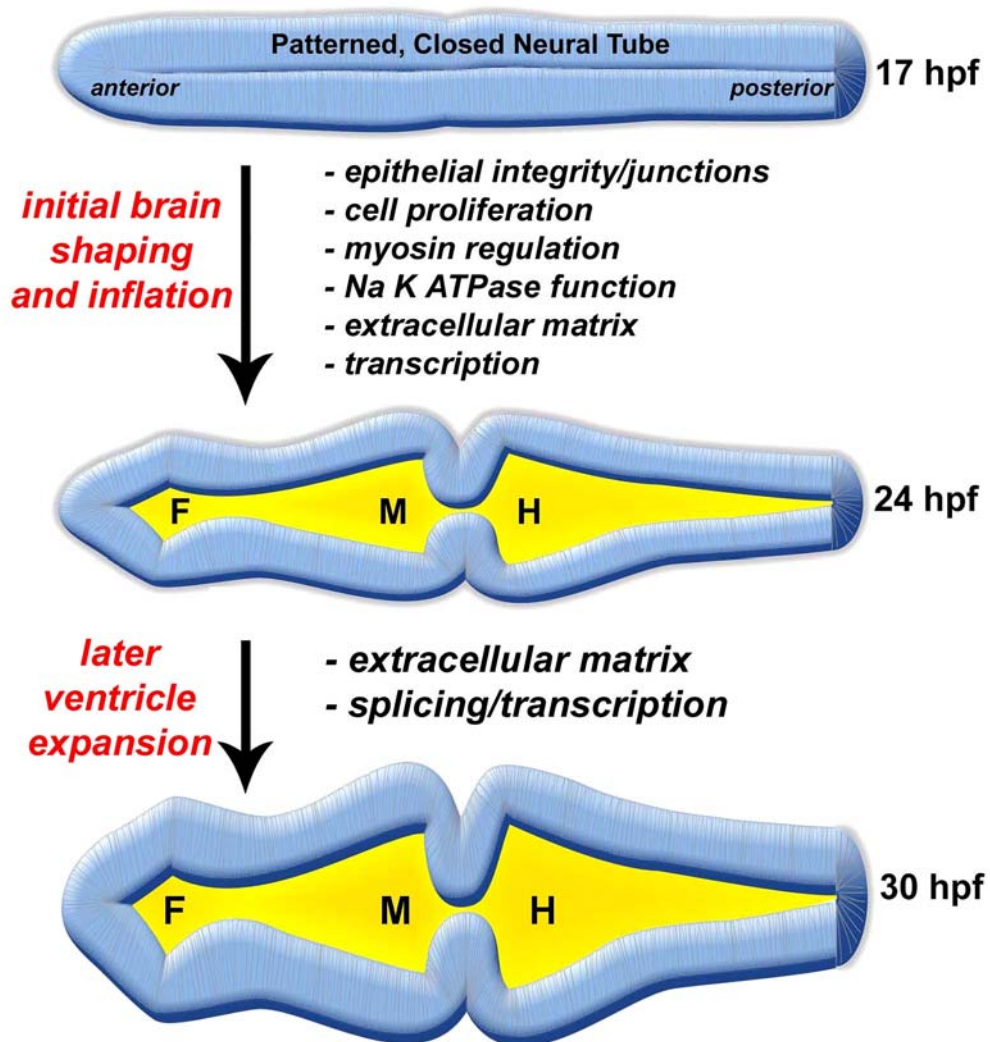




**Figure 3.6 Gene functions required for early brain morphogenesis.**

Processes involved in initial brain shaping include midline separation (requiring epithelial integrity/junctions, cell proliferation regulation, myosin regulation), brain lumen inflation (requiring  $\text{Na}^+ \text{K}^+$  ATPase activity), midbrain-hindbrain boundary formation (requiring extracellular matrix), and other mechanisms affecting brain morphology at these early stages (requiring transcription, among other unknown factors). Later brain ventricle expansion requires the extracellular matrix in order to maintain normal ventricle height, as well as splicing/transcription, which contributes to normal brain morphology. F: forebrain ventricle, M: midbrain ventricle, H: hindbrain ventricle.





## References

- Amsterdam, A., R. M. Nissen, Z. Sun, E. C. Swindell, S. Farrington and N. Hopkins (2004). Identification of 315 genes essential for early zebrafish development. *Proc Natl Acad Sci U S A* 101(35): 12792-7.
- Antonova, E., T. Sharma, R. Morris and V. Kumari (2004). The relationship between brain structure and neurocognition in schizophrenia: a selective review. *Schizophr Res* 70(2-3): 117-45.
- Bayer, S. A. and J. Altman (2007). *The human brain during the early first trimester*. Boca Raton, CRC Press.
- Biehlmaier, O., Y. Makhankov and S. C. Neuhauss (2007). Impaired retinal differentiation and maintenance in zebrafish laminin mutants. *Invest Ophthalmol Vis Sci* 48(6): 2887-94.
- Bingham, S., S. Chaudhari, G. Vanderlaan, M. Itoh, A. Chitnis and A. Chandrasekhar (2003). Neurogenic phenotype of mind bomb mutants leads to severe patterning defects in the zebrafish hindbrain. *Dev Dyn* 228(3): 451-63.
- Chitnis, A. B. and J. Y. Kuwada (1990). Axonogenesis in the brain of zebrafish embryos. *J Neurosci* 10(6): 1892-905.
- Conaway, R. C., S. Sato, C. Tomomori-Sato, T. Yao and J. W. Conaway (2005). The mammalian Mediator complex and its role in transcriptional regulation. *Trends Biochem Sci* 30(5): 250-5.
- Crespo-Facorro, B., L. Barbadillo, J. M. Pelayo-Teran and J. M. Rodriguez-Sanchez (2007). Neuropsychological functioning and brain structure in schizophrenia. *Int Rev Psychiatry* 19(4): 325-36.
- Eto, M., J. A. Kirkbride and D. L. Brautigan (2005). Assembly of MYPT1 with protein phosphatase-1 in fibroblasts redirects localization and reorganizes the actin cytoskeleton. *Cell Motil Cytoskeleton* 62(2): 100-9.
- Eto, M., L. Wong, M. Yazawa and D. L. Brautigan (2000). Inhibition of myosin/moesin phosphatase by expression of the phosphoinhibitor protein CPI-17 alters microfilament organization and retards cell spreading. *Cell Motil Cytoskeleton* 46(3): 222-34.
- Gilmore, J. H., J. J. van Tol, H. Lewis Streicher, K. Williamson, S. B. Cohen, R. S. Greenwood, H. C. Charles, M. A. Kliewer, J. K. Whitt, S. G. Silva, B. S. Hertzberg and N. C. Chescheir (2001). Outcome in children with fetal mild ventriculomegaly: a case series. *Schizophr Res* 48(2-3): 219-26.
- Gray, H. and C. D. Clemente (1985). *Anatomy of the human body*. Philadelphia, Lea & Febiger.
- Grinblat, Y., J. Gamse, M. Patel and H. Sive (1998). Determination of the zebrafish forebrain: induction and patterning. *Development* 125(22): 4403-16.

- Guo, S., S. W. Wilson, S. Cooke, A. B. Chitnis, W. Driever and A. Rosenthal (1999). Mutations in the zebrafish unmask shared regulatory pathways controlling the development of catecholaminergic neurons. *Dev Biol* 208(2): 473-87.
- Hardan, A. Y., N. J. Minshew, M. Mallikarjunn and M. S. Keshavan (2001). Brain volume in autism. *J Child Neurol* 16(6): 421-4.
- Harland, R. M. (1991). In situ hybridization: an improved whole-mount method for *Xenopus* embryos. *Methods Cell Biol* 36: 685-95.
- Hong, S. K., C. E. Haldin, N. D. Lawson, B. M. Weinstein, I. B. Dawid and N. A. Hukriede (2005). The zebrafish *kohtalo/trap230* gene is required for the development of the brain, neural crest, and pronephric kidney. *Proc Natl Acad Sci U S A* 102(51): 18473-8.
- Horne-Badovinac, S., D. Lin, S. Waldron, M. Schwarz, G. Mbamalu, T. Pawson, Y. Jan, D. Y. Stainier and S. Abdelilah-Seyfried (2001). Positional cloning of heart and soul reveals multiple roles for PKC lambda in zebrafish organogenesis. *Curr Biol* 11(19): 1492-502.
- Hsu, Y. C., J. J. Willoughby, A. K. Christensen and A. M. Jensen (2006). Mosaic Eyes is a novel component of the Crumbs complex and negatively regulates photoreceptor apical size. *Development* 133(24): 4849-59.
- Itoh, M., C. H. Kim, G. Palardy, T. Oda, Y. J. Jiang, D. Maust, S. Y. Yeo, K. Lorick, G. J. Wright, L. Ariza-McNaughton, A. M. Weissman, J. Lewis, S. C. Chandrasekharappa and A. B. Chitnis (2003). Mind bomb is a ubiquitin ligase that is essential for efficient activation of Notch signaling by Delta. *Dev Cell* 4(1): 67-82.
- Jensen, A. M. and M. Westerfield (2004). Zebrafish mosaic eyes is a novel FERM protein required for retinal lamination and retinal pigmented epithelial tight junction formation. *Curr Biol* 14(8): 711-7.
- Jiang, Y. J., M. Brand, C. P. Heisenberg, D. Beuchle, M. Furutani-Seiki, R. N. Kelsh, R. M. Warga, M. Granato, P. Haffter, M. Hammerschmidt, D. A. Kane, M. C. Mullins, J. Odenthal, F. J. van Eeden and C. Nusslein-Volhard (1996). Mutations affecting neurogenesis and brain morphology in the zebrafish, *Danio rerio*. *Development* 123: 205-16.
- Jo, H., L. A. Lowery, V. Tropepe and H. Sive (2005). The zebrafish as a model for analyzing neural tube defects. *Neural Tube Defects: From Origin to Treatment*. D. F. Wyszynski, Oxford University Press: 29-41.
- Karlstrom, R. O., T. Trowe, S. Klostermann, H. Baier, M. Brand, A. D. Crawford, B. Grunewald, P. Haffter, H. Hoffmann, S. U. Meyer, B. K. Muller, S. Richter, F. J. van Eeden, C.

- Nusslein-Volhard and F. Bonhoeffer (1996). Zebrafish mutations affecting retinotectal axon pathfinding. *Development* 123: 427-38.
- Kim, S., X. Xu, A. Hecht and T. G. Boyer (2006). Mediator is a transducer of Wnt/beta-catenin signaling. *J Biol Chem* 281(20): 14066-75.
- Kimmel, C. B., W. W. Ballard, S. R. Kimmel, B. Ullmann and T. F. Schilling (1995). Stages of embryonic development of the zebrafish. *Dev Dyn* 203(3): 253-310.
- Krauss, S., J. P. Concordet and P. W. Ingham (1993). A functionally conserved homolog of the *Drosophila* segment polarity gene *hh* is expressed in tissues with polarizing activity in zebrafish embryos. *Cell* 75(7): 1431-44.
- Krauss, S., T. Johansen, V. Korzh and A. Fjose (1991). Expression of the zebrafish paired box gene *pax[zf-b]* during early neurogenesis. *Development* 113(4): 1193-206.
- Kurokawa, K., K. Nakamura, T. Sumiyoshi, H. Hagino, T. Yotsutsuji, I. Yamashita, M. Suzuki, M. Matsui and M. Kurachi (2000). Ventricular enlargement in schizophrenia spectrum patients with prodromal symptoms of obsessive-compulsive disorder. *Psychiatry Res* 99(2): 83-91.
- Loncle, N., M. Boube, L. Joulia, C. Boschiero, M. Werner, D. L. Cribbs and H. M. Bourbon (2007). Distinct roles for Mediator Cdk8 module subunits in *Drosophila* development. *Embo J* 26(4): 1045-54.
- Lowery, L. A., J. Rubin and H. Sive (2007). Whitesnake/*sfpq* is required for cell survival and neuronal development in the zebrafish. *Dev Dyn* 236(5): 1347-57.
- Lowery, L. A. and H. Sive (2004). Strategies of vertebrate neurulation and a re-evaluation of teleost neural tube formation. *Mech Dev* 121(10): 1189-97.
- Lowery, L. A. and H. Sive (2005). Initial formation of zebrafish brain ventricles occurs independently of circulation and requires the *nagio oko* and *snakehead/atp1a1a.1* gene products. *Development* 132(9): 2057-67.
- Malicki, J., S. C. Neuhauss, A. F. Schier, L. Solnica-Krezel, D. L. Stemple, D. Y. Stainier, S. Abdelilah, F. Zwartkruis, Z. Rangini and W. Driever (1996). Mutations affecting development of the zebrafish retina. *Development* 123: 263-73.
- Mizuno, T., K. Tsutsui and Y. Nishida (2002). *Drosophila* myosin phosphatase and its role in dorsal closure. *Development* 129(5): 1215-23.
- Mueller, T. and M. Wullmann (2005). *Atlas of Early Zebrafish Brain Development*, Elsevier.
- Nopoulos, P., L. Richman, N. C. Andreasen, J. C. Murray and B. Schutte (2007). Abnormal brain structure in adults with Van der Woude syndrome. *Clin Genet* 71(6): 511-7.

- Omori, Y. and J. Malicki (2006). *oko meduzy* and related crumbs genes are determinants of apical cell features in the vertebrate embryo. *Curr Biol* 16(10): 945-57.
- Oxtoby, E. and T. Jowett (1993). Cloning of the zebrafish *krox-20* gene (*krx-20*) and its expression during hindbrain development. *Nucleic Acids Res* 21(5): 1087-95.
- Parsons, M. J., S. M. Pollard, L. Saude, B. Feldman, P. Coutinho, E. M. Hirst and D. L. Stemple (2002). Zebrafish mutants identify an essential role for laminins in notochord formation. *Development* 129(13): 3137-46.
- Philibert, R. A., P. Bohle, D. Secrest, J. Deaderick, H. Sandhu, R. Crowe and D. W. Black (2007). The association of the HOPA(12bp) polymorphism with schizophrenia in the NIMH genetics initiative for schizophrenia sample. *Am J Med Genet B Neuropsychiatr Genet* 144(6): 743-7.
- Pleasure, S. J., M. E. Selzer and V. M. Lee (1989). Lamprey neurofilaments combine in one subunit the features of each mammalian NF triplet protein but are highly phosphorylated only in large axons. *J Neurosci* 9(2): 698-709.
- Pollard, S. M., M. J. Parsons, M. Kamei, R. N. Kettleborough, K. A. Thomas, V. N. Pham, M. K. Bae, A. Scott, B. M. Weinstein and D. L. Stemple (2006). Essential and overlapping roles for laminin alpha chains in notochord and blood vessel formation. *Dev Biol* 289(1): 64-76.
- Rau, M. J., S. Fischer and C. J. Neumann (2006). Zebrafish *Trap230/Med12* is required as a coactivator for *Sox9*-dependent neural crest, cartilage and ear development. *Dev Biol* 296(1): 83-93.
- Rehn, A. E. and S. M. Rees (2005). Investigating the neurodevelopmental hypothesis of schizophrenia. *Clin Exp Pharmacol Physiol* 32(9): 687-96.
- Reimann, J. D., E. Freed, J. Y. Hsu, E. R. Kramer, J. M. Peters and P. K. Jackson (2001). *Emi1* is a mitotic regulator that interacts with *Cdc20* and inhibits the anaphase promoting complex. *Cell* 105(5): 645-55.
- Riley, B. B., M. Y. Chiang, E. M. Storch, R. Heck, G. R. Buckles and A. C. Lekven (2004). Rhombomere boundaries are Wnt signaling centers that regulate metameric patterning in the zebrafish hindbrain. *Dev Dyn* 231(2): 278-91.
- Rohr, S., N. Bit-Avragim and S. Abdelilah-Seyfried (2006). Heart and soul/*PRKCi* and *nagie oko/Mpp5* regulate myocardial coherence and remodeling during cardiac morphogenesis. *Development* 133(1): 107-15.
- Sagerstrom, C. G., Y. Grinbalt and H. Sive (1996). Anteroposterior patterning in the zebrafish, *Danio rerio*: an explant assay reveals inductive and suppressive cell interactions. *Development* 122(6): 1873-83.



- Schier, A. F., S. C. Neuhauss, M. Harvey, J. Malicki, L. Solnica-Krezel, D. Y. Stainier, F. Zwartkruis, S. Abdelilah, D. L. Stemple, Z. Rangini, H. Yang and W. Driever (1996). Mutations affecting the development of the embryonic zebrafish brain. *Development* 123: 165-78.
- Tan, C., B. Stronach and N. Perrimon (2003). Roles of myosin phosphatase during *Drosophila* development. *Development* 130(4): 671-81.
- Trevarrow, B., D. L. Marks and C. B. Kimmel (1990). Organization of hindbrain segments in the zebrafish embryo. *Neuron* 4(5): 669-79.
- Trinh, L. A. and D. Y. Stainier (2004). Fibronectin regulates epithelial organization during myocardial migration in zebrafish. *Dev Cell* 6(3): 371-82.
- Tropepe, V. and H. L. Sive (2003). Can zebrafish be used as a model to study the neurodevelopmental causes of autism? *Genes Brain Behav* 2(5): 268-81.
- Wang, X., N. Yang, E. Uno, R. G. Roeder and S. Guo (2006). A subunit of the mediator complex regulates vertebrate neuronal development. *Proc Natl Acad Sci U S A* 103(46): 17284-9.
- Wei, X. and J. Malicki (2002). *nagie oko*, encoding a MAGUK-family protein, is essential for cellular patterning of the retina. *Nat Genet* 31(2): 150-7.
- Westerfield, M. (1995). *The Zebrafish Book: A guide for the laboratory use of zebrafish*, University of Oregon Press.
- Wiellette, E., Y. Grinblat, M. Austen, E. Hirsinger, A. Amsterdam, C. Walker, M. Westerfield and H. Sive (2004). Combined haploid and insertional mutation screen in the zebrafish. *Genesis* 40(4): 231-40.
- Xia, D., J. T. Stull and K. E. Kamm (2005). Myosin phosphatase targeting subunit 1 affects cell migration by regulating myosin phosphorylation and actin assembly. *Exp Cell Res* 304(2): 506-17.
- Yelon, D., S. A. Horne and D. Y. Stainier (1999). Restricted expression of cardiac myosin genes reveals regulated aspects of heart tube assembly in zebrafish. *Dev Biol* 214(1): 23-37.
- Yoda, A., H. Kouike, H. Okano and H. Sawa (2005). Components of the transcriptional Mediator complex are required for asymmetric cell division in *C. elegans*. *Development* 132(8): 1885-93.



## Chapter Four

### **Initial Formation of Zebrafish Brain Ventricles Occurs Independently of Circulation and Requires the *nagie oko* and *snakehead/atp1a1* Gene Products**

Published as:

Laura Anne Lowery and Hazel Sive. Initial formation of zebrafish brain ventricles occurs independently of circulation and requires the *nagie oko* and *snakehead/atp1a1a.1* gene products. *Development* 132, 2005.



## Abstract

The mechanisms by which the vertebrate brain develops its characteristic three-dimensional structure are poorly understood. The brain ventricles are a highly conserved system of cavities that form very early during brain morphogenesis, and that are required for normal brain function. We have initiated a study of zebrafish brain ventricle development and show here that the neural tube expands into primary forebrain, midbrain, and hindbrain ventricles rapidly, over a four hour window during mid-somitogenesis. Circulation is not required for initial ventricle formation, only for later expansion. Cell division rates in the neural tube surrounding the ventricles are higher than between ventricles, and consistently, cell division is required for normal ventricle development. Two zebrafish mutants which both do not develop brain ventricles are *snakehead* and *nagie oko*. We show that *snakehead* is allelic to *small heart*, which has a mutation in the Na<sup>+</sup>K<sup>+</sup> ATPase gene *atp1a1*. The *snakehead* neural tube undergoes normal ventricle morphogenesis; however the ventricles do not inflate, likely due to impaired ion transport. In contrast, mutants in *nagie oko*, which was previously shown to encode a MAGUK family protein, fail to undergo ventricle morphogenesis. This correlates with an abnormal brain neuroepithelium, with no clear midline and disrupted junctional protein expression. This study defines three steps that are required for brain ventricle development and that occur independently of circulation: 1) morphogenesis of the neural tube, requiring *nok* function; 2) lumen inflation requiring *atp1a1* function, and 3) localized cell proliferation. We suggest that mechanisms of brain ventricle development are conserved throughout the vertebrates.

## Introduction

The vertebrate brain has a characteristic and complex three-dimensional structure, the development of which is not well understood. Brain morphogenesis begins during, and continues subsequent to, neural tube closure. One aspect of brain structure that is highly conserved throughout the vertebrates is the brain ventricular system.

The brain ventricles are cavities lying deep within the brain, which contain cerebrospinal fluid (CSF) and form a circulatory system in the brain (Cushing 1914; Milhorat et al 1971; Pollay and Curl 1967). This system is believed to have essential roles in brain function including waste removal, nutrition, protection, and pressure equilibration (Novak et al 2000). Recent evidence suggests that CSF directly regulates neuronal proliferation in the embryonic brain and is part of a non-synaptic communication system in the adult (Miyan et al 2003; Owen-Lynch et al 2003; Skinner and Caraty 2002). In addition, certain neurons send processes into the ventricular space, suggesting that their activity may be connected with regulating CSF homeostasis (Vigh and Vigh-Teichmann 1998). CSF contains hormones, proteoglycans, and ions, and its composition varies between ventricles and over time, suggesting a changing function for the ventricles during development (Alonso et al 1998; Skinner and Caraty 2002). Abnormalities in brain ventricle structure can lead to hydrocephaly, one of the most common birth defects (McAllister and Chovan 1998; Rekate 1997), and abnormal brain ventricle size and development have been correlated with mental health disorders such as autism and schizophrenia (Hardan et al 2001; Kurokawa et al 2000).

While the adult brain ventricles have a complex shape, the embryonic brain begins as a simple tube, the lumen of which forms the brain ventricles. During and after neurulation, the anterior neural tube dilates in three specific locations to form the future forebrain, midbrain, and hindbrain ventricles (also called brain vesicles). This dilation pattern is highly conserved in all vertebrates. Elegant studies in chick embryos have shown that intraluminal pressure resulting from the accumulation of CSF inside the brain ventricles is necessary for normal brain ventricle expansion and cell proliferation (Desmond 1985; Desmond and Levitan 2002), and levels of proteoglycans such as chondroitin sulfate affect this process (Alonso et al 1998; Alonso et al 1999). However, the molecular mechanisms underlying brain ventricle formation are almost completely unknown. This has been due, in part, to lack of a genetic model in which early brain ventricle development could be observed.

We have considered whether the zebrafish is a good model for analyzing brain morphogenesis. One issue is whether the zebrafish neural tube forms by a similar mechanism to the amniote neural tube, since teleost neurulation involves formation of a solid neural keel, whereas amniote and amphibian neurulation involves rolling of the neuroepithelium into a tube. Our evaluation of the primary literature clearly indicates that teleost, amniote, and amphibian neurulation occur via fundamentally similar topological mechanisms, supporting the use of zebrafish as a model for brain morphogenesis (Lowery and Sive 2004). We therefore initiated a project to analyze brain ventricle formation using the zebrafish as a model. Brain ventricle mutants have been identified in several mutagenesis screens (Guo et al 1999; Jiang et al 1996; Schier et al 1996), however most have not been further studied.

In this study, we characterize normal brain ventricle formation in the zebrafish, and examine in detail the phenotypes of two severe brain ventricle mutants, *nagie oko* and *snakehead*. Our data define a series of steps necessary for brain ventricle development and demonstrate the utility of the zebrafish as a system for in-depth analysis of this process.

## Results

### Initial opening of zebrafish brain ventricles is rapid

We first characterized brain ventricle formation in wild-type zebrafish embryos using a live imaging method. The hindbrain ventricle was injected with Texas-Red conjugated to dextran, which diffused throughout the brain cavities (Fig. 4.1A), and micrographs taken under light and fluorescent illumination were superimposed (Fig. 4.1B-K). Using this method, it is apparent that initial ventricle opening is rapid, taking place over a four hour period between 18 hours post fertilization (hpf) (Fig. 4.1B) and 22 hpf (Fig. 4.1D), during mid-somitogenesis and prior to the onset of heartbeat, which begins at 24 hpf (Fig. 4.1E). Further expansion of the brain ventricles occurs as circulation begins (Fig. 4.1F). Both the midbrain and hindbrain ventricles are shaped by lateral hinge-points, regions of the neuroepithelium that bend sharply (asterisks, Fig. 4.1E,J). The hindbrain ventricle is first to open and does so in a diamond-shaped region formed by the pulling apart of two hinge-points, located between the upper and lower halves of the rhombic lip (the rhombomere 0 and 1 junction) (Koster and Fraser 2001; Moens and Prince 2002) (Fig. 4.1B-E). Using time-lapse confocal microscopy on living embryos (Fig. 4.1L-O), we

show that the hindbrain ventricle opens from anterior to posterior, with the apical surfaces of the neuroepithelium pulling apart, to form the ventricular space (Fig. 4.1M-O).

These data show that initial brain ventricle formation occurs rapidly, before heartbeat begins, and that the hindbrain ventricle opens in a sequential fashion.

### **Circulation is not required for initial brain ventricle opening, but is required for later expansion**

The demonstration that brain ventricle opening occurs before the onset of heartbeat contrasts with previous speculations that circulation is required for initial brain ventricle development (Schier et al 1996). In order to further explore this point, we analyzed this process in *silent heart (sih)* mutants. The *sih* gene encodes a cardiac-specific troponin, and while the heart forms normally, heartbeat and circulation never occur (Sehnert et al 2002). *Silent heart* mutants form brain ventricles indistinguishable from wild type by 24 hpf (Fig. 4.2A,B). This continues through 27 hpf (Fig. 4.2C,D). Later during development, by 36 hpf, when wild-type ventricles have expanded their volume significantly (Fig. 4.2E), *sih* mutants show a smaller ventricle height (and therefore volume) relative to wild-type embryos (Fig. 4.2F). These data confirm that initial steps in brain ventricle formation are independent of heartbeat and circulation, but that a later step contributing to ventricle expansion does require circulation. We subsequently focused our attention on the initial opening of the brain ventricles, prior to 24hpf.

### **Requirement for cell proliferation but not cell death in brain ventricle opening**

We began to address the mechanism of initial ventricle opening by first asking whether cell proliferation is involved. Whole-mount immunocytochemistry was performed to label mitotic cells with an antibody to phosphorylated histone H3 (PH3) (Hendzel et al 1997; Saka and Smith 2001) (Fig. 4.3A-C). In particular, we asked whether patterns and amounts of cell division along the anteroposterior (A/P) neuraxis correlated with location of the ventricles. In the straight neural tube, at 17 hpf, prior to ventricle opening, PH3 labeling was uniform along the A/P axis (Fig. 4.3A) ( $n=8$ ,  $p=0.627$ ). However, by 21 hpf, the number of PH3- positive cells appeared higher in the neural tube surrounding the midbrain and hindbrain ventricles relative to levels in the midbrain-hindbrain boundary (MHB) that does not open to form a ventricle (Fig. 4.3B). Quantitation of PH3-positive cells showed that at 21 hpf, there were approximately two-



fold more PH3-positive cells in the hindbrain than in the midbrain-hindbrain boundary (n= 8, p= 0.008) (Fig. 4.3C).

In order to ask whether these different levels of proliferation were significant for ventricle opening, we inhibited cell proliferation by treatment with aphidicolin which blocks DNA synthesis (Harris and Hartenstein 1991). Inhibition extended from 15 hpf, prior to ventricle opening, through 24 hpf, when ventricles would normally have opened (9 hr total) (Fig. 4.1). This treatment resulted in reduction of cell proliferation with varying levels (Fig. 4.3G and data not shown). Reduction in ventricle size was correlated with reduction in cell proliferation (Fig. 4.3D-G). However, even with extremely reduced levels of PH3 staining, some ventricle opening was observed, and correct ventricle shape and hinge-points were maintained.

We also asked whether cell death was correlated with ventricle opening (Fig. 4.3H-J). Using TUNEL staining in whole-mount embryos, no patterns of localized cell death were apparent from 17 hpf to 24 hpf (Fig. 4.3H,I and data not shown). Quantification of cell death demonstrated that while more death occurred at 17 hpf than at 21 hpf, no brain region examined displayed a significant difference in amount of cell death relative to other regions (Fig. 4.3J) (n=10, p=0.575 at 17 hpf, p=0.368 at 21 hpf).

These results suggest that regulated cell proliferation is necessary for initial brain ventricle formation, although other processes are crucial. Localized cell death does not appear to regulate initial brain ventricle formation.

### **The *snakehead* mutant is allelic to *small heart* and corresponds to a point mutation in $\text{Na}^+\text{K}^+$ ATPase *atp1a1***

In order to identify brain ventricle mutants, we performed a “shelf” screen of ENU and insertional zebrafish mutants (Amsterdam et al 2004; Jiang et al 1996; Schier et al 1996). We focused on mutants that were previously suggested to have a ventricle phenotype, although none of their brain phenotypes have been studied further. From this screen, we have identified 33 mutants with a brain ventricle phenotype, with the important criterion that these show healthy neural tissue, with no obvious necrosis (not shown).

One of the most severe ventricle phenotypes is seen in the *snakehead* (*snk*) mutant. *snk*<sup>10273a</sup> was derived from a large-scale chemical screen and is therefore presumed to be caused by a point mutation (Jiang et al 1996). In addition to a lack of brain ventricles, *snk* embryos

have heart defects, delayed body pigmentation, and no touch response (Schier et al 1996). We noticed that the *snk* phenotype appeared identical to that of the *small heart (slh)* mutant, which was isolated in an ENU screen (Yuan and Joseph 2004). We therefore performed complementation analysis between *snk* and *slh* and determined that they do not complement, and are likely to be different alleles of the same locus. In a cross of *snk* and *slh* heterozygotes, 77% showed a wild-type phenotype, 23% a mutant phenotype (78 embryos total). *slh* has been cloned and encodes a Na<sup>+</sup>K<sup>+</sup> ATPase, *Atp1a1* (previously named  $\alpha 1B1$ ). The *heart and mind (had)* mutant also has a mutation in the *atp1a1* gene (Shu et al 2003).

We asked whether the *snakehead* phenotype was due to a mutation in *atp1a1* by comparing cDNA sequences from the wild type and *snakehead*<sup>*to273a*</sup> mutant. This analysis revealed that the *to273a* allele of *snakehead* contains a G to A mutation at position 812 in the *atp1a1* coding sequence which results in an amino acid change from glycine to aspartate at position 271 in the amino acid sequence (Fig. 4.4 and data not shown). The location of this mutation is in the M2-M3 cytoplasmic loop, which is necessary for catalytic activity and may play a role in ion pumping action (Kaplan 2002). Additional mutations in this loop have been shown to alter the kinetic properties of the protein in other systems (Kaplan 2002), and thus we predict that the glycine to aspartate mutation in the *snakehead*<sup>*to273a*</sup> mutant substantially reduces or eliminates Na<sup>+</sup>K<sup>+</sup> ATPase *atp1a1* function.

It is not clear whether *snk*<sup>*to273a*</sup> is a null mutant. However, *small heart* is thought to be a null or severe hypomorph (Yuan and Joseph 2004), and we are unable to distinguish *snk* and *slh* phenotypes. Furthermore, inhibition of *atp1a1* function by anti-sense morpholino oligonucleotides does not lead to a more severe phenotype than seen in *snk* or *slh* (Yuan and Joseph 2004). Together, these data indicate that *snk*<sup>*to273a*</sup> is a null or severe loss of function allele of *atp1a1*.

### ***snakehead* and *nagie oko* mutants fail to form brain ventricles by different mechanisms**

Another mutant with a severe brain ventricle phenotype is *nagie oko (nok)*, that encodes a MAGUK family kinase required for epithelial cell polarity in the zebrafish eye and gut (Wei and Malicki 2002; Horne-Badovinac et al 2003). We analyzed a retroviral insertion allele of *nagie oko*, isolated in our laboratory, and this hypomorphic allele shows absence of brain ventricles, but does not show the eye phenotype of the ENU-derived *nok* allele, suggesting these may be

separable functions, or that there is a quantitatively different requirement for Nok in different tissues (Wei and Malicki 2002; Wiellette et al 2004).

By light microscopy of living embryos, brain ventricles appear completely absent from both mutants in either dorsal views (Fig. 4.5A-C) or in lateral views (Fig. 4.5D-F). However, unlike *nok* mutants, the entire *snk* embryo displays a characteristic refractivity. In particular, in dorsal view, the outline of the neural tube is not visible, even though a neural tube is present (see below). The refractivity of the neural tube thus cannot be distinguished from that of surrounding tissues, unlike the case in wild-type embryos. In order to ask whether absence of ventricles in both mutants reflected disruption of a similar process, we further analyzed the brain morphology of the mutants.

Transverse sections of fixed embryos show that the phenotypes of *snk* and *nok* are strikingly distinct (Fig. 4.5G-O). In wild-type embryos at 22 hpf, different regions of the brain show characteristic brain ventricle morphology. The forebrain ventricle opens into a diamond shape (Fig. 4.5G), the midbrain ventricle shows a cruciform morphology with lateral and dorsoventral hinge-points (asterisks, Fig. 4.5J), while the hindbrain ventricle shows lateral hinge-points as well as a very thin dorsal epithelial covering (Fig. 4.5M). Sections of *snk* show that these morphologies are present in *snk* embryos (Fig. 4.5H,K,N), however, there are no visible extra-cellular spaces, all cells seem stuck together, and the lumen never opens. Normal morphogenesis is most clearly visible in the *snk* midbrain, which shows the wild-type cruciform shape (Fig. 4.5K), and hindbrain, which has a thin covering sheet (Fig. 4.5N). In contrast, the *nok* mutant neural tube remains uniform in transverse section, with no lateral hinge-points (Fig. 4.5I,L,O), resembling the 17 hpf neural tube prior to ventricle morphogenesis (not shown). In some *nok* embryos, the dorsal neural tube does appear thinner in the hindbrain region (not shown), indicating this aspect of brain morphogenesis is normal. Confocal microscopy of living embryos confirms the different phenotypes of these two mutants (Fig. 4.5P-R). Thus, while *snk* brain morphology appears normal except for the lack of brain ventricle inflation (Fig. 4.5Q), the *nok* neuroepithelium fails to undergo morphogenesis with no midbrain or hindbrain lateral hinge-points (Fig. 4.5R).

These data show that both *snk* and *nok* have an early ventricle phenotype, by 20 hpf, prior to the onset of heartbeat. Significantly, the “no ventricle” phenotypes of *snk* and *nok* mutants are quite different, and indicate that the mechanisms by which these genes affect brain ventricle morphogenesis are distinct.

### ***nokie* mutants retain epithelial polarity but lose epithelial integrity in the brain**

Previous analyses of *nokie* mutants have concluded that within the brain, epithelial polarity is normal, whereas in the retina, epithelial polarity is abnormal and correlated with retinal disorganization (Wei and Malicki 2002). However, the brain epithelium has not been extensively examined, and we therefore analyzed *nokie* epithelial organization in more detail. We first examined transverse brain sections at 17 hpf, when the neural tube is normally straight and ventricle morphogenesis has not yet begun. Sections of wild-type embryos show a clear midline, with nuclei lined up on either side (Fig. 4.6A), while *nokie* mutant sections show disorganized nuclear position and no continuous midline (Fig. 4.6B). However, in most sections of *nokie* mutants extending from forebrain to hindbrain, there were small, intermittent regions with a clear midline (not shown).

Since epithelial polarity and junctions have not been thoroughly examined in the *nokie* brain epithelium, we analyzed expression of various junction and cell polarity markers in *nokie* mutants using immunohistochemistry. As indicators of adherens junctions,  $\beta$ -catenin and actin expression were analyzed, while occludin expression was used as a tight junction marker (Furuse et al 1993; Nagafuchi 2001), all of which are normally found at the apical side of tightly-connected cells of an epithelium. In *nokie* mutants,  $\beta$ -catenin, actin, and occludin proteins were localized apically, and no ectopic foci were observed at other regions of the cell membrane, indicating correct apical/basal polarity was present (Fig. 4.6C-L). However, consistent with histological sections, labeling did not occur along a distinct brain midline, and instead there were regions where labeling was missing (compare Fig. 4.6E and F, 4.6G and H, 4.6I and J). This was particularly apparent when observing actin foci at high magnification (Fig. 4.6K,L). In a three-dimensional confocal image of the labeled wild-type brain, an actin belt surrounding the apicolateral surface of each cell in the epithelium is visible (Fig. 4.6K). However, this belt is not present in *nokie* mutants and instead the actin foci are disorganized (Fig. 4.6L). As a further test for correct apical/basal polarity, we also asked in our *nokie* hypomorphic allele whether residual *nokie* protein was correctly localized, using an antibody to Nok (Wei and Malicki 2002). A small amount of protein is correctly localized in the *nokie* mutant (Fig. 4.6N), however this appears much reduced compared to wild type (Fig. 4.6M).

In summary, we show that in the future brain, the *nok* neuroepithelium is highly disorganized, and that while this displays proper apical/basal organization, junctional actin belts do not form cohesively, and there is no clear or continuous midline.

### **Epistasis analysis of *snakehead/atp1a1* and *nogie oko***

Since both *snk* and *nok* mutants fail to form ventricles, we performed epistasis analysis to determine whether the *atp1a1* and *nok* genes function in the same or separate genetic pathways (Fig. 4.7). To create double mutant embryos, heterozygote carriers were mated and their progeny raised. Double mutants were identified by morphology and PCR. Light microscopy and histology showed that the double mutant *snk;nok* had a composite of both mutant phenotypes (Fig. 4.7D,H,L,P). In the double mutant, the altered refractivity and lack of extracellular spaces of the *snk* phenotype was present (Fig. 4.7C,G,K,O). However, the narrower brain tube, disorganized epithelium, and lack of hinge-points characteristic of the *nok* phenotype was also present (Fig. 4.7B,F,J,N and Fig. 4.7D,H,L,P).

We wondered whether the *nok*-like ventricle morphology indicated that *nok* is required to activate *atp1a1* function. In order to address this, we asked whether Atp1a1 was correctly localized in *nok* mutants (Fig. 4.8A,B). An antibody ( $\alpha 6F$ ) that recognizes multiple Na<sup>+</sup>K<sup>+</sup>ATPases was used (Drummond et al 1998; Takeyasu et al 1988) since Atp1a1-specific antibodies are not yet available. In both wild-type and *nok* embryos,  $\alpha 6F$  antibody staining was present at the apical surface of the neuroepithelium, whether or not the ventricle had opened (Fig. 4.8A,B).

In addition, we assayed Nok localization in the *snk* mutant. In both wild-type and *snk* embryos, Nok antibody staining was localized apically (Fig. 4.8C,D), suggesting that Atp1a1 function is not necessary for correct targeting of Nok to the apical membrane. Moreover, actin associated-adherens junctions were intact in the *snk* mutant, as shown by phalloidin-Texas Red labeling (data not shown), further substantiating that Atp1a1 is not affecting epithelial integrity.

In summary, the composite double mutant phenotype and correct localization of  $\alpha 6F$  staining and Nok protein in *nok* and *snk* mutants, respectively, suggests that *nogie oko* and *atp1a1* function in separate pathways.

## Discussion

### Multiple steps are required for brain ventricle development

Brain ventricle formation is one of the earliest manifestations of three-dimensional brain structure. Using the zebrafish as a model, we can distinguish several steps required for ventricle development (Fig. 4.9). Three early steps occur rapidly, over a four hour period, and are circulation-independent. One step leads to morphogenesis of the closed neural tube and to formation of lateral hinge-points at specific anteroposterior positions. Morphogenesis requires an intact, polarized epithelium and is dependent on *Nagie oko* protein function. A second step is inflation of the ventricle lumen that requires activity of the *Atp1a1* ion pump, and presumably subsequent osmosis to open the ventricular spaces. Regulated cell proliferation appears to be a third input into ventricle development. A later process of ventricle expansion occurs after circulation has begun, and is circulation dependent.

### Two distinct periods during initiation and expansion of brain ventricles: the role of circulation

Most zebrafish mutants that show brain ventricle defects also display heart or circulation defects (Schier et al 1996). Previous studies have shown that circulation is necessary for maintenance of brain ventricle size in adult animals, and that reduction in blood pressure leads to reduction in CSF secretion and pressure within the ventricles (Deane and Segal 1979). It was therefore suggested that zebrafish brain ventricle defects developed secondarily to the circulation defect (Schier et al 1996). This reasoning also stemmed from studies in chick which showed that after the onset of circulation, a positive CSF pressure inside the brain ventricles is necessary for brain ventricle expansion (Desmond 1985; Desmond and Jacobson 1977; Desmond and Levitan 2002).

Our data show that initial stages of ventricle formation are not dependent on circulation. Why do many mutants with brain ventricle defects also display heart or circulation defects? One possibility is that some of these mutants show a “late” ventricle phenotype and reflect a deficit in circulation-dependent ventricle expansion. Another possibility is that genes required for heart and brain ventricle morphogenesis are shared and the phenotype of a particular mutant is therefore pleiotropic. In support of this, both *nagie oko* and *snakehead* mutants show heart defects.

### **The role of cell proliferation in brain ventricle development**

The lowest level of cell proliferation we observed along the anteroposterior axis of the brain epithelium is at the midbrain-hindbrain boundary (MHB), and this deficit may be one of the reasons that the MHB does not open into a ventricular space. How might cell proliferation contribute to normal ventricle development? One possibility is that a critical mass of cells is necessary for ventricle morphogenesis while a second is that cells must be actively cycling to respond to signals leading to cell movement or shape changes. A third possibility is that cell proliferation is required for lumen inflation, rather than for ventricle morphogenesis. However, the smaller, but normally shaped ventricles observed after inhibition of DNA replication do not resemble the defects seen in *nok* or *snk* mutants, and neither of these mutants show differences in cell proliferation (or cell death) relative to wild-type embryos (not shown). We therefore hypothesize that cell proliferation defines an independent step during ventricle formation. We cannot rule out that embryos in which cell proliferation has been inhibited are generally disrupted; however, other regions of such embryos appear normal, including somite number and shape (not shown). Overproliferation of the neuroepithelium also suppresses ventricle opening, as shown in the *mindbomb* and *curlyfry* mutants (Bingham et al 2003; Song et al 2004), and the connection between these data and the requirement for cell proliferation is not clear.

Previous reports have indicated that in mice, blocking cell death by caspase gene ablation causes an overgrowth of the brain tissue, with obscured or obstructed brain ventricles (Kuida et al 1996). Conversely, mutations which cause too much cell death in the brain lead to a reduction in brain tissue and over-expansion of the brain ventricles (Keino et al 1994). Our data do not suggest an early role for regulated cell death in initial brain ventricle development, and it is likely that these phenotypes reflect late outcomes of perturbing cell death.

### **The *nagie oko* phenotype indicates a requirement for epithelial integrity in ventricle formation**

The *nagie oko* gene encodes a MAGUK family scaffolding protein that localizes to junctions at the apical surface of epithelia and regulates epithelial polarity (Wei and Malicki 2002). MAGUK proteins likely function in the assembly of protein complexes that control the formation or maintenance of cell junctions, and the Nok homolog in other organisms (*Stardust* in

*Drosophila*, PALS1 in mammals) is part of the Crumbs protein complex, one of the key regulators of epithelial junction formation (Bachmann et al 2001; Hong et al 2001; Hurd et al 2003; Knust and Bossinger 2002; Muller and Bossinger 2003; Tepass 2002).

Brain ventricle morphogenesis may require a cohesive epithelium, and *nok* mutants may fail to undergo morphogenesis because the brain neuroepithelium lacks normal epithelial junctions and therefore lacks this cohesiveness. Additionally, in *nok* mutants, there is no continuous midline, at which opposing epithelial surfaces would normally separate. The *nok* phenotype may therefore arise because the neuroepithelium is glued shut by cells straddling the midline. In support of this, *nok* mutants often show short stretches of a clear midline, and perhaps correlated with this, sometimes show very small ventricular openings.

### **Atp1a1 plays a role in lumen inflation**

The mechanism by which the brain ventricles initially inflate is not known. The Na<sup>+</sup>K<sup>+</sup> ATPase Atp1a1 protein is likely to be necessary to create an osmotic gradient that would drive movement of water into the closed ventricles after their morphogenesis (Blanco and Mercer 1998; Speake et al 2001; Therien and Blostein 2000). We therefore hypothesize that Atp1a1 functions to direct initial brain ventricle lumen inflation. The sequential opening of each ventricle may reflect sequential activation of this ion pump, thus blowing up the ventricles like a balloon. Alternately, Atp1a1 function may be continuous along the length of the brain, and another mechanism may regulate where initial lumen inflation occurs. Interestingly, although the Na<sup>+</sup>K<sup>+</sup> ATPase family is large, other members cannot compensate for the loss of embryonic Atp1a1 function. This is consistent with previous results showing that similar alpha subunits of Na<sup>+</sup>K<sup>+</sup> ATPase do not show the same expression patterns and cannot substitute for each other during zebrafish heart development or ear development (Canfield et al 2002; Shu et al 2003; Blasiolo et al 2003).

In the older brain, the choroid plexuses are the main source of CSF secretion, although the brain ependymal cells also contribute (Wright 1978; Brown et al 2004; Bruni 1998). Na<sup>+</sup>K<sup>+</sup> ATPases localize to the ventricular surface of secretory brain epithelia in adult mammals and amphibia and are necessary for the secretion of CSF (Masuzawa et al 1984; Saito and Wright 1983). Thus, this gene family may be used at different times of development to initiate and later maintain ventricular fluid secretion. We hypothesize that earlier during development, when the brain ventricles are initially forming and before the choroid plexuses have formed, the



ependymal cells lining the ventricles are the source of CSF, through the action of the *Atp1a1* protein.

### **Zebrafish as a model for vertebrate brain ventricle development**

In some respects, formation of the zebrafish neural tube appears different from that of frog, since in the brain region, the zebrafish neural tube is initially straight whereas in the frog *Xenopus*, the presumptive brain undergoes some morphogenesis prior to neural tube closure. However, the number, position, and shape of the initial brain ventricles are essentially identical in all vertebrates. We have previously compared processes of trunk neural tube formation between teleosts and other vertebrates, and have concluded that these are very similar (Lowery and Sive 2004 and see Introduction). These considerations suggest that zebrafish ventricle formation is likely to be fundamentally the same as that of other vertebrates. We are beginning to analyze the phenotypes of other zebrafish ventricle mutants, and this is likely to uncover additional genetic mechanisms regulating brain ventricle formation. Of particular interest is the relationship between genes that regulate neural patterning and the positioning and shaping of the ventricles, the interaction of *nok* with other genes that regulate epithelial polarity, and the mechanism by which *atp1a1* and other genes regulate lumen inflation.

## **Experimental Procedures**

### **Fish lines and maintenance**

*Danio rerio* fish were raised and bred according to standard methods (Westerfield 1995). Embryos were kept at 28.5°C and staged according to (Kimmel et al 1995). Times of development are expressed as hours post-fertilization (hpf).

Lines used were: Tübingen Long Fin, *sih<sup>tc300B</sup>* (Sehnert et al 2002), *snk<sup>to273a</sup>* (Jiang et al 1996), *nok<sup>wi83</sup>* (Wiellette et al 2004), *snk<sup>to273a</sup>;nok<sup>wi83</sup>*, *slh<sup>m291</sup>* (Yuan and Joseph 2004). Double mutant *snk<sup>to273a</sup>;nok<sup>wi83</sup>* were constructed using standard genetic techniques. To genotype double mutant embryos, PCR analysis of *nok* and morphology analysis for *snk* was used. After sorting *snk* mutant embryos phenotypically, the heads from each individual were removed, fixed in 2% paraformaldehyde, 1% glutaraldehyde, and processed for sectioning as described below. The remaining body was digested with proteinase K (1 mg/mL) in lysis buffer (10mM Tris pH8,

1mM EDTA, 0.3% Tween-20, 0.3% NP40) and used for PCR genotyping for the *nok* locus. Because *nok<sup>wi83</sup>* has a retroviral insertion in the *nok* gene, mutant individuals could be identified by PCR. Primers used: nokf 5'-GGTGAGCTGCCACTTTTCGGACA-3', nokr 5'-TAGCGACCCGTCACATAACA-3', retroviral-specific primer 5'-CCATGCCTTGCAAATGGCGTTACTTAAGC-3' (MWG Biotech). To identify the wild-type allele, nokf and nokr primers were used. To identify the *nok<sup>wi83</sup>* allele, nokf and insertion primers were used.

### **Brain ventricle imaging**

Embryos were anesthetized in 0.1 mg/mL Tricaine (Sigma) dissolved in embryo medium (Westerfield 1995) prior to injection and imaging. The hindbrain ventricle was micro-injected with 2-10 nL dextran conjugated to Rhodamine or Texas Red® (5% in 0.2M KCl, Sigma), the fluorescent molecule then diffused through the brain cavities, and micrographs were taken with light and fluorescent illumination within ten minutes of injection. These two images were superimposed in Photoshop 6 (Adobe). Injected embryos survive and develop normally. Comparisons of injected and non-injected brains show ventricle size is not perturbed by injection.

### **Live confocal imaging**

Bodipy-ceramide (Fl C5, Molecular Probes) was dissolved in DMSO to a stock concentration of 5 mM. Embryos were soaked in 50 nM bodipy-ceramide solution overnight in the dark. The embryos were then washed, dechorionated, and placed in wells in 1% agarose for confocal microscopy. Confocal imaging was performed using a Zeiss LSM510 laser-scanning microscope, using standard confocal imaging techniques (Cooper et al., 1999). Confocal images were analyzed using LSM software (Zeiss) and Photoshop 6.0 (Adobe).

### **Histology**

Embryos were fixed in 2% paraformaldehyde, 1% glutaraldehyde in PBS overnight 4°C, then washed in PBS, dechorionated, dehydrated, and embedded in plastic according to manufacturer's instructions (JB-4 Plus Embedding Kit, Polysciences). 5µm to 8 µm sections were cut on Leica RM2065 microtome and stained with hematoxylin and eosin using standard staining methods (Polysciences).

## **Immunohistochemistry**

For labeling with anti-phosphohistone H3 antibody, anti-Nagie oko antibody, and phalloidin-Texas Red, embryos were fixed in 4% paraformaldehyde 2 hours at room temperature, then rinsed in PBS and dechorionated. For labeling with anti- $\beta$ -catenin polyclonal antibody, anti-occludin polyclonal antibody, and anti-alpha Na<sup>+</sup>K<sup>+</sup> ATPase  $\alpha$ 6F antibody, dechorionated embryos were fixed in Dent's fixative (80% methanol, 20% DMSO) for 2 hours at room temperature, then rinsed in PBS (Dent et al 1989). Blocking was done for 4 hours at room temperature in 0.5 % Triton X, 4% normal goat serum, in phosphate buffer. Whole-mount immunostaining was carried out using anti-phosphohistone H3 rabbit polyclonal antibody (Upstate Biotechnology, 1:800), anti- $\beta$ -catenin rabbit polyclonal antibody (Zymed Laboratories Inc, 1:50), anti-occludin rabbit polyclonal antibody (Zymed Laboratories Inc, 1:50), anti-Nagie oko rabbit polyclonal antibody (Wei and Malicki 2002, 1:500), and mouse monoclonal antibody alpha6F, raised against chicken alpha1 subunit of Na<sup>+</sup>K<sup>+</sup> ATPase (Takeyasu et al 1988, 1:100) which was obtained from the Developmental Studies Hybridoma Bank. Goat anti-rabbit IgG Alexa Fluor 488 (Molecular Probes, 1:500) and goat anti-mouse Alexa Fluor 488 (Molecular Probes, 1:500) were used as secondary antibodies. Phalloidin conjugated to Texas Red (Sigma, 1:1000) was used as to label actin filaments. Brains were flat-mounted in glycerol and imaged with confocal microscope. For transverse sections, brains were embedded in 4% low melting agarose and sectioned with a vibratome (200 $\mu$ m sections) prior to confocal imaging.

For cell proliferation quantification, phosphohistone H3-labeled cells in each z-series of the midbrain-hindbrain boundary and hindbrain regions were counted and averaged. Average z-series area of the regions were measured using Scion Image software (Scion Corporation), and by determining the approximate area occupied by each cell, total cell number and the percentage of labeled cells in each region were calculated. To determine the statistical difference among different regions at the same time point, statistical analyses were performed using a paired sample t-test with SPSS 13.0 for Windows (SPSS). Cell death quantification was performed similarly, using an ANOVA test for comparison of multiple groups. P < 0.05 was considered significant.

## **Cell death labeling**

DNA fragmentation during apoptosis was detected by the TUNEL method, using "ApopTag®" kit (Chemicon). Embryos were fixed in 4% paraformaldehyde in PBS 2 hours,

then rinsed in PBS and dechorionated. Embryos were dehydrated to 100% ethanol, stored at -20°C overnight, then rehydrated to PBS. Embryos were further permeabilized by incubation in proteinase K (5 µg/mL) 5 minutes, then rinsed in PBS. TdT labeling was followed per manufacturer's instructions. Anti-DIG-AP (Gibco, 1:100) was used to detect the DIG labeled ends. Brains were flat-mounted in glycerol and imaged.

### **Inhibition of cell proliferation**

Cell proliferation was inhibited by treating embryos with 100 µg/mL aphidicolin (Sigma) in 1% DMSO from 15 hpf until 24 hpf. This treatment significantly slows, although does not stop, cell proliferation. Previous studies have indicated that in zebrafish it is not possible to completely inhibit cell proliferation at the stages observed without severe cell death which interferes with brain ventricle development (Ikegami et al 1997). Reduction in cell proliferation was measured using an antibody to phosphorylated histone H3 as described above.

### **Detection of *snakehead* mutation**

Total RNA was extracted from mutant embryos and wild-type siblings using Trizol reagent (Invitrogen), followed by chloroform extraction and isopropanol precipitation. cDNA synthesis was performed with Super Script II Reverse Transcriptase (Invitrogen) and random hexamers. PCR was then performed using five sets of previously published primers, which amplify the coding region of *atp1a1* (Shu et al 2003). RT-PCR products were used for sequencing analysis, performed by Northwoods DNA, Inc (Solway MN). Sequencing data were analyzed using the BLAST program (<http://www.ncbi.nlm.nih.gov/BLAST/>), and the cDNA sequence of *atp1a1* was obtained from GenBank database ([NM\\_131686](#)). Seven single-nucleotide changes in the *snakehead* cDNA were found, but only one, within primer set 2, changed the amino acid sequence.

### **Acknowledgements**

We thank members of the Sive lab for helpful comments and Ben Pratt for fish husbandry. Many thanks to Randall Peterson for clutches of *silent heart* mutant embryos, Shipeng Yuan and Calum Macrae for providing unpublished information related to the *small heart* mutation, the Nusslein-Volhard lab for providing us with the *snakehead* mutant, Jarema Malicki and Xiangyun Wei for *nok* morpholino sequence, Nok antibody and *nok*<sup>m227</sup>, Ryan

Murphy (Zon lab) for information on blocking cell proliferation, and Jaunian Chen for helpful discussions. This work was conducted utilizing the W.M. Keck Foundation Biological Imaging Facility at the Whitehead Institute. Supported by NIH MH70926 and MH59942 to HLS.



**Figure 4.1 Time-course of zebrafish brain ventricle formation.**

(A-K) Ventricles were visualized by microinjecting a fluorescent dye, Texas Red-dextran, into the hindbrain ventricle of anesthetized embryos. (A) Ventricle injection schematic: lateral view of 24 hpf embryo with microinjection needle at injection site of hindbrain ventricle. (B-K) Developmental profile of brain ventricle morphology at 18 hpf, 20 hpf, 22 hpf, 24 hpf, and 30 hpf following dye injection, (B-F) dorsal views, (G-J) lateral views; anterior to left. Heart beat onset at 24 hpf (E), after brain ventricles have formed. A anterior, P posterior.

(L-O) Cell morphology of hindbrain ventricle was visualized by confocal microscopy after overnight immersion in fluorescent molecule bodipy-ceramide. (L) Lateral view of 18 hpf embryo, with horizontal plane used for confocal time lapse imaging indicated by green line. (M-O) Confocal time lapse imaging of hindbrain ventricle of living, anesthetized embryo, beginning at 19 hpf and ending at 20 hpf. Asterisks label hinge-points from which opening begins, and arrows point to locations of apparent adhesion which release as ventricle opens anterior to posterior. F forebrain ventricle, M midbrain ventricle, H hindbrain ventricle. Asterisks: midbrain and hindbrain hinge-points. Scale bar = 50µm.

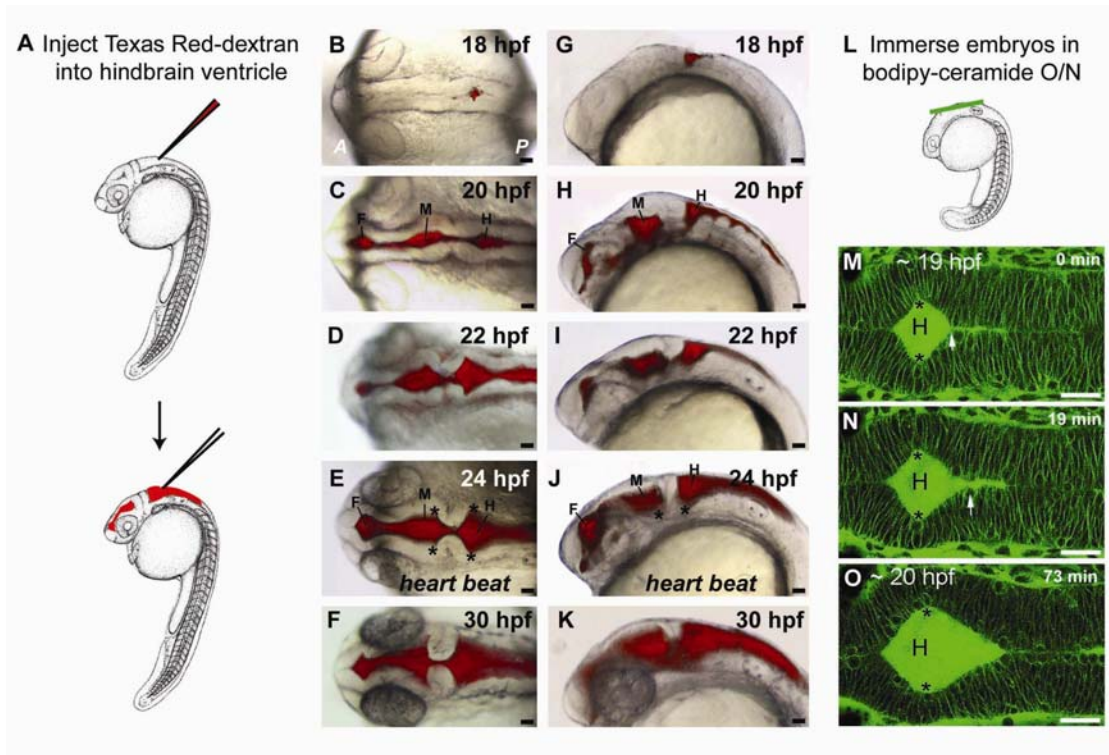






**Figure 4.2 Initial brain ventricle formation is normal in the absence of circulation.**

Living, anesthetized embryos from a heterozygous cross of the *silent heart (sih)* mutant were injected with Texas Red-dextran. At 24 hpf, the pattern of ventricle formation is identical in wild type (A) and *sih* mutant (B). At 27 hpf, dorsal views of ventricles are still identical in wild type (C) and mutant (D). At 36 hpf, the volume of brain ventricles is smaller in *sih* (F) than in wild type (E). (A-D) dorsal views, (E,F) side views, anterior to left. Scale bar = 50 $\mu$ m.

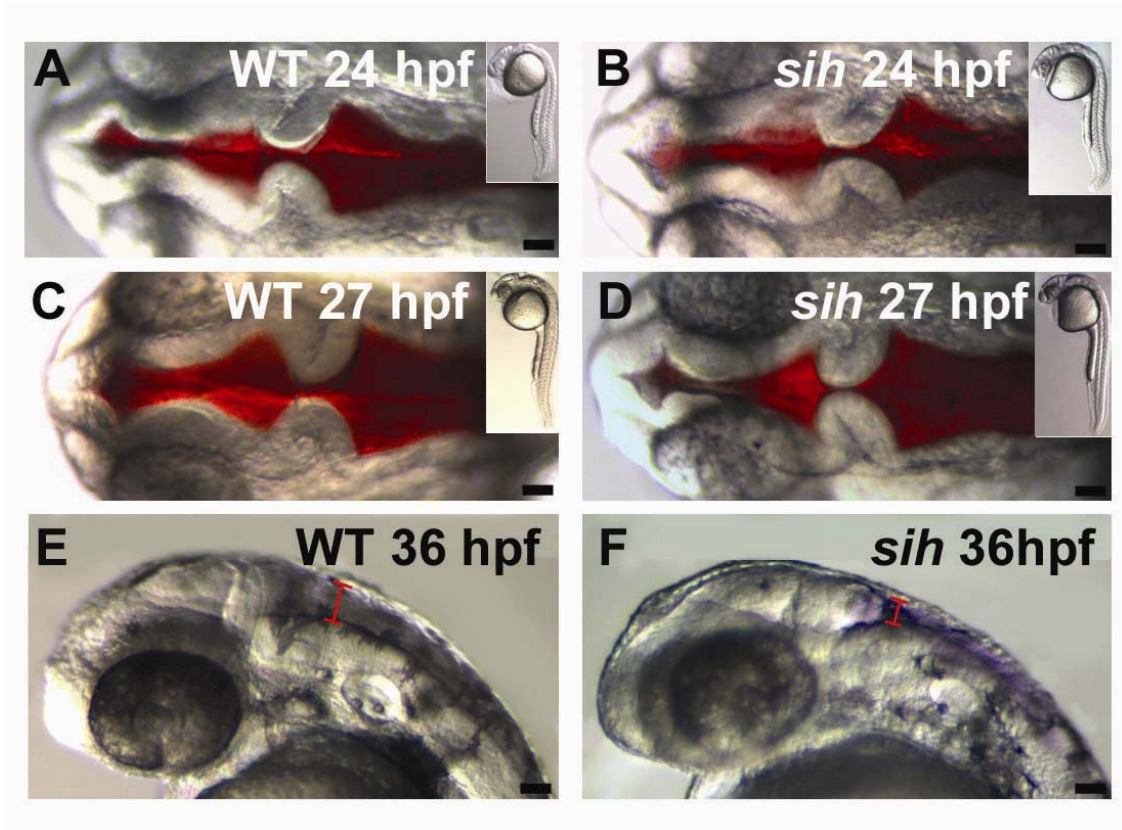




**Figure 4.3 Cell proliferation and cell death analysis in wild type and mutant embryos.**

(A-C) Cell proliferation analysis, using phosphorylated histone H3 antibody labeling. (A,B) fixed and labeled wild-type brain at 17 hpf and 21 hpf, (C) quantification comparing midbrain hindbrain boundary region and hindbrain, n=8, p=0.627 at 17 hpf; p=0.008 at 21 hpf. Cell proliferation at 21 hpf is statistically significant, showing almost two-fold higher amount of proliferation in the hindbrain (H) than in the midbrain-hindbrain boundary (MHB).

(D-G) Ventricule formation after inhibition of cell proliferation by aphidicolin treatment. (D,F) live control or drug embryos after ventricule injection at 24 hpf, (E,G) same embryo as in (D,F) fixed and labeled for cell proliferation. Reduced cell proliferation leads to a decrease in ventricule opening.

(H-J) Cell death analysis, using TUNEL labeling with ApopTag kit. (H,I) fixed and labeled wild-type brain at 17 hpf and 21 hpf, (J) quantification comparing midbrain, midbrain-hindbrain boundary, and hindbrain regions, n=10, p=0.575 at 17 hpf; p=0.368 at 22 hpf. Error bars denote standard error. M midbrain ventricule, MHB midbrain-hindbrain boundary, H hindbrain ventricule. Scale bar = 50µm.

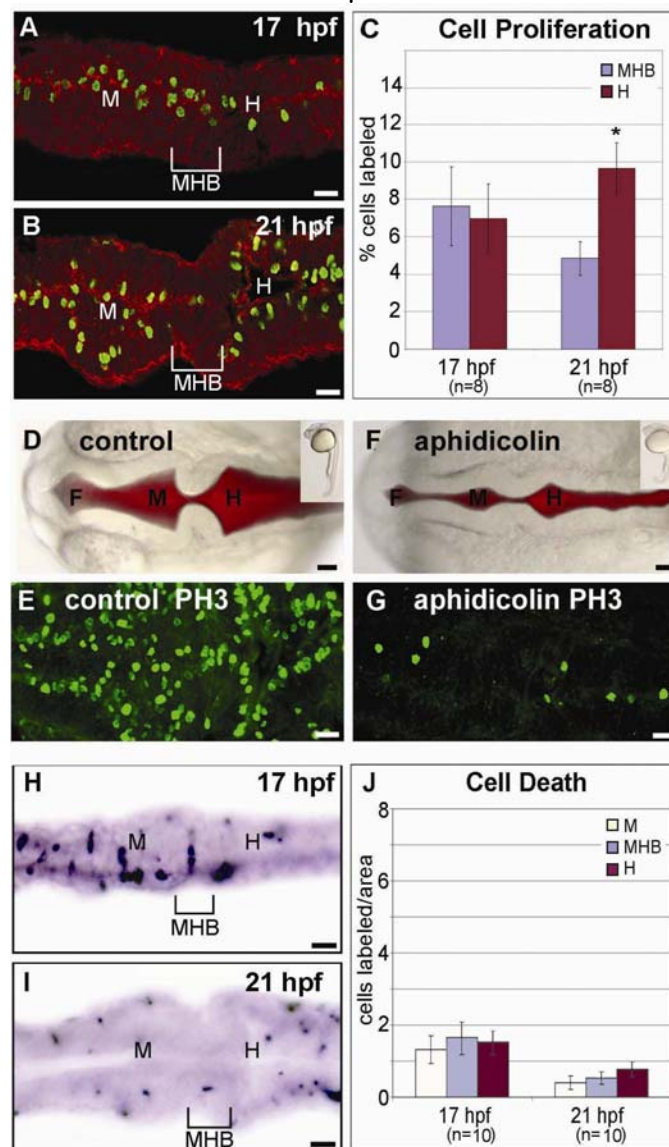




**Figure 4.4 *snk* encodes the zebrafish Na<sup>+</sup>K<sup>+</sup> ATPase Atp1a1 protein.**

Predicted structure of the Na<sup>+</sup>K<sup>+</sup> ATPase Atp1a1 protein. Red dot in the M2-M3 loop represents site of amino acid change from glycine to aspartate at residue 271 in the *snk*<sup>to273a</sup> mutant. RT-PCR and sequencing was performed on the *snk* mutants from 3 *snk* carrier clutches (107 embryos), embryos from a *snk* sibling non-carrier clutch (76 embryos), and a wild-type clutch (79 embryos). In 100% embryos, *snk* mutants, identified phenotypically, showed the G to A mutation, which would result in the glycine to aspartate amino acid change, whereas 100% wild-type embryos showed the normal G nucleotide.

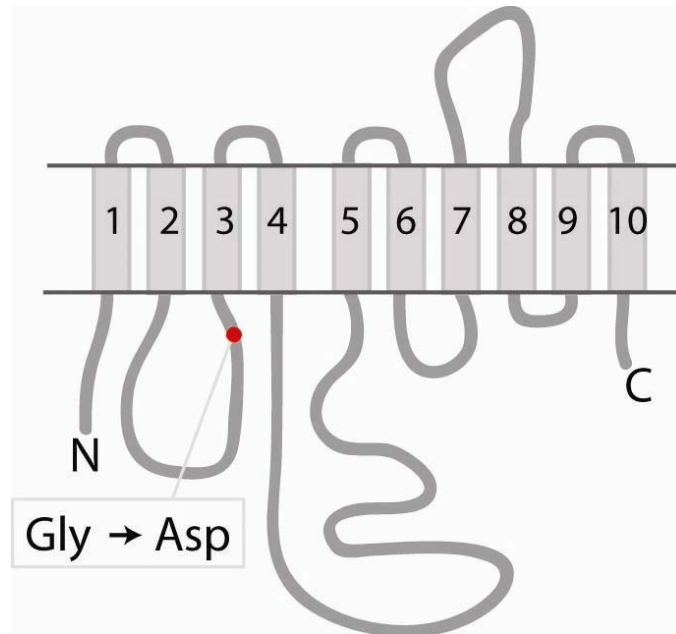




**Figure 4.5 Morphological analysis of *snakehead* and *nagie oko* brain ventricle mutants.** (A-F) Light microscopy images of brain at 28 hpf. Dorsal views (A-C) or side views (D-F) of living, anesthetized embryos are shown, anterior to left. Relative to wild type (A,D), brain ventricles in *snakehead* (B,E) and *nagie oko* (C,F) mutants appear to be absent (*nok* mutants sometimes form a small hindbrain ventricle that never enlarges). Note the characteristic refractivity of the neural tube in *snk*, in that neither the outline of the neural tube nor the brain folds are visible in the *snk* mutant (B,E). In addition, note that arrows in A and C point to the midbrain-hindbrain boundary (MHB) constriction in WT and *nok*, respectively. By light microscopy, the *snk* MHB constriction is not visible (even though it is in the proper location, see Q below). (G-O) Histology of *snk* and *nok* mutants. Embryos were fixed and transverse-sectioned at 22 hpf, at the level of forebrain, midbrain, or hindbrain, and stained with hematoxylin and eosin. Relative to wild-type embryos (G,J,M), *snk* mutant embryos (H,K,N) show appropriate ventricle morphology, however the cells appear stuck together and no lumen is present. In contrast, *nok* mutant embryos (I,L,O) fail to undergo any ventricle morphogenesis, and the epithelium appears disorganized. Asterisks label midbrain hinge-points in wild type (J) and *snk* (K), but hinge-points are absent in *nok* (L). (P-R) Confocal images through mid- and hindbrain ventricles of 24 hpf living embryos stained with bodipy ceramide. (P) wild type, (Q) *snk*, (R) *nok*. Note that *snk* embryos (Q) assume correct ventricle morphology but fail to open the ventricles. In contrast, the brain tube in *nok* embryos (R) remains straight and no hinge-points form (although the MHB constriction remains). F forebrain ventricle, M midbrain ventricle, H hindbrain ventricle. Scale bar = 50 $\mu$ m. Asterisks: hinge-points.





Figure 4.5 Continued

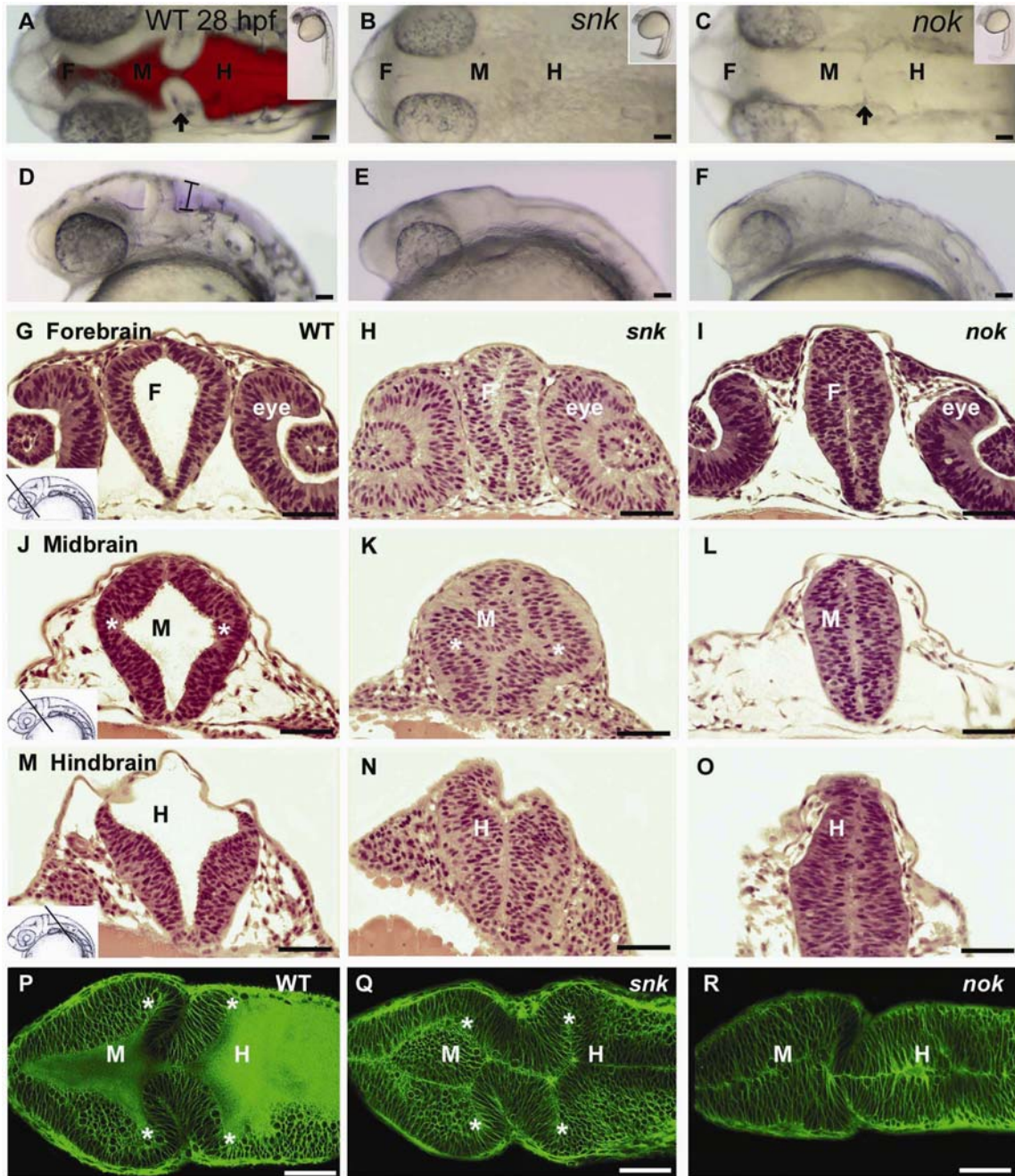




**Figure 4.6 Analysis of epithelial integrity in *nok* mutants.**

(A-L) Transverse sections through brains of wild type and *nok* embryos at 17 hpf (A,B) or 22 hpf (C-L). (A,B) shows clear midline in wild type (A; arrow) and disorganization in *nok* (B). (C,D) labeled with phosphohistone H3 antibody (mitosis marker) (green) and actin (red), dividing nuclei localize apically in both WT (C) and mutant (D). (E,F) labeled with  $\beta$ -catenin antibody, (G,H) labeled with actin marker, phalloidin-Texas Red, (I,J) labeled with occludin antibody and phalloidin-Texas Red counterstain, (K,L) High magnification of 3D compilation of transverse sections through forebrain, labeled with phalloidin-Texas Red. In the *nok* mutant, all junction markers localize apically as in wild type but show disorganization. (M,N) Nok antibody labeling (green) at 22 hpf in horizontal section through midbrain and hindbrain of wild type (M) and *nok* mutant (N), with phalloidin-Texas Red as counterstain (red). Scale bar = 20 $\mu$ m.

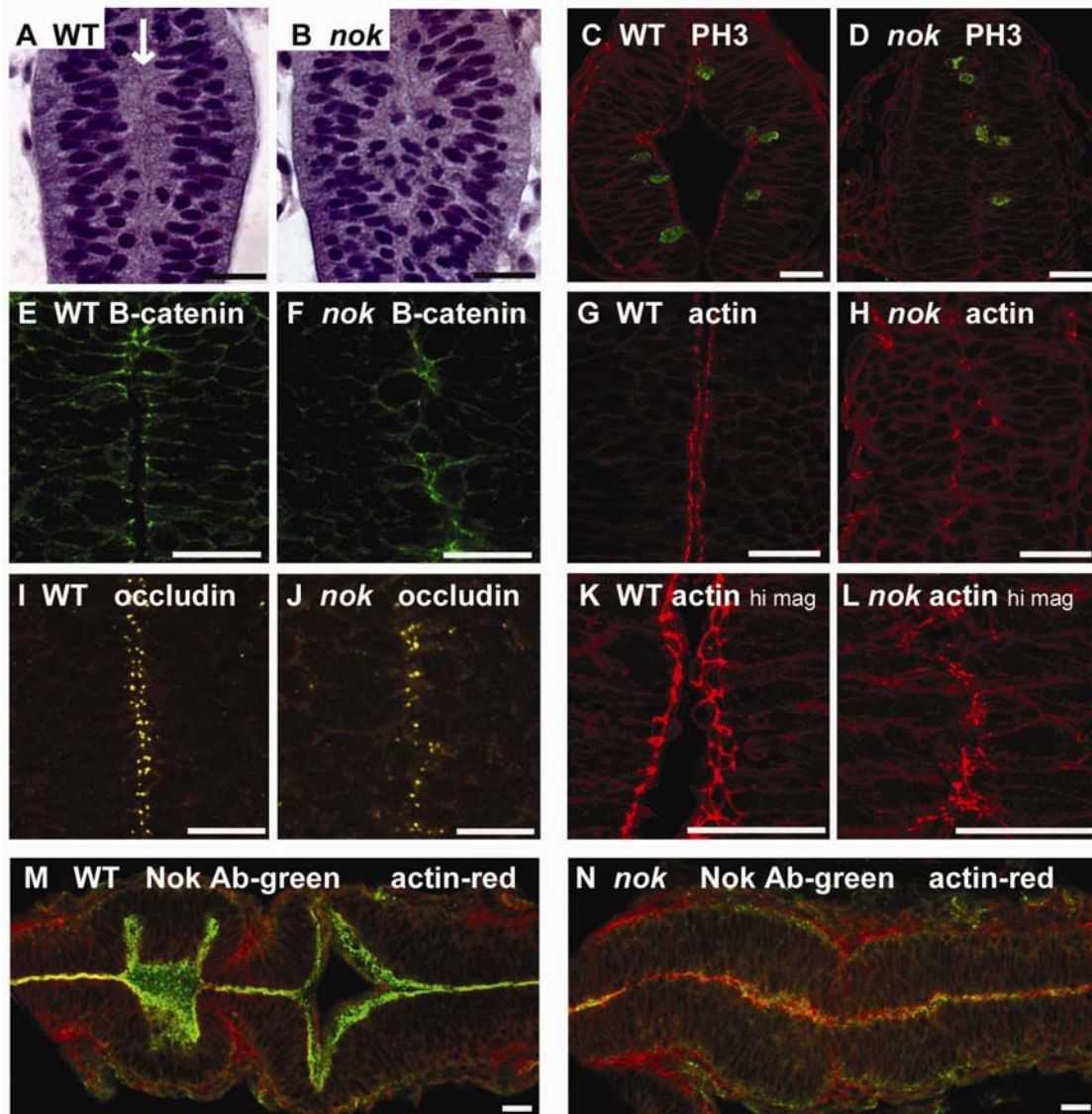




**Figure 4.7 Epistasis analysis of brain ventricle mutants *snk* and *nok*.**

(A-H) Lateral and dorsal views of anesthetized, living embryos at 25 hpf. (A,E) Wild type (70/139 embryos, 50%); (B,F) *nogie oko* mutants (29/139 embryos, 21%); (C,G) *snakehead* mutants (30/139 embryos, 22%); (D,H) *snakehead;nogie oko* double mutants (10/139, 7%) show overall composite phenotype. Asterisks mark hinge-points which are visible in wild type but not visible in the mutants (although hinge-points are present in the *snk* mutant, see K). Arrow marks midbrain-hindbrain constriction which is visible in wild type and *nok* mutant but is not visible in *snk* nor *snk;nok* due to the altered refractivity of the *snk* tissue.

(I-L) Histological sections through midbrain at 22 hpf of wild type (I), *nok* (J), *snk* (K), and *snk;nok* (L). The phenotype appears to be additive, suggesting *nogie oko* and *snakehead* function in separate pathways. (M-P) Drawings of brain outline and ventricle lumen in I-L shows composite phenotype more clearly. M midbrain ventricle, H hindbrain ventricle. Scale bar = 50  $\mu$ m.

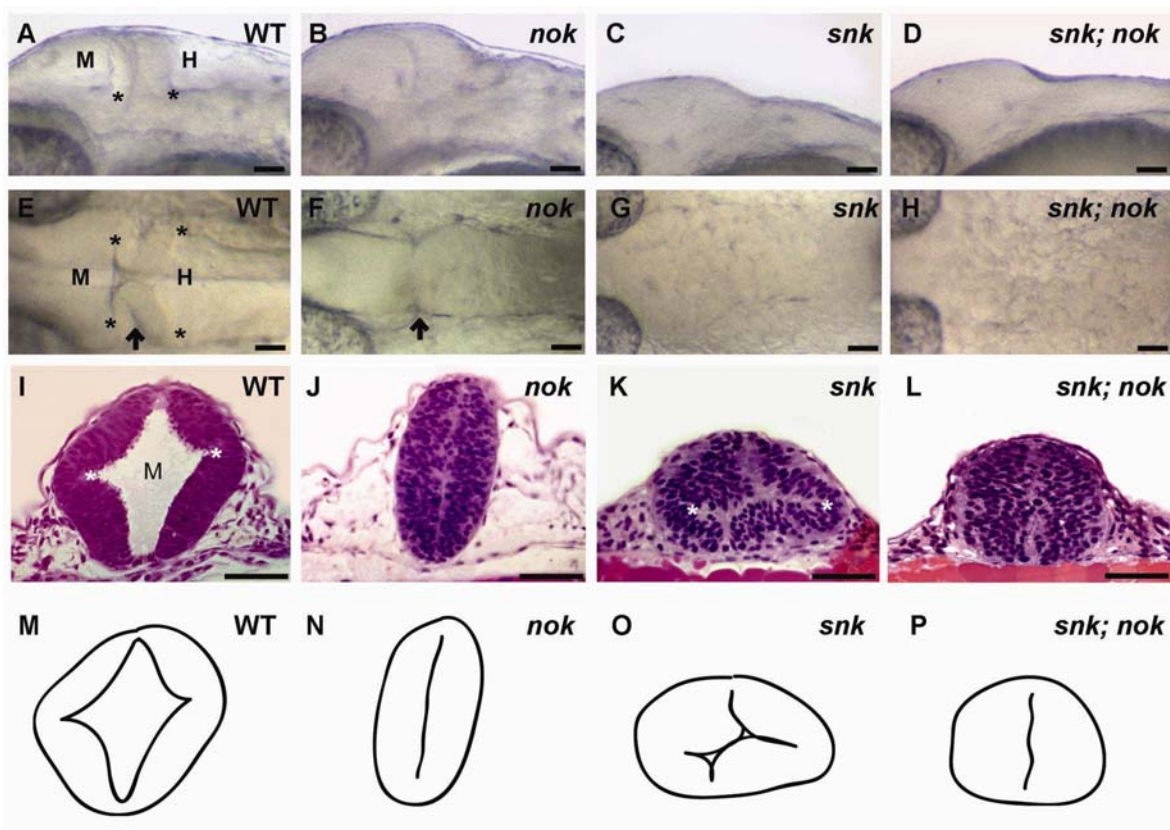




**Figure 4.8  $\alpha$ -Na<sup>+</sup>K<sup>+</sup> ATPase localization in *nok* mutants and Nok localization in *snk* mutants appears normal.**

(A,B) a6F antibody labeling (green) at 24 hpf in horizontal section through midbrain and hindbrain of wild type (A) and *nok* mutant (B) with phalloidin-Texas red as counterstain (red). Note that while the *nok* mutant hindbrain ventricle is severely reduced, a6F antibody still labels apical membrane. (C,D) Nok antibody labeling (green) at 24 hpf in horizontal section through midbrain and hindbrain of wild type (C) and *snk* mutant (D), with phalloidin-Texas Red as counterstain (red). Nok localizes at the apical membrane in both wild type (C) and mutant (D), suggesting that Snk is not necessary for Nok targeting to apical surface. Note: the *snk* mutant does have normal hinge-points in the midbrain and hindbrain, although they are not present in the optical section shown in D. Scale bar = 50 $\mu$ m.

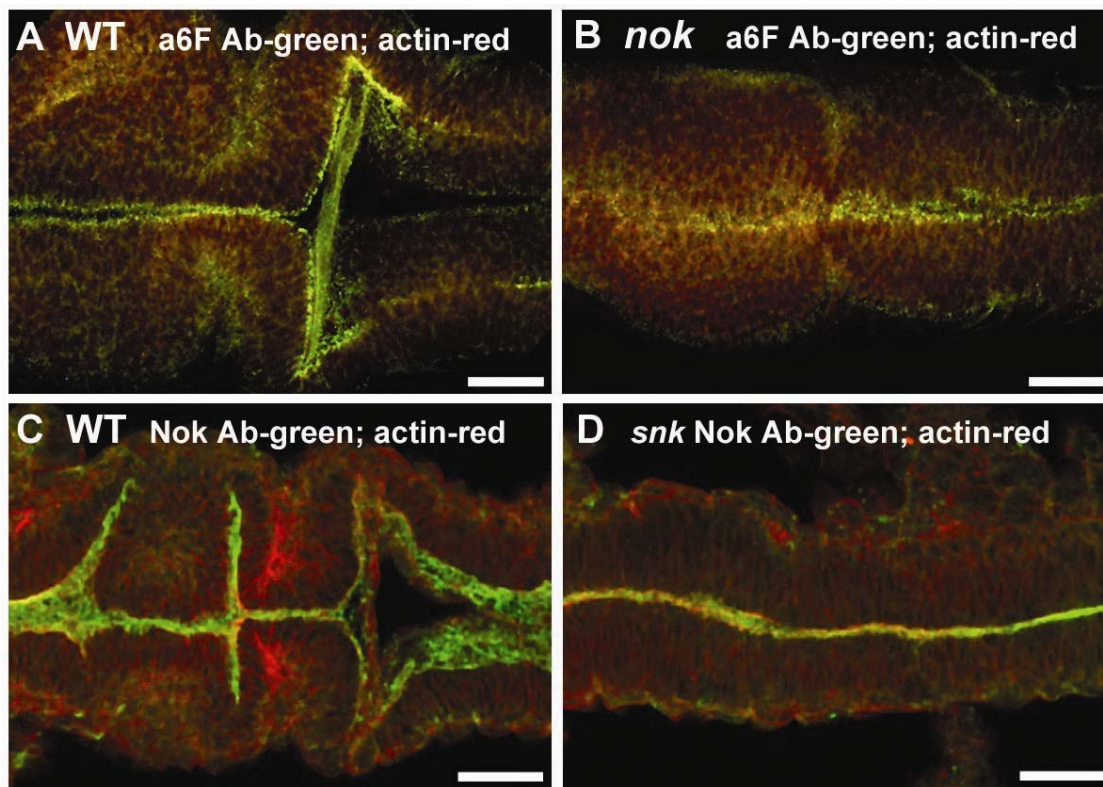


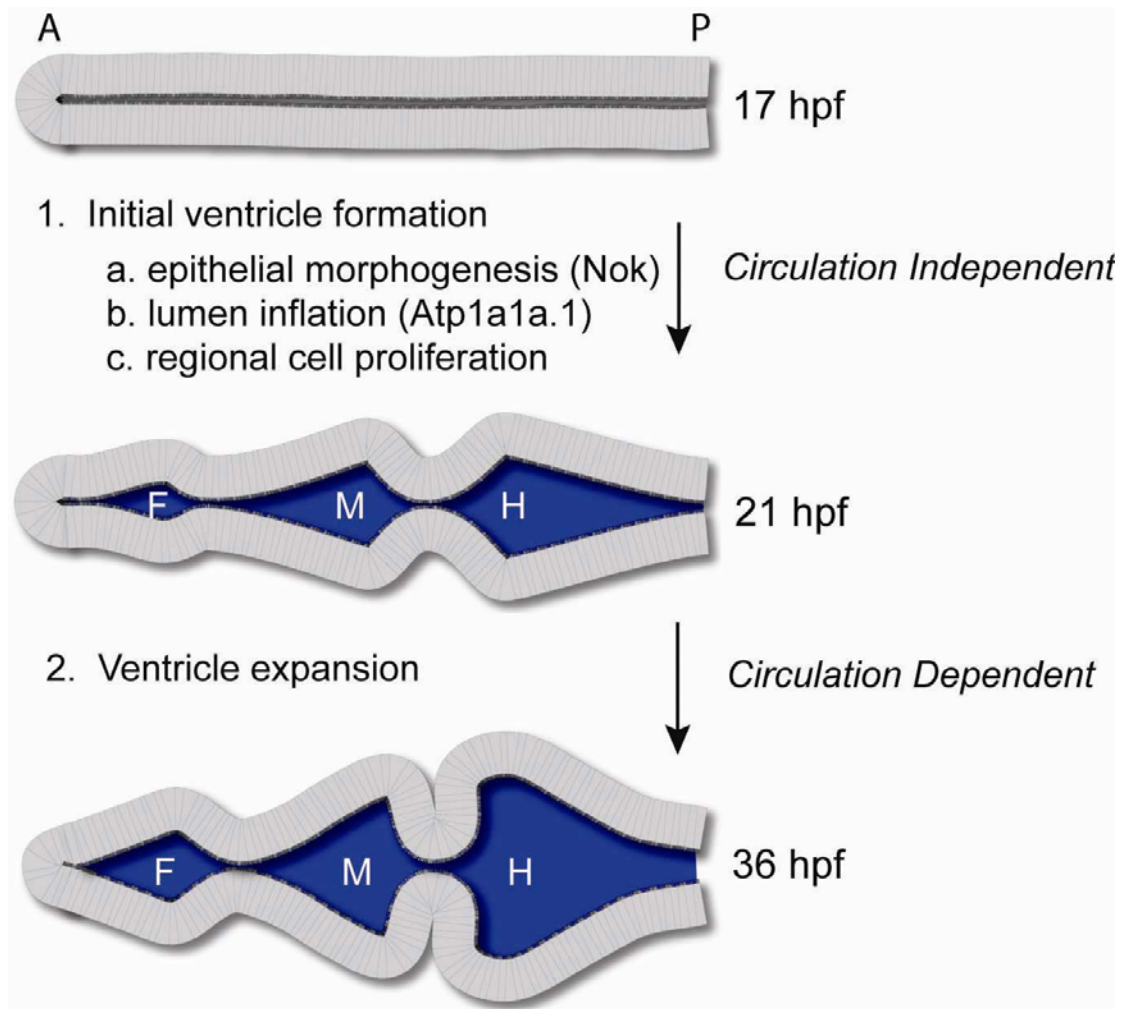




**Figure 4.9 Multiple steps are required for brain ventricle formation.**

Three steps have been identified during initial brain ventricle formation and occur independently of circulation. The Nagie oko protein helps maintain epithelial polarity and/or integrity that is required for normal ventricle morphogenesis. Atp1a1 (previously named Atp1a1a.1) is essential to inflate the ventricular space with fluid, and localized cell proliferation also appears to be necessary. Later brain ventricle expansion requires circulation.

A anterior, P posterior, F forebrain ventricle, M midbrain ventricle, H hindbrain ventricle.





## References

- Alonso, M. I., Gato, A., Moro, J. A. and Barbosa, E. (1998). Disruption of proteoglycans in neural tube fluid by beta-D-xyloside alters brain enlargement in chick embryos. *Anat Rec* 252, 499-508.
- Alonso, M. I., Gato, A., Moro, J. A., Martin, P. and Barbosa, E. (1999). Involvement of sulfated proteoglycans in embryonic brain expansion at earliest stages of development in rat embryos. *Cells Tissues Organs* 165, 1-9.
- Amsterdam, A., Nissen, R. M., Sun, Z., Swindell, E. C., Farrington, S. and Hopkins, N. (2004). Identification of 315 genes essential for early zebrafish development. *Proc Natl Acad Sci U S A* 101, 12792-7.
- Bachmann, A., Schneider, M., Theilenberg, E., Grawe, F. and Knust, E. (2001). *Drosophila* Stardust is a partner of Crumbs in the control of epithelial cell polarity. *Nature* 414, 638-43.
- Bingham, S., Chaudhari, S., Vanderlaan, G., Itoh, M., Chitnis, A. and Chandrasekhar, A. (2003). Neurogenic phenotype of mind bomb mutants leads to severe patterning defects in the zebrafish hindbrain. *Dev Dyn* 228, 451-63.
- Blanco, G. and Mercer, R. W. (1998). Isozymes of the Na-K-ATPase: heterogeneity in structure, diversity in function. *Am J Physiol* 275, F633-50.
- Blasiolo, B., Degraeve, A., Canfield, V., Boehmler, W., Thisse, C., Thisse, B., Mohideen, M. A. and Levenson, R. (2003). Differential expression of Na,K-ATPase alpha and beta subunit genes in the developing zebrafish inner ear. *Dev Dyn* 228, 386-92.
- Brown, P. D., Davies, S. L., Speake, T. and Millar, I. D. (2004). Molecular mechanisms of cerebrospinal fluid production. *Neuroscience* 129, 955-68.
- Bruni, J. E. (1998). Ependymal development, proliferation, and functions: a review. *Microsc Res Tech* 41, 2-13.
- Canfield, V. A., Loppin, B., Thisse, B., Thisse, C., Postlethwait, J. H., Mohideen, M. A., Rajarao, S. J. and Levenson, R. (2002). Na,K-ATPase alpha and beta subunit genes exhibit unique expression patterns during zebrafish embryogenesis. *Mech Dev* 116, 51-9.
- Cooper, M. S., D'Amico, L. A. and Henry, C. A. (1999). Confocal microscopic analysis of morphogenetic movements. *Methods Cell Biol* 59, 179-204.
- Cushing, H. (1914). Studies on the cerebrospinal fluid. I. Introduction. *J Med Res* 26, 1-19.
- Deane, R. and Segal, M. B. (1979). The effect of vascular perfusion of the choroid plexus on the secretion of cerebrospinal fluid [proceedings]. *J Physiol* 293, 18P-19P.

- Dent, J. A., Polson, A. G. and Klymkowsky, M. W. (1989). A whole-mount immunocytochemical analysis of the expression of the intermediate filament protein vimentin in *Xenopus*. *Development* 105, 61-74.
- Desmond, M. E. (1985). Reduced number of brain cells in so-called neural overgrowth. *Anat Rec* 212, 195-8.
- Desmond, M. E. and Jacobson, A. G. (1977). Embryonic brain enlargement requires cerebrospinal fluid pressure. *Dev Biol* 57, 188-98.
- Desmond, M. E. and Levitan, M. L. (2002). Brain expansion in the chick embryo initiated by experimentally produced occlusion of the spinal neurocoel. *Anat Rec* 268, 147-59.
- Drummond, I. A., Majumdar, A., Hentschel, H., Elger, M., Solnica-Krezel, L., Schier, A. F., Neuhauss, S. C., Stemple, D. L., Zwartkruis, F., Rangini, Z. et al. (1998). Early development of the zebrafish pronephros and analysis of mutations affecting pronephric function. *Development* 125, 4655-67.
- Furuse, M., Hirase, T., Itoh, M., Nagafuchi, A., Yonemura, S. and Tsukita, S. (1993). Occludin: a novel integral membrane protein localizing at tight junctions. *J Cell Biol* 123, 1777-88.
- Guo, S., Wilson, S. W., Cooke, S., Chitnis, A. B., Driever, W. and Rosenthal, A. (1999). Mutations in the zebrafish unmask shared regulatory pathways controlling the development of catecholaminergic neurons. *Dev Biol* 208, 473-87.
- Hardan, A. Y., Minshew, N. J., Mallikarjunn, M. and Keshavan, M. S. (2001). Brain volume in autism. *J Child Neurol* 16, 421-4.
- Harris, W. A. and Hartenstein, V. (1991). Neuronal determination without cell division in *Xenopus* embryos. *Neuron* 6, 499-515.
- Henzel, M. J., Wei, Y., Mancini, M. A., Van Hooser, A., Ranalli, T., Brinkley, B. R., Bazett-Jones, D. P. and Allis, C. D. (1997). Mitosis-specific phosphorylation of histone H3 initiates primarily within pericentromeric heterochromatin during G2 and spreads in an ordered fashion coincident with mitotic chromosome condensation. *Chromosoma* 106, 348-60.
- Hong, Y., Stronach, B., Perrimon, N., Jan, L. Y. and Jan, Y. N. (2001). *Drosophila* Stardust interacts with Crumbs to control polarity of epithelia but not neuroblasts. *Nature* 414, 634-8.
- Horne-Badovinac, S., Rebagliati, M., and Stainier, D.Y. (2003). A cellular framework for gut-looping morphogenesis in zebrafish. *Science* 302, 662-5.

- Hurd, T. W., Gao, L., Roh, M. H., Macara, I. G. and Margolis, B. (2003). Direct interaction of two polarity complexes implicated in epithelial tight junction assembly. *Nat Cell Biol* 5, 137-42.
- Ikegami, R., Rivera-Bennetts, A. K., Brooker, D. L. and Yager, T. D. (1997). Effect of inhibitors of DNA replication on early zebrafish embryos: evidence for coordinate activation of multiple intrinsic cell-cycle checkpoints at the mid-blastula transition. *Zygote* 5, 153-75.
- Jiang, Y. J., Brand, M., Heisenberg, C. P., Beuchle, D., Furutani-Seiki, M., Kelsh, R. N., Warga, R. M., Granato, M., Haffter, P., Hammerschmidt, M. et al. (1996). Mutations affecting neurogenesis and brain morphology in the zebrafish, *Danio rerio*. *Development* 123, 205-16.
- Kaplan, J. H. (2002). Biochemistry of Na,K-ATPase. *Annu Rev Biochem* 71, 511-35.
- Keino, H., Masaki, S., Kawarada, Y. and Naruse, I. (1994). Apoptotic degeneration in the rhinencephalic brain of the mouse mutant *Pdn/Pdn*. *Brain Res Dev Brain Res* 78, 161-8.
- Kimmel, C. B., Ballard, W. W., Kimmel, S. R., Ullmann, B. and Schilling, T. F. (1995). Stages of embryonic development of the zebrafish. *Dev Dyn* 203, 253-310.
- Knust, E. and Bossinger, O. (2002). Composition and formation of intercellular junctions in epithelial cells. *Science* 298, 1955-9.
- Koster, R. W. and Fraser, S. E. (2001). Direct imaging of in vivo neuronal migration in the developing cerebellum. *Curr Biol* 11, 1858-63.
- Kuida, K., Zheng, T. S., Na, S., Kuan, C., Yang, D., Karasuyama, H., Rakic, P. and Flavell, R. A. (1996). Decreased apoptosis in the brain and premature lethality in *CPP32*-deficient mice. *Nature* 384, 368-72.
- Kurokawa, K., Nakamura, K., Sumiyoshi, T., Hagino, H., Yotsutsuji, T., Yamashita, I., Suzuki, M., Matsui, M. and Kurachi, M. (2000). Ventricular enlargement in schizophrenia spectrum patients with prodromal symptoms of obsessive-compulsive disorder. *Psychiatry Res* 99, 83-91.
- Lowery, L. A. and Sive, H. (2004). Strategies of vertebrate neurulation and a re-evaluation of teleost neural tube formation. *Mech Dev* 121, 1189-97.
- Masuzawa, T., Ohta, T., Kawamura, M., Nakahara, N. and Sato, F. (1984). Immunohistochemical localization of Na<sup>+</sup>, K<sup>+</sup>-ATPase in the choroid plexus. *Brain Res* 302, 357-62.
- McAllister, J. P., 2nd and Chovan, P. (1998). Neonatal hydrocephalus. Mechanisms and consequences. *Neurosurg Clin N Am* 9, 73-93.
- Milhorat, T. H., Hammock, M. K., Fenstermacher, J. D. and Levin, V. A. (1971). Cerebrospinal fluid production by the choroid plexus and brain. *Science* 173, 330-2.

- Miyan, J. A., Nabiyouni, M. and Zendah, M. (2003). Development of the brain: a vital role for cerebrospinal fluid. *Can J Physiol Pharmacol* 81, 317-28.
- Moens, C. B. and Prince, V. E. (2002). Constructing the hindbrain: insights from the zebrafish. *Dev Dyn* 224, 1-17.
- Muller, H. A. and Bossinger, O. (2003). Molecular networks controlling epithelial cell polarity in development. *Mech Dev* 120, 1231-56.
- Nagafuchi, A. (2001). Molecular architecture of adherens junctions. *Curr Opin Cell Biol* 13, 600-3.
- Novak, Z., Krupa, P., Zlatos, J. and Nadvornik, P. (2000). The function of the cerebrospinal fluid space and its expansion. *Bratisl Lek Listy* 101, 594-7.
- Owen-Lynch, P. J., Draper, C. E., Mashayekhi, F., Bannister, C. M. and Miyan, J. A. (2003). Defective cell cycle control underlies abnormal cortical development in the hydrocephalic Texas rat. *Brain* 126, 623-31.
- Pollay, M. and Curl, F. (1967). Secretion of cerebrospinal fluid by the ventricular ependyma of the rabbit. *Am J Physiol* 213, 1031-8.
- Rekate, H. L. (1997). Recent advances in the understanding and treatment of hydrocephalus. *Semin Pediatr Neurol* 4, 167-78.
- Saito, Y. and Wright, E. M. (1983). Bicarbonate transport across the frog choroid plexus and its control by cyclic nucleotides. *J Physiol* 336, 635-48.
- Saka, Y. and Smith, J. C. (2001). Spatial and temporal patterns of cell division during early *Xenopus* embryogenesis. *Dev Biol* 229, 307-18.
- Schier, A. F., Neuhauss, S. C., Harvey, M., Malicki, J., Solnica-Krezel, L., Stainier, D. Y., Zwartkruis, F., Abdelilah, S., Stemple, D. L., Rangini, Z. et al. (1996). Mutations affecting the development of the embryonic zebrafish brain. *Development* 123, 165-78.
- Sehnert, A. J., Huq, A., Weinstein, B. M., Walker, C., Fishman, M. and Stainier, D. Y. (2002). Cardiac troponin T is essential in sarcomere assembly and cardiac contractility. *Nat Genet* 31, 106-10.
- Shu, X., Cheng, K., Patel, N., Chen, F., Joseph, E., Tsai, H. J. and Chen, J. N. (2003). Na,K-ATPase is essential for embryonic heart development in the zebrafish. *Development* 130, 6165-73.
- Skinner, D. C. and Caraty, A. (2002). Measurement and possible function of GnRH in cerebrospinal fluid in ewes. *Reprod Suppl* 59, 25-39.

- Song, M. H., Brown, N. L. and Kuwada, J. Y. (2004). The *cfy* mutation disrupts cell divisions in a stage-dependent manner in zebrafish embryos. *Dev Biol* 276, 194-206.
- Speake, T., Whitwell, C., Kajita, H., Majid, A. and Brown, P. D. (2001). Mechanisms of CSF secretion by the choroid plexus. *Microsc Res Tech* 52, 49-59.
- Takeyasu, K., Tamkun, M. M., Renaud, K. J. and Fambrough, D. M. (1988). Ouabain-sensitive ( $\text{Na}^+ + \text{K}^+$ )-ATPase activity expressed in mouse L cells by transfection with DNA encoding the alpha-subunit of an avian sodium pump. *J Biol Chem* 263, 4347-54.
- Tepass, U. (2002). Adherens junctions: new insight into assembly, modulation and function. *Bioessays* 24, 690-5.
- Therien, A. G. and Blostein, R. (2000). Mechanisms of sodium pump regulation. *Am J Physiol Cell Physiol* 279, C541-66.
- Vigh, B. and Vigh-Teichmann, I. (1998). Actual problems of the cerebrospinal fluid-contacting neurons. *Microsc Res Tech* 41, 57-83.
- Wei, X. and Malicki, J. (2002). *nagie oko*, encoding a MAGUK-family protein, is essential for cellular patterning of the retina. *Nat Genet* 31, 150-7.
- Westerfield, M. (1995). *The Zebrafish Book: A guide for the laboratory use of zebrafish*: University of Oregon Press.
- Wiellette, E., Grinblat, Y., Austen, M., Hirsinger, E., Amsterdam, A., Walker, C., Westerfield, M. and Sive, H. (2004). Combined haploid and insertional mutation screen in the zebrafish. *Genesis* 40, 231-240.
- Wright, E. M. (1978). Transport processes in the formation of the cerebrospinal fluid. *Rev Physiol Biochem Pharmacol* 83, 3-34.
- Yuan, S. and Joseph, E. M. (2004). The small heart mutation reveals novel roles of  $\text{Na}^+/\text{K}^+$ -ATPase in maintaining ventricular cardiomyocyte morphology and viability in zebrafish. *Circ Res* 95, 595-603.





## Chapter Five

### **The Spatial and Temporal Requirements for Na<sup>+</sup> K<sup>+</sup> ATPase during Brain Ventricle Development**

To be submitted as:

Laura Anne Lowery, Jenny Ruan, and Hazel Sive. The spatial and temporal requirements for Na<sup>+</sup> K<sup>+</sup> ATPase during brain ventricle development.

Contributions:

JR is an undergraduate whom LAL supervised. JR performed the Na<sup>+</sup> K<sup>+</sup> ATPase beta subunit in situ hybridizations of Figure 5.7 and provided technical assistance for Figure 5.5. LAL performed all other work for this manuscript. HS edited the final manuscript.



## Abstract

The brain ventricles are a highly conserved system of fluid-filled cavities that form during the earliest stages of brain development. The mechanisms which regulate formation of the brain ventricles and the embryonic cerebrospinal fluid they contain are poorly understood. We have previously shown that mutation in the Na<sup>+</sup>K<sup>+</sup> ATPase alpha subunit *atp1a1* leads to absence of brain ventricle inflation in the zebrafish. Here we present analysis of the temporal and spatial requirements for Na<sup>+</sup>K<sup>+</sup> ATPase function during brain ventricle development. We find that Atp1a1 function is required at two distinct steps of brain development. Early in development, requiring maternal RNA translation, Atp1a1 is necessary for formation of the intact neuroepithelium, including tight and adherens junctions. Later, Atp1a1 is not required for maintenance of the junctions, but is required for inflation of the brain ventricular lumen. This is likely due to formation of an osmotic gradient that drives flow of fluid into the ventricle space. Expression of Atp1a1 exclusively in the neuroepithelium is necessary and sufficient for normal brain ventricle formation. However, we find a dose-dependency for Atp1a1 function, with the forebrain ventricle requiring highest levels of Atp1a1 activity. Furthermore, we show that the Na<sup>+</sup>K<sup>+</sup> ATPase beta subunit *atp1b3a* is most strongly expressed surrounding the forebrain and midbrain ventricles, and is required specifically for forebrain and midbrain ventricle inflation. In sum, these data show that the Na<sup>+</sup>K<sup>+</sup> ATPase Atp1a1 plays different roles before and after neurulation. Additionally, we show, for the first time, that inflation of different brain ventricles is under spatially independent control.

## Introduction

The brain ventricles are a highly conserved system of cavities within the brain that form during the earliest stages of brain development. Inflation of these ventricles with fluid is a crucial step in brain ventricle formation. As they form, the ventricles fill with embryonic cerebrospinal fluid (eCSF), a complex, protein-rich fluid whose composition changes during different developmental stages and also between ventricles (Parada et al 2005; Parada et al 2006; Zappaterra et al 2007). While adult CSF is formed mainly by the choroid plexus located in each of the ventricles (Speake et al 2001; Brown et al 2004; Praetorius 2007), initial eCSF production and brain ventricle inflation occurs several weeks prior to choroid plexus formation in humans (Bayer and Altman 2008). Despite evidence suggesting that eCSF plays crucial roles during brain development (Miyani et al 2003), the mechanisms which regulate formation of eCSF and brain ventricle inflation are poorly understood.

We have previously shown that mutation in the  $\text{Na}^+\text{K}^+$  ATPase alpha subunit *atp1a1* leads to absence of brain ventricle inflation in the zebrafish.  $\text{Na}^+\text{K}^+$  ATPase is a heterodimeric transmembrane protein, composed of one alpha and one beta subunit, that transports  $\text{Na}^+$  and  $\text{K}^+$  across the plasma membrane to establish chemical and electrical gradients (Thomas 1972; Lingrel and Kuntzweiler 1994; Blanco and Mercer 1998; Therien and Blostein 2000). Multiple isoforms of  $\text{Na}^+\text{K}^+$  ATPase subunits have been described, although the specific functions of each subunit during vertebrate development have not been established. The mammalian genome contains four alpha subunits and three beta subunits, whereas the zebrafish genome encodes nine alpha subunits and six beta subunits (Rajarao et al 2001; Serluca et al 2001; Blasiolo et al 2002; Canfield et al 2002). While in vitro evidence demonstrates that any alpha and beta combination composes a functional  $\text{Na}^+\text{K}^+$  ATPase enzyme (Crambert et al., 2000; Lemas et al., 1994; Schmalzing et al., 1997), other experiments suggest that different isoforms have distinct biochemical properties (Blanco and Mercer 1998). Furthermore, in vivo assays show that different  $\text{Na}^+\text{K}^+$  ATPase subunits have unique physiological functions in the heart and ear (Shu et al 2003; Blasiolo et al 2006). Within the embryonic nervous system, expression of each  $\text{Na}^+\text{K}^+$  ATPase subunit displays striking spatial and temporal specificity (Orlowski and Lingrel 1988; Good et al 1990; Herrera et al 1994; Martin-Vasallo et al 1997; Serluca et al 2001; Canfield et al 2002). However, while many aspects of brain function require  $\text{Na}^+\text{K}^+$  ATPase activity, its roles during embryonic brain development have not been addressed.

Here we present analysis of the temporal and spatial requirements for Na<sup>+</sup>K<sup>+</sup> ATPase function during zebrafish brain development. Our data indicate temporally separable roles for Atp1a1 during neuroepithelial junction formation and lumen inflation. Furthermore, we present evidence that spatially restricted Na<sup>+</sup>K<sup>+</sup> ATPase activity independently inflates specific brain ventricles.

## Results

### *Brain ventricle inflation requires atp1a1 at the time of inflation*

During wild-type zebrafish brain development, the neuroepithelium undergoes morphogenesis to form the forebrain, midbrain, and hindbrain ventricles. Brain ventricle opening begins at 18 hours post fertilization (hpf), and stereotypically-shaped embryonic brain ventricles are formed by 22 hpf (Fig. 5.1A,A') (Lowery and Sive 2005). By 24 hpf, the brain ventricles have expanded in width and height (Fig. 5.1B-C,B'-C'). We previously showed that the *snakehead* (*snk*) mutant lacks visible brain ventricles at 28 hpf and has a mutation in the *atp1a1* gene (Lowery and Sive 2005). From this analysis, it was not clear when Atp1a1 function was required for brain ventricle inflation, and whether it was required in all ventricles, or only in a pivotal subset.

We began this study by asking when Atp1a1 function is required. We first asked when the *snk* mutant phenotype is apparent. The brain of the *snk* mutant looks similar to wild-type siblings at 18 hpf (data not shown), although by 22 hpf, the brain ventricles are not apparent by brightfield microscopy (Fig. 5.1D,D'). By 24 hpf, the *snk* brain tissue displays an altered refractility in which morphological landmarks of the brain, including the ventricles and the brain outline, are not visible (Fig. 5.1E,E'). However, forebrain, midbrain, and hindbrain tissue regions are apparent in lateral views (Fig. 5.1F,F'), and confocal microscopy previously showed that *snk* brain shaping is otherwise normal (Lowery and Sive 2005) (Fig. 5.1A'-F').

Atp1a1 is expressed throughout embryonic development, and a central question is whether lack of brain ventricle inflation is due to an earlier loss of Atp1a1 function. To address the temporal requirement of Atp1a1, we used a heat shock promoter to drive *atp1a1* expression in *snk* embryos and wild-type siblings at 22 hpf, after brain ventricle inflation normally initiates. We determined that expression of *atp1a1* at 22 hpf is sufficient to rescue *snk* ventricle inflation

within 2 hours after induction (Fig. 5.1H, rescue in 3/12 (25%) *snk* embryos), suggesting that *atp1a1* plays a direct role at the time of brain ventricle inflation.

### ***Brain phenotype severity depends on the timing of atp1a1 ion pump inhibition***

In order to distinguish possible maternal and zygotic *Atp1a1* requirements, we compared the effects of antisense morpholino oligonucleotide inhibition of *atp1a1* mRNA translation (Nasevicius and Ekker 2000) and pre-mRNA splicing (Draper et al 2001). The morpholino which blocks translation can potentially target both maternal and zygotic gene products, whereas blocking splicing only targets zygotic gene function.

For the translation (start-site) morpholino, we used an oligonucleotide previously documented to knock down *atp1a1* function (Yuan and Joseph 2004), which targets bases -11 to +14 of the mRNA sequence. This morpholino has a very strong, dose-dependent effect on brain ventricle inflation. A standard control morpholino (2 ng) does not affect brain ventricle inflation (Fig. 5.2A, 100% wild-type ventricles, n=41). As little as 0.25 ng of *atp1a1* start-site morpholino results in reduced brain ventricle inflation at 24 hpf (data not shown, 48% absent ventricles, 32% reduced ventricles, 20% WT, n=101), whereas 0.75 ng morpholino leads to a complete absence of brain ventricles, identical to the *snk* phenotype (Fig. 5.2C, 100% absent ventricles, n=69). Specificity of the phenotype was shown by phenotypic rescue after injection of mRNA that does not complement the morpholino sequence (Fig. 5.2E, 300-500 pg *atp1a1* mRNA rescued brain ventricle inflation in 18/19 embryos).

We determined that the *atp1a1* splice morpholino, targeted to the exon 5-intron 5 boundary, prevents normal splicing of the zygotically-synthesized *atp1a1* transcript. This results in intron 5 incorporation in all detectable mRNA by RT-PCR (Fig. 5.2B), introducing a stop codon at residue 206 and truncating the *Atp1a1* protein to 1/3 its normal size, after the second transmembrane domain (Fig. 5.2B'), which will render the protein non-functional. Injection of 5-8 ng of this morpholino results in a reduction in brain ventricle inflation (Fig. 5.2D, 75% reduced brain ventricles, n=24), however this phenotype is less severe than that of the *atp1a1* start-site morphant (compare to Fig. 5.2C). Increased doses of splicing morpholino do not result in a more severe phenotype. The morphant phenotype can be rescued by injection of 300 pg *atp1a1* mRNA (Fig. 5.2F). These data indicate that the severity of the brain phenotype depends on timing of *Atp1a1* loss, and is consistent with separable maternal and zygotic requirements.

While  $\text{Na}^+\text{K}^+$  ATPases are traditionally known as ion pumps, they have recently been shown to have a pump-independent role during *Drosophila* tracheal tube development (Paul et al 2007), where they may be involved in junction formation. To determine whether loss of ion pumping is specifically responsible for the absence of brain ventricle inflation in the *atp1a1* morphants, we treated wild-type embryos with 5 mM ouabain, an inhibitor of  $\text{Na}^+\text{K}^+$  ATPase ion pumping (Linask and Gui 1995), either beginning at 5 hpf (during gastrulation) or 16 hpf (directly prior to brain ventricle inflation). Treatment at 5 hpf leads to severely disrupted morphogenesis in all parts of the embryo, and no brain morphology is visible (Fig. 5.2G, n=30). In contrast, ouabain treatment at 16 hpf, two hours prior to ventricle inflation, gives a milder phenotype, resembling the *snk* phenotype (Fig. 5.2H, n=42). Thus, this confirms that the ion pumping activity of  $\text{Na}^+\text{K}^+$  ATPase is responsible for inflation of the brain ventricles, at a time after neurulation, and directly preceding ventricle inflation.

#### ***Loss of maternal versus zygotic atp1a1 results in differences in brain morphology and dye retention***

An unanswered question is whether the brain ventricles that form in the absence of Atp1a1 function are stuck shut. We attempted to manually inflate the ventricles with a fluorescent-dextran solution and found that the *snk* brain opens into ventricles that are shaped similarly to wild type (compare *snk* in Fig. 5.3B-B'' to wild type in Fig. 5.3A-A''). Furthermore, the introduction of fluid into the brain lumen alters the *snk* phenotype such that the ventricles become visible by brightfield microscopy (Fig. 5.3B'), indicating that the abnormal refractility in embryos lacking Atp1a1 function is due to lack of fluid in the lumen. In contrast, in 60% of the *atp1a1* start-site morphants, the brain ventricles do not open upon fluid injection, and instead dye diffuses throughout the entire head region and beyond (Fig. 5.3C''). However, the splice site morphant ventricles do not show this defect and instead inflate similarly to *snk* (Fig. 5.3D''). These data confirm that loss of maternal *atp1a1* function leads to a more severe brain defect than loss of zygotic *atp1a1*. These data suggest that the neuroepithelium is “leaky” when both maternal and zygotic Atp1a1 translation is blocked, suggesting that epithelial junctions are abnormal.

#### ***Atp1a1 ion pumping is required for neuroepithelial formation, but not maintenance***

The apparent leakiness of the brain after maternal and zygotic Atp1a1 loss of function led us to hypothesize that Atp1a1 plays an early role in neuroepithelial junction formation, in

addition to a later role in brain ventricle inflation. To address this question, we used immunohistochemistry to analyze the organization of nuclei, adherens-junction associated actin, and the apical junction marker ZO-1, within the neuroepithelium. In wild type, nuclei are organized to either side of the midline, with actin foci and ZO-1 lining the ventricular surface (Fig. 5.4A-E). In the *snk* mutant, which has maternal but not zygotic *atp1a1* function, the midline looks normal with nuclei lined up on either side, and the junction markers line the apical surface similar to wild type (Fig. 5.4F-J). However, we saw a striking phenotype in the start-site morphants, in which the midline does not form continuously and cells of the neuroepithelium are highly disorganized (Fig. 5.4K-O). Both actin foci and ZO-1 markers are localized apically but in a punctate manner (Fig. 5.4M-O). This brain phenotype also occurs after ouabain treatment from 5-22 hpf (Fig. 5.4P-T), suggesting that early embryonic  $\text{Na}^+\text{K}^+$  ATPase ion pumping is required for neuroepithelial junction formation.

Neither the splice-site morphants nor the late-treated ouabain (16-22 hpf) embryos show neuroepithelial defects, and instead they appear similar to *snk* mutants (data not shown). This is the case even when ouabain treatment is extended until 48 hpf (data not shown), suggesting that neuroepithelial disintegration is not the result of an extended ouabain treatment per se. These data also imply that  $\text{Na}^+\text{K}^+$  ATPase ion pumping is required specifically for neuroepithelial junction formation, but not maintenance, as neither 48 hpf *snk* mutants nor embryos treated with ouabain beginning at 16 hpf show defects in neuroepithelial organization (Fig. 5.4V and data not shown). Rather, both have ZO-1 labelled junctions that appear similar to wild type (Fig. 5.4U).

Our data suggest that *snk* mutants form a normal neuroepithelium due to maternal contribution providing the early *atp1a1* requirement. Another possibility, however, is that the *snk to273a* *Atp1a1* might retain some residual activity, since the *snk to273a* mutation is a single base pair mutation which results in an amino acid change from glycine to aspartate at position 271 in the amino acid sequence, within the M2-M3 cytoplasmic loop necessary for catalytic activity (Kaplan 2002). We predict that this mutation eliminates  $\text{Na}^+\text{K}^+$  ATPase *atp1a1* function by preventing ion pumping. However, we also examined a known *atp1a1* null, the *had m883* allele. In the *m883* allele, a non-sense mutation truncates half of the protein, including the catalytic domain, 5 of the transmembrane domains, and the  $\text{Na}^+\text{K}^+$  ATPase beta-subunit binding domain (Ellertsdottir et al 2006). We were unable to detect any differences between the phenotypes of *had m883* and *snk to273a* (Fig. 5.4V,W), indicating that once the neuroepithelium is formed, *Atp1a1* function is no longer required.



We also investigated the possibility that epithelial barrier function is compromised in the *snk* mutant, even though junction markers localize normally. For example, blocking Na<sup>+</sup>K<sup>+</sup> ATPase activity in retinal pigmented epithelial cell culture leads to increased tight junction permeability that is not accompanied by a change in actin localization (Rajasekaran et al 2003). Thus, we assayed for epithelial barrier function using a modified assay previously used in zebrafish (Bagnat et al 2007), testing the ability of the neuroepithelium to maintain various molecular weights of rhodamine-conjugated dextran. However, the *snk* and wild-type neuroepithelia behave similarly in terms of barrier function (data not shown), and thus it is unlikely that the permeability of *snk* neuroepithelial junctions is abnormal.

### ***Atp1a1 is spatially required within the neuroepithelium for brain ventricle inflation***

At the time of brain ventricle inflation, *atp1a1* is expressed ubiquitously throughout the embryo (Ellertsdottir et al 2006). In order to address whether *atp1a1* plays a direct role to inflate the brain, or whether brain ventricle inflation depends on a global requirement for *atp1a1* function, we used a CNS-specific promoter (miR124) to target expression of Atp1a1 to the brain in an otherwise *snk* background. In transgenic embryos expressing a CNS-driven *atp1a1* (Fig. 5.5C,F), the brain ventricles recover and show the same amount of inflation recovery that occurs with a ubiquitous *atp1a1* promoter (Fig. 5.5H). Ventricle inflation does not occur with a somite-specific promoter (miR206) (Fig. 5.5G). These data demonstrate that Atp1a1 plays a direct role within the neuroepithelium to promote brain ventricle inflation.

### ***Atp1a1 dosage requirements for brain ventricle inflation***

While initial inflation of the brain ventricles requires Atp1a1 activity within the neuroepithelium at the time of inflation, a key next question was whether Atp1a1 functions throughout the entire neuroepithelium or in distinct regions.

In order to determine the regional requirements for Atp1a1 for eCSF formation, we first used a transplantation technique to create mosaic embryos. Wild-type embryos with 10-20% *snk* mutant brain tissue have brain ventricle inflation indistinguishable from wild-type transplant controls (Fig. 5.6A,B). Quantification of forebrain and hindbrain ventricle widths confirmed this result (p=0.6840, n=17). Thus, this demonstrates that brain ventricle inflation does not require Atp1a1 function throughout the entire neuroepithelium. However, surprisingly, the reciprocal experiment, transplanting 10-20% wild-type donor tissue into *snk* host, results in *snk*-like brains

100% of the time (n=9), with no partial inflation (Fig. 5.6C). This result suggests that either there is a threshold level of Atp1a1 activity required for brain ventricle inflation, and/or there is a particular regional requirement which we were not meeting with the transplantation technique.

Supporting the threshold requirement, we observed that *snk* heterozygotes sometimes show transiently-reduced brain ventricle inflation, suggesting that 50% Atp1a1 function may be near the threshold limit. Additionally, we observed that brain ventricle inflation is sensitive to increased Atp1a1 levels as well, particularly within the forebrain ventricle. Wild-type embryos expressing increased *atp1a1* either by mRNA injection or CNS-driven *atp1a1* transgenics have forebrain ventricles that are 1.3 times larger than wild-type controls (Fig. 5.6G-I). Together, these results suggest that brain ventricle inflation requires a certain threshold amount of Atp1a1 function, and that the forebrain ventricle is particularly sensitive to Na<sup>+</sup>K<sup>+</sup> ATPase mediated inflation.

### ***Atp1b3a is specifically required for forebrain and midbrain ventricle inflation***

It was still unclear whether Na<sup>+</sup>K<sup>+</sup> ATPase activity occurs throughout the entire neuroepithelium or in discrete regions. Although the forebrain appears especially sensitive to levels of Atp1a1, a general antibody to Na<sup>+</sup>K<sup>+</sup> ATPase alpha subunits show expression throughout the brain at the time of brain ventricle inflation (Lowery and Sive 2005). However, the alpha subunit of Na<sup>+</sup>K<sup>+</sup> ATPase requires dimerization to a beta subunit for functionality, and it is possible that localization of the beta subunit could regulate Atp1a1 activity in a regionally-restricted fashion. We therefore analyzed Na<sup>+</sup>K<sup>+</sup> ATPase beta subunit expression patterns at the beginning of ventricle inflation, 18 hpf, using in situ hybridization (Fig. 5.7A-F). Whereas neither *atp1b1b* nor *atp1b2b* expression is detectable within the neuroepithelium at this stage (Fig. 5.7B,D), both *atp1b1a* and *atp1b3b* are expressed ubiquitously (Fig. 5.7A,F), and *atp1b2a* is specific to known locations of neuronal differentiation (Fig. 5.7C). Conversely, expression of *atp1b3a* is highly enriched surrounding the forebrain and midbrain ventricles, but is absent in the anterior hindbrain, with weak expression in the more posterior hindbrain (Fig. 5.7E). This *atp1b3a* expression pattern persists through 24 hpf (data not shown). Thus, *atp1b3a* is the only beta subunit whose expression is regionally-restricted in the neuroepithelium at the time of inflation.

In order to address the function of the beta subunits expressed in the the 18 hpf neuroepithelium, we designed antisense morpholino oligonucleotides to the translation initiation

sites of each mRNA. Only the morpholino targeted to *atp1b3a* gives a brain ventricle inflation defect (Fig. 5.7H, and data not shown). Compared to embryos injected with a control morpholino (Fig. 5.7G), embryos injected with the *atp1b3a* start site morpholino exhibited significantly reduced forebrain and midbrain ventricle inflation at 24 hpf, but only mildly reduced in the hindbrain (Fig. 5.7H). In order to confirm the knock-down phenotype, we also designed a splice site morpholino which causes approximately 70% of the zygotic *atp1b3a* mRNA to be abnormally spliced, as confirmed by RT-PCR (Fig. 5.7R). This leads to a protein that lacks the transmembrane domain and thus is non-functional. Injection of this morpholino also leads to reduced forebrain and midbrain ventricles (Fig. 5.7I). The specificity of the morpholinos was confirmed by rescuing the morphant phenotypes by co-injecting mRNA encoding *atp1b3a* which does not bind to either morpholino (Fig. 5.7J, and data not shown).

These data suggest that the Atp1a1 partner utilized in the forebrain and midbrain during brain ventricle inflation is Atp1b3a. In order to test this hypothesis, we injected sub-effective amounts of *atp1a1* and *atp1b3a* MOs, either alone or together. Whereas injecting 3 ng of *atp1a1* splice MO alone (Fig. 5.7O), or 1.5 ng of *atp1b3a* MO alone (Fig. 5.7P), does not result in a strong ventricle inflation defect, co-injection of these significantly reduced forebrain and midbrain ventricle inflation (Fig. 5.7Q). These experiments support the notion that Atp1b3a may spatially restrict Atp1a1 activity in the forebrain and midbrain ventricles to promote ventricle inflation (Fig. 5.8).

## Discussion

While significant work has investigated the role of  $\text{Na}^+\text{K}^+$  ATPases during brain function, no previous research has focused on the functions of these proteins during embryonic brain development. In this study, we demonstrate distinct temporal and spatial requirements for *Atp1a1* function during brain development.

### ***Differential requirement of Atp1a1 for neuroepithelial formation, but not maintenance***

Our data identify a previously undescribed role for *Atp1a1* activity and  $\text{Na}^+\text{K}^+$  ATPase ion pumping during neuroepithelial formation. The comparison of our data with that from other systems highlights that the particular junction requirement for  $\text{Na}^+\text{K}^+$  ATPase activity varies greatly depending on cell type (Rajasekaran et al 2001; Paul et al 2003; Rajasekaran et al 2003; Violette et al 2006; Cibrian-Uhalte et al 2007; Rajasekaran et al 2007).

In the zebrafish neuroepithelium, we observed that junction formation, but not maintenance, requires  $\text{Na}^+\text{K}^+$  ATPase activity. While the *snk* mutant data may be explained by another  $\text{Na}^+\text{K}^+$  ATPase compensating for loss of *atp1a1* later in development, the fact that late but long-lasting ouabain treatment has no effect on neuroepithelial junctions suggests that  $\text{Na}^+\text{K}^+$  ATPase does not play a role in junction maintenance. Perhaps this is because  $\text{Na}^+\text{K}^+$  ATPase activity is particularly important for the formation of nascent junctions during neurulation, as prior to this stage in zebrafish, neuroepithelial junctions do not exist (Geldmacher-Voss et al 2003). This role for *Atp1a1* is opposite of that observed during zebrafish heart morphogenesis, whereby  $\text{Na}^+\text{K}^+$  ATPase ion pumping promotes the maintenance but not the formation of the heart epithelium, in the junction-compromised *nagie oko* mutant background (Cibrian-Uhalte et al 2007).

$\text{Na}^+\text{K}^+$  ATPase functions distinctly in different tissue culture lines as well. In MDCK cells, loss of  $\text{Na}^+\text{K}^+$  ATPase activity prevents the localization of tight junction markers, whereas in human retinal pigment epithelial cells and human pancreatic epithelial cells, junction markers localize normally but junction permeability is abnormally increased (Rajasekaran et al 2001; Rajasekaran et al 2003; Rajasekaran et al 2007). Thus,  $\text{Na}^+\text{K}^+$  ATPase activity appears to regulate tight junctions through different mechanisms depending on cell type.

What is the molecular role for  $\text{Na}^+\text{K}^+$  ATPase function in epithelial junction formation? Because  $\text{Na}^+\text{K}^+$  ATPases control a variety of ion and metabolite transport systems, inhibition

induces multiple biochemical changes including abnormally high levels of intracellular  $\text{Na}^+$ , altered  $\text{Ca}^{2+}$  signaling, altered cell volume and pH, abnormal membrane potential, as well as defects in signaling pathways (Rajasekaran et al 2005). While Abdelilah-Seyfried and colleagues suggest that correct ionic gradients stabilize the integrity of the tight junctions (Cibrian-Uhalte et al 2007), Rajasekaran and colleagues suggest a specific mechanism in which abnormal  $\text{Na}^+$  levels directly impact junction formation through mediation of downstream signaling pathways (reviewed in (Rajasekaran and Rajasekaran 2003)).

Alternatively,  $\text{Na}^+\text{K}^+$  ATPase may act directly in junction formation as a scaffolding protein. In *Drosophila melanogaster* tracheal tube development,  $\text{Na}^+\text{K}^+$  ATPase is essential for the formation and function of septate junctions, apically localized structures similar to vertebrate tight junctions (Genova and Fehon 2003; Paul et al 2003). Mutation in  $\text{Na}^+\text{K}^+$  ATPase alpha subunit *ATPalpha* disrupts junction formation but is rescued with catalytically inactive *ATPalpha*, suggesting that junction function requires a pump-independent role of  $\text{Na}^+\text{K}^+$  ATPase (Paul et al 2007). This possible scaffolding role is supported by tissue culture experiments which show that the  $\text{Na}^+\text{K}^+$  ATPase beta subunit acts as a homophilic cell adhesion molecule (Cereijido et al 2004), and thus it is possible that  $\text{Na}^+\text{K}^+$  ATPase acts directly in epithelial junction formation and function in some systems. However, our data showing that ouabain, an ion pump inhibitor, blocks neuroepithelial formation suggests that at least one function of  $\text{Na}^+\text{K}^+$  ATPase in brain development requires ion pumping.

Thus, in this study we describe a novel role for *Atp1a1* during brain development. Further investigation of the requirement for  $\text{Na}^+\text{K}^+$  ATPase activity will be required to determine the molecular mechanism of action within the neuroepithelium. This system provides a highly tractable in vivo model for analyzing the regulation of  $\text{Na}^+\text{K}^+$  ATPase activity during epithelial junction formation.

### ***Atp1a1 plays a direct role in brain ventricle inflation***

In this paper, we show that zygotically-produced *Atp1a1* is specifically required within the neuroepithelium for brain ventricle inflation in the zebrafish. This role is distinct from the earlier requirement for junction formation but also involves ion pumping. Notably, the lack of brain ventricle inflation in the *snk* mutant is not indirectly due to a lack of functional *Atp1a1* earlier in development, as expression of *Atp1a1* at the time of inflation, or even after normal

inflation onset, can rescue brain ventricle inflation in the *snk* mutant within several hours. Thus, Atp1a1 plays a direct role at the time of brain ventricle inflation.

We hypothesize that Atp1a1 ion pumping forms the osmotic gradient that drives fluid flow into the ventricular space. Na<sup>+</sup>K<sup>+</sup> ATPases function in this manner to drive fluid flow during mouse embryonic blastocyst formation (Watson et al 2004), development of the ear epithelium (Yen et al 1993), zebrafish gut lumen formation (Bagnat et al 2007), and clearance of lung edema (Dada and Sznajder 2003; Mutlu and Sznajder 2005). This also occurs during adult CSF production in the choroid plexus, and thus, this demonstrates that despite the significant differences between adult and embryonic CSF composition (Zheng and Chodobski 2005), both critically require Na<sup>+</sup>K<sup>+</sup> ATPase function. However, Atp1a1 may also be affecting brain ventricle inflation by a different mechanism. Rather than simply forming an osmotic gradient that drives fluid secretion, the electrical gradient created by Atp1a1 activity may also alter the conformation and activity of proteins regulating eCSF secretion. Endogenous electrical fields have been shown to play a role in embryonic development in other systems such as the chick (Hotary and Robinson 1992), and it is likely that the Na<sup>+</sup>K<sup>+</sup> ATPase pump contributes to formation of an electrical gradient during development of the nervous system, as has been shown to occur in amphibian embryos (Shi and Borgens 1995). Similarly, changes in Na<sup>+</sup> and K<sup>+</sup> concentration inside the neuroepithelial cells may directly modulate the activity of molecular transporters or secretory processes. However, the exact mechanism by which Atp1a1 activity affects embryonic CSF secretion remains to be determined.

### ***Atp1b3a specifically regulates forebrain and midbrain ventricle inflation***

Numerous isoforms of both alpha and beta subunits of Na<sup>+</sup>K<sup>+</sup> ATPase exist in the vertebrate genome, and a point of contention regarding Na<sup>+</sup>K<sup>+</sup> ATPase diversity is whether the proteins have unique or redundant developmental functions. Within the embryonic nervous system, each Na<sup>+</sup>K<sup>+</sup> ATPase subunit displays striking spatial and temporal specificity, suggesting distinct functions (Orlowski and Lingrel 1988; Good et al 1990; Herrera et al 1994; Martin-Vasallo et al 1997; Serluca et al 2001; Canfield et al 2002).

We observed a specific requirement for *atp1b3a* function during brain ventricle inflation. Our evidence also suggests that Atp1a1 and Atp1b3a synergize to direct brain ventricle formation and thus these two subunits may dimerize to form a functional Na<sup>+</sup>K<sup>+</sup> ATPase within the forebrain and midbrain (Fig. 5.8). Atp1a1 synergizes with a different beta subunit, Atp1b2b,

during inner ear development (otolith biogenesis) (Blasiolo et al 2006), further suggesting that beta subunit function defines the specificity of Na<sup>+</sup>K<sup>+</sup> ATPases in different tissue types. Furthermore, in *Drosophila*, there is only one alpha gene but three beta genes which have different subcellular localizations, and it has been suggested that the beta subunits play a key role in defining the subcellular localization and specificity of Na<sup>+</sup>K<sup>+</sup> ATPase function (Paul et al 2007).

We also observed that the beta subunit Atp1b3a specifically promotes brain ventricle inflation in the forebrain and midbrain. The forebrain ventricle is particularly sensitive to Na<sup>+</sup>K<sup>+</sup> ATPase function as reducing or increasing Atp1a1 levels leads to a corresponding decrease or increase in ventricle size. Currently, it is unclear how hindbrain ventricle inflation is regulated and why there appears to be a distinct mechanism for the forebrain and midbrain ventricles. Perhaps opening of the forebrain and midbrain ventricles is more dependent on inflation forces, whereas hindbrain ventricle opening may be more dependent on tissue morphogenesis and formation of the roof plate.

In conclusion, this study demonstrates that the Na<sup>+</sup>K<sup>+</sup> ATPase alpha subunit, Atp1a1, plays two critical roles during brain development (Fig 5.8B). Additionally, the beta subunit, Atp1b3a, spatially restricts Na<sup>+</sup>K<sup>+</sup> ATPase ion pumping to inflate the forebrain and midbrain ventricles and may highlight a spatially-distinct regulatory mechanism for inflation of these ventricles.

## Experimental Procedures

### Fish lines and maintenance

*Danio rerio* fish were raised and bred according to standard methods (Westerfield 1995). Embryos were kept at 28.5°C and staged according to (Kimmel et al 1995). Times of development are expressed as hours post-fertilization (hpf).

Lines used were: AB, *snk*<sup>to273a</sup> (Jiang et al 1996), *snk*<sup>m883</sup> (Ellertsdottir et al 2006), *snk*<sup>hi3475</sup> (Amsterdam et al 2004). For PCR genotyping, tails or embryos were digested with proteinase K (1 mg/mL) in lysis buffer (10mM Tris pH8, 1mM EDTA, 0.3% Tween-20, 0.3% NP40). Because *snk*<sup>hi3475</sup> mutants have a retroviral insertion in the *atp1a1* gene, mutant individuals and carriers could be identified by PCR.

Primer sequences are listed in Table 5.1. To identify the wild-type *atp1a1* allele, *atp1a1F* and *atp1a1R* primers were used. To identify the *snk*<sup>hi3475</sup> allele, *atp1a1F* and *snk* retroviralR primers were used.

### **Brightfield Microscopy Imaging**

Embryos were anesthetized in 0.1 mg/mL Tricaine (Sigma) dissolved in embryo medium (Westerfield 1995) during imaging. Micrographs were taken using a Leica dissecting scope and a KT Spot Digital Camera (RT KE Diagnostic Instruments). Images were adjusted for brightness, contrast, and coloring in Photoshop CS (Adobe). Line tracings of brain morphology were made using Xara Xtreme Pro (Xara Group Ltd).

### **RNA injections**

Full-length *atp1a1* cDNA constructs in pCS2+ and pCS2+-His-Myc were obtained from the Chen and Abdelilah-Seyfried labs, respectively (Shu et al 2003; Cibrian-Uhalte et al 2007). To incorporate the *snk to273a* G to A mutation into the *atp1a1* cDNA (Lowery and Sive 2005), the Quik Change II XL site-directed mutagenesis kit was used following the instructions of the manufacturer (Stratagene). Primers used for mutagenesis: *snkma* and *snkmb* (Table 5.1). The mutated cDNA was verified by DNA sequencing (Northwoods DNA), using primers described previously (Lowery and Sive 2005).

A full-length *atp1b3a* construct, with a minimal Kozak consensus sequence adjacent to the initiating ATG, was generated by RTPCR with primers *b3aF* and *b3aR* (Table 5.1). The PCR fragments were subcloned into pGEM-T Easy Vector (Promega), and then subcloned into the EcoRI site in pCS2+.

A construct encoding membrane-targeted CAAX-eGFP in PCS2+, used for control injections, was obtained from the Green lab (Harvard Medical School).

Capped *atp1a1*, *atp1a1*<sup>GtoA</sup>, *HisMyc-atp1a1*, *atp1b3a*, and membrane-GFP mRNAs were transcribed in vitro using the SP6 mMessage mMachine kit (Ambion), after linearization by NotI. Embryos were injected at the one-cell stage with 100-800 pg mRNA. The embryos phenotypically rescued by mRNA injection were identified as mutants by genotyping.

### **Morpholino oligo injections**

Antisense morpholino oligonucleotides (MO) (Gene Tools, LLC) were injected into



embryos at the 1-2 cell stage. The MOs used were *atp1a1start* (Table 5.2) and has been used previously to knock down *atp1a1* (Yuan and Joseph 2004), *atp1a1splice*, *atp1b3astart*, *atp1b3asplice*, *atp1b3b start*, *atp1b1a start*, *atp1b2a start*, *atp1b2b start*, *atp1b3b splice*, and Gene Tools standard control MO. Between 0.5 - 1 nl was injected into the single cell of each embryo with a MO concentration of 3 - 6 ng/nl. Final amounts used are noted in the Results.

## **RT-PCR**

RNA was extracted from individual morphant and control embryos using Trizol reagent (Invitrogen), followed by chloroform extraction and isopropanol precipitation. RNA was pelleted by centrifugation, resuspended in 30uL distilled water, then precipitated with LiCl. cDNA synthesis was performed with Super Script II Reverse Transcriptase (Invitrogen) and random hexamers. PCR was then performed using primers which amplified the exonic and intronic sequence surrounding the splice MO target. *atp1a1* primers: *atp1a1 testF* and *atp1a1 testR*. *atp1b3a* primers: *B3A TESTF*, *B3A TESTR*.

## **Transgenic analysis**

To make F<sub>0</sub> transgenic embryos for analysis, microinjections of plasmid DNA with meganuclease were carried out as described by (Thermes et al 2002). Briefly, 1 cell embryos were injected with: 1X I-SceI buffer, 0.2 units I-SceI enzyme, and 50ng plasmid DNA. Embryos injected with empty vector and uninjected embryos were used as controls. *miR124* and *miR206* promoters were cloned previously (Shkumatava et al, in preparation 2008). *Beta-actin* promoter and IRES-GFP from Chien lab (University of Utah). After analysis, embryos were digested for PCR genotyping.

## **Heat shock driven-*atp1a1* transgenic analysis**

We generated the GFP:HSE:*atp1a1* construct, expressing both GFP and *atp1a1*. We used the artificial heat-shock promoter (Bajoghli et al 2004), driving bidirectional expression of both genes. The heatshock treatment was performed from 22 hpf, following sorting of mutant and wild-type sibling embryos, as described by (Bajoghli et al 2004). After heat shock treatment, *snk* mutant embryos were analyzed every hour for evidence of brain ventricle inflation and GFP expression in the brain.

## **Ouabain treatment**

Embryos were incubated in 5mM ouabain (Sigma) in embryo media at various time-points, as noted in text (Yuan and Joseph 2004). Not all the embryos responded to ouabain soaking at 16 hpf, and it is possible that ouabain has difficulty in penetrating the embryonic epidermis at this stage. To bypass this issue, we also injected 1nL 5 mM ouabain directly into the brain tissue.

## **Brain ventricle injection experiments**

Methods for brain ventricle imaging after ventricle injection have been described previously (Lowery and Sive 2005). Briefly, for the manual inflation assay, embryos were anesthetized in 0.1 mg/mL Tricaine (Sigma) dissolved in embryo medium (Westerfield 1995) prior to injection and imaging. The hindbrain ventricle was micro-injected with 2-15 nL 2000K MW dextran conjugated to Rhodamine (Sigma, 12% in water), using enough pressure to inflate all the ventricles with dye. For the tight junction permeability tests, various molecular weight dextrans conjugated to Rhodamine (Sigma, 12% in water) were used, ranging from 4K to 2000K. Micrographs were taken with light and fluorescent illumination prior to and following injection, with a Leica dissecting microscope, using a KT Spot Digital Camera (RT KE Diagnostic Instruments). Images were superimposed in Photoshop 6 (Adobe).

## **Immunohistochemistry**

For labeling with phalloidin-Alexa Fluor 488 and SYTO nuclei dye, embryos were fixed in 4% paraformaldehyde 2 hours at room temperature, then rinsed in PBS and dechorionated. For labeling with anti-ZO1 monoclonal antibody and anti-alpha  $\text{Na}^+\text{K}^+$  ATPase  $\alpha 6\text{F}$  antibody, dechorionated embryos were fixed in Dent's fixative (80% methanol, 20% DMSO) for 2 hours at room temperature, then rinsed in PBS (Dent et al., 1989). Blocking was done for 4 hours at room temperature in 0.5 % Triton X, 10% normal goat serum, in phosphate buffer. Whole-mount immunostaining was carried out phalloidin-Alexa Fluor 488 (Molecular Probes, 1:200), SYTO 83 nuclei dye (Molecular Probes, 1:1000), anti-ZO-1 monoclonal antibody (Zymed Laboratories Inc, 1:200), and mouse monoclonal antibody alpha6F, raised against chicken alpha subunit of  $\text{Na}^+\text{K}^+$  ATPase (Takeyasu et al., 1988, 1:100) which was obtained from the Developmental Studies Hybridoma Bank. Goat anti-mouse Alexa Fluor 488 (Molecular Probes,

1:500) was used as secondary antibodies. Brains were flat-mounted in glycerol and imaged with Zeiss LSM scanning confocal microscope. Some images are a compilation of several z-scans.

### **In situ hybridization**

RNA probes containing digoxigenin (DIG)-11-UTP were synthesized from linearized plasmid DNA, as described (Harland 1991). Standard methods for hybridization and for single color labeling were used as described elsewhere (Sagerstrom et al 1996). After staining, embryos were fixed in 4% paraformaldehyde overnight at 4 degrees C, washed in phosphate buffered saline (PBS), dehydrated in methanol, and then cleared in a 3:1 benzyl benzoate/benzyl alcohol (BB/BA) solution before mounting and imaging with a Nikon compound microscope.

### **Transplantations**

Transplantations were performed using a protocol modified from the Mullins Lab. Donor embryos were injected with Rhodamine-dextran at the 1 cell stage, and host embryos with membrane-GFP mRNA. Embryos were dechorionated and placed in a dish coated with agarose, in 1x Ringers with high calcium (116 mM NaCl, 2.9 mM KCl, 10mM CaCl<sub>2</sub>, 5 mM HEPES, pH 7.2)/1.6% egg white solution. Addition of egg whites helps in quick healing of transplant. Using a hair knife or pulled glass capillary knife, cells from blastoderm were removed from donor and transferred into same stage host embryos, near the animal cap. Embryos were left in Ringers/Egg whites 10 minutes then transferred to agarose-coated petri dish containing 1/3x Ringers using a glass transfer pipet. To prepare the cleared chicken egg whites, egg whites were whipped from one chicken egg with a whisk until the whites turned glossy and their tips stood tall. Egg whites were then left for 20 minutes, and the clear egg white solution from beneath the foam was collected and frozen in aliquots at -20 degrees C.

### **Forebrain ventricle size quantification**

Brightfied images of live anesthetized images were taken as described above. The forebrain ventricle size as viewed dorsally was measured, blind to the genotype, with ImageJ software and statistics were performed with GraphPad InStat software.

## **Acknowledgements**

We thank members of the Sive lab for helpful comments and Olivier Paugois for fish husbandry. Many thanks to the Nusslein-Volhard lab for providing us with the *snakehead* mutant, Jaunian Chen for providing *atp1a1*-PCS2+, Abdelilah-Seyfried for providing *atp1a1*-PCS2+-HisMyc, Jeremy Green for memGFP plasmid, T. Czerny for the GFP:HSE construct, Mullins lab for transplant protocol. Special thanks to Alena Shkumatava for providing the *miR-124* and *206* promoters prior to publication. This work was conducted utilizing the W.M. Keck Foundation Biological Imaging Facility at the Whitehead Institute. Supported by NIH MH70926 to HLS, NIH NRSA pre-doctoral fellowship and Abraham J. Siegel Fellowship at the Whitehead Institute to LAL.

**Table 5.1 Primer sequences used in this study.**

<b>Primer Name</b>	<b>Sequence</b>
<i>atp1a1F</i>	5'- GCAGCAAAATGGGACGAGGAG -3'
<i>atp1a1R</i>	5'- TGCGCACATTTTCATTCATT -3'
<i>snk retroviralR</i>	5'- GCTAGCTTGCCAAACCTACAGGT -3'
<i>snkma</i>	5'- CCGCACAGTCATGGATCGTATTGCCACTCTCG -3'
<i>snkmb</i>	5'- CGAGAGTGGCAATACGATCCATGACTGTGCGG -3'
<i>b3aF</i>	5'- CACCATGTCTAAAAAGAGCGAAAAT -3'
<i>b3aR</i>	5'- AGCACAAGTTCCCTTCAGC -3'
<i>atp1a1 testF</i>	5'- CTCTTTCAAGAATTTGGTTCCC -3'
<i>atp1a1 testR</i>	5'- CTCGATCTCAATAGAGATGGGGGTGC -3'
<i>B3a TESTF</i>	5'- GCAGTGATTTTCAGCCTCCTC -3'
<i>B3a TESTR</i>	5'- GTATCCTCCATCCCAGAGCA -3'

**Table 5.2 Morpholino (MO) sequences used in this study.**

<b>MO name</b>	<b>MO sequence</b>
<i>atp1a1start</i>	5'- AAAGCAGCAAAATGGGACGAGGAGA -3'
<i>atp1a1splice</i>	5'- AATATAATATCAATAAGTACCTGGG -3'
<i>atp1b3astart</i>	5'- CGCTCTTTTTAGACATGCTGAAATG -3'
<i>atp1b3asplice</i>	5'- AACTGCACACTAACAACTTACCTG -3'
<i>atp1b3bstart</i>	5'- CATAGTGTGGAGAGGATAGATAAAC -3'
<i>atp1b1astart</i>	5'- ACCATCTTTATTTGCGGGCATTTC -3'
<i>atp1b2astart</i>	5'- GCCATGTCTCCGGTAGATTCTCGGT -3'
<i>atp1b2bstart</i>	5'- TTTCCTGGACTAAATGTGCGCTCAC -3'
<i>atp1b3bsplice</i>	5'- TAAAAGAGGAATATAAGAGCTGCGG -3',
Control	5'- CCTCTTACCTCAGTTACAATTTATA -3'

**Figure 5.1 Brain ventricle inflation requires *Atp1a1* at the time of inflation.**

(A-K) Brightfield microscopy images of live zebrafish embryos at 22-24 hpf, all are dorsal views except for side views in (C) and (F). (A'-I') Tracings of brain morphology visible by brightfield microscopy are shown in black, while morphology which is present but not visible is shown in dotted grey. (A, A') Brain of wild-type sibling at 22 hpf, forebrain, midbrain, and hindbrain ventricles are inflated, (B, B') inflation continues and midbrain and hindbrain ventricles of 24 hpf wild-type sibling are increased in size, (C, C') same embryo as in B, side view. (D, D') *snk to273a* at 22 hpf, hindbrain opening is just visible and outline of brain tube is apparent, but there is no other visible ventricle morphology. (E, E') By 24 hpf, *snk* brain morphology has altered refractivity such that no brain morphology is visible, although the three brain regions, forebrain, midbrain, and hindbrain, are apparent in side views of same embryo (F, F'). (G-I) F0 transgenic *snk* embryos expressing a heat-shock driven GFP do not rescue *snk* brain ventricle inflation after heat-shock (G,G'), but the ventricles of those expressing *atp1a1* begin to inflate within 2 hours after heat-shock (H, H'). (I) is fluorescent image of embryo in (H). Anterior to left. F forebrain, M midbrain, H hindbrain. Scale bars 50  $\mu$ m.

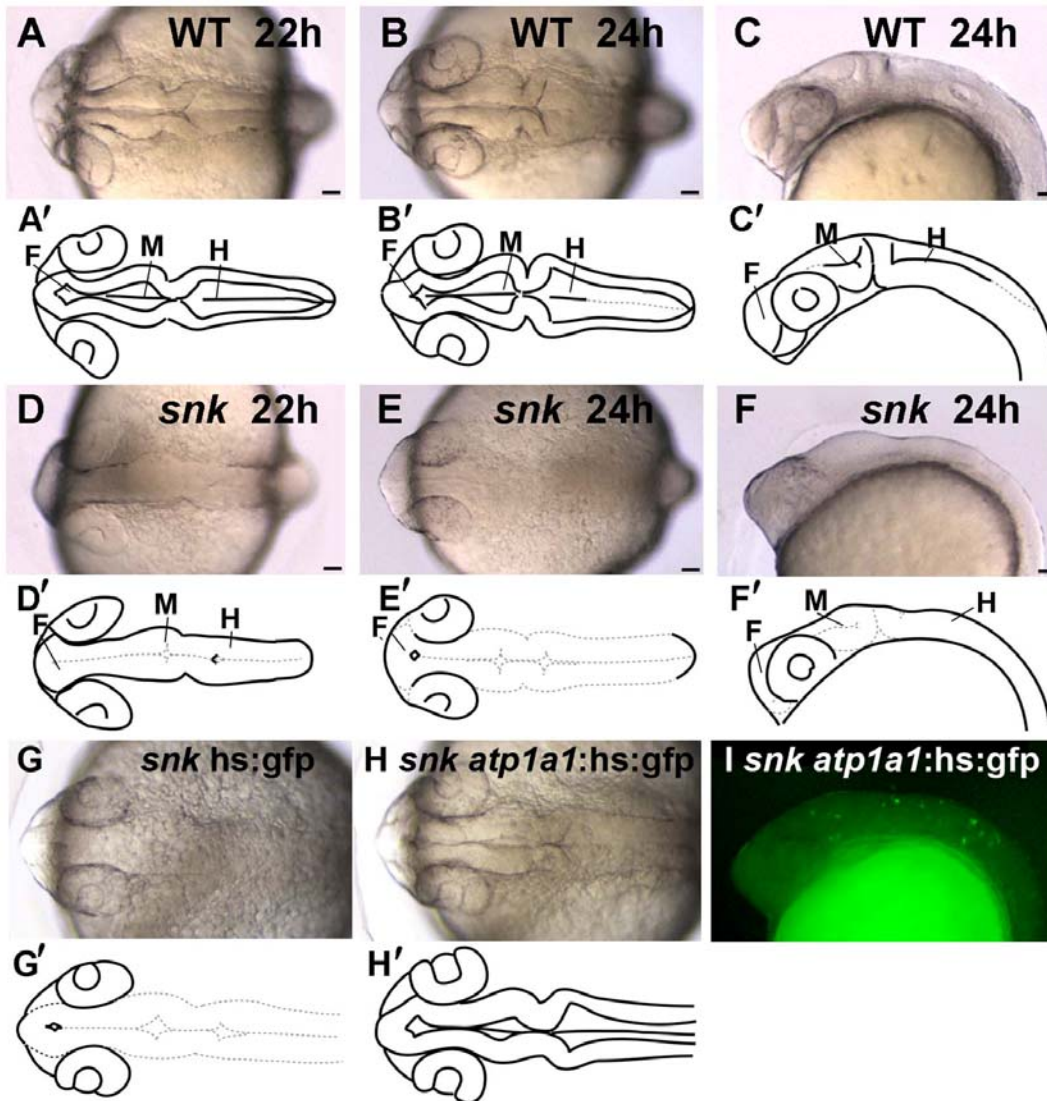






### Figure 5.2 Brain phenotype severity depends on the timing of Atp1a1 ion pump inhibition

(A,C-H) Brightfield microscopy images of live zebrafish embryos at 22-24 hpf, dorsal views. (A',C'-H') Tracings of brain morphology visible by brightfield microscopy are shown in black, while morphology which is present but not visible is shown in dotted grey. (A, A') Control morpholino does not affect brain ventricle morphology. (B) RT-PCR with primers specific to *atp1a1* demonstrates that *atp1a1* splice morphants have a larger splicing product than control morphants. An intron is abnormally incorporated, which causes a nonsense mutation and truncation of the protein after the second transmembrane domain, shown in (B'). (C, C') Morpholino to the *atp1a1* translation start site mimics the *snk* brain inflation phenotype, and (E,E') injection of *atp1a1* mRNA which does not bind to the morpholino rescues the inflation defect. (D, D') Morpholino designed to inhibit *atp1a1* splicing results in brain ventricle inflation less severe than the *snk* phenotype. The ventricles do not inflate, although the brain tube outline is normal and a small hindbrain ventricle opening is visible. (F, F') The *atp1a1* splice morphant phenotype is rescued by injection of *atp1a1* mRNA. (G, G') Incubation of wild-type embryos in ouabain, a Na<sup>+</sup>K<sup>+</sup>ATPase inhibitor, at 5 hpf results in a phenotype similar to, but more severe, than the *atp1a1* start-site morphant phenotype. No ventricles are visible, and neither is eye morphology (H, H') Incubation of wild-type embryos in ouabain at 17 hpf results in a phenotype similar to the *snk* phenotype. No ventricles are visible, although the outline of the brain tube is barely discernible. Anterior to left. F forebrain, M midbrain, H hindbrain. Scale bars 50  $\mu$ m.

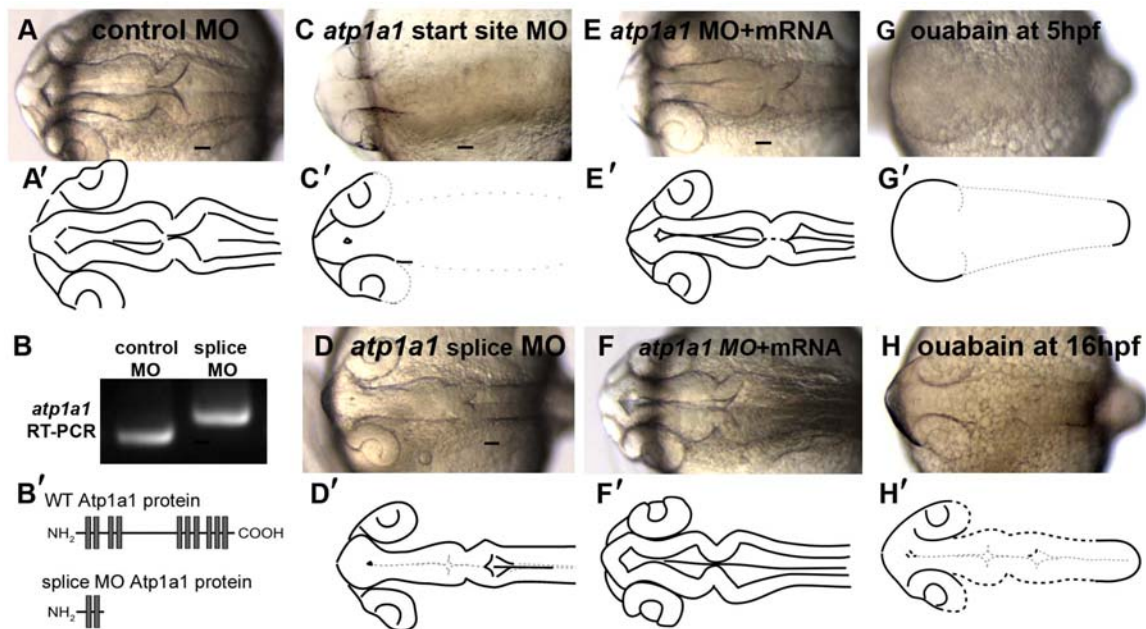




**Figure 5.3 Loss of maternal versus zygotic *atp1a1* results in differences in brain morphology and dye retention.**

(A-D, A'-D') Brightfield microscopy images of live zebrafish embryos at 24 hpf, immediately prior to and following manual ventricle inflation with Rhodamine-dextran. (A''-D'') Superimposition of brightfield and fluorescent images following ventricle inflation. Each row depicts different images of the same embryo. (A) Wild-type embryo: prior to ventricle inflation, wild-type ventricles are open and visible (A), whereas after ventricle inflation, ventricle size is slightly increased (A'). Dye stays within the ventricle cavities (A''), and highlights the internal ventricle hinge-points in the forebrain, midbrain, and hindbrain (A'', asterisks). (B) *snk* embryo: prior to ventricle inflation, *snk* ventricle morphology is not apparent (B), however after manual inflation, refractility is altered and ventricles are visible (B'), although smaller than wild type. (B'') *snk* ventricle morphology is relatively normal, with three pairs of hinge-points in the forebrain, midbrain, and hindbrain (B'', asterisks), as in wild type (A''). (C) *atp1a1* start site morphant (1ng MO): prior to ventricle inflation, no morphology is visible (C). Ventricle inflation does not proceed normally, with much of the dye spilling out of the brain region and into the surrounding areas (C''), midbrain and hindbrain ventricle morphology following injection is not apparent, however the forebrain ventricle does open somewhat normally in this embryo (C'', asterisks). (D) *atp1a1* splice site morphant embryo: prior to ventricle inflation, visible ventricle morphology is reduced (D). After inflation, ventricles are apparent (D') and normally shaped (D'', asterisks). Anterior to left. Scale bars 50  $\mu$ m.

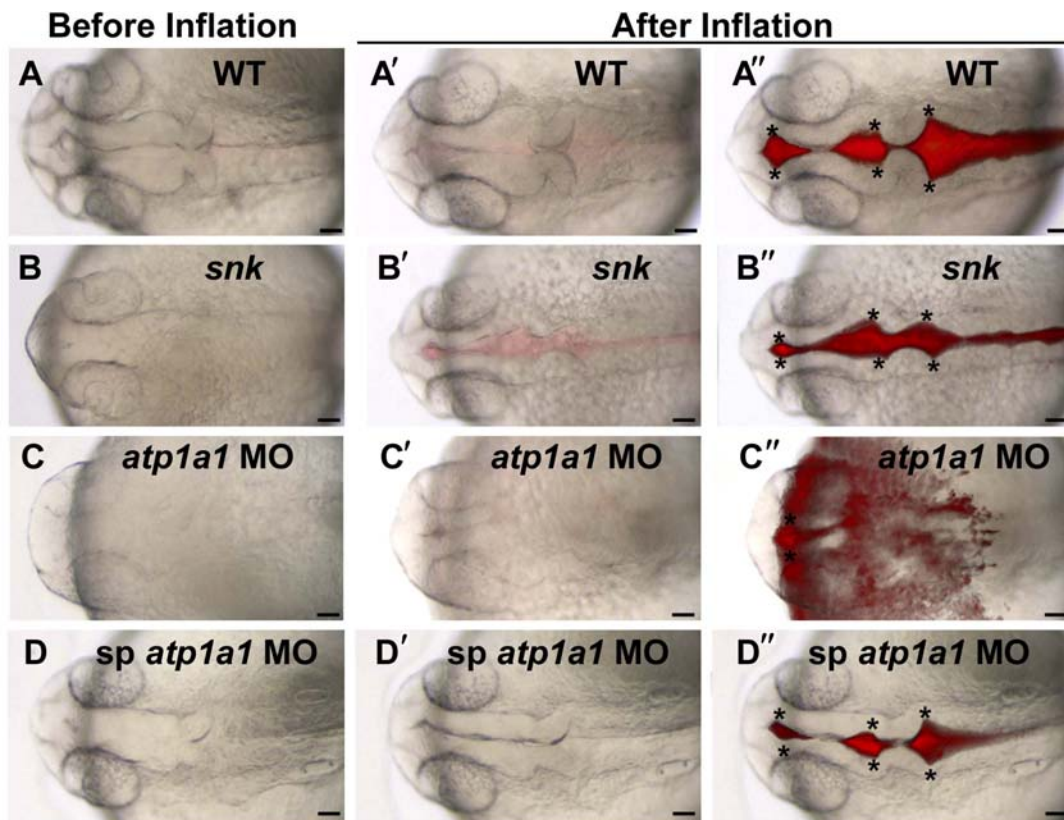




**Figure 5.4 Atp1a1 ion pumping is required for neuroepithelial formation, but not maintenance.**

(A-T) Horizontal confocal sections through the midbrains of 22 hpf wild-type embryos (A-E), *snk* embryos (F-J), *atp1a1* start site morphants (K-O), wild-type embryos treated in 5mM ouabain from 5-22hpf (P-T), except for (D, I, N, S) which are 3D projections of 30um confocal z-series of the midbrain and hindbrain. (A-E) Wild-type embryos show normal brain morphology, including apical-associated actin foci (phalloidin-Alexa Fluor 488 is green, A and C), organized nuclei (red, A and B), and the junction marker ZO-1 localizes to the ventricular surface (D, E). (F-J) *snk* mutants have closed ventricles but the midline forms normally, nuclei are organized, and junctions are connected. (K-O) *atp1a1* start site morphants do not form a continuous midline, the nuclei are disorganized, and the junctions are not continuous. Instead there are random puncta of ZO-1 labeling throughout the brain region (K, M, O). (P-T) Embryos treated from 5-22hpf with ouabain show a similar phenotype as the *atp1a1* start site morphants, with disorganized nuclei and junctions. (U-W) Horizontal confocal projection through the brains of 48 hpf wild type (U), *snk to273a* (V), and *had m883* (W) following labeling with the ZO-1 antibody. Anterior to top left corner. Scale bars 50 um.



Figure 5.4 continued

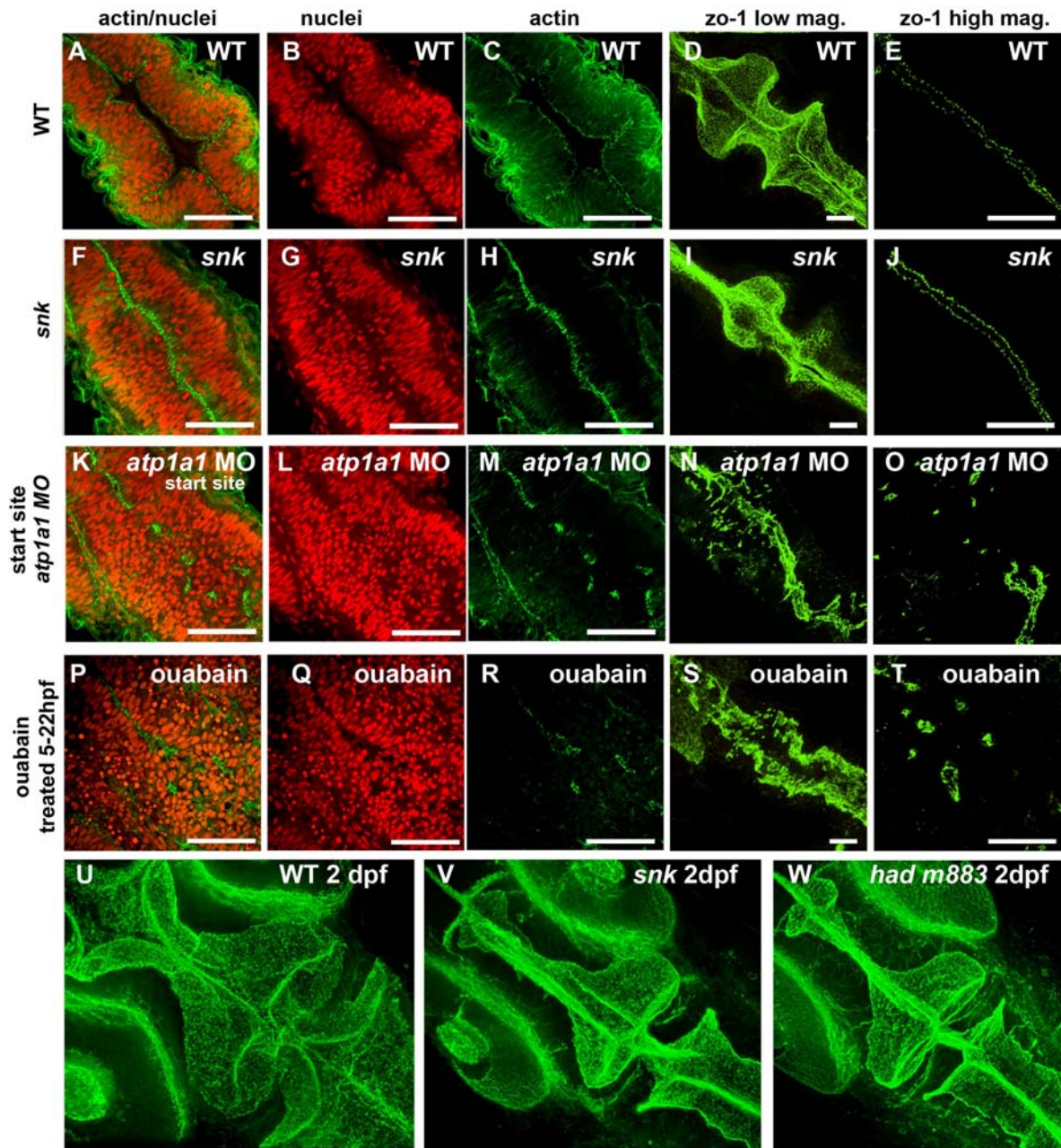






**Figure 5.5 Atp1a1 is spatially required within the neuroepithelium for brain ventricle inflation.**

(A-F) Brightfield microscopy of live embryos at 26 hpf, dorsal views (A-C) and lateral views (D-F). (A,D) F0 transgenic wild-type sibling expressing the empty vector transgene; (B,E) F0 transgenic *snk* mutant expressing the empty vector transgene shows no ventricle morphology; (C,F) F0 transgenic *snk* mutant expressing CNS-specific *atp1a1* displays visible ventricle morphology; (G) F0 transgenic *snk* mutant expressing somite-specific *atp1a1* shows no ventricle morphology; (H) F0 transgenic *snk* mutant expressing ubiquitous *atp1a1* displays visible ventricle morphology. The transgenic *snk* ventricles do not inflate completely with either the CNS-specific (C) or ubiquitous promoters (H), but this is likely due to the mosaicism of F0 transgenics and the ventricle inflation is still substantial.

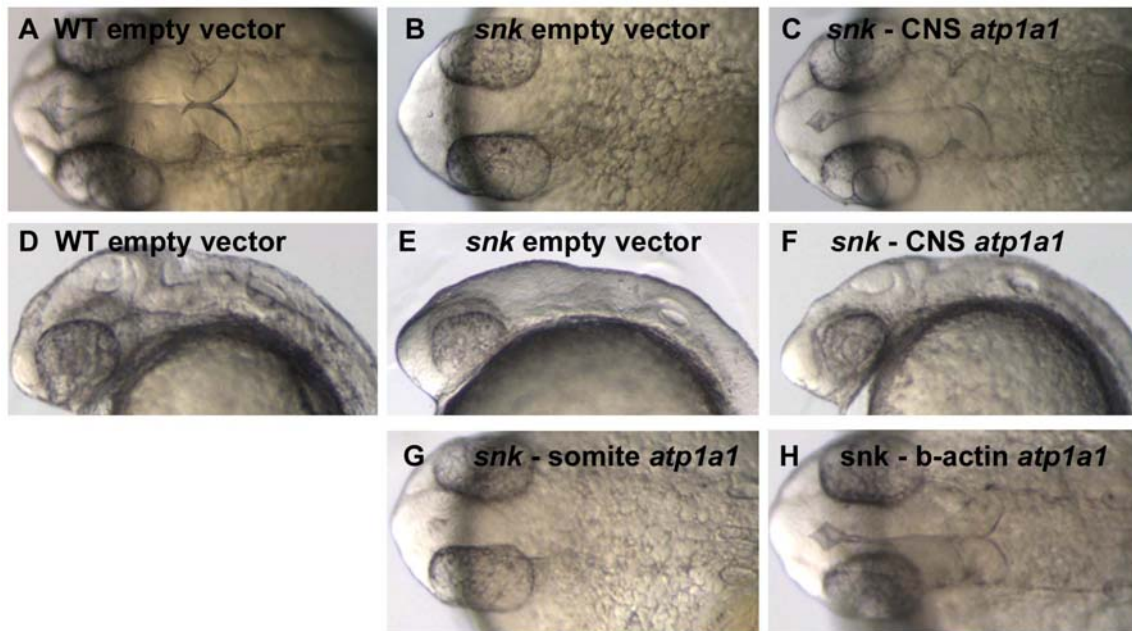




**Figure 5.6 Atp1a1 dosage requirements for brain ventricle inflation.**

(A-F) Juxtaposition of brightfield and fluorescent microscopy images of mosaic embryos at 24 hpf, dorsal views (A-C) and lateral views (D-F). Donor tissue is pink and host tissue is unlabeled. (A,D) WT donor tissue into WT host control; (B,E) *snk* donor tissue into WT host; (C,F) WT donor tissue into *snk* host. (G,H) Brightfield microscopy images of dorsal views of forebrain ventricles of living 28 hpf embryos. (G) wild type, (H) F0 transgenic wild type expressing CNS-specific *atp1a1* shows increased forebrain ventricle size, (I) quantification of forebrain ventricle size, n = 10 for each data set.

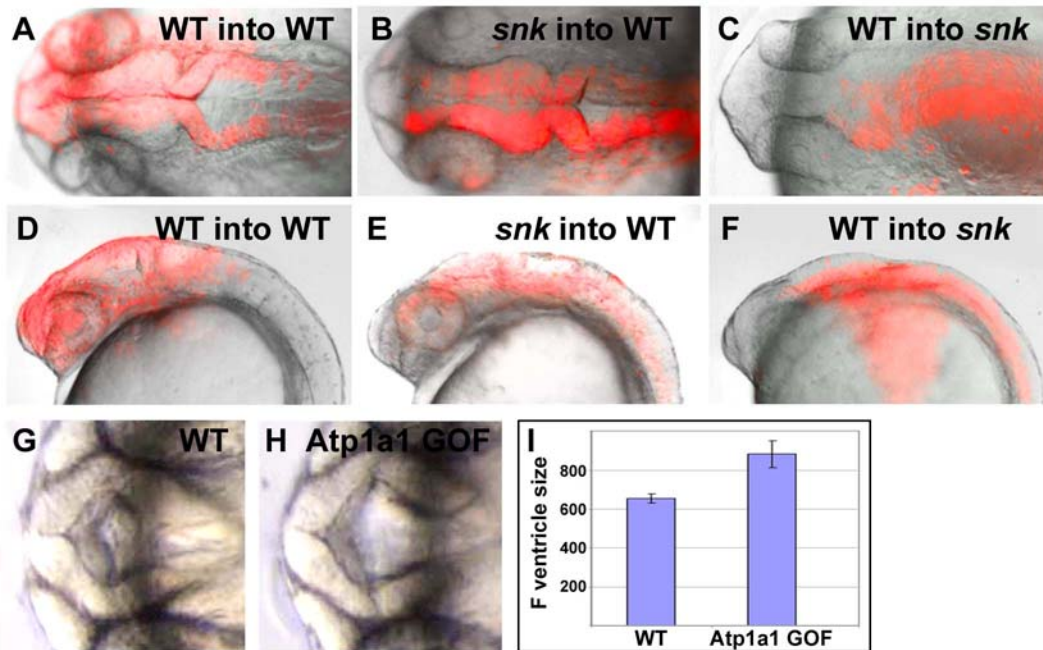




**Figure 5.7 *atp1b3a* is specifically required for forebrain and midbrain ventricle inflation.** Dorsal views of brain flat-mounts after in situ hybridization with probes for *atp1b1a* (A), *atp1b1b* (B), *atp1b2a* (C), *atp1b2b* (D), *atp1b3a* (E), *atp1b3b* (F). Both *atp1b1a* and *atp1b3b* are expressed ubiquitously (A,F), *atp1b2a* is expressed neuronally (C), *atp1b3a* expressed in forebrain, midbain, eyes, and posterior hindbrain (E), and *atp1b1b* and *atp1b2b* are expressed at very low levels (B,D). (A-G) Brightfield microscopy images of dorsal views of living 24 hpf embryos. (A'-D') Higher magnification views of the forebrain ventricles of embryos in (A-D). (A''-D'') Tracings of forebrain ventricles in (A'-D'). (A) control morphant shows normal brain ventricle opening; (B, D) *atp1b3a* start site- and splice site- morphants show severely reduced forebrain ventricle opening but relatively normal hindbrain ventricle opening. The midbrain ventricle appears partially reduced in size. (D) Injection of *atp1b3a* mRNA into the morphant embryos recovers forebrain ventricle inflation. (E-G) Brightfield microscopy images of dorsal views of living 22 hpf embryos. Suboptimal amounts of *atp1a1* MO (E) and *atp1b3a* MO (F) appear normal, but the combination of both (G) strongly inhibits forebrain and midbrain, but not hindbrain, ventricle opening. (H) RT-PCR showing abnormal *atp1b3a* mRNA splicing due to the splicing MO. Approximately 2/3 of the mRNA is abnormally spliced.

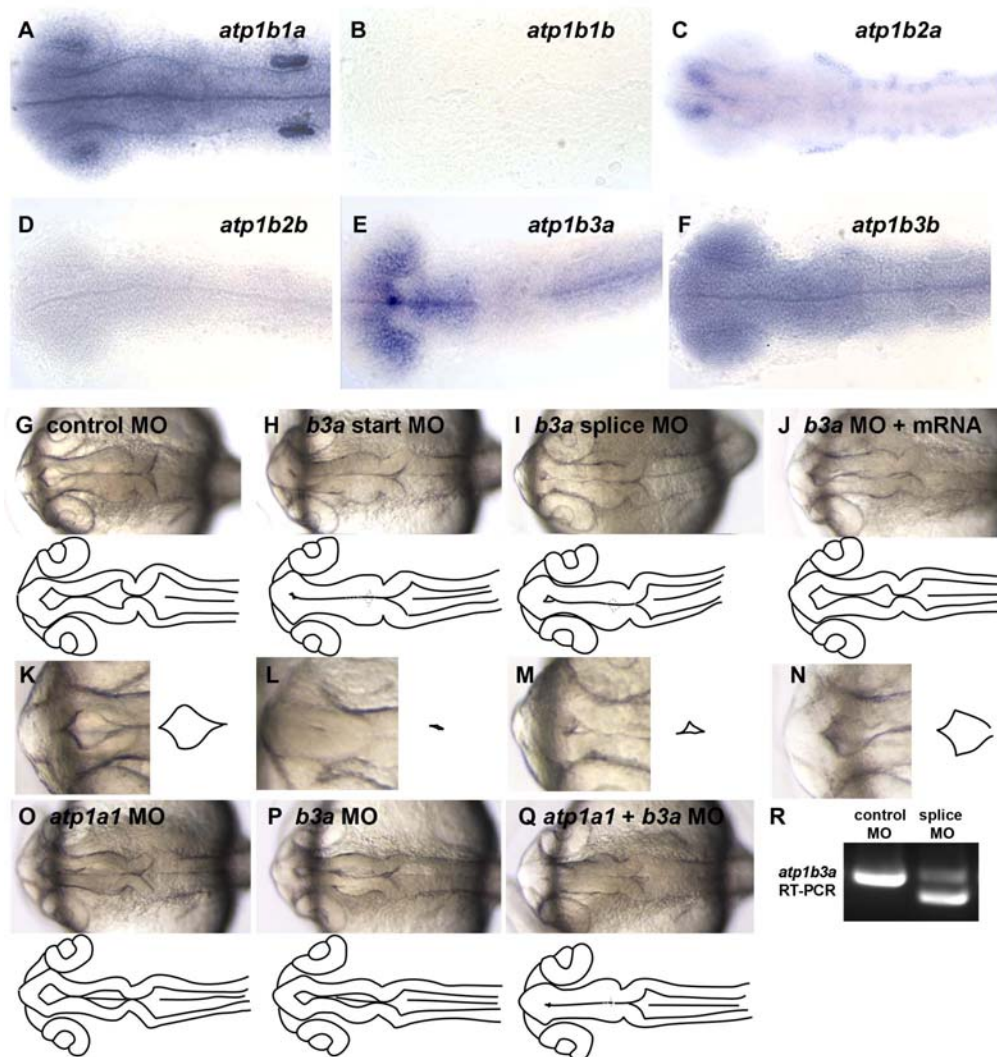
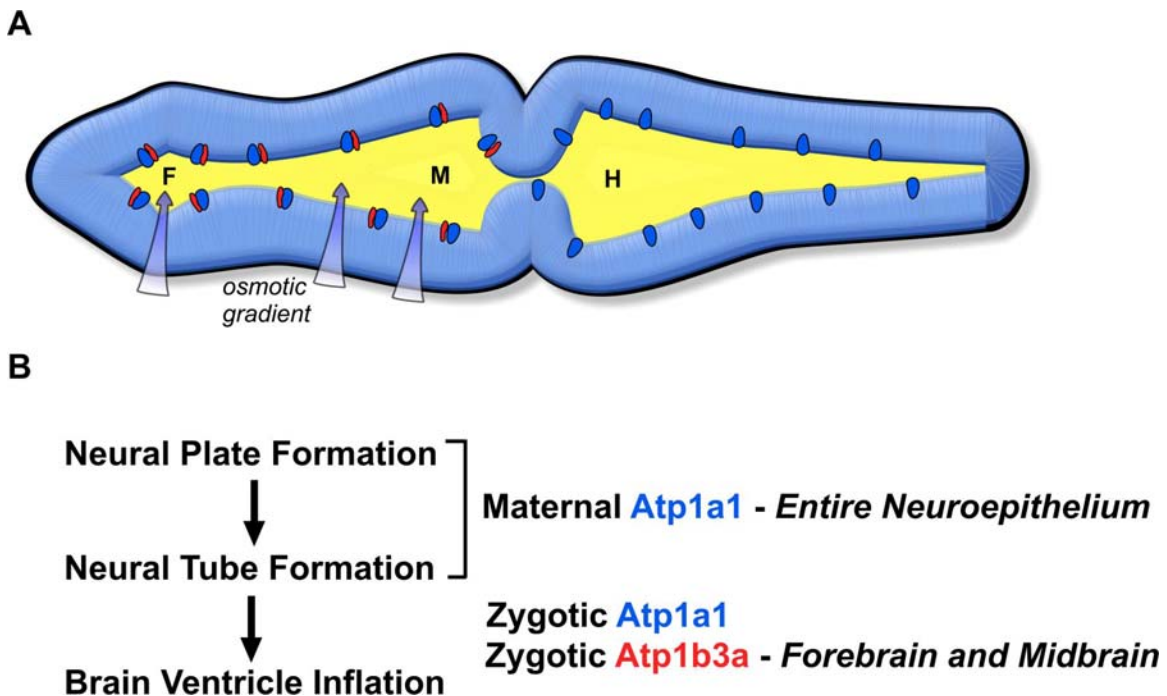




### Figure 5.8 Roles of Atp1a1 and Atp1b3a during brain development

(A) Atp1a1 (blue oval) is expressed throughout the neuroepithelium, whereas Atp1b3a (red oval) spatially restricts  $\text{Na}^+\text{K}^+$  ATPase ion pumping to inflate the forebrain and midbrain ventricles and may highlight a spatially-distinct regulatory mechanism for inflation of these ventricles. (B) Atp1a1 plays two roles during brain development.

Early in development, Atp1a1 is necessary for formation of the intact neuroepithelium, including tight and adherens junctions. Later, Atp1a1 is required for inflation of the brain ventricular lumen. This is likely due to formation of an osmotic gradient that drives flow of fluid into the ventricle space.







## References

- Amsterdam, A., R. M. Nissen, Z. Sun, E. C. Swindell, S. Farrington and N. Hopkins (2004). "Identification of 315 genes essential for early zebrafish development." Proc Natl Acad Sci U S A **101**(35): 12792-7.
- Bagnat, M., I. D. Cheung, K. E. Mostov and D. Y. Stainier (2007). "Genetic control of single lumen formation in the zebrafish gut." Nat Cell Biol **9**(8): 954-60.
- Bajoghli, B., N. Aghaallaei, T. Heimbucher and T. Czerny (2004). "An artificial promoter construct for heat-inducible misexpression during fish embryogenesis." Dev Biol **271**(2): 416-30.
- Bayer, S. A. and J. Altman (2008). The human brain during the early first trimester. Boca Raton, Fla.; London, CRC.
- Blanco, G. and R. W. Mercer (1998). "Isozymes of the Na-K-ATPase: heterogeneity in structure, diversity in function." Am J Physiol **275**(5 Pt 2): F633-50.
- Blasiolo, B., V. Canfield, A. Degraeve, C. Thisse, B. Thisse, J. Rajarao and R. Levenson (2002). "Cloning, mapping, and developmental expression of a sixth zebrafish Na,K-ATPase alpha1 subunit gene (atp1a1a.5)." Gene Expr Patterns **2**(3-4): 243-6.
- Blasiolo, B., V. A. Canfield, M. A. Vollrath, D. Huss, M. A. Mohideen, J. D. Dickman, K. C. Cheng, D. M. Fekete and R. Levenson (2006). "Separate Na,K-ATPase genes are required for otolith formation and semicircular canal development in zebrafish." Dev Biol **294**(1): 148-60.
- Brown, P. D., S. L. Davies, T. Speake and I. D. Millar (2004). "Molecular mechanisms of cerebrospinal fluid production." Neuroscience **129**(4): 957-70.
- Canfield, V. A., B. Loppin, B. Thisse, C. Thisse, J. H. Postlethwait, M. A. Mohideen, S. J. Rajarao and R. Levenson (2002). "Na,K-ATPase alpha and beta subunit genes exhibit unique expression patterns during zebrafish embryogenesis." Mech Dev **116**(1-2): 51-9.
- Cereijido, M., R. G. Contreras and L. Shoshani (2004). "Cell adhesion, polarity, and epithelia in the dawn of metazoans." Physiol Rev **84**(4): 1229-62.
- Cibrian-Uhalte, E., A. Langenbacher, X. Shu, J. N. Chen and S. Abdelilah-Seyfried (2007). "Involvement of zebrafish Na<sup>+</sup>,K<sup>+</sup> ATPase in myocardial cell junction maintenance." J Cell Biol **176**(2): 223-30.
- Dada, L. A. and J. I. Sznajder (2003). "Mechanisms of pulmonary edema clearance during acute hypoxemic respiratory failure: role of the Na,K-ATPase." Crit Care Med **31**(4 Suppl): S248-52.

- Draper, B. W., P. A. Morcos and C. B. Kimmel (2001). "Inhibition of zebrafish fgf8 pre-mRNA splicing with morpholino oligos: a quantifiable method for gene knockdown." Genesis **30**(3): 154-6.
- Ellertsdottir, E., J. Ganz, K. Durr, N. Loges, F. Biemar, F. Seifert, A. K. Ettl, A. K. Kramer-Zucker, R. Nitschke and W. Driever (2006). "A mutation in the zebrafish Na,K-ATPase subunit atp1a1a.1 provides genetic evidence that the sodium potassium pump contributes to left-right asymmetry downstream or in parallel to nodal flow." Dev Dyn **235**(7): 1794-808.
- Geldmacher-Voss, B., A. M. Reugels, S. Pauls and J. A. Campos-Ortega (2003). "A 90-degree rotation of the mitotic spindle changes the orientation of mitoses of zebrafish neuroepithelial cells." Development **130**(16): 3767-80.
- Genova, J. L. and R. G. Fehon (2003). "Neuroglian, Gliotactin, and the Na<sup>+</sup>/K<sup>+</sup> ATPase are essential for septate junction function in Drosophila." J Cell Biol **161**(5): 979-89.
- Good, P. J., K. Richter and I. B. Dawid (1990). "A nervous system-specific isotype of the beta subunit of Na<sup>+</sup>,K(+) -ATPase expressed during early development of Xenopus laevis." Proc Natl Acad Sci U S A **87**(23): 9088-92.
- Harland, R. M. (1991). "In situ hybridization: an improved whole-mount method for Xenopus embryos." Methods Cell Biol **36**: 685-95.
- Herrera, V. L., T. Cova, D. Sassoon and N. Ruiz-Opazo (1994). "Developmental cell-specific regulation of Na(+)-K(+)-ATPase alpha 1-, alpha 2-, and alpha 3-isoform gene expression." Am J Physiol **266**(5 Pt 1): C1301-12.
- Hotary, K. B. and K. R. Robinson (1992). "Evidence of a role for endogenous electrical fields in chick embryo development." Development **114**(4): 985-96.
- Jiang, Y. J., M. Brand, C. P. Heisenberg, D. Beuchle, M. Furutani-Seiki, R. N. Kelsh, R. M. Warga, M. Granato, P. Haffter, M. Hammerschmidt, D. A. Kane, M. C. Mullins, J. Odenthal, F. J. van Eeden and C. Nusslein-Volhard (1996). "Mutations affecting neurogenesis and brain morphology in the zebrafish, Danio rerio." Development **123**: 205-16.
- Kimmel, C. B., W. W. Ballard, S. R. Kimmel, B. Ullmann and T. F. Schilling (1995). "Stages of embryonic development of the zebrafish." Dev Dyn **203**(3): 253-310.
- Linask, K. K. and Y. H. Gui (1995). "Inhibitory effects of ouabain on early heart development and cardiomyogenesis in the chick embryo." Dev Dyn **203**(1): 93-105.
- Lingrel, J. B. and T. Kuntzweiler (1994). "Na<sup>+</sup>,K(+) -ATPase." J Biol Chem **269**(31): 19659-62.
- Lowery, L. A. and H. Sive (2005). "Initial formation of zebrafish brain ventricles occurs independently of circulation and requires the nagie oko and snakehead/atp1a1a.1 gene products." Development **132**(9): 2057-67.

- Martin-Vasallo, P., E. Lecuona, S. Luquin, D. Alvarez de la Rosa, J. Avila, T. Alonso and L. M. Garcia-Segura (1997). "Cellular and developmental distribution of the Na,K-ATPase beta subunit isoforms of neural tissues." Ann N Y Acad Sci **834**: 110-4.
- Miyan, J. A., M. Nabiyouni and M. Zendah (2003). "Development of the brain: a vital role for cerebrospinal fluid." Can J Physiol Pharmacol **81**(4): 317-28.
- Mutlu, G. M. and J. I. Sznajder (2005). "Mechanisms of pulmonary edema clearance." Am J Physiol Lung Cell Mol Physiol **289**(5): L685-95.
- Nasevicius, A. and S. C. Ekker (2000). "Effective targeted gene 'knockdown' in zebrafish." Nat Genet **26**(2): 216-20.
- Orlowski, J. and J. B. Lingrel (1988). "Tissue-specific and developmental regulation of rat Na,K-ATPase catalytic alpha isoform and beta subunit mRNAs." J Biol Chem **263**(21): 10436-42.
- Parada, C., A. Gato, M. Aparicio and D. Bueno (2006). "Proteome analysis of chick embryonic cerebrospinal fluid." Proteomics **6**(1): 312-20.
- Parada, C., A. Gato and D. Bueno (2005). "Mammalian embryonic cerebrospinal fluid proteome has greater apolipoprotein and enzyme pattern complexity than the avian proteome." J Proteome Res **4**(6): 2420-8.
- Paul, S. M., M. J. Palladino and G. J. Beitel (2007). "A pump-independent function of the Na,K-ATPase is required for epithelial junction function and tracheal tube-size control." Development **134**(1): 147-55.
- Paul, S. M., M. Ternet, P. M. Salvaterra and G. J. Beitel (2003). "The Na<sup>+</sup>/K<sup>+</sup> ATPase is required for septate junction function and epithelial tube-size control in the Drosophila tracheal system." Development **130**(20): 4963-74.
- Praetorius, J. (2007). "Water and solute secretion by the choroid plexus." Pflugers Arch **454**(1): 1-18.
- Rajarao, S. J., V. A. Canfield, M. A. Mohideen, Y. L. Yan, J. H. Postlethwait, K. C. Cheng and R. Levenson (2001). "The repertoire of Na,K-ATPase alpha and beta subunit genes expressed in the zebrafish, *Danio rerio*." Genome Res **11**(7): 1211-20.
- Rajasekaran, A. K. and S. A. Rajasekaran (2003). "Role of Na-K-ATPase in the assembly of tight junctions." Am J Physiol Renal Physiol **285**(3): F388-96.
- Rajasekaran, S. A., S. P. Barwe, J. Gopal, S. Ryazantsev, E. E. Schneeberger and A. K. Rajasekaran (2007). "Na-K-ATPase regulates tight junction permeability through occludin phosphorylation in pancreatic epithelial cells." Am J Physiol Gastrointest Liver Physiol **292**(1): G124-33.
- Rajasekaran, S. A., S. P. Barwe and A. K. Rajasekaran (2005). "Multiple functions of Na,K-ATPase in epithelial cells." Semin Nephrol **25**(5): 328-34.

- Rajasekaran, S. A., J. Hu, J. Gopal, R. Gallemore, S. Ryazantsev, D. Bok and A. K. Rajasekaran (2003). "Na,K-ATPase inhibition alters tight junction structure and permeability in human retinal pigment epithelial cells." *Am J Physiol Cell Physiol* **284**(6): C1497-507.
- Rajasekaran, S. A., L. G. Palmer, S. Y. Moon, A. Peralta Soler, G. L. Apodaca, J. F. Harper, Y. Zheng and A. K. Rajasekaran (2001). "Na,K-ATPase activity is required for formation of tight junctions, desmosomes, and induction of polarity in epithelial cells." *Mol Biol Cell* **12**(12): 3717-32.
- Sagerstrom, C. G., Y. Grinbalt and H. Sive (1996). "Anteroposterior patterning in the zebrafish, *Danio rerio*: an explant assay reveals inductive and suppressive cell interactions." *Development* **122**(6): 1873-83.
- Serluca, F. C., A. Sidow, J. D. Mably and M. C. Fishman (2001). "Partitioning of tissue expression accompanies multiple duplications of the Na<sup>+</sup>/K<sup>+</sup> ATPase alpha subunit gene." *Genome Res* **11**(10): 1625-31.
- Shi, R. and R. B. Borgens (1995). "Three-dimensional gradients of voltage during development of the nervous system as invisible coordinates for the establishment of embryonic pattern." *Dev Dyn* **202**(2): 101-14.
- Shu, X., K. Cheng, N. Patel, F. Chen, E. Joseph, H. J. Tsai and J. N. Chen (2003). "Na,K-ATPase is essential for embryonic heart development in the zebrafish." *Development* **130**(25): 6165-73.
- Speake, T., C. Whitwell, H. Kajita, A. Majid and P. D. Brown (2001). "Mechanisms of CSF secretion by the choroid plexus." *Microsc Res Tech* **52**(1): 49-59.
- Therien, A. G. and R. Blostein (2000). "Mechanisms of sodium pump regulation." *Am J Physiol Cell Physiol* **279**(3): C541-66.
- Thermes, V., C. Grabher, F. Ristoratore, F. Bourrat, A. Choulika, J. Wittbrodt and J. S. Joly (2002). "I-SceI meganuclease mediates highly efficient transgenesis in fish." *Mech Dev* **118**(1-2): 91-8.
- Thomas, R. C. (1972). "Electrogenic sodium pump in nerve and muscle cells." *Physiol Rev* **52**(3): 563-94.
- Violette, M. I., P. Madan and A. J. Watson (2006). "Na<sup>+</sup>/K<sup>+</sup> -ATPase regulates tight junction formation and function during mouse preimplantation development." *Dev Biol* **289**(2): 406-19.
- Watson, A. J., D. R. Natale and L. C. Barcroft (2004). "Molecular regulation of blastocyst formation." *Anim Reprod Sci* **82-83**: 583-92.
- Westerfield, M. (1995). *The Zebrafish Book: A guide for the laboratory use of zebrafish.* University of Oregon Press.

- Yen, P. T., P. Herman and P. Tran Ba Huy (1993). "Ion transport processes and middle ear physiopathology. An experimental approach using cell culture." Acta Otolaryngol **113**(3): 358-63.
- Yuan, S. and E. M. Joseph (2004). "The small heart mutation reveals novel roles of Na<sup>+</sup>/K<sup>+</sup>-ATPase in maintaining ventricular cardiomyocyte morphology and viability in zebrafish." Circ Res **95**(6): 595-603.
- Zappaterra, M. D., S. N. Lisgo, S. Lindsay, S. P. Gygi, C. A. Walsh and B. A. Ballif (2007). "A comparative proteomic analysis of human and rat embryonic cerebrospinal fluid." J Proteome Res **6**(9): 3537-48.
- Zheng, W. and A. Chodobski (2005). The blood-cerebrospinal fluid barrier. Boca Raton, Taylor & Francis.



# Chapter Six

## **Conclusions and Future Directions**





In this thesis, I present work which has established zebrafish as a powerful system for studying brain ventricle development. In the zebrafish, the straight neural tube expands into embryonic forebrain, midbrain, and hindbrain ventricles over a four-hour window during mid-somitogenesis. Using wild-type and mutant analysis, I defined numerous genes and broad mechanisms required for the formation of the embryonic brain ventricles. These mechanisms include neural tube patterning, regulated cell proliferation, tissue morphogenesis, neuronal development, and regulation of embryonic cerebrospinal fluid (eCSF). Thus, my studies have set the framework for further elucidation of the complex mechanisms controlling brain morphogenesis, and already several projects have stemmed from this work investigating more detailed aspects of this process. Moreover, I established a collection of over 20 lines of zebrafish mutants affecting various steps in brain ventricle formation, and many are now being studied by members of the Sive lab.

### **Future studies of eCSF formation and function**

While my work identified the ion pump,  $\text{Na}^+ \text{K}^+$  ATPase, as a critical regulator of eCSF formation, ion pumping is only one of many mechanisms involved in eCSF regulation. Proteomic analyses have identified approximately 200 different proteins, including signaling and growth factors, extracellular matrix proteins, transport and carrier proteins, enzymes and proteases (Parada et al 2005; Parada et al 2006; Zappaterra et al 2007). Additionally, eCSF composition changes during different developmental stages and also between ventricles, further increasing the complexity of eCSF regulation. Clearly, ion pumps play an important role to drive fluid into the ventricles, however it will be interesting to uncover the mechanisms which secrete proteins into eCSF. For example, is all the neuroepithelium secretory, or are there distinct regions which secrete specific proteins? My data suggest that there is at least some ventricle-specific regulation of ion pumping in the zebrafish, and it follows that there may be more complex regional-specific mechanisms for protein secretion as well.

#### *Elucidation of additional ion pumps and channels involved in eCSF formation*

In addition to  $\text{Na}^+ \text{K}^+$  ATPase, other ion pumps and channels, such as the  $\text{Na}^+ \text{HCO}_3^-$  co-transporter Nbc1, play a role in adult CSF formation (Brown et al 2004). These channels may also function during eCSF formation, which could be tested in a relatively straight-forward manner in the zebrafish by using a combination of pharmacological inhibitors and antisense

oligonucleotides to knock down function of specific ion pumps. These experiments could provide further insight into the early mechanisms of eCSF formation and brain ventricle inflation, especially if the genes show regionally restricted expression like *atp1b3a*.

#### *Choroid Plexus Formation – a potential site of eCSF regulation*

As mentioned in Chapter 1, adult CSF is formed mainly by the choroid plexuses located in each of the ventricles (Speake et al 2001; Brown et al 2004; Praetorius 2007), although this is not the origin for eCSF, as substantial embryonic brain ventricle expansion occurs prior to noticeable choroid plexus formation (Bayer and Altman 2008). One key question is whether tissue that is destined to become choroid plexus (“embryonic choroid plexus”) may play a role in eCSF production yet is a morphologically indistinct region of the embryonic neuroepithelium. For instance, fetal choroid plexus tissue is quite unlike adult choroid plexus tissue. While adult tissue is composed of a distinctive frond-like monolayer of cuboidal cells around a capillary core, fetal choroid plexus is a smooth pseudostratified epithelium similar to the embryonic neuroepithelium (Dohrmann 1970; Dziegielewska et al 2001; Bayer and Altman 2008). Thus, it is possible that embryonic choroid plexus tissue may be regulating eCSF formation in a regionally-restricted manner, although it is unclear how early this tissue is specified and when it begins functioning.

During my studies of wild-type zebrafish embryos, I never observed any tissue in the brain that resembled the traditional frond-like choroid plexus. Whether this is because I was looking too early in development, or whether the zebrafish choroid plexus appears morphologically more similar to fetal choroid plexus, is unknown. The zebrafish choroid plexus has yet to be definitively identified at any developmental stage, including the adult. Thus, prior to analyzing a possible role of choroid plexus during eCSF formation in zebrafish, it will first be necessary to identify the choroid plexus organs and their development in the zebrafish.

However, I did make a possible choroid plexus observation in my study of  $\text{Na}^+ \text{K}^+$  ATPase function during eCSF formation. As discussed in Chapter 5, brain ventricle inflation shows a dose-dependent response to knock down of *atp1a1* by antisense morpholino oligonucleotides (Table 6.1). A low dose of the *atp1a1* start-site morpholino (0.50ng) caused a *snk*-like ventricle inflation defect in 60% of the embryos at 24 hours post fertilization (hpf), but by 48 hpf, half of those (30% total) were completely recovered, whereas the other half (30% total) were only partially recovered. Additionally, in these partially recovered embryos, there

was a striking overgrowth of undulating tissue from the hindbrain roofplate (Fig. 6.1B-D,F-G), which was never observed in wild-type embryos (Fig. 6.1A). The location of this outgrowth is where the hindbrain choroid plexus forms in other vertebrate systems. Thus, I speculate that hyperplasia of this tissue may result from feedback mechanisms which are activated when the embryonic brain senses low levels of eCSF fluid. Alternatively, this tissue could be a normally-sized choroid plexus which is simply more visible due to the smaller size of the ventricles, perhaps causing the tissue to be pushed out of the ventricle. In wild-type embryos, skin pigment obscures the hindbrain roof-plate tissue at this stage and so it is unclear if this type of tissue normally occurs within the ventricles (Fig. 6.1A,E). If this is choroid plexus tissue, then that means that the zebrafish hindbrain choroid plexus forms at least by 48 hpf, and it would be relatively simple to examine earlier stages using histological techniques until the first morphological observations of choroid plexus tissue are apparent. Numerous molecular markers, specific to choroid plexus tissue, exist which could facilitate this analysis.

Interestingly, in one case report of human choroid plexus hyperplasia (a rare disorder of unknown origin which results in hydrocephalus), the researchers observed that aquaporin immunoreactivity was significantly reduced compared to normal controls (Smith et al 2007). While the authors proposed that aquaporin levels were reduced in response to the hyperplasia, it also seems possible, in light of my potential findings, that the choroid plexus hyperplasia was stimulated by reduced aquaporin activity.

### *eCSF flow*

Another area of potential interest includes the mechanisms responsible for eCSF flow and possible functions of the flow. In adult ventricles, CSF is believed to flow in a directional manner (Fig. 1.1C), beginning in the lateral ventricles and ending at the fourth ventricle, before it exits into the subarachnoid space covering the brain outer surface where it is likely absorbed. It is thought that the CSF flow is directed by pressure gradients produced by the one-way secretion and absorption as well as by beating cilia located on the ependymal epithelium that lines the ventricles (Nicholson 1999). The flow within the embryonic brain ventricles has not been addressed, although beating cilia line the ventricular surface by the beginning of brain ventricle formation. I made preliminary movies of eCSF flow in the zebrafish embryo midbrain ventricle, which show a circular flow with eCSF going in an anterior direction dorsally and a posterior direction ventrally, in addition to a general anterior to posterior flow from the forebrain

to midbrain to hindbrain ventricles (Fig. 6.2). Future experiments should include confirming this directional flow in addition to analyzing the other ventricles more carefully, as well as determining when flow begins and how it changes during brain development.

Integral to CSF flow is CSF absorption, which occurs in the arachnoid villi and dural venous sinuses in the subarachnoid space in the adult brain ventricles (Davson and Segal 1996). But there is no subarachnoid space in the embryonic ventricles, and it is unclear if eCSF is absorbed, and if so, how it occurs. There are data that loss of cilia function in the ventricles leads to hydrocephalus in the embryonic brain in both mice and zebrafish (Ibanez-Tallon et al 2004; Kramer-Zucker et al 2005), but it is unclear how cilia-mediated flow normally contributes to eCSF absorption mechanisms. Recently, it was shown that the CSF flow in the lateral ventricles of adult rats creates a gradient of SLIT2 protein and directs migration of neuroblasts to the olfactory bulb (Sawamoto et al 2006). It will be interesting to determine whether flow in the embryonic brain ventricles also plays a role in neuroblast migration or other aspects of brain development.

#### *eCSF function*

One exciting project I initiated is a study investigating the function of eCSF during zebrafish brain development. Data from other systems suggest that factors within the eCSF are required for brain development. For example, several studies show that drainage of eCSF leads to reduced cell proliferation and increased apoptosis in the developing chick brain (Desmond and Jacobson 1977; Desmond 1985; Mashayekhi and Salehi 2006; Salehi and Mashayekhi 2006), and eCSF can also promote neuroepithelial stem cell growth in culture (Gato et al 2005; Miyan et al 2006). Investigation of the functional roles of eCSF has gained recent attention as a promising avenue of neurodevelopment research and may play a critical role in the success of neural stem cell technology (Cottingham 2007; Zappaterra et al 2007).

However, the current understanding of the roles of eCSF during brain development is vague, and the exact requirements for specific proteins within the fluid are unclear. In particular, it is not known whether eCSF is required solely for neuroepithelial cell proliferation in a general sense, or whether specific factors are required for the neurogenesis of certain neuronal classes. Current research has not addressed this distinction.

Some of the reagents I acquired during my analysis of  $\text{Na}^+ \text{K}^+$  ATPase function and eCSF formation will be useful points of entry for defined studies of eCSF function during brain

development. The *snakehead* mutant, which lacks eCSF, is a unique tool which currently does not exist in any other organism. Complementing use of the *snk* mutant, I also designed an assay in which the brain is partially severed from the spinal cord prior to brain ventricle inflation, resulting in a morphological brain phenotype almost identical to the *snk* mutant (Fig. 6.3). Assays of this nature will be useful to confirm that a particular *snk* brain defect is due to loss of fluid and not to some other cellular function of  $\text{Na}^+ \text{K}^+ \text{ATPase}$ .

Based on the timing of neurogenesis and eCSF formation, I hypothesize that eCSF is required for secondary, but not primary, neurogenesis in the zebrafish. The terms “primary” and “secondary” refer to different neurogenesis waves in zebrafish than in amniotes. In amniotes such as zebrafish and *Xenopus*, “primary” neurogenesis refers to the generation of mostly transitory neurons such as somatosensory Rohon-Beard neurons (Reyes et al 2004) and the first differentiated brain neurons forming the early axon scaffold (Chitnis and Kuwada 1990). Primary neurogenesis in zebrafish begins by the end of gastrulation and early neurulation (10-18 hpf), prior to inflation of the brain ventricles (Park et al 2000). On the other hand, “secondary” neurogenesis in zebrafish begins by 48 hpf, and refers to all neurogenesis which produces the majority of neurons found in the adult central nervous system (Mueller and Wullimann 2005). Preliminary analysis of hindbrain reticulospinal axon tracts in the *snk* mutant at 3 days post fertilization shows variable defects in pathfinding and fasciculation (Fig. 6.4), whereas axon tracts at 24 hpf do not appear different from wild type (not shown), supporting my hypothesis.

Another graduate student in the Sive lab has continued this project to determine the specific roles eCSF plays during brain development, using the *snk* mutant as well as eCSF drainage assays. This project has the potential to uncover how eCSF controls the process of neuronal development.

## **Na<sup>+</sup> K<sup>+</sup> ATPase function during brain development**

### *Specificity of brain function for Na<sup>+</sup> K<sup>+</sup> ATPase isoforms*

My work has described the early brain functions of two Na<sup>+</sup> K<sup>+</sup> ATPase isoforms, the alpha subunit *Atp1a1* and the beta subunit *Atp1b3a*. But the zebrafish genome encodes at least 9 different alpha subunits and 6 beta subunits, each with their own distinct expression patterns during embryonic brain development (Rajarao et al 2001; Serluca et al 2001; Blasiolo et al 2002; Canfield et al 2002). It has become apparent that each Na<sup>+</sup> K<sup>+</sup> ATPase isoform plays specific functional roles during embryonic development of other organs, such as the heart and the ear (Shu et al 2003; Blasiolo et al 2006), but the function of most Na<sup>+</sup> K<sup>+</sup> ATPase isoforms have not been studied in the brain.

Relevant to brain ventricle inflation, there are several isoforms strongly expressed in the neuroepithelium at the onset of inflation, in addition to *atp1a1* and *atp1b3a*. In particular, *atp1a1b* has an interesting expression pattern, as it is solely expressed surrounding the brain ventricles in a developmental-stage-dependent manner. At the onset of brain ventricle inflation, expression surrounds only the forebrain ventricle, then at later embryonic stages it localizes to the ventricular zones of all three ventricles (Thisse et al 2001). *Atp1a1b* is perfectly situated to play a direct role in eCSF formation, and it will be useful to determine if there is a phenotype after gene knockdown.

One area of Na<sup>+</sup> K<sup>+</sup> ATPase biology which is quite puzzling is how the alpha subunit is localized at the sub-cellular level. Traditionally, the Na<sup>+</sup> K<sup>+</sup> ATPase enzyme is thought to localize to the basolateral membrane of most epithelial cells, including in the kidney and in the gastrointestinal tract (Kyte 1976; McNeill et al 1990). However, there are several tissues in which at least certain isoforms of Na<sup>+</sup> K<sup>+</sup> ATPase (including *Atp1a1*) are localized apically, such as the embryonic neuroepithelium (Lowery and Sive 2005), the adult choroid plexus (Wright 1972, Rizzolo 1999), the prostate (Mobasher et al 2001), and the mammalian embryonic trophoectoderm (Barcroft et al 2002). The mechanism by which Na<sup>+</sup> K<sup>+</sup> ATPase localizes is not known, although it has been proposed that the beta subunit directs sub-cellular localization (Geering 2001). The zebrafish would be a useful system to further address this question, using a combination of beta gene knockdown by antisense morpholino oligonucleotides, gene over-expression, and immunohistochemistry to determine whether particular beta subunits direct alpha subunit localization.

### *Possible connection between Na<sup>+</sup>K<sup>+</sup> ATPase activity and RhoA GTPase in brain development*

As described in Chapter 5, I identified an early role for Atp1a1 activity and Na<sup>+</sup> K<sup>+</sup> ATPase ion pumping during formation, but not maintenance, of the neuroepithelium. While this is consistent with previous data implicating Na<sup>+</sup> K<sup>+</sup> ATPase activity during junction formation in a wide variety of cell types, the direct connection between Na<sup>+</sup> K<sup>+</sup> ATPase function and epithelial junctions is not clear (Rajasekaran et al 2001; Rajasekaran et al 2003; Violette et al 2006; Cibrian-Uhalte et al 2007; Rajasekaran et al 2007).

How might Na<sup>+</sup> K<sup>+</sup> ATPase function regulate epithelial junctions? Rajasekaran et al suggest a specific mechanism in which abnormal Na<sup>+</sup> levels directly impact junction formation through RhoA GTPase mediation (Rajasekaran and Rajasekaran 2003). Ouabain treatment, which blocks Na<sup>+</sup> K<sup>+</sup> ATPase ion pumping and prevents junction formation in tissue culture, also inhibits RhoA activity (Rajasekaran et al 2001). Intriguingly, over-expression of RhoA rescues ouabain-induced junction defects, suggesting that RhoA mediates epithelial junction formation downstream of Na<sup>+</sup> K<sup>+</sup> ATPase activity (Rajasekaran et al 2001). As a direct signaling connection has not been shown to occur in vivo, the zebrafish neuroepithelium may provide a highly tractable in vivo system for analyzing the role of Na<sup>+</sup>K<sup>+</sup> ATPase activity and possible signaling pathways such as RhoA during epithelial junction formation. In particular, it may be interesting to ascertain whether inhibition of RhoA GTPase activity, shown to occur after ouabain treatment in cell culture, also happens in the early neuroepithelium of *atp1a1* start-site morphants. These and other experiments have significant potential to elucidate the connection between Na<sup>+</sup>K<sup>+</sup> ATPase activity and epithelial junction formation.

It is also possible that a connection between Na<sup>+</sup>K<sup>+</sup> ATPase and RhoA GTPase would not be specific to junction formation during neurulation but may occur during brain ventricle formation as well. Supporting this connection in zebrafish, a dominant-negative construct that should block all Rho guanine nucleotide exchange factor (RhoGEF) and RhoA activity causes significantly reduced brain ventricles that appear similar to the *snk* mutant (Panizzi et al 2007). Moreover, RhoA regulates Na<sup>+</sup> K<sup>+</sup> ATPase sub-cellular localization in the zebrafish embryonic pronephros and in cultured renal epithelial cells (Maeda et al 2002; Panizzi et al 2007). Thus, it is plausible that RhoA activity is also regulating eCSF formation by affecting Na<sup>+</sup>K<sup>+</sup> ATPase localization and function in the brain, in addition to its possible role in neuroepithelial junction formation.

### **Relationship between cell proliferation and brain ventricle opening**

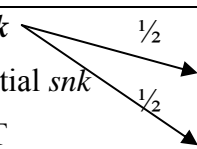
In Chapter 4, I discussed data which showed that cell proliferation plays a role in brain ventricle development, as there is increased mitosis surrounding the ventricles, and pharmacologically blocking cell proliferation results in smaller but normally shaped ventricles. These observations indicate that cell proliferation may provide increased tissue for ventricle opening to occur. However, my analysis of the *fbxo5* mutant suggests that the role of cell proliferation during brain ventricle opening may be more complex.

The *fbxo5* mutant is putatively caused by a retroviral insertion in the *F-box protein 5* gene, the zebrafish homolog of the mitotic regulator Emi1 (Reimann et al 2001). I observed that *fbxo5* mutants display significantly reduced cell proliferation, increased cell size, and no body growth (Fig. 6.5A-G). Moreover, the *fbxo5* brain ventricle phenotype is significantly more severe than that observed when cell proliferation is reduced pharmacologically, showing defective midline separation (Fig. 6.5I). It is unclear whether the Fbxo5 protein has a non-cell proliferation function, or whether abnormal/reduced cell proliferation is leading to the brain ventricle phenotype. Two possibilities are that cells must be actively cycling in order to respond to signals that promote certain cell movement or shape changes, or that differential proliferation within the neuroepithelium regulates later cell behavior by promoting loss of cell-cell interactions at the midline. In the zebrafish neuroepithelium, control of the plane of cell division is intimately connected with apicobasal and planar cell polarity, and disrupting signaling pathways controlling cell polarity lead to abnormal cell behavior following division and defective daughter cell intercalation into the neuroepithelium (Geldmacher-Voss et al 2003; Ciruna et al 2006; Tawk et al 2007). As *fbxo5* mutant brain ventricles appear somewhat similar to mutants with apicobasal polarity defects, this is a likely connection between cell proliferation and brain ventricle defects, and perhaps epithelial intercalation is disrupted in the *fbxo5* mutant. However, further analysis of the *fbxo5* mutant, and in particular, confocal time-lapse imaging of cell behavior during brain morphogenesis, will be required to elucidate the underlying cause of the *fbxo5* brain phenotype.



**Table 6.1 Dose-dependent brain phenotypes with *atp1a1* MO at 1 and 2 dpf.**

Note: for treatment with 0.5ng MO, 60% of the embryos showed a *snk*-like brain phenotype. Of these embryos, one-half showed a partial recovery along with hindbrain ventricle roofplate hyperplasia, whereas the remaining half appeared wild type.

MO amount	1 day post fertilization	2 days post fertilization
1 ng	100% <i>snk</i> 0% partial <i>snk</i> 0% WT	100% <i>snk</i> 0% partial with roofplate hyperplasia 0% WT
0.5 ng	<b>60% <i>snk</i></b>  30% partial <i>snk</i> 10% WT	0% <i>snk</i> <b>30% partial with roofplate hyperplasia</b> 70% WT
0.25 ng	35% <i>snk</i> 25% partial <i>snk</i> 40% WT	0% <i>snk</i> 0% partial with roofplate hyperplasia 100% WT



**Figure 6.1 Possible choroid plexus identification in zebrafish embryos.**

(A-H) Lateral views of live 2 days post fertilization embryos, injected with antisense morpholino oligonucleotides (MO) at the 1-cell stage. (E-H) are higher magnification view of (A-D). (A,E) Hindbrain ventricle roofplate in control MO has a smooth surface, although pigment obscures ventricle. (B-D, F-H) 30% of embryos injected with 0.5 ng *atp1a1* MO show hindbrain ventricle roofplate hyperplasia, possibly of choroid plexus tissue (arrows).

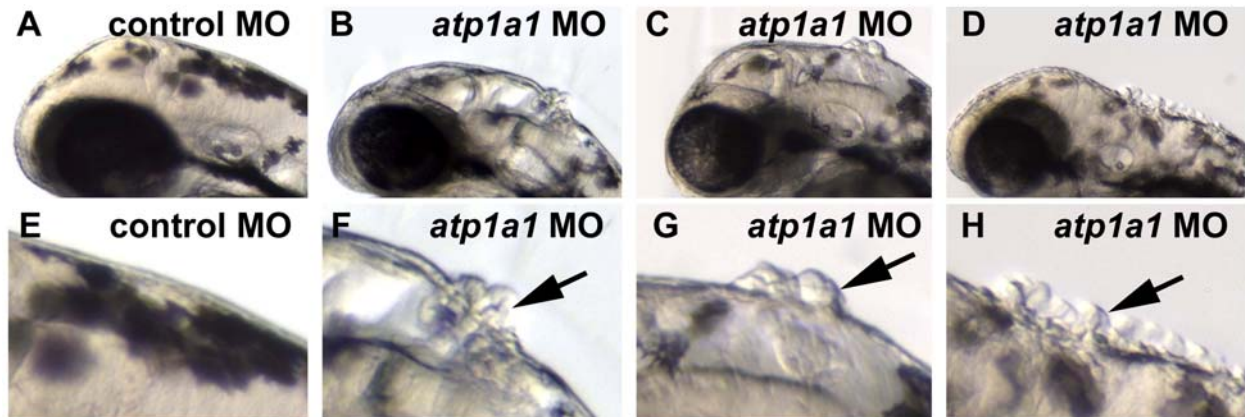




**Figure 6.2 Preliminary schematic of zebrafish embryo eCSF flow.**

Preliminary cartoon schematic based on 4 movies of eCSF fluorescent dextran flow in 24-26 hours post fertilization embryos. Black line depicts outline of ventricle, red line depicts eCSF flow. F forebrain ventricle, M midbrain ventricle, H hindbrain ventricle.

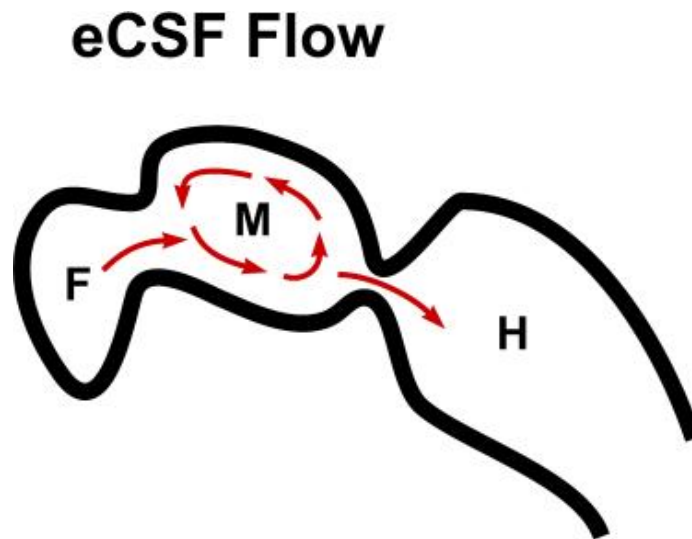




**Figure 6.3 Severed head assay results in *snk*-like head phenotype.**

(A-C) Lateral views of live embryos at 2 dpf. (A) Wild-type embryos: midbrain and hindbrain hinge-points apparent (asterisks) and hindbrain ventricle is inflated (red bar notes ventricle height). (B) Wild-type embryos after severed brain from the rest of the body at 18 hpf: brain ventricles do not inflate and appear similar to *snk* embryos (C).

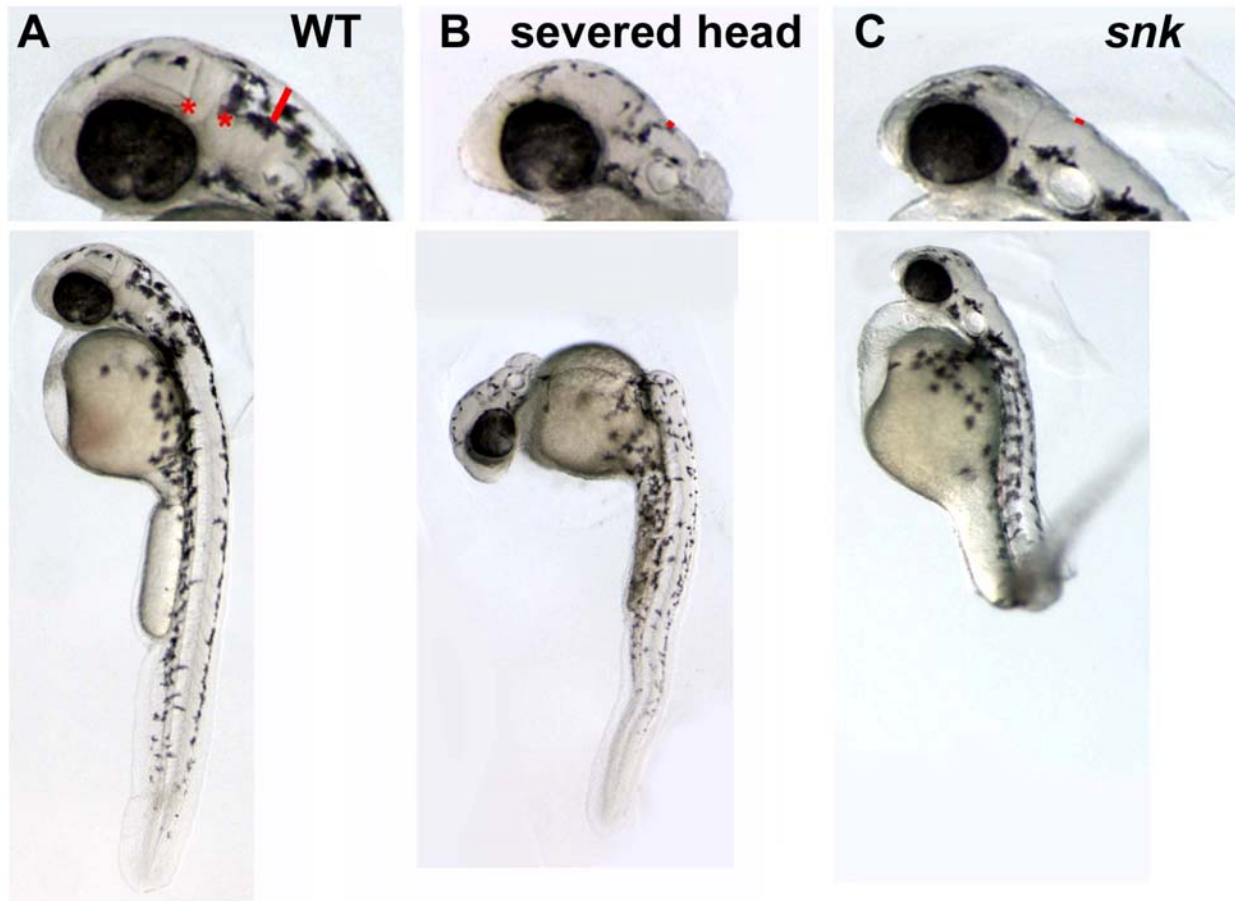






**Figure 6.4 Defects in *snk* hindbrain neurons at 3 dpf.**

(A-D) Confocal images of zebrafish dorsal hindbrain flatmounts after immunohistochemistry for Neurofilament M, which labels hindbrain reticulospinal neurons. (A) Wild-type sibling of *snk* clutch. (B-D) Three different *snk* mutants show variable defects in axon structure and organization.

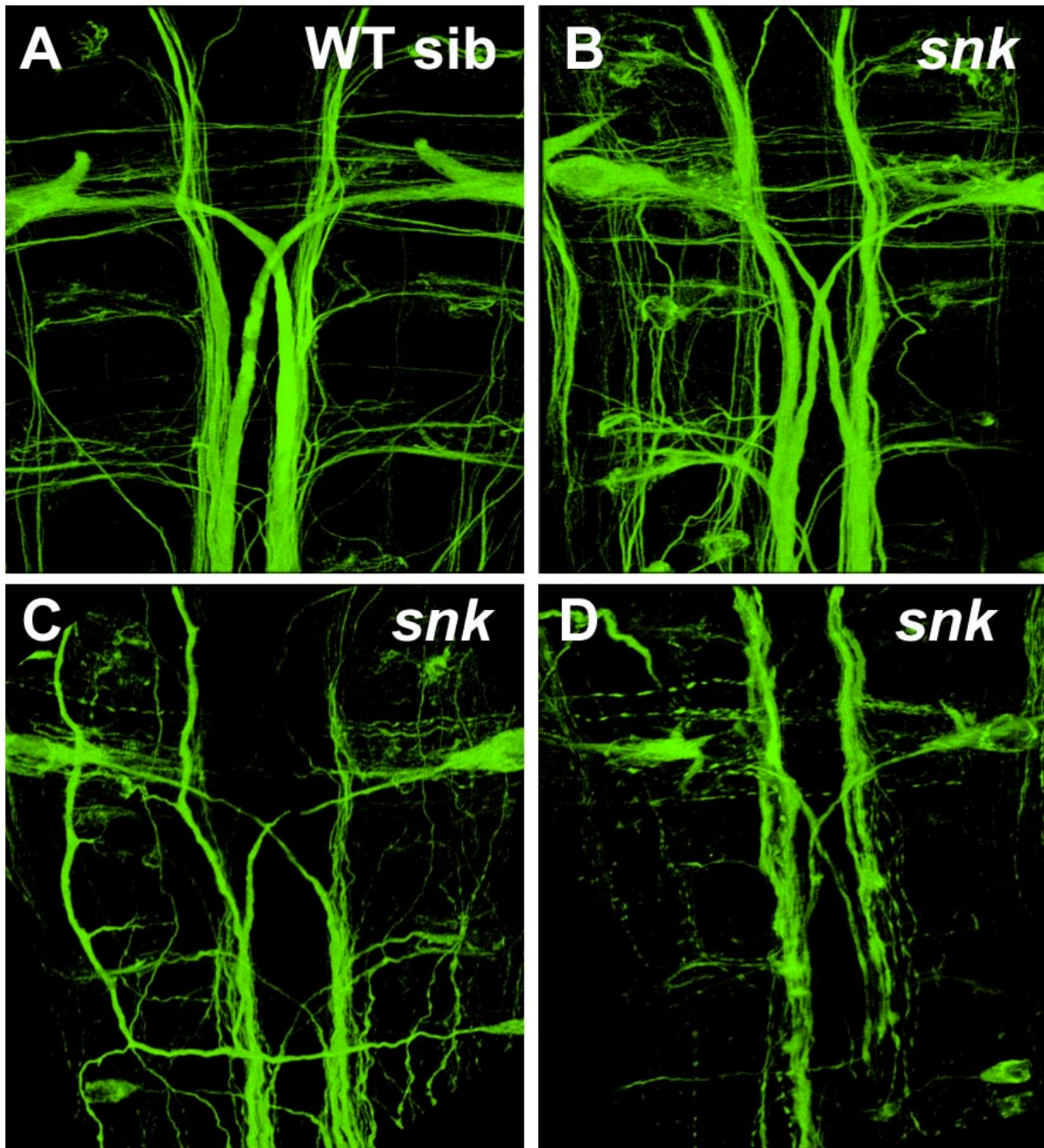
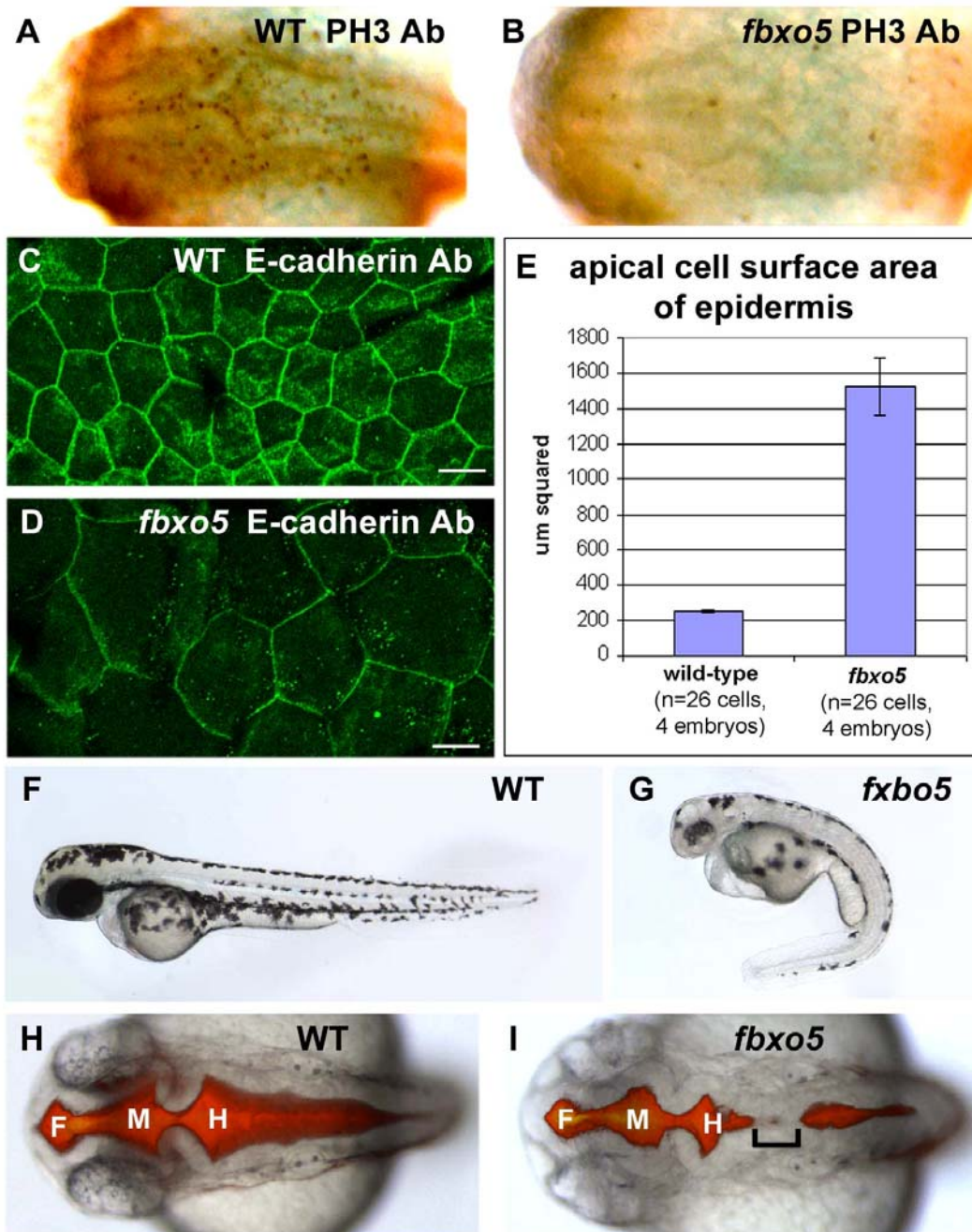




**Figure 6.5 *fbxo5* mutants show reduced cell proliferation, increased cell size, and midline opening brain ventricle defects.** (A,B) Brightfield microscopy dorsal views of 24 hpf embryos after immunolabeling with the PH3 Ab. (C,D) Confocal microscopy of epidermis overlying the brain of 24 hpf embryos after immunolabeling with E-cadherin Ab. Cell surface area quantitated in (E). (F,G) Brightfield microscopy lateral views of 4 dpf live embryos. (H,I) Superimposition of brightfield and fluorescent microscopy after ventricle injection with fluorescent-dextran at 26 hpf. Bracket in (I) refers to area of defective midline opening in *fbxo5* mutant. F forebrain ventricle, M midbrain ventricle, H hindbrain ventricle.





## References

- Barcroft, L. C., S. E. Gill and A. J. Watson (2002). "The gamma-subunit of the Na-K-ATPase as a potential regulator of apical and basolateral Na<sup>+</sup>-pump isozymes during development of bovine pre-attachment embryos." *Reproduction* 124(3): 387-97.
- Bayer, S. A. and J. Altman (2008). *The human brain during the early first trimester*. Boca Raton, Fla.; London, CRC.
- Blasiolo, B., V. Canfield, A. Degraeve, C. Thisse, B. Thisse, J. Rajarao and R. Levenson (2002). "Cloning, mapping, and developmental expression of a sixth zebrafish Na,K-ATPase alpha1 subunit gene (atp1a1a.5)." *Gene Expr Patterns* 2(3-4): 243-6.
- Blasiolo, B., V. A. Canfield, M. A. Vollrath, D. Huss, M. A. Mohideen, J. D. Dickman, K. C. Cheng, D. M. Fekete and R. Levenson (2006). "Separate Na,K-ATPase genes are required for otolith formation and semicircular canal development in zebrafish." *Dev Biol* 294(1): 148-60.
- Brown, P. D., S. L. Davies, T. Speake and I. D. Millar (2004). "Molecular mechanisms of cerebrospinal fluid production." *Neuroscience* 129(4): 957-70.
- Canfield, V. A., B. Loppin, B. Thisse, C. Thisse, J. H. Postlethwait, M. A. Mohideen, S. J. Rajarao and R. Levenson (2002). "Na,K-ATPase alpha and beta subunit genes exhibit unique expression patterns during zebrafish embryogenesis." *Mech Dev* 116(1-2): 51-9.
- Chitnis, A. B. and J. Y. Kuwada (1990). "Axonogenesis in the brain of zebrafish embryos." *J Neurosci* 10(6): 1892-905.
- Cibrian-Uhalte, E., A. Langenbacher, X. Shu, J. N. Chen and S. Abdelilah-Seyfried (2007). "Involvement of zebrafish Na<sup>+</sup>,K<sup>+</sup> ATPase in myocardial cell junction maintenance." *J Cell Biol* 176(2): 223-30.
- Ciruna, B., A. Jenny, D. Lee, M. Mlodzik and A. F. Schier (2006). "Planar cell polarity signalling couples cell division and morphogenesis during neurulation." *Nature* 439(7073): 220-4.
- Cottingham, K. (2007). "The complex composition of embryonic CSF." *J Proteome Res* 6(9): 3366.
- Davson, H. and M. B. Segal (1996). *Physiology of the CSF and blood-brain barriers*. Boca Raton, CRC Press.
- Desmond, M. E. (1985). "Reduced number of brain cells in so-called neural overgrowth." *Anat Rec* 212(2): 195-8.
- Desmond, M. E. and A. G. Jacobson (1977). "Embryonic brain enlargement requires cerebrospinal fluid pressure." *Dev Biol* 57(1): 188-98.

- Dohrmann, G. J. (1970). "The choroid plexus: a historical review." *Brain Res* 18(2): 197-218.
- Dziegielewska, K. M., J. Ek, M. D. Habgood and N. R. Saunders (2001). "Development of the choroid plexus." *Microsc Res Tech* 52(1): 5-20.
- Ellertsdottir, E., J. Ganz, K. Durr, N. Loges, F. Biemar, F. Seifert, A. K. Ettl, A. K. Kramer-Zucker, R. Nitschke and W. Driever (2006). "A mutation in the zebrafish Na,K-ATPase subunit *atp1a1a.1* provides genetic evidence that the sodium potassium pump contributes to left-right asymmetry downstream or in parallel to nodal flow." *Dev Dyn* 235(7): 1794-808.
- Gato, A., J. A. Moro, M. I. Alonso, D. Bueno, A. De La Mano and C. Martin (2005). "Embryonic cerebrospinal fluid regulates neuroepithelial survival, proliferation, and neurogenesis in chick embryos." *Anat Rec A Discov Mol Cell Evol Biol* 284(1): 475-84.
- Geering, K. (2001). "The functional role of beta subunits in oligomeric P-type ATPases." *J Bioenerg Biomembr* 33(5): 425-38.
- Geldmacher-Voss, B., A. M. Reugels, S. Pauls and J. A. Campos-Ortega (2003). "A 90-degree rotation of the mitotic spindle changes the orientation of mitoses of zebrafish neuroepithelial cells." *Development* 130(16): 3767-80.
- Ibanez-Tallon, I., A. Pagenstecher, M. Fliegauf, H. Olbrich, A. Kispert, U. P. Ketelsen, A. North, N. Heintz and H. Omran (2004). "Dysfunction of axonemal dynein heavy chain *Mdnah5* inhibits ependymal flow and reveals a novel mechanism for hydrocephalus formation." *Hum Mol Genet* 13(18): 2133-41.
- Kramer-Zucker, A. G., F. Olale, C. J. Haycraft, B. K. Yoder, A. F. Schier and I. A. Drummond (2005). "Cilia-driven fluid flow in the zebrafish pronephros, brain and Kupffer's vesicle is required for normal organogenesis." *Development* 132(8): 1907-21.
- Kyte, J. (1976). "Immunoferritin determination of the distribution of (Na<sup>+</sup> + K<sup>+</sup>) ATPase over the plasma membranes of renal convoluted tubules. I. Distal segment." *J Cell Biol* 68(2): 287-303.
- Maeda, A., M. Amano, Y. Fukata and K. Kaibuchi (2002). "Translocation of Na(+),K(+)-ATPase is induced by Rho small GTPase in renal epithelial cells." *Biochem Biophys Res Commun* 297(5): 1231-7.
- Mashayekhi, F. and Z. Salehi (2006). "The importance of cerebrospinal fluid on neural cell proliferation in developing chick cerebral cortex." *Eur J Neurol* 13(3): 266-72.
- McNeill, H., M. Ozawa, R. Kemler and W. J. Nelson (1990). "Novel function of the cell adhesion molecule uvomorulin as an inducer of cell surface polarity." *Cell* 62(2): 309-16.
- Miyan, J. A., M. Zendah, F. Mashayekhi and P. J. Owen-Lynch (2006). "Cerebrospinal fluid supports viability and proliferation of cortical cells in vitro, mirroring in vivo development." *Cerebrospinal Fluid Res* 3: 2.

- Mobasheri, A., D. Oukrif, S. P. Dawodu, M. Sinha, P. Greenwell, D. Stewart, M. B. Djamgoz, C. S. Foster, P. Martin-Vasallo and R. Mobasheri (2001). "Isoforms of Na<sup>+</sup>, K<sup>+</sup>-ATPase in human prostate; specificity of expression and apical membrane polarization." *Histol Histopathol* 16(1): 141-54.
- Mueller, T. and M. Wullimann (2005). *Atlas of Early Zebrafish Brain Development*, Elsevier.
- Nicholson, C. (1999). "Signals that go with the flow." *Trends Neurosci* 22(4): 143-5.
- Panizzi, J. R., J. R. Jessen, I. A. Drummond and L. Solnica-Krezel (2007). "New functions for a vertebrate Rho guanine nucleotide exchange factor in ciliated epithelia." *Development* 134(5): 921-31.
- Parada, C., A. Gato, M. Aparicio and D. Bueno (2006). "Proteome analysis of chick embryonic cerebrospinal fluid." *Proteomics* 6(1): 312-20.
- Parada, C., A. Gato and D. Bueno (2005). "Mammalian embryonic cerebrospinal fluid proteome has greater apolipoprotein and enzyme pattern complexity than the avian proteome." *J Proteome Res* 4(6): 2420-8.
- Park, H. C., S. K. Hong, H. S. Kim, S. H. Kim, E. J. Yoon, C. H. Kim, N. Miki and T. L. Huh (2000). "Structural comparison of zebrafish Elav/Hu and their differential expressions during neurogenesis." *Neurosci Lett* 279(2): 81-4.
- Praetorius, J. (2007). "Water and solute secretion by the choroid plexus." *Pflugers Arch* 454(1): 1-18.
- Rajarao, S. J., V. A. Canfield, M. A. Mohideen, Y. L. Yan, J. H. Postlethwait, K. C. Cheng and R. Levenson (2001). "The repertoire of Na,K-ATPase alpha and beta subunit genes expressed in the zebrafish, *Danio rerio*." *Genome Res* 11(7): 1211-20.
- Rajasekaran, A. K. and S. A. Rajasekaran (2003). "Role of Na-K-ATPase in the assembly of tight junctions." *Am J Physiol Renal Physiol* 285(3): F388-96.
- Rajasekaran, S. A., S. P. Barwe, J. Gopal, S. Ryazantsev, E. E. Schneeberger and A. K. Rajasekaran (2007). "Na-K-ATPase regulates tight junction permeability through occludin phosphorylation in pancreatic epithelial cells." *Am J Physiol Gastrointest Liver Physiol* 292(1): G124-33.
- Rajasekaran, S. A., J. Hu, J. Gopal, R. Gallemore, S. Ryazantsev, D. Bok and A. K. Rajasekaran (2003). "Na,K-ATPase inhibition alters tight junction structure and permeability in human retinal pigment epithelial cells." *Am J Physiol Cell Physiol* 284(6): C1497-507.
- Rajasekaran, S. A., L. G. Palmer, S. Y. Moon, A. Peralta Soler, G. L. Apodaca, J. F. Harper, Y. Zheng and A. K. Rajasekaran (2001). "Na,K-ATPase activity is required for formation of tight junctions, desmosomes, and induction of polarity in epithelial cells." *Mol Biol Cell* 12(12): 3717-32.

- Reimann, J. D., E. Freed, J. Y. Hsu, E. R. Kramer, J. M. Peters and P. K. Jackson (2001). "Emi1 is a mitotic regulator that interacts with Cdc20 and inhibits the anaphase promoting complex." *Cell* 105(5): 645-55.
- Reyes, R., M. Haendel, D. Grant, E. Melancon and J. S. Eisen (2004). "Slow degeneration of zebrafish Rohon-Beard neurons during programmed cell death." *Dev Dyn* 229(1): 30-41.
- Salehi, Z. and F. Mashayekhi (2006). "The role of cerebrospinal fluid on neural cell survival in the developing chick cerebral cortex: an in vivo study." *Eur J Neurol* 13(7): 760-4.
- Sawamoto, K., H. Wichterle, O. Gonzalez-Perez, J. A. Cholfin, M. Yamada, N. Spassky, N. S. Murcia, J. M. Garcia-Verdugo, O. Marin, J. L. Rubenstein, M. Tessier-Lavigne, H. Okano and A. Alvarez-Buylla (2006). "New neurons follow the flow of cerebrospinal fluid in the adult brain." *Science* 311(5761): 629-32.
- Serluca, F. C., A. Sidow, J. D. Mably and M. C. Fishman (2001). "Partitioning of tissue expression accompanies multiple duplications of the Na<sup>+</sup>/K<sup>+</sup> ATPase alpha subunit gene." *Genome Res* 11(10): 1625-31.
- Shu, X., K. Cheng, N. Patel, F. Chen, E. Joseph, H. J. Tsai and J. N. Chen (2003). "Na,K-ATPase is essential for embryonic heart development in the zebrafish." *Development* 130(25): 6165-73.
- Smith, Z. A., P. Moftakhar, D. Malkasian, Z. Xiong, H. V. Vinters and J. A. Lazareff (2007). "Choroid plexus hyperplasia: surgical treatment and immunohistochemical results. Case report." *J Neurosurg* 107(3 Suppl): 255-62.
- Speake, T., C. Whitwell, H. Kajita, A. Majid and P. D. Brown (2001). "Mechanisms of CSF secretion by the choroid plexus." *Microsc Res Tech* 52(1): 49-59.
- Tawk, M., C. Araya, D. A. Lyons, A. M. Reugels, G. C. Girdler, P. R. Bayley, D. R. Hyde, M. Tada and J. D. Clarke (2007). "A mirror-symmetric cell division that orchestrates neuroepithelial morphogenesis." *Nature* 446(7137): 797-800.
- Thisse, B., S. Pflumio, M. Fürthauer, B. Loppin, V. Heyer, A. Degrave, R. Woehl, A. Lux, T. Steffan, X. Q. Charbonnier and C. Thisse (2001). "Expression of the zebrafish genome during embryogenesis." ZFIN Direct Data Submission (<http://zfin.org>).
- Violette, M. I., P. Madan and A. J. Watson (2006). "Na<sup>+</sup>/K<sup>+</sup> -ATPase regulates tight junction formation and function during mouse preimplantation development." *Dev Biol* 289(2): 406-19.
- Zappaterra, M. D., S. N. Lisgo, S. Lindsay, S. P. Gygi, C. A. Walsh and B. A. Ballif (2007). "A comparative proteomic analysis of human and rat embryonic cerebrospinal fluid." *J Proteome Res* 6(9): 3537-48.



# Appendix One

## ***whitesnake/sfpq* is Required for Cell Survival and Neuronal Development in the Zebrafish**

Published As:

Laura Anne Lowery, Jamie Rubin and Hazel Sive. Whitesnake/sfpq is Required for Cell Survival and Neuronal Development in the Zebrafish. *Developmental Dynamics* 236, 2007.

Contributions:

Jamie Rubin was an undergraduate student who provided technical assistance for several experiments, namely all RT-PCR data and the in situ hybridizations in Figure A1.4. I performed the remaining experiments, and I wrote the paper with editing by Hazel Sive.

## Abstract

Organogenesis involves both the development of specific cell types and their organization into a functional three-dimensional structure. We are using the zebrafish to assess the genetic basis for brain organogenesis. We show that the *whitesnake* mutant corresponds to the *sfpq* (splicing factor, proline/glutamine rich) gene, encoding the PSF protein (polypyrimidine tract-binding protein-associated splicing factor). In vitro studies have shown that PSF is important for RNA splicing and transcription, and is a candidate brain-specific splicing factor, however the in vivo function of this gene is unclear. *sfpq* is expressed throughout development and in the adult zebrafish, with strong expression in the developing brain, particularly in regions enriched for neuronal progenitors. In the *whitesnake* mutant, a brain phenotype is visible by 28 hours after fertilization, when it becomes apparent that the midbrain and hindbrain are abnormally shaped. Neural crest, heart, and muscle development or function is also abnormal. *sfpq* function appears to be required in two distinct phases during development. First, loss of *sfpq* gene function leads to increased cell death throughout the early embryo, suggesting that cell survival requires functional PSF protein. Second, *sfpq* function is required for differentiation, but not for determination, of specific classes of brain neurons. These data indicate that, in vertebrates, *sfpq* plays a key role in neuronal development, and is essential for normal brain development.

## Introduction

The development of organs is complex, involving both generation of appropriate cell types and tissues and organization of these in the correct three-dimensional structure. We have begun to examine brain organogenesis, using the zebrafish as a model and by studying mutants suggested to be defective in brain development (Jiang et al., 1996; Schier et al., 1996; Amsterdam et al., 2004).

The *whitesnake* (*wis*) mutant was isolated from a chemical mutagenesis screen, and shows a distinct brain phenotype (Jiang et al., 1996; Schier et al., 1996). Here, we show that the zebrafish *whitesnake* (*wis*) mutant corresponds to disruption of the *sfpq* gene. *sfpq* (*splicing factor, proline/glutamine rich*), which encodes the polypyrimidine tract binding protein associated splicing factor (PSF), is enriched in differentiating neurons in the mouse brain and has been suggested to play a role in neural-specific splicing (Chanas-Sacre et al., 1999). PSF was first identified as an essential pre-mRNA splicing factor (Patton et al., 1993) and has since been shown to exhibit multiple functions in nucleic acid synthesis and processing in vitro and in tissue culture including transcriptional co-repression, DNA unwinding, and linking RNA transcripts with RNA polymerase II (Emili et al., 2002; Shav-Tal and Zipori, 2002). In addition, it has been suggested to play a role in tumorigenesis as well as apoptosis, as *sfpq* translocation occurs in papillary renal cell carcinoma (Clark et al., 1997), and nuclear relocalization and hyperphosphorylation of PSF occur during apoptosis (Shav-Tal et al., 2001).

In this report, we present the first whole animal study of *sfpq* loss of function. Our data suggest that *sfpq* function is required for cell survival, and that it is also required for the differentiation, but not determination, of specific neuronal classes.

## Results and Discussion

### The *whitesnake* mutation disrupts normal brain and body development

The *whitesnake* (*wis*) mutant was isolated from a chemical mutagenesis screen, and shows a distinct brain phenotype (Jiang et al., 1996; Schier et al., 1996). Phenotypic abnormalities are first visible during mid-somitogenesis. By 22 hours post fertilization (hpf), there is a subtle change in the curvature of the entire body, with the tail remaining more curved than wild-type siblings and the hindbrain more flat (not shown). In addition, *wis* mutants lack

myotomal contractions, and the somites are abnormally organized (not shown). The *wis* phenotype is more pronounced by 24 hpf, with absence of eye pigmentation, and slightly reduced brain ventricle width (Fig. A1.1B,E). By 28 hpf, mutants show an absence or severe reduction in body pigmentation, flattening of the brain, a curved and thick yolk extension, reduced heartbeat, and a lack of touch response (Fig. A1.1H, and not shown). Injecting the brain cavity with a fluorescent dye (Lowery and Sive, 2005) highlights structural abnormalities by this stage - all the embryonic brain ventricles are reduced, with the midbrain ventricle most severely affected, however there is variability in the extent of ventricle reduction (Fig. A1.1H and Fig. A1.2). At 2 days post fertilization (dpf), the *wis* brain is smaller than in wild-type siblings, and the size of all brain ventricle cavities are severely reduced, with the midbrain ventricle almost completely absent (Fig. A1.1J-Q). The tail does become straight, though all other 24 hpf defects persist. *wis* mutant embryos die by 4 dpf, when cells appear to become necrotic and the embryo disintegrates. The two alleles analyzed, *tr241* and *m427*, have indistinguishable phenotypes.

These results show that loss of *wis* function leads to profound morphological defects affecting several organ systems, with specific defects in the brain. The brain morphology defect appears relatively late, after the initial shaping of the brain.

### **The *whitesnake* mutant corresponds to the *sfpq* gene, encoding the PSF protein**

We observed that the *wis* phenotype appears very similar to that of the *sfpq hi1779* retroviral insertion mutant (compare Fig. A1.1B and C, E and F, H and I), although only preliminary analysis of the *sfpq* phenotype has been reported (Amsterdam et al., 2004). The *sfpq* gene (splicing factor, proline/glutamine (q) rich) encodes the PSF (polypyrimidine tract-binding protein-associated splicing factor) protein, a 619-amino-acid nuclear factor. In vitro assays using cell extracts indicate that PSF can participate in a variety of functions, including RNA splicing and transcriptional regulation (Patton et al., 1993; Shav-Tal and Zipori, 2002).

Crosses between the *wis<sup>tr241</sup>* and *sfpq* mutants showed that they fail to complement, and are therefore likely to be different alleles of the same locus. In a cross of *wis* and *sfpq* heterozygotes, 144 (73%) showed a wild-type phenotype and 54 (27%) a mutant phenotype, as expected for non-complementing loci (198 embryos total).

*sfpq<sup>hi1779</sup>* has a 6kb retroviral insertion at base 553 in the coding sequence, which leads to a truncation of the protein at amino acid 197 (Fig. A1.1R). This truncation removes the RNA recognition motifs and the two nuclear localization sequences needed for protein function (Dye

and Patton, 2001), suggesting that the *hi1779* PSF protein is not functional. We asked whether the *wis* phenotype is due to a mutation in the *sfpq* gene by comparing cDNA sequences from wild type, *wis<sup>tr241</sup>* and *wis<sup>m427</sup>* mutants. The *tr241* allele of *wis* contains a C to T mutation at position 499 in the *sfpq* coding sequence, which results in a premature stop codon at amino acid position 167 (Fig. A1.1R) and severe truncation of the protein. The *wis<sup>m427</sup>* allele has incorrect splicing of the last exon which truncates the last 39 amino acids, removing the last nuclear localization sequence previously shown to be necessary for protein function (Dye and Patton, 2001). There are no obvious mutations in the *wis<sup>m427</sup>* genomic DNA coding sequence which could account for the splicing error, and thus it is likely that the mutation exists elsewhere, perhaps in intronic sequence. We used RT-PCR to analyze *sfpq* RNA levels in *wis<sup>m427</sup>*, and did not see gross differences in levels between mutant and wildtype (data not shown).

We further confirmed gene assignment by rescuing the *wis* phenotype with *sfpq* mRNA. Injection of 100 - 200 pg *sfpq* mRNA partially rescues the *wis* brain ventricle, yolk extension, pigment, and movement defects at 28 hpf (n=17, 94% rescue, Fig. A1.3B,E). The incomplete rescue is likely to be due to degradation of the injected mRNA by later stages of development. Consistently, we were able to partially phenocopy the *wis* phenotype by injecting 8 ng antisense morpholino oligonucleotides targeted to the *sfpq* start site (Fig. A1.3G-L). These morphant embryos showed the *wis* brain morphology defect, mild tail curvature, and reduced pigmentation in 100% of injected embryos (n=89) (Fig. A1.3H,K), although myotomal contractions and touch response were not eliminated, suggesting we were not able to completely deplete *sfpq* function with the morpholino.

### ***sfpq* is expressed throughout the embryo and adult zebrafish and is enriched in the brain during neuronal development**

PSF protein is localized to differentiating neurons in the embryonic mouse brain (Chanas-Sacre et al., 1999), but the expression pattern of this gene has not been thoroughly examined during development. We therefore examined the expression patterns and level of *sfpq* RNA during zebrafish development, using RT-PCR and whole mount in situ hybridization. RT-PCR shows that *sfpq* is expressed both maternally and zygotically, with maximal expression at 18 hpf and continuing through 3 dpf. Expression is also strong in the adult brain, but there are varying levels of weaker expression in the eyes, gut, heart, and body muscle (Fig. A1.4A). In situ hybridization demonstrates that *sfpq* expression is ubiquitous until mid-somitogenesis (Fig.

A1.4B-G). By 18 hpf, *sfpq* expression is slightly stronger in presumptive rhombomere 4 (Fig. A1.4H, arrow) as well as in the developing telencephalon (Fig. A1.4H, bracket). By 24 hpf, expression appears much stronger in the brain than in non-neural tissue (Fig. A1.4I), with strongest expression in the telencephalon, midbrain, hindbrain and retina (Fig. A1.4J,K). At 2-3 dpf, *sfpq* expression is apparent only in distinct regions of the brain (Fig. A1.4L-Q). At 2 dpf, expression is strong in the ventral hindbrain and in dorsoventral stripes throughout the hindbrain (Fig. A1.4M,N). At 3 dpf, expression is strongly detected in a region ventral to the brain, but also faintly along many axon tracts (Fig. A1.4O-Q). By the more sensitive RT-PCR assay, *sfpq* is also expressed in the tail at 3 dpf (Fig. A1.4A, lane 9).

The strong expression of *sfpq* in distinct areas of the brain prompted us to ask whether this gene is expressed in regions of active neurogenesis. We addressed this question by double-labeling 24 hpf embryos for *sfpq* RNA by in situ hybridization followed by antibody labeling for HuC/D, an early marker for post-mitotic neurons (Marusich et al., 1994). This confirmed that multiple regions in the brain with the strongest *sfpq* expression overlap with regions labeled with HuC/D (Fig. A1.5). This overlap is particularly apparent in the telencephalon (Fig. A1.5A,C bracket) and in the hindbrain (Fig. A1.5B,D bracket). A higher magnification view of the hindbrain shows two darker stripes along its anteroposterior extent, with less expression medially (Fig. A1.5B, dark stripe in brackets). HuC/D labeling in the hindbrain occurs only within the region of stronger *sfpq* expression (Fig. A1.5D).

These data show that differentiating neurons express high levels of *sfpq* in the zebrafish, and together with a report of high PSF levels in differentiating mouse brain neurons (Chanas-Sacre et al., 1999), suggest that PSF may have brain-specific activity, functioning during neuronal differentiation. However, *sfpq* is also expressed broadly during zebrafish embryonic development and in the adult, consistent with PSF expression in non-neural human and rat tissues (Shav-Tal et al., 2000; Dong et al., 2005). Reminiscent of the case for *sfpq*, the RNA binding proteins, Nova1 and Nova2, have been proposed to be brain-specific splicing factors in mammals, and aberrant splicing of neural genes is seen in Nova knock-out mutants (Yang et al., 1998; Jensen et al., 2000; Ule et al., 2005). However, both Nova1 and Nova2 are also expressed in one or more non-neural tissues, including liver and lung (Buckanovich et al., 1993; Yang et al., 1998). Thus, splicing factors with tissue-specific activity may also have more general activity. This is the case for the essential splicing factor ASF/SF2, which has been implicated in cardiac-specific splicing (Xu et al., 2005b), while the ubiquitously expressed PTB, the

polypyrimidine-tract-binding protein, specifically represses neuron-specific splicing of the GABA (A) receptor in non-neuronal cells (Ashiya and Grabowski, 1997).

### **Loss of *sfpq* function does not affect cell proliferation but leads to widespread cell death**

While extensive in vitro analysis has shown that PSF protein can participate in a variety of functions (Shav-Tal and Zipori, 2002), loss of PSF function has not been examined in any whole animal. In order to characterize the PSF loss of function phenotype, we analyzed levels of cell proliferation in *wis* embryos at 24 hpf, by labeling mitotic cells with an antibody to phosphorylated histone H3 (PH3) (Hendzel et al., 1997; Saka and Smith, 2001). There are no obvious differences in cell proliferation levels between *wis* mutants and their wild-type siblings (Fig. A1.6A,B), and quantitation of PH3 positive cells in the hindbrain and trunk region show no statistical difference between mutant and wild type embryos (n=8, p=0.8046, Fig. A1.6C, and data not shown).

In contrast, analysis of cell death at 24 hpf by TUNEL labeling shows that *wis* mutants display twice the normal amount of cell death throughout the embryo (Fig. A1.6D-F, n=14, p<0.0001, and data not shown). Increased cell death continues through 2 dpf (data not shown), occurring in many tissues, even those which express *sfpq* at low levels. This could be due to loss of low level *sfpq* expression, or it could be a result of loss of *sfpq* at earlier timepoints. Regardless, these results suggest that *sfpq* is not required for regulation of cell proliferation, but is involved in regulating cell death. Several lines of evidence suggest that PSF responds to and/or can modulate apoptosis. In apoptotic cells, PSF dissociates from a partner, PTB, and binds new partners, including the splicing factors U1-70K and SR proteins (Shav-Tal et al., 2001). Additionally, during apoptosis, PSF relocates into globular nuclear structures, rather than in the nuclear “speckles” (interchromatin granules) normally observed (Shav-Tal et al., 2001). Interestingly, PSF induces apoptosis when over-expressed in mammalian cell culture (Xu et al., 2005a), and it is not clear how this observation relates to the increase in apoptosis we observe in *wis/sfpq* mutants.

### ***sfpq* is required for the differentiation, but not determination, of certain neuronal cell types**

Since *sfpq* is strongly expressed in the brain, and particularly in determined, post-mitotic neuronal precursors, we asked whether and when *sfpq* alters neuronal development. We first analyzed neural patterning in *wis* mutants at 24 hpf. Expression of the anteroposterior neural

markers *krox20*, *pax2.1*, and the dorsoventral markers *opl*, and *shh* (Krauss et al., 1991; Krauss et al., 1993; Oxtoby and Jowett, 1993; Grinblat et al., 1998) is identical in *wis* mutants and wild-type siblings (Fig. A1.7A,B, and data not shown), suggesting that *sfpq* is not required for early neural patterning. Second, we analyzed early neurogenesis in *wis* mutants. Expression of *zash1B*, a proneural gene expressed exclusively in cycling neural progenitors (Allende and Weinberg, 1994; Mueller and Wullimann, 2003), is similar between *wis* mutants and wild-type siblings (data not shown). Similarly, expression of HuC/D, one of the earliest markers for post-mitotic neuronal precursors (Marusich et al., 1994), shows no difference between *wis* and wild-type siblings (Fig. A1.7C-G). Quantitation of HuC/D cell labeling in the spinal cord confirms that the number of Hu-positive cells is the same between *wis* and wild-type embryos (Fig. A1.7E-G, n=5, p=0.2672). These results indicate that *sfpq* is not required for early neural patterning and neuronal determination, and show that the number of post-mitotic neuronal precursors is normal in the *wis* mutant.

In contrast, markers for later neuronal differentiation show obvious expression defects in *wis* mutants. Labeling the 24 hpf embryonic axon scaffolds with anti-acetylated tubulin or anti-HNK-1 (Metcalf et al., 1990) demonstrates a large reduction in the number of axon tracts throughout the brain (Fig. A1.8A-J). Immunostaining with a monoclonal antibody directed against Neurofilament M, which labels both cell bodies and axons of hindbrain reticulospinal neuronal (Pleasure et al., 1989), shows a complete absence of all reticulospinal neurons in the hindbrain except the Mauthner neurons (Fig. A1.8K,L). By 2 dpf, Mauthner neurons appear somewhat abnormal, with a rounded cell body and occasional axonal pathfinding abnormalities (Fig. A1.8M,N, and not shown). No other hindbrain reticulospinal neurons are present. Importantly, not all neuronal cell types are affected in *wis*, as labeling with an anti-islet antibody which marks differentiated motoneuron cell bodies (Ericson et al., 1992) shows no differences between *wis* and wild-type siblings in the brain (Fig. A1.8O,P) or in the spinal cord (Fig. A1.8Q,R). Quantitation in the brain demonstrates identical numbers of labeled cells are present in this region (n=5, p=0.7517, Fig. A1.9). One caveat to these conclusions is that we have analyzed survival of motoneuron cell bodies but not axons, raising the interesting possibility that cell bodies survive while axons degenerate. However, this is clearly not generally true, as both cell bodies and axons were absent from *wis* reticulospinal neurons.

These data suggest that a second phase of *sfpq* function is neural-specific. In particular, only specific classes of differentiated neurons are absent in the *sfpq/wis* mutants, while other



classes are present in normal numbers. Furthermore, the number of post-mitotic neuronal precursors identified by HuC/D labeling is indistinguishable between wild type and mutant at 24 hpf. Thus, even with increased cell death throughout the embryo, normal numbers of determined and post-mitotic neurons are recruited. Together, the data indicate that neuronal differentiation, but not neuronal determination, requires *sfpq* function.

### **Conclusion: Separable functions for *sfpq*?**

Is the increase in cell death we observe in *sfpq/wis* mutants simply the result of removing a housekeeping function from the embryo? The notion of housekeeping functions has become complex, where some genes have both ubiquitously required functions and cell type-specific functions, such as the essential splicing factor ASF/SF2, implicated in cardiac-specific splicing (Xu et al., 2005b), and the ubiquitously expressed PTB, the polypyrimidine-tract-binding protein, which represses neuron-specific splicing in non-neuronal cells (Ashiya and Grabowski, 1997). PSF may also have both general and tissue-specific functions.

Clearly, there is an embryo-wide requirement for PSF protein. Our data suggest that PSF normally suppresses apoptosis, although the mechanisms by which it interfaces with the apoptotic machinery is not clear. A report that overexpressed PSF promotes apoptosis in mammalian tissue culture contradicts our finding in whole animals (Xu et al., 2005a), and suggests either that cells respond to either too much or too little PSF, or indicates a species-specific difference in PSF function.

Later in development, a second effect of loss of PSF function is apparent, as specific neuronal classes fail to differentiate. This is not a general phenotype, as formation of some neuronal classes is unaffected, while numbers of neurons in other classes are profoundly decreased or are absent. Consistent with two phases of *sfpq* function is the replacement of low level, ubiquitous early expression of *sfpq* with later and very strong expression that is enriched in developing brain relative to the rest of the embryo. This suggests separable early and late functions for *sfpq*. Our data are consistent with other reports that demonstrate PSF has numerous cellular functions (Shav-Tal and Zipori, 2002).

Is specific neuronal loss linked to the effects of PSF on apoptosis? We cannot yet distinguish whether particular neuronal classes are absent because they do not survive or because they cannot differentiate. This question will be best answered by defining whether neuronal

progenitors die in *spfq/wis* mutants. Definition of PSF target genes will also help answer this question. An alternate explanation is that another function of PSF is necessary for differentiation of specific neuronal classes. In particular, PSF could play a role in brain-specific splicing or transcriptional regulation. *whitesnake/spfq* mutants will be indispensable tools to investigate whether PSF function depends on its splicing activity or on another function of this protein, and to characterize potential targets of PSF.

## Experimental Procedures

### Fish lines and maintenance

*Danio rerio* were raised and bred according to standard methods (Westerfield, 1995). Embryos were kept at 28.5°C and staged according to Kimmel et al. (Kimmel et al., 1995). Times of development are expressed as hours post-fertilization (hpf) or days post-fertilization (dpf).

Lines used were: AB, Tübingen Long Fin, *spfq*<sup>hi1779</sup> (Amsterdam et al., 2004), *wis*<sup>tr241</sup> (Jiang et al., 1996), *wis*<sup>m427</sup> (Schier et al., 1996). For PCR genotyping, tails or embryos were digested with proteinase K (1 mg/ml) in lysis buffer (10 mmol/l Tris pH 8, 1 mmol/l EDTA, 0.3% Tween-20, 0.3% NP40). Because *spfq*<sup>hi1779</sup> has a retroviral insertion in the *spfq* gene, mutant individuals could be identified by PCR. Primers used: 1779c: 5'-cagcagactcccaccgtcg-3', MSL4: 5'-gctagcttgccaaacctacaggt-3' (MWG Biotech). MSL4 detects the retroviral insertion which is located 553 base pairs downstream from the *spfq* start site in the *hi1779* mutant. The C to T mutation present in *wis*<sup>tr241</sup> introduces an AccI restriction site and thus can be detected by PCR followed by digestion. All procedures on live animals and embryos were approved by the Massachusetts Institute of Technology Committee on Animal Care.

### Brain ventricle imaging

Methods for brain ventricle imaging have been described previously (Lowery and Sive, 2005). Briefly, embryos were anesthetized in 0.1 mg/ml Tricaine (Sigma) dissolved in embryo medium prior to hindbrain ventricle microinjection with 2-10 nl dextran conjugated to Rhodamine (5% in 0.2 mol/l KCl, Sigma), and then embryos were imaged by light and fluorescence microscopy

with a Leica dissecting microscope, using a KT Spot Digital Camera (RT KE Diagnostic Instruments). Images were superimposed in Photoshop 6 (Adobe).

### **Detection of *whitesnake* mutation**

Total RNA was extracted from mutant embryos and wild-type siblings using Trizol reagent (Invitrogen), followed by chloroform extraction and isopropanol precipitation. cDNA synthesis was performed with Super Script II Reverse Transcriptase (Invitrogen) and random hexamers. PCR was then performed using five sets of primers, which amplify the coding region of *sfpq*.

Primers used: *sfpq*1F 5'-tgagggtgctctctctttg-3', *sfpq*1R 5'-gagagcgttgcttcaattc-3',  
*sfpq*2F 5'-tccaccgaagatccagtctc-3', *sfpq*2R 5'-ggcagctggcttagaagaaa-3',  
*sfpq*3F 5'-gaggttgcaagcagagtt-3', *sfpq*3R 5'-tcctctctctctctctctac-3',  
*sfpq*4F 5'-aggcagcaagtggagaaaaa-3', *sfpq*4R 5'-gccacaaatgggatgagttt-3'  
*sfpq*5F 5'-gcaaacgcgaggaatcttac-3', *sfpq*5R 5'-ttttgggagaaccaactgc-3'

RT-PCR products were used for sequencing analysis, performed by Northwoods DNA, Inc. (Solway MN). Sequencing data were analyzed using the BLAST program (<http://www.ncbi.nlm.nih.gov/BLAST/>), and the cDNA sequence of *sfpq* was obtained from the GenBank database (NM\_213278).

### **RNA injections**

Full-length *sfpq* cDNAs were generated by RTPCR with primers including ClaI/XbaI sites, ClaI-*sfpq*1F 5'-ccat/cgattgagggtgctctctctttg-3', XbaI-*sfpq*5R 5'-gct/ctagattttgggagaaccaactgc-3'. The PCR fragments were subcloned into pCS2+, and the pCS2+ constructs were linearized by NotI. Capped mRNA was transcribed in vitro using the SP6 mMessage mMachine kit (Ambion). Embryos were injected at the one-cell stage with 100-300 pg mRNA. The embryos phenotypically rescued by mRNA injection were identified as mutants by genotyping.

### **Morpholino oligo injections**

A morpholino antisense oligonucleotide (MO) targeted to the translation start site of zebrafish *sfpq* (5'-ccatgccaccgcgatccccattcc-3') was injected into 1-2 cell embryos. The final amounts used were 8 ng of *sfpq* or control MO (provided by Gene Tools Inc).

### **RT-PCR time course**

Total RNA was extracted from staged wild-type embryos or adult dissected tissue using Trizol reagent (Invitrogen), followed by chloroform extraction and isopropanol precipitation. cDNA synthesis was performed with Super Script II Reverse Transcriptase (Invitrogen) and random hexamers. PCR was then performed using *sfpq*4F and *sfpq*4R (listed above), and *actinF* 5'-tatccacgagaccacctcaactcc-3', *actinR* 5'-ctgcttgetgatccacatctgctgg-3'

### **In situ hybridization**

RNA probes containing digoxigenin-11-UTP were synthesized from linearized plasmid DNA for *sfpq*, *pax2.1* (Krauss et al., 1991), *krox20* (Oxtoby and Jowett, 1993), *opl* (Grinblat et al., 1998), *shh* (Krauss et al., 1993), and *zash1B* (Allende and Weinberg, 1994) as described (Harland, 1991). Standard methods for hybridization and for single color labeling were used as described elsewhere (Sagerstrom et al., 1996). After staining, embryos were fixed in 4% paraformaldehyde overnight at 4 degrees C, washed in PBS, dehydrated in methanol, and then cleared in a 3:1 benzyl benzoate/ benzyl alcohol (BB/BA) solution prior to mounting and imaging with a Nikon compound microscope.

### **Immunohistochemistry**

Whole-mount immunostaining was carried out using rabbit anti-phosphohistone H3 (Upstate Biotechnology, 1:800), mouse anti-acetylated tubulin (Sigma, 1:1000), mouse anti-neurofilament RM044 (Zymed #13-0500, 1:50), mouse HNK-1/zn-12 (Zebrafish International Resource Center, 1:500), mouse 39.4D5 anti-islet (Developmental Studies Hybridoma Bank, 1:100), mouse anti-HuC (Molecular Probes, 1:500), and mouse MF20 IgG2b (Developmental Studies Hybridoma Bank, 1:10). Goat anti-rabbit IgG Alexa Fluor 488 (Molecular Probes, 1:500), goat anti-mouse Alexa Fluor 488 (Molecular Probes, 1:500), goat anti-mouse IgG HRP (Sigma, 1:500), goat anti-rabbit IgG HRP (Sigma, 1:500), and goat anti-mouse IgG2b Alexa Fluor 568 (Molecular Probes, 1:500) were used as secondary antibodies.

For labeling with anti-phosphohistone H3, anti-acetylated tubulin, HNK-1 antibody, 39.4D5 antibody, anti-HuC, and MF20 antibody, dechorionated embryos were fixed in 4% paraformaldehyde for 2 hours at room temperature, then rinsed in PBS. For anti-phosphohistone H3 and anti-HuC, endogenous peroxidase activity was quenched in 10% hydrogen peroxide in

PBT for 1 hour. For all antibodies, blocking was done for 4 hours at room temperature in 0.5% Triton X, 4% normal goat serum, in phosphate buffer. Detection of HRP was performed with the DAB substrate peroxidase kit (Vector Laboratories). Fluorescent secondary antibodies were visualized by confocal microscopy (LSM510). Brains were flat-mounted in glycerol and imaged. Images are composites of several scans.

For labeling with RM044 antibody, dechorionated embryos were fixed in 2% trichloroacetic acid 3 hours at room temperature, washed in PBS, blocked in 10% normal goat serum in PBT for 3 hours, prior to incubation in antibody. The brains were partially dissected and mounted for visualization by confocal microscopy.

To block pigmentation, embryos were incubated in 0.2mM 1-phenyl-2-thiourea in embryo media beginning at 22 hpf.

### **Cell death labeling**

DNA fragmentation during apoptosis was detected by the TUNEL method, using 'ApopTag' kit (Chemicon). Embryos were fixed in 4% paraformaldehyde in PBS for 2 hours, then rinsed in PBS and dechorionated. Embryos were dehydrated to 100% ethanol, stored at  $-20^{\circ}\text{C}$  overnight, then rehydrated in PBS. Embryos were further permeabilized by incubation in proteinase K (5  $\mu\text{g}/\text{ml}$ ) for 5 minutes, then rinsed in PBS. TdT labeling was followed per manufacturer's instructions. Anti-DIG-AP (Gibco, 1:100) was used to detect the DIG labeled ends. Brains were flat-mounted in glycerol and imaged.

### **Statistical analysis**

To quantify amount of cell proliferation, cell death, or antibody staining, labeled cells in a defined area of the brain and/or tail were counted and then compared statistically using an unpaired t-test (InStat v.3, GraphPad software).

### **Acknowledgements**

We thank members of the Sive Lab for helpful comments and Olivier Paugois for fish husbandry. Many thanks to the Nusslein-Volhard lab for providing us with the *wis tr241* mutant, the Zebrafish International Resource Center for the *wis m427* mutant and zn-12 antibody, Adam Amsterdam and Nancy Hopkins for *sfpq hi1779* mutant. The 39.4D5 antibody developed by

Thomas Jessell, and the MF20 antibody developed by Donald Fischman, were obtained from the Developmental Studies Hybridoma Bank developed under the auspices of the NICHD and maintained by the University of Iowa, Department of Biogoical Sciences, Iowa City, IA 52242. This work was conducted utilizing the W.M. Keck Foundation Biological Imaging Facility at the Whitehead Institute. The Zebrafish International Resource Center is supported by grant #RR12546 from the NIH-NCRR. Supported by NIH MH70926 to HLS, NIH NRSA pre-doctoral fellowship and Abraham J. Siegel Fellowship at the Whitehead Institute to LAL.

**Figure A1.1 Phenotype of *whitesnake/sfpq* mutants.**

Brain ventricles were visualized by microinjecting a fluorescent dye, Rhodamine-dextran, into the hindbrain ventricle of living anesthetized embryos at 24 hpf (A-F), 28 hpf (G-I), and 2 dpf (J-Q). At 24 hpf, the *wis*<sup>tr241</sup> mutant has reduced brain ventricles and abnormal curvature of the tail (B,E), as compared to wild type (A,D), and the *sfpq*<sup>hi1779</sup> mutant phenotype is similar (C,F). At 28 hpf, both *wis*<sup>tr241</sup> and *sfpq*<sup>hi1779</sup> show variable reduction in brain ventricle size and reduced pigmentation (H,I). By 48 hpf, the *wis* brain ventricle reduction becomes more severe compared to wild type, especially in the midbrain (J-Q). Dorsal views (A-C, G-I, N-Q); side views (D-F, J-M). F, forebrain; M, midbrain; H, hindbrain. Scale bar 100  $\mu$ m.

(R) *sfpq* gene/PSF protein and corresponding mutations. *wis*<sup>tr241</sup> has a C to T mutation at position 491 of coding sequence, which results in an early stop codon at amino acid 167. *sfpq*<sup>hi1779</sup> has a 6kb retroviral insertion (which has a stop codon early in the insertion sequence). *wis*<sup>m427</sup> mRNA has aberrant splicing resulting in 200 base pairs of intronic sequence inserted before the last exon. Both *sfpq*<sup>hi1779</sup> and *wis*<sup>tr241</sup> are truncated near the end of P/Q-rich region, and *wis*<sup>m427</sup> lacks the last NLS. P/Q, proline/glutamine-rich region; RRM, RNA recognition motifs; NLS, nuclear localization sequence.





Figure A1.1 Continued

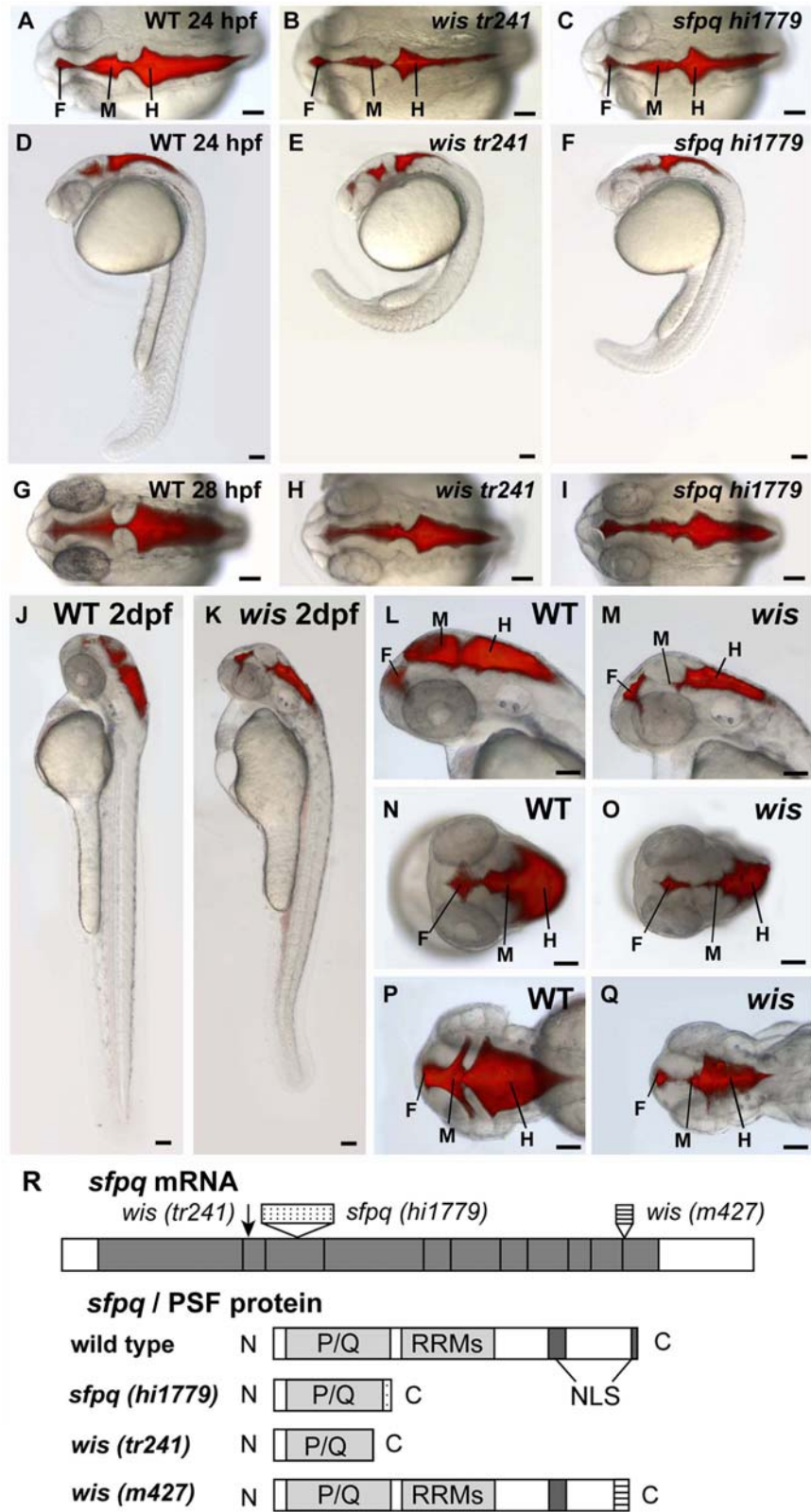




**Figure A1.2 Brain phenotype of the *whitesnake/sfpq* mutant is variable.**

Brain ventricles were visualized by microinjecting a fluorescent dye, Rhodamine-dextran, into hindbrain ventricle of living anesthetized embryos at 28 hpf. Both *wis*<sup>tr241</sup> and *sfpq*<sup>hi1779</sup> show variable reduction in brain ventricle size. (A,B) show most severe phenotype, while (C,D) show least severe. Dorsal views, anterior left. Scale bar 100  $\mu$ m.

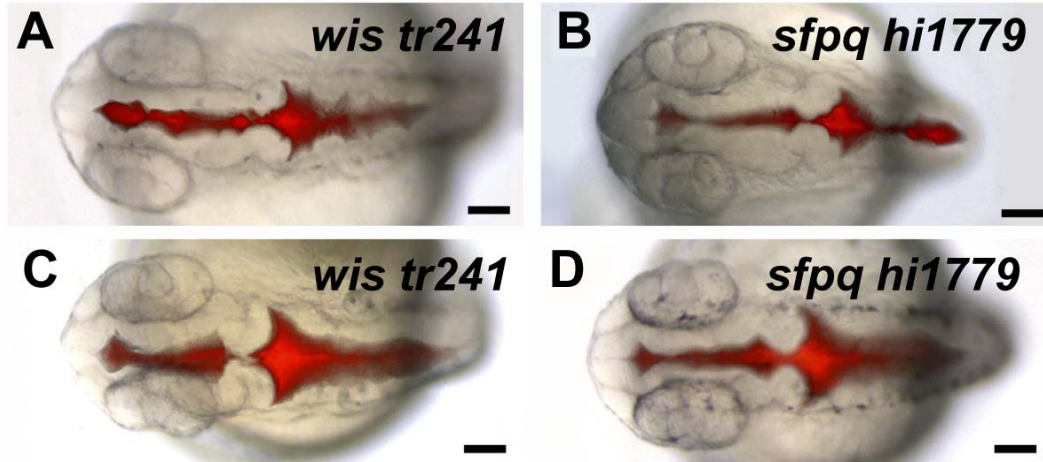




**Figure A1.3 *sfpq* mRNA partially rescues the *whitesnake* phenotype and *sfpq* morpholino phenocopies mutant phenotype at 28 hpf.**

(A,D) WT sibling of *wis*<sup>tr241</sup> (B,E) *wis*<sup>tr241</sup> mutant injected with ~100 pg *sfpq* mRNA (C,F) *wis*<sup>tr241</sup> mutant. (G,J) WT injected with 8ng control morpholino, (H,K) WT injected with 8ng *sfpq* morpholino, (I,L) *sfpq*<sup>hi1779</sup> mutant. (A-C, G-I) dorsal views; (D-F, J-L) lateral views. Scale bar 100  $\mu$ m.

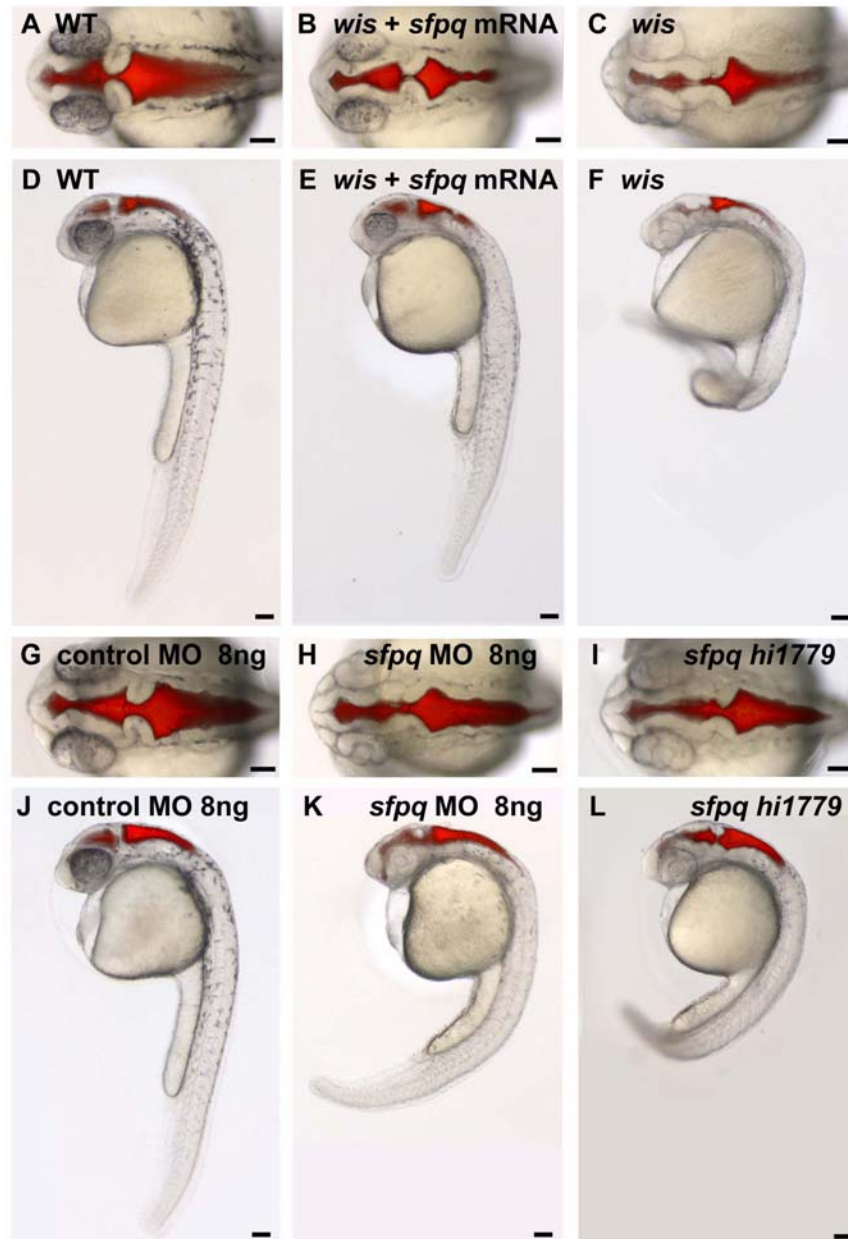




**Figure A1.4 *sfpq* expression patterns.**

(A) RTPCR for *sfpq* in embryonic tissue shows that *sfpq* is expressed beginning at 1 hpf (lane 1) and peaks at 18 hpf (lane 5). Adult tissue also has *sfpq* expression, with the brain showing the highest level (lane 11) and heart and body muscle showing lower levels (lanes 14, 15). Actin RTPCR was used as control for RNA levels.

(B-Q) *sfpq* in situ hybridization time course shows that *sfpq* is expressed throughout embryogenesis. (B) 1 hpf (4 cell stage), side view; (C) 4 hpf (blastula stage), side view; (D) 8 hpf (75% epiboly stage), side view, dorsal right; (E) 12 hpf (6 somite stage), side view, dorsal right, anterior top. (F-H) 18 hpf, strongest expression in the forebrain (H, bracket) and in presumptive rhombomere 4 (H, arrow). (I-K) 24 hpf. (L-N) 2 dpf, expression appears restricted to strong longitudinal strips in the ventral brain (M, arrow) and in weaker transverse stripes in the hindbrain. (O-Q) 3 dpf, expression ventral to brain (P, arrow) and along axon tracts. (F-G, I-J, L-M, O-P) side views, anterior left. (H,K,N,Q) dorsal views, anterior left. Note: in I-Q, regions without staining may not be in focus, as to allow high magnification imaging of the stained regions. In areas of staining, the fuzziness sometimes observed is due to low levels of diffuse staining, not poor imaging. Scale bar 100  $\mu$ m.





Figure A1.4 Continued

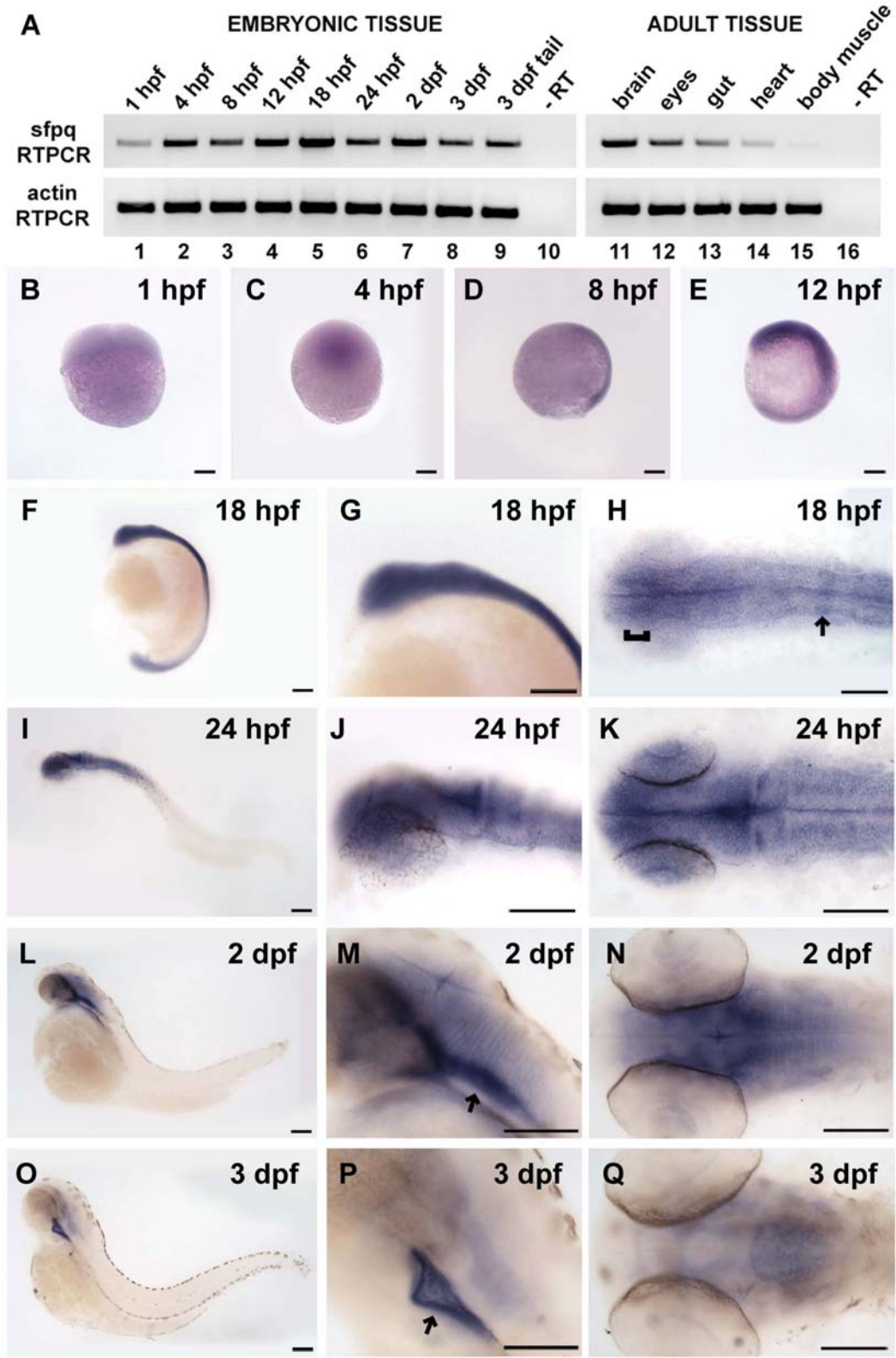




**Figure A1.5 *sfpq* is strongly expressed in regions of neurogenic activity.**

(A,B) 24 hpf wild-type embryos labeled for *sfpq* expression by in situ hybridization only, and (C,D) wild-type sibling embryos double labeled for *sfpq* mRNA expression and HuC protein by immunohistochemistry show that regions of strongest *sfpq* expression in the brain (brackets) overlap with HuC, a marker for post-mitotic neuronal precursors. (B,D) show higher magnification of hindbrain; brackets mark strong *sfpq* expression overlapping with HuC labeling. Midline staining is an artifact of the staining process, since it is not observed in embryos cut open prior to staining. (A-D) Dorsal views. Anterior left. Scale bar 100  $\mu$ m.

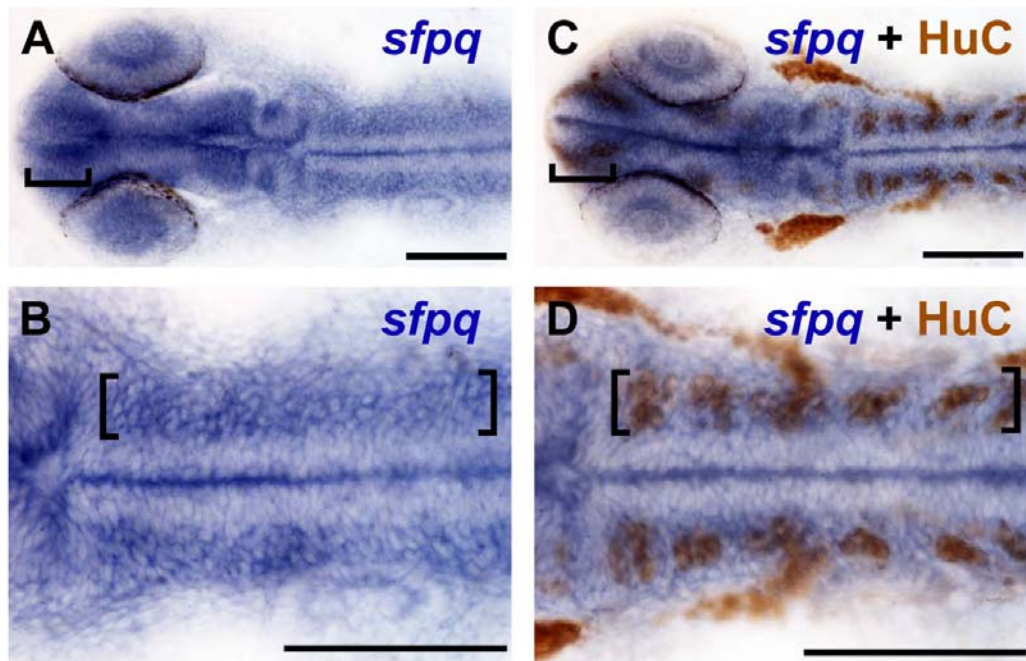




**Figure A1.6 Cell proliferation and cell death analysis in *whitesnake* mutants.**

(A-C) Cell proliferation analysis, using PH3 antibody labeling. (A,B) Fixed and labeled wild type and *wis* brain at 24 hpf. (C) Quantification comparing labeling in hindbrain shows no difference between wild type and mutant,  $n=8$ ,  $p=0.8046$ . (D-F) Cell death analysis, using TUNEL staining. (D,E) Fixed and labeled wild type and *wis* brain at 24 hpf. (F) Quantification comparing labeling in hindbrain shows approximately twice the amount of cell death in the mutant than in wild type,  $n=14$ ,  $p<0.0001$ . Error bars denote standard error. (A-B, D-E) Dorsal views. Boxes mark region used for quantitation. F forebrain, M midbrain, H hindbrain. Scale bar 100  $\mu\text{m}$ .

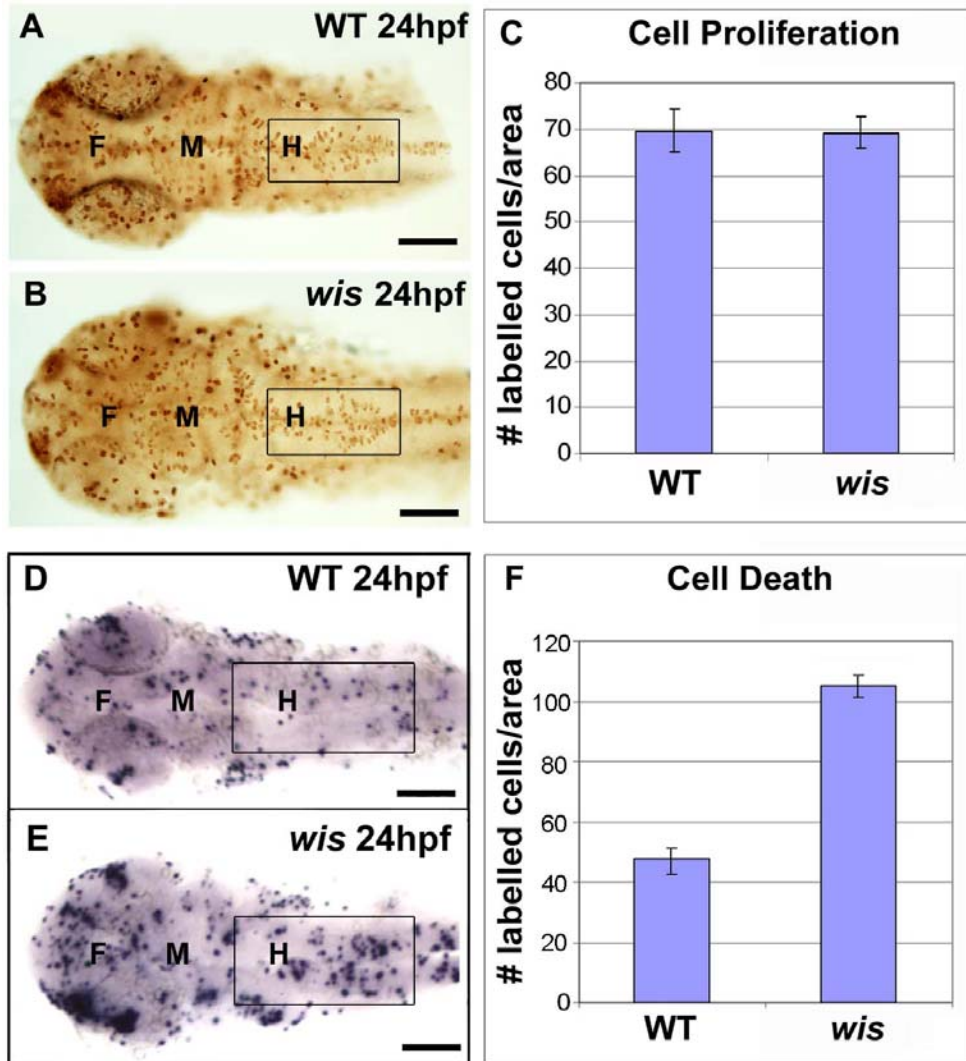




**Figure A1.7 Neuronal determination is normal in *whitesnake* mutants.**

(A,B) in situ hybridization for *pax2a* (labeling nasal placodes, midbrain-hindbrain boundary, and otic vesicles - arrowheads) and *krox20* (labeling rhombomeres 3 and 5 - arrows) show similar staining patterns in wild type and mutant. (C,D) immunohistochemistry for HuC, a marker for post-mitotic neurons, shows identical patterns between wild type and mutant. This has been quantified in graph (E), which depicts the number of HuC labeled cells per unit area in the spinal cords of wild type and *wis* (F,G). F forebrain, M midbrain, H hindbrain. Scale bar 100  $\mu$ m.

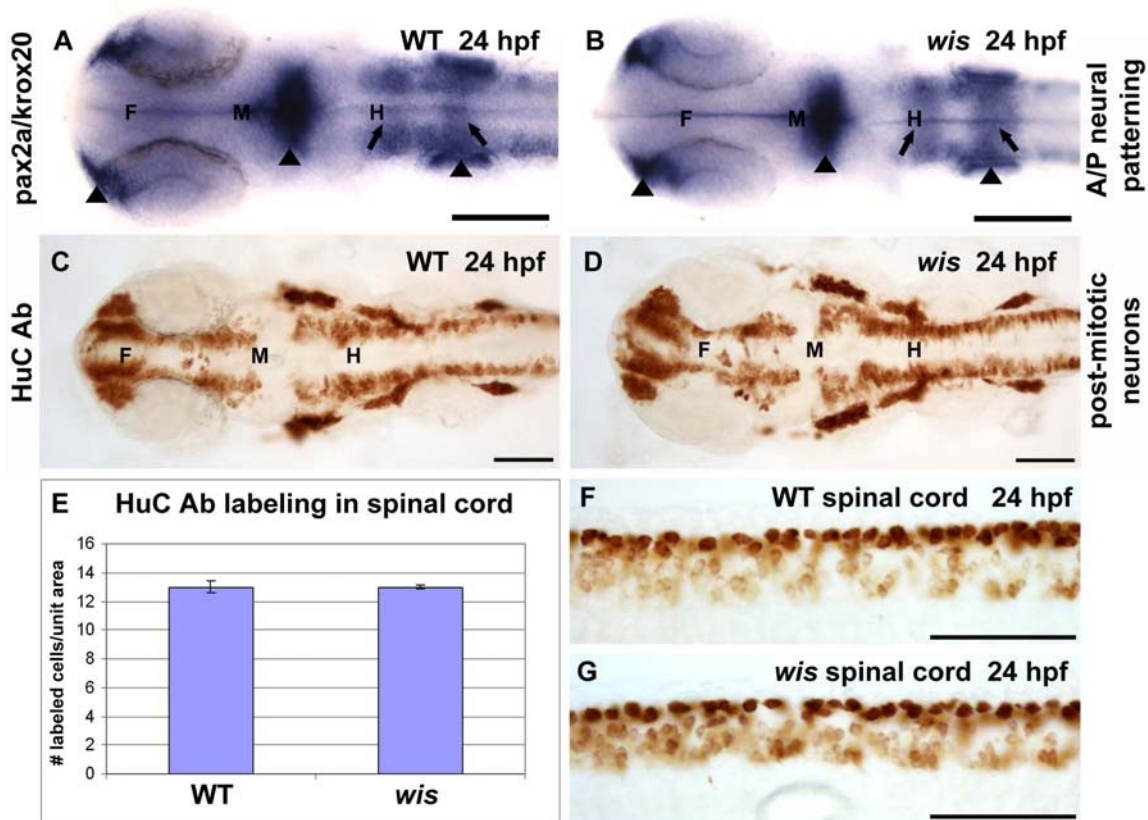






**Figure A1.8 Specific neurons are absent in *whitesnake* mutants.**

(A-F) acetylated tubulin antibody labeling, and (G-J) HNK-1 antibody labeling, both of which mark most differentiated neurons and their axons, show reduced number of axons in *wis* mutant in the hindbrain (B,D,H), midbrain (F) and eyes/forebrain (J) compared to wild type (A,C,E,G,I); (K-N) RM044 Ab, which labels reticulospinal neurons, shows an absence of all reticulospinal neurons in the *wis* hindbrain except Mauthner neurons (labeled with M) at both 24 hpf (L) and 2 dpf (N), compared to wild type (K,M); (O-R) 4D5 Islet antibody, labeling motoneurons, shows no loss of motoneurons in *whitesnake* in the dorsal diencephalon (P) or spinal cord (R) compared to wild type (O,Q). A anterior, P posterior. (A-D, G-P) dorsal views. (E-F, Q-R) side views. Scale bar 50  $\mu$ m.

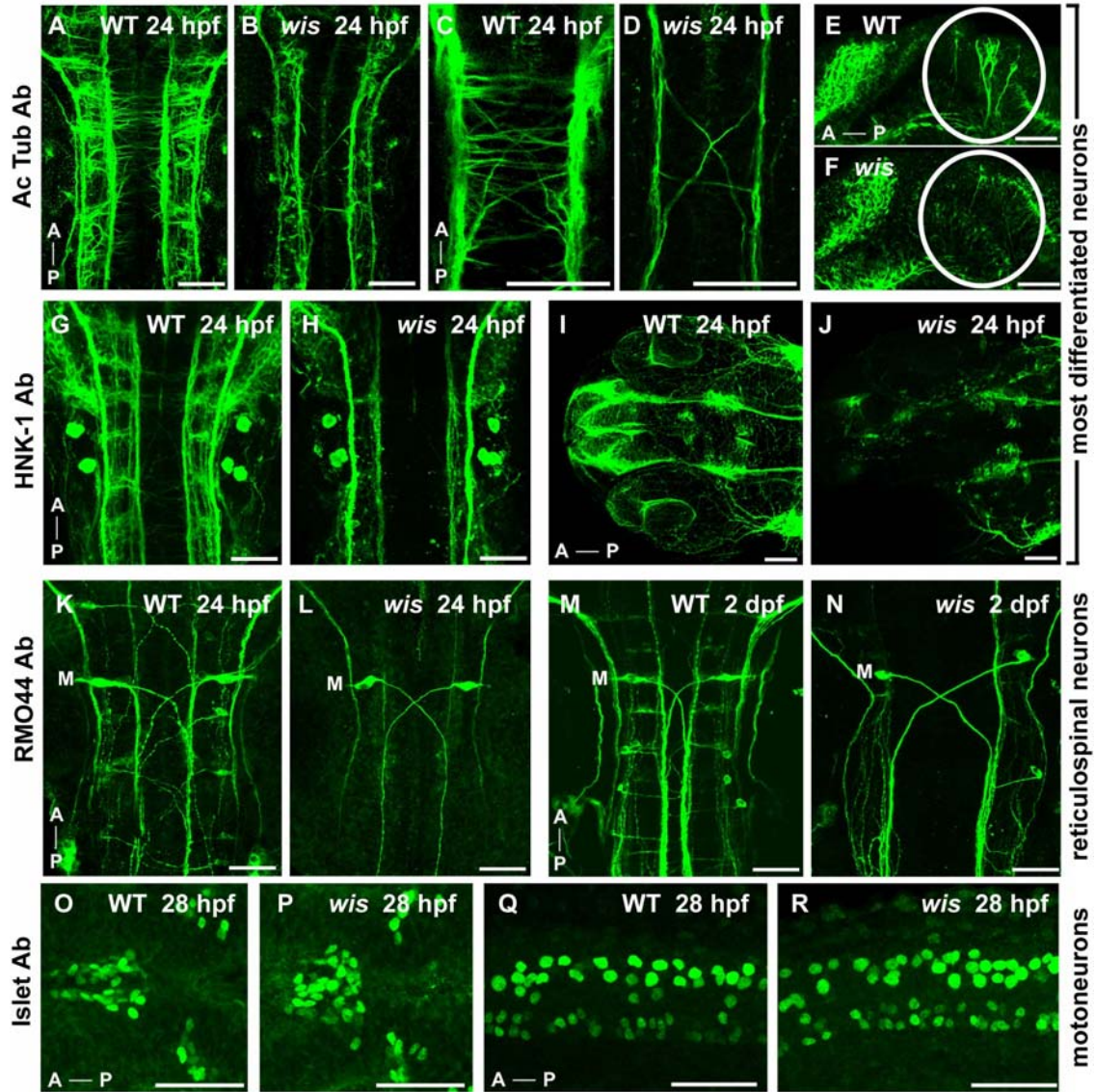
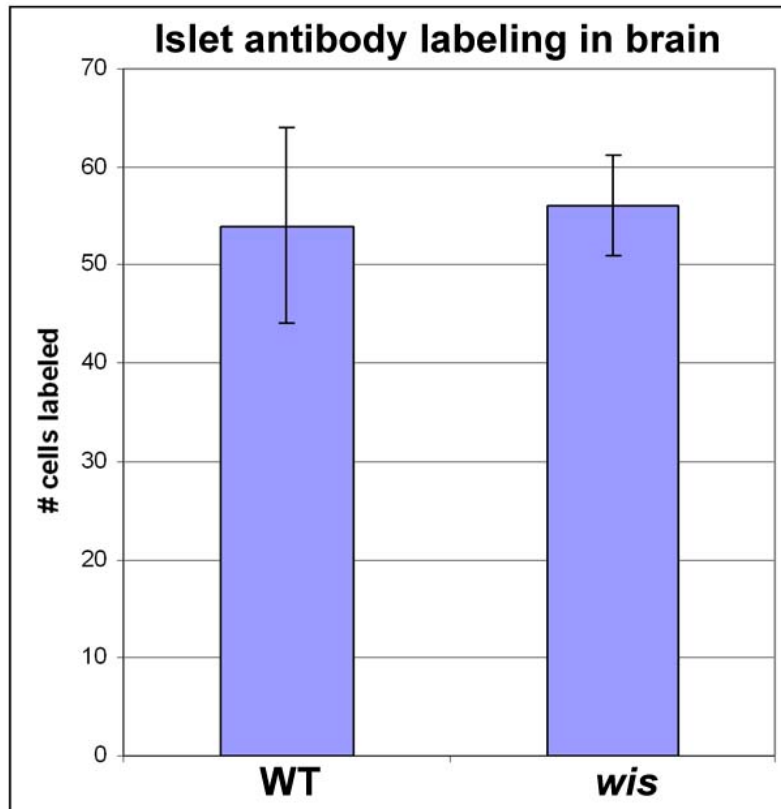




**Figure A1.9 Quantification of Islet antibody labeling in brain.**

Quantification comparing Islet antibody labeling in brain shows approximately the same amount of labeling in *wis* mutants as in wild-type embryo at 24 hpf,  $n=5$ ,  $p=0.7517$ . Error bars denote standard error.





## References

- Allende ML, Weinberg ES. 1994. The expression pattern of two zebrafish achaete-scute homolog (ash) genes is altered in the embryonic brain of the cyclops mutant. *Dev Biol* 166:509-530.
- Amsterdam A, Nissen RM, Sun Z, Swindell EC, Farrington S, Hopkins N. 2004. Identification of 315 genes essential for early zebrafish development. *Proc Natl Acad Sci U S A* 101:12792-12797.
- Ashiya M, Grabowski PJ. 1997. A neuron-specific splicing switch mediated by an array of pre-mRNA repressor sites: evidence of a regulatory role for the polypyrimidine tract binding protein and a brain-specific PTB counterpart. *Rna* 3:996-1015.
- Buckanovich RJ, Posner JB, Darnell RB. 1993. Nova, the paraneoplastic Ri antigen, is homologous to an RNA-binding protein and is specifically expressed in the developing motor system. *Neuron* 11:657-672.
- Chanas-Sacre G, Mazy-Servais C, Wattiez R, Pirard S, Rogister B, Patton JG, Belachew S, Malgrange B, Moonen G, Leprince P. 1999. Identification of PSF, the polypyrimidine tract-binding protein-associated splicing factor, as a developmentally regulated neuronal protein. *J Neurosci Res* 57:62-73.
- Clark J, Lu YJ, Sidhar SK, Parker C, Gill S, Smedley D, Hamoudi R, Linehan WM, Shipley J, Cooper CS. 1997. Fusion of splicing factor genes PSF and NonO (p54nrb) to the TFE3 gene in papillary renal cell carcinoma. *Oncogene* 15:2233-2239.
- Dong X, Shylnova O, Challis JR, Lye SJ. 2005. Identification and characterization of the protein-associated splicing factor as a negative co-regulator of the progesterone receptor. *J Biol Chem* 280:13329-13340.
- Dye BT, Patton JG. 2001. An RNA recognition motif (RRM) is required for the localization of PTB-associated splicing factor (PSF) to subnuclear speckles. *Exp Cell Res* 263:131-144.
- Emili A, Shales M, McCracken S, Xie W, Tucker PW, Kobayashi R, Blencowe BJ, Ingles CJ. 2002. Splicing and transcription-associated proteins PSF and p54nrb/nonO bind to the RNA polymerase II CTD. *Rna* 8:1102-1111.
- Ericson J, Thor S, Edlund T, Jessell TM, Yamada T. 1992. Early stages of motor neuron differentiation revealed by expression of homeobox gene *Islet-1*. *Science* 256:1555-1560.
- Grinblat Y, Gamse J, Patel M, Sive H. 1998. Determination of the zebrafish forebrain: induction and patterning. *Development* 125:4403-4416.
- Harland RM. 1991. In situ hybridization: an improved whole-mount method for *Xenopus* embryos. *Methods Cell Biol* 36:685-695.

- Hendzel MJ, Wei Y, Mancini MA, Van Hooser A, Ranalli T, Brinkley BR, Bazett-Jones DP, Allis CD. 1997. Mitosis-specific phosphorylation of histone H3 initiates primarily within pericentromeric heterochromatin during G2 and spreads in an ordered fashion coincident with mitotic chromosome condensation. *Chromosoma* 106:348-360.
- Jensen KB, Dredge BK, Stefani G, Zhong R, Buckanovich RJ, Okano HJ, Yang YY, Darnell RB. 2000. Nova-1 regulates neuron-specific alternative splicing and is essential for neuronal viability. *Neuron* 25:359-371.
- Jiang YJ, Brand M, Heisenberg CP, Beuchle D, Furutani-Seiki M, Kelsh RN, Warga RM, Granato M, Haffter P, Hammerschmidt M, Kane DA, Mullins MC, Odenthal J, van Eeden FJ, Nusslein-Volhard C. 1996. Mutations affecting neurogenesis and brain morphology in the zebrafish, *Danio rerio*. *Development* 123:205-216.
- Kimmel CB, Ballard WW, Kimmel SR, Ullmann B, Schilling TF. 1995. Stages of embryonic development of the zebrafish. *Dev Dyn* 203:253-310.
- Krauss S, Concordet JP, Ingham PW. 1993. A functionally conserved homolog of the *Drosophila* segment polarity gene *hh* is expressed in tissues with polarizing activity in zebrafish embryos. *Cell* 75:1431-1444.
- Krauss S, Johansen T, Korzh V, Fjose A. 1991. Expression of the zebrafish paired box gene *pax[zf-b]* during early neurogenesis. *Development* 113:1193-1206.
- Lowery LA, Sive H. 2005. Initial formation of zebrafish brain ventricles occurs independently of circulation and requires the *nagie oko* and *snakehead/atp1a1a.1* gene products. *Development* 132:2057-2067.
- Marusich MF, Furneaux HM, Henion PD, Weston JA. 1994. Hu neuronal proteins are expressed in proliferating neurogenic cells. *J Neurobiol* 25:143-155.
- Metcalf WK, Myers PZ, Trevarrow B, Bass MB, Kimmel CB. 1990. Primary neurons that express the L2/HNK-1 carbohydrate during early development in the zebrafish. *Development* 110:491-504.
- Mueller T, Wullmann MF. 2003. Anatomy of neurogenesis in the early zebrafish brain. *Brain Res Dev Brain Res* 140:137-155.
- Oxtoby E, Jowett T. 1993. Cloning of the zebrafish *krox-20* gene (*krx-20*) and its expression during hindbrain development. *Nucleic Acids Res* 21:1087-1095.
- Patton JG, Porro EB, Galceran J, Tempst P, Nadal-Ginard B. 1993. Cloning and characterization of PSF, a novel pre-mRNA splicing factor. *Genes Dev* 7:393-406.
- Pleasure SJ, Selzer ME, Lee VM. 1989. Lamprey neurofilaments combine in one subunit the features of each mammalian NF triplet protein but are highly phosphorylated only in large axons. *J Neurosci* 9:698-709.

- Sagerstrom CG, Grinbalt Y, Sive H. 1996. Anteroposterior patterning in the zebrafish, *Danio rerio*: an explant assay reveals inductive and suppressive cell interactions. *Development* 122:1873-1883.
- Saka Y, Smith JC. 2001. Spatial and temporal patterns of cell division during early *Xenopus* embryogenesis. *Dev Biol* 229:307-318.
- Schier AF, Neuhauss SC, Harvey M, Malicki J, Solnica-Krezel L, Stainier DY, Zwartkruis F, Abdelilah S, Stemple DL, Rangini Z, Yang H, Driever W. 1996. Mutations affecting the development of the embryonic zebrafish brain. *Development* 123:165-178.
- Shav-Tal Y, Cohen M, Lapter S, Dye B, Patton JG, Vandekerckhove J, Zipori D. 2001. Nuclear relocalization of the pre-mRNA splicing factor PSF during apoptosis involves hyperphosphorylation, masking of antigenic epitopes, and changes in protein interactions. *Mol Biol Cell* 12:2328-2340.
- Shav-Tal Y, Lee B, Bar-Haim S, Vandekerckhove J, Zipori D. 2000. Enhanced proteolysis of pre-mRNA splicing factors in myeloid cells. *Exp Hematol* 28:1029-1038.
- Shav-Tal Y, Zipori D. 2002. PSF and p54(nrb)/NonO--multi-functional nuclear proteins. *FEBS Lett* 531:109-114.
- Ule J, Ule A, Spencer J, Williams A, Hu JS, Cline M, Wang H, Clark T, Fraser C, Ruggiu M, Zeeberg BR, Kane D, Weinstein JN, Blume J, Darnell RB. 2005. Nova regulates brain-specific splicing to shape the synapse. *Nat Genet* 37:844-852.
- Westerfield M. 1995. *The Zebrafish Book: A guide for the laboratory use of zebrafish*. University of Oregon Press.
- Xu J, Zhong N, Wang H, Elias JE, Kim CY, Woldman I, Pifl C, Gygi SP, Geula C, Yankner BA. 2005a. The Parkinson's disease-associated DJ-1 protein is a transcriptional co-activator that protects against neuronal apoptosis. *Hum Mol Genet* 14:1231-1241.
- Xu X, Yang D, Ding JH, Wang W, Chu PH, Dalton ND, Wang HY, Bermingham JR, Jr., Ye Z, Liu F, Rosenfeld MG, Manley JL, Ross J, Jr., Chen J, Xiao RP, Cheng H, Fu XD. 2005b. ASF/SF2-regulated CaMKIIdelta alternative splicing temporally reprograms excitation-contraction coupling in cardiac muscle. *Cell* 120:59-72.
- Yang YY, Yin GL, Darnell RB. 1998. The neuronal RNA-binding protein Nova-2 is implicated as the autoantigen targeted in POMA patients with dementia. *Proc Natl Acad Sci U S A* 95:13254-13259.





# Appendix Two

## **Formation of the midbrain-hindbrain boundary constriction requires laminin-dependent basal constriction**

To Be Published As:

Jennifer H. Gutzman<sup>\*</sup>, Ellie G. Graeden<sup>\*</sup>, Laura Anne Lowery, Heidi S. Holley, and Hazel Sive. Formation of the midbrain-hindbrain boundary constriction requires laminin-dependent basal constriction. <sup>\*</sup>authors contributed equally

Contributions:

LAL performed preliminary experiments identifying *sly* and *gup* as MHB constriction mutants, examined wild-type MHB formation by time-lapse confocal microscopy, and proposed the hypothesis that MHB constriction requires laminin but not ventricle inflation or apical epithelial integrity. LAL also assisted in editing the manuscript. JHG did the immunohistochemistry and some of the live confocal imaging used in this paper, and co-wrote the manuscript with EG, who also did the live confocal imaging and quantification of cell shape changes. HSH did the brain ventricle imaging.

**Abstract**

The midbrain-hindbrain boundary (MHB) is a highly conserved fold in the embryonic vertebrate brain. We have termed the point of deepest constriction of this fold the “MHB constriction” (MHBC), and have begun to define the mechanisms by which it develops. The MHBC is formed soon after neural tube closure in the zebrafish, concomitant with other aspects of brain morphogenesis, including inflation of the brain ventricles. We show that zebrafish MHBC formation begins as cells at the MHB shorten to 75% of the length of surrounding cells. This is followed by basal constriction and apical expansion of a small group of cells that contribute to the MHBC. Brain ventricle inflation is not necessary for basal constriction at the MHBC, demonstrating that this process is likely to be actively regulated. Furthermore, basal constriction, but not the earlier cell shortening, requires laminin. This study demonstrates laminin-dependent basal constriction as a previously undescribed molecular mechanism for brain morphogenesis.

## Introduction

During development of the vertebrate brain, the neural tube acquires complex structure including the brain ventricles and conserved folds and bends. These folds and bends delineate functional units of the brain, and are likely to shape the brain such that it can pack into the skull. The midbrain-hindbrain boundary (MHB) is the site of one of the earliest bends in the developing brain. In the embryo, the MHB functions as an embryonic organizing center (Brand et al., 1996; Joyner, 1996; Puelles and Martinez-de-la-Torre, 1987; Sato et al., 2004) and later becomes the cerebellum and part of the tectum (Louvi et al., 2003).

We have called the point of deepest constriction in the MHB the “midbrain-hindbrain boundary constriction” (MHBC). In the present study, we ask what processes are necessary for MHBC morphogenesis, using the zebrafish as a model. In the zebrafish, the MHBC forms between 17 and 24 hours post fertilization (hpf), concomitant with formation of the brain ventricles. At this stage of development, the neuroepithelium is a pseudostratified-columnar epithelium where apical cell surfaces face the brain ventricle lumen, and basal cell surfaces, on the outside of the tube, are lined by the basement membrane, a major component of the extracellular matrix (ECM). The organization of the neuroepithelium, and correlation with brain ventricle inflation led us to consider three factors potentially relevant for MHBC morphogenesis: (1) changes in cell shape during bending, (2) fluid pressure on the inside of the neural tube as the brain ventricles inflate (Lowery and Sive, 2005), and (3) interactions with the ECM on the outside of the tube.

We show that MHBC morphogenesis involves at least two processes, cell shortening at the MHB and basal constriction of the neuroepithelial cells that comprise the MHBC. We demonstrate that basal constriction is dependent upon laminin function, but not upon inflation of the brain ventricles. These data indicate that the MHBC forms through changes in cell shape, dependent on the ECM, which have not been previously described during brain morphogenesis.

## Results and Discussion

### Zebrafish MHBC morphogenesis occurs soon after neural tube closure

In the zebrafish, brain morphogenesis begins after neural tube closure at 17 hpf (Kimmel et al., 1995; Lowery and Sive, 2005). At this stage, a slight indentation, visible on the outside of the tube at the MHB anlage (Fig. A2.1A), corresponds to the basal side of the neuroepithelium. Beginning at 18 hpf, the opposing apical sides of the neuroepithelium separate along the midline and inflate to form the fore-, mid-, and hindbrain ventricles (Lowery and Sive, 2005). However, midline cells at the MHB remain closely apposed. At 21 hpf, after the midbrain and hindbrain ventricles have opened further, the indentation at the MHB outside the tube is more prominent, but still shallow (Fig. A2.1B). By 24 hpf, the MHB is bent acutely at the basal surface creating a sharp point on the outside of the tube (Fig. A2.1C). This is clearly visualized by staining the outside of the neural tube with a laminin antibody as in wild-type embryos (Fig. A2.1D). We have called this sharp point, equivalent to the site of deepest constriction, as the midbrain-hindbrain boundary constriction (MHBC). This constriction is highly conserved amongst the vertebrates (Rhinn and Brand, 2001).

### A sharp MHBC forms in ventricle inflation mutants but not in the laminin mutants

In order to determine the mechanisms regulating MHBC morphogenesis, we asked whether brain ventricle inflation and/or the extracellular matrix play a role in this process. First, we hypothesized that pressure from the embryonic cerebrospinal fluid (eCSF) within the brain ventricles is required to form the MHBC (Desmond and Levitan, 2002; Lowery and Sive, 2005). Consistent with this hypothesis, blood flow through the heart modifies heart chamber morphology and stimulates valve morphogenesis (Berdougo et al., 2003; Hove et al., 2003; Seidman and Seidman, 2001).

We therefore analyzed MHBC morphogenesis in two zebrafish mutants lacking inflated brain ventricles, *snakehead* (*snk*), with a mutation in *atp1a1* encoding a Na<sup>+</sup>K<sup>+</sup> ATPase (Lowery and Sive, 2005) and *nagie oko* (*nok*), a mutant allele of the MAGUK scaffolding protein, MPP5 (Wei and Malicki, 2002). *snk* and *nok* embryos were imaged at 24 hpf to examine the overall outline of the neural tube, and shape of the MHBC. The abnormal refractility in *snk* embryos prevents visualization of the MHBC by brightfield microscopy (Fig. A2.1E). However, laminin staining of these embryos revealed that the MHBC does define a sharp point, although this is less

acute than that of wild-type embryos (Fig. A2.1F). Brightfield imaging did not clearly indicate morphology of the MHBC in *nok* mutants (Fig. A2.1G); however, laminin staining indicated that the MHBC also defined a sharp point (Fig. A2.1H). These data indicate that brain ventricle inflation is not essential for formation of an acutely bent MHBC.

We also hypothesized that the basement membrane, which lies adjacent to the MHBC on the outside of the brain primordium, may play a role in its formation. Laminin interacts with integrins to mediate adhesion of the basement membrane to the cytoskeleton of the overlying cells (Miner and Yurchenco, 2004). A role for laminin has been demonstrated during mouse salivary gland branching, for axon pathfinding in multiple organisms, and for zebrafish notochord development (Bernfield et al., 1984; Garcia-Alonso et al., 1996; Karlstrom et al., 1996; Parsons et al., 2002; Paulus and Halloran, 2006). Laminin has not previously been implicated in brain morphogenesis in any system.

We tested the requirement for laminin by examining the MHBC in the *sleepy* mutant (*sly<sup>m86</sup>*), which has a mutation in the *gamma1* laminin gene (*lamc1*) (Miner and Yurchenco, 2004) and in the *grumpy* mutant (*gup<sup>hi113b</sup>*), which has a viral insertion in the first intron of the laminin *beta1* gene (*lamb1*), (Amsterdam et al., 2004 and A. Amsterdam, personal communication). By brightfield imaging, *sly* mutants showed an initially normally shaped neural tube (Fig. A2.1I,J), but by 24 hpf, the MHBC remained a shallow indentation (Fig. A2.1K). Similar results were observed with *gup* mutants (data not shown). Consistent with brightfield imaging, at 24 hpf, a shallow MHBC was observed in *gup* mutant embryos stained with the laminin 1 antibody (Fig. A2.1L). *gup* embryos were used because, as previously reported, the laminin 1 antibody is not immunoreactive in *sly* mutants (Parsons et al., 2002). These data showed that laminin function is essential for the sharp bend normally seen at the MHBC and define a new role for laminin in brain morphogenesis.

### **Cells shorten and basally constrict at the MHBC**

Bends or folds in epithelial sheets are often driven by changes in cell length and shape such as the cell shortening and apical constriction during neurulation in *Xenopus*, optic vesicle formation in mice, and ventral furrow invagination in *Drosophila* (Lee et al., 2007; Smith et al., 1994; Svoboda and O'Shea, 1987; Sweeton et al., 1991). We therefore hypothesized that wedge shaped cells would be required to form the deep constriction in the neuroepithelium at the MHBC. However, based on the orientation of the MHBC, we speculated that such wedge-

shaped cells would be basally, rather than apically, constricted. Basal constriction has previously been mentioned only briefly in reference to *Drosophila* salivary gland morphogenesis (Fristrom, 1988).

In order to test this hypothesis, we analyzed cell shape at the MHBC in wild-type embryos by expressing membrane-localized green fluorescent protein (memGFP) and imaging live embryos by laser-scanning confocal microscopy. At 17 hpf, cells in the midbrain, hindbrain, and MHB are uniform in length and are both spindle and columnar-shaped (Fig. A2.2A,A'), with some rounded dividing cells visible. In contrast, by 21 hpf, MHB cells are shorter in length (0.76 the apical-basal length) than those in either the midbrain or hindbrain (Fig. A2.2B,B',J).

Do these MHB cells shorten relative to surrounding cells, or do they fail to lengthen in concert with the rest of the neuroepithelium? We addressed this by imaging wild-type embryos expressing memGFP, using spinning-disk confocal microscopy between 17 and 21 hpf. A single cell at the MHB was followed in a live time-lapse data series (Fig. A2.2D-I). Thus, a first step in MHBC formation is the shortening of cells at the MHB.

Subsequent to cell shortening, we found that, by 24 hpf, a group of cells at the MHBC had become wedge-shaped, with constriction at their basal surface (Fig. A2.2C,C'). Within a single plane (Z-section) three to four wedge-shaped cells meet at a sharp point at the MHBC (Fig. A2.2C',L). We further found that the apical width of the wedge-shaped cells at the MHBC is 1.6 times that of cells outside the MHBC (outlined cells in Fig. A2.2C', Fig. A2.2K). Interestingly, although the midline in the MHB does not separate, we found that the basally constricted MHBC cells were not apposed at the midline, but instead are oriented such that their apical surface was exposed to the midbrain ventricle lumen (Fig. A2.2C,C'). These data demonstrate that cells at the MHBC undergo basal constriction and apical expansion, following an initial cell-shortening step.

### **Basal constriction at the MHBC occurs without ventricle inflation, but requires laminin**

In order to address whether basally constricted cells formed independent of brain ventricle inflation, we examined the MHBC in *snk* and *nok* mutants. Cells at the MHBC in both mutants demonstrated basal constriction (Fig. A2.3A-C'). However, unlike wild type, the basally constricted cells in these mutants did not show apical expansion, relative to adjacent cells in the same embryo (Fig. A2.4A). This may be because apical expansion requires that cells have

an unconstrained apical surface, which occurs when wild-type MHBC cells abut the midbrain lumen, and which does not occur when the ventricles do not inflate and the midline of the brain primordium does not separate. These data show that the basal constriction in the MHBC can occur independent of brain ventricle inflation, and independent of apical expansion.

In order to determine what aspect of MHBC formation is disrupted in laminin mutants, we analyzed *sly* embryos for changes in cell length and shape (Fig. A2.3D-F'). At 17 hpf, the cells at the MHB of *sly* mutants appeared similar to wild type (compare Fig. A2.2A' with Fig. A2.3D'). By 21 hpf, cells at the MHBC in *sly* mutants were 0.76 the length of cells on either side (Fig. A2.3D,D'), similar to wild type (Fig. A2.4B). By 24 hpf, cells at the MHBC in *sly* mutants have not basally constricted (Fig. A2.3F'). These data indicate that laminin is not necessary for the cell shortening at the MHB, but is necessary for the second step of basal constriction. Moreover, basal constriction is required for formation of the sharp MHBC bend, and cell shortening is insufficient for this process. A role for laminin in mediating basal constriction has not previously been described.

### **Mechanisms of MHBC morphogenesis**

The model presented in Fig. A2.5 summarizes our data that describe morphogenesis of a major embryonic brain fold, the MHBC, and demonstrates two steps that are involved. In the first step, cells of the MHB shorten relative to the surrounding cells. This is followed by laminin-dependent basal constriction and coordinate apical expansion of a small group of cells that contribute to the sharp bend of the MHBC. Basal constriction apparently occurs independently of apical expansion in mutants lacking ventricle inflation, suggesting that it is an active process. The mechanisms underlying basal constriction are not known; however, our data indicate that laminin provides a crucial function, perhaps through exerting force on adjacent cells and likely requiring integrin function (Hynes, 2002; Wang and Ingber, 1994). Future analysis will explore the cell biology involved in MHBC formation and the mechanisms by which this fold is positioned.

### **Experimental Procedures**

#### **Fish lines and Maintenance**

Zebrafish lines were maintained and stages determined as previously described (Kimmel et al., 1995; Westerfield, 1995). Strains used include wild-type AB, *sly*<sup>m86</sup> (Schier et al., 1996), *gup*<sup>hi1113b</sup> (Amsterdam et al., 2004), *nok*<sup>m227</sup> (Malicki et al., 1996), and *snk*<sup>to273a</sup> (Jiang et al., 1996).

### **Live imaging**

Brain ventricle imaging was carried out as previously described (Lowery and Sive, 2005). For confocal imaging, single cell embryos were micro-injected with CAAX-eGFP mRNA (memGFP) (kindly provided by J. B. Green, Dana-Farber Cancer Institute Boston, MA) transcribed with the mMessage mMachine kit (Ambion). The embryos were mounted inverted in 0.7% agarose (Sigma) and imaged by fluorescent, laser-scanning confocal microscopy (Zeiss LSM510) or with spinning disk confocal microscopy (Perkin Elmer Ultraview RS). Time-lapse data were analyzed using Imaris (Bitplane).

### **Quantitation of cell length and apical cell width**

Slices for measurement were chosen based on the ability to outline the entire extent of a cell from the apical to basal surface of the neuroepithelium, and by following the cell through a full Z-series. The length of three cells at the MHBC and four cells outside the MHBC were measured using Imaris (Bitplane) software, and the ratio between cell lengths at and outside the MHBC were calculated for each embryo and averaged. The width of two wedge shaped cells at the MHBC and three unconstricted cells outside the MHBC at 24 hpf in each embryo were measured using Imaris (Bitplane). The error bars in Fig. A2.2 indicate the standard deviation between the ratios found for each embryo.

### **Immunohistochemistry**

Embryos were fixed in 4% paraformaldehyde and dehydrated in methanol. After rehydrating in PBT, embryos were permeabilized with 2.5  $\mu$ g/ml proteinase K for 1 minute, and blocked in PBT, 0.1% Triton X, 1% BSA, and 1% NGS. Embryos were incubated overnight at room temperature in laminin antibody (laminin rabbit anti-mouse, Sigma L-9393, 1:150), washed, and incubated in secondary antibody, (goat anti-rabbit IgG Alexa Fluor 488, Invitrogen, 1:500) in combination with propidium iodide (PI) (Invitrogen, 1:1000). Embryos were flat mounted in



glycerol, imaged using a Zeiss LSM510 laser-scanning confocal microscope, and images analyzed with LSM software (Zeiss) and Photoshop.

### **Acknowledgements**

We thank the members of the Sive lab for helpful comments and Olivier Paugois for fish husbandry. Thanks to Nancy Hopkins and Adam Amsterdam for the *gup<sup>hi1113b</sup>* mutant and to James Evans for advice and expertise in live imaging. This work was conducted using the Whitehead Institute-MIT Bioimaging Center at MIT and the W. M. Keck Foundation Biological Imaging Facility at the Whitehead Institute. HS is supported by NIH. JHG is supported by a MIT CSBi/Merck postdoctoral fellowship. EGG is supported by an NSF pre-doctoral fellowship. LAL is supported by a NIH NRSA pre-doctoral fellowship.



**Figure A2.1 Zebrafish MHB morphogenesis occurs between 17 and 24 hpf, and requires laminin but not ventricle inflation.**

(A-C) Brightfield and fluorescent images and schematics of wild-type (WT) MHBC formation. (D) WT embryo at 24 hpf was stained with anti-laminin 1 antibody (green); nuclei were stained with propidium iodide (red). Laminin lines the basal surface of the neuroepithelium. (E) Brightfield image of *snk*, a ventricle inflation mutant, at 24 hpf. Outside of neural tube in *snk* embryos is not visible by brightfield imaging. (F) *snk* embryo at 24 hpf stained as in D. (G) Brightfield image and schematic of *nok*, a ventricle inflation mutant, at 24 hpf. (H) *nok* embryo at 24 hpf stained as in as D. (I-K) Brightfield and fluorescent images and schematics of MHBC formation in the laminin mutant, *sly*. (L) *gup* embryo at 24 hpf stained as in D. Arrowheads indicate MHB at 21 hpf and MHBC at 24 hpf. F, forebrain; M, midbrain; H, hindbrain. Scale bars: A-C, E, G, I-K = 100  $\mu$ M, D, F, H, L = 6  $\mu$ M.

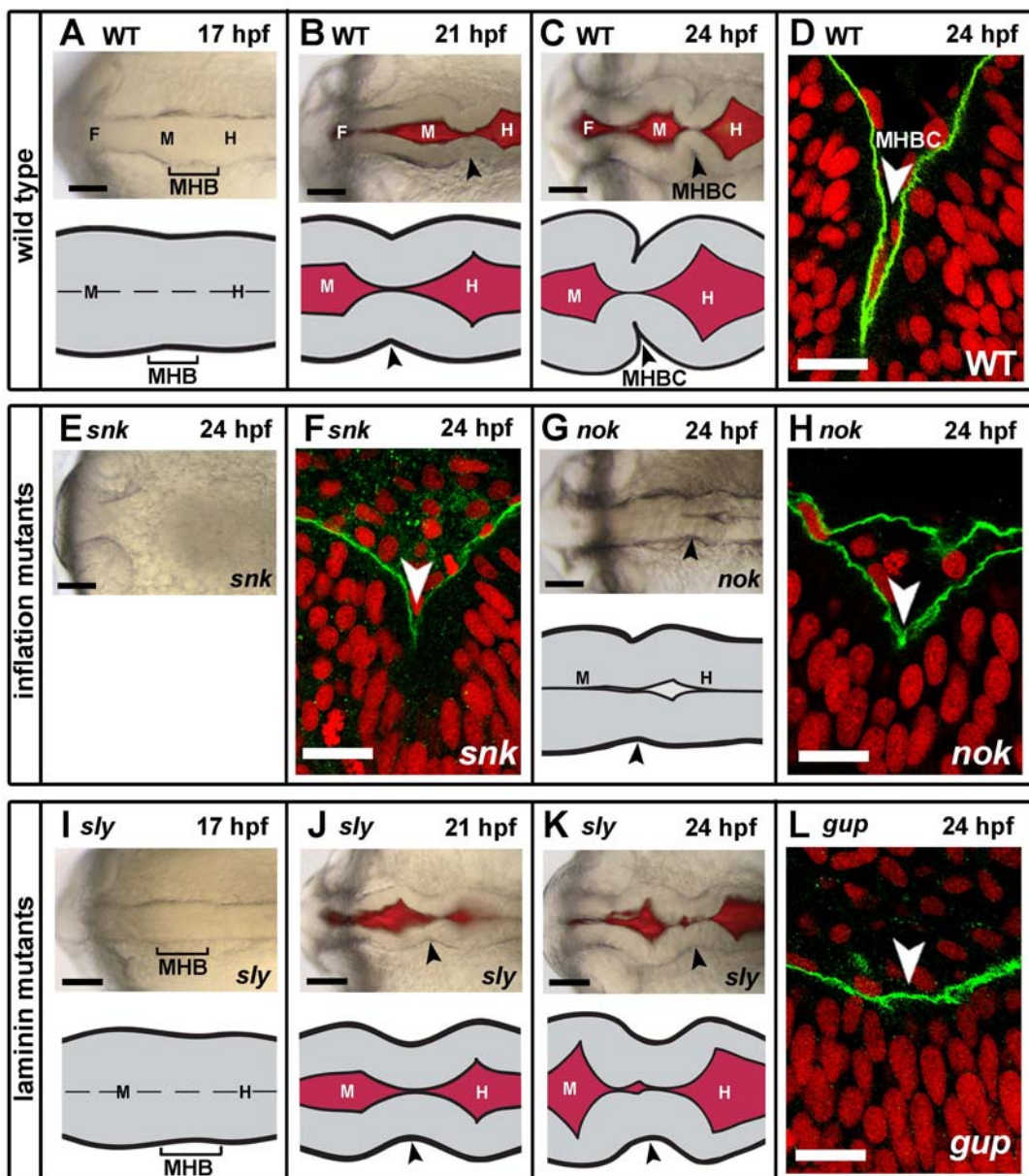




**Figure A2.2 MHBC formation requires cell shortening and basal constriction.**

(A-C') Live laser-scanning confocal imaging of wild-type embryos injected with memGFP mRNA at the one cell stage and imaged at 17, 21, and 24 hpf. Boxed regions from A-C are enlarged for panels A'-C'. Individual cells in the MHB are outlined, and a dividing cell is indicated by an arrow in B. Asterisks in A-C mark cells outlined in A'-C'. Cells with two asterisks are outside the MHB. (A') At 17 hpf, cells at the MHB are similar in length to the cells in the surrounding tissue. (B') At 21 hpf, cells at the MHB are shorter than the cells in the surrounding tissue. (C') At 24 hpf, cells at the MHBC are basally constricted and apically expanded. In A-C' some green fluorescence within outlined cells is due to the plane of section that includes the cell membrane. (D-I) Time-course of MHB morphogenesis beginning at 17 hpf. A single cell is outlined and followed through the time course. Cells at the MHB shorten relative to those surrounding ( $n = 6$  embryos). (J) Relative cell lengths at and outside the MHB in 21 hpf wild-type embryos. Cells at the MHB were 0.76 times the length of those outside the MHB ( $\pm 0.06$  s.d.) ( $n = 8$  embryos, 3 cells at the MHB and 4 cells outside the MHB were measured per embryo). (K) Relative apical width of unwedged cells (those outside the MHBC) and basally constricted cells (at the MHBC) in wild-type embryos at 24 hpf. Cells at the MHBC had 1.6 times the apical width of those outside the MHBC ( $\pm 0.29$  s.d.) ( $n = 6$  embryos, 2 cells at the MHBC and 3 cells outside the MHBC were measured per embryo). (L) Numbers of basally constricted cells at the MHBC in wild-type embryos at 24 hpf ( $n = 9$  embryos). Arrowheads indicate the MHBC. M, midbrain. Scale bars: A-C = 20  $\mu$ M, A'-C' = 9  $\mu$ M, D-I = 30  $\mu$ M.



Figure A2.2 Continued

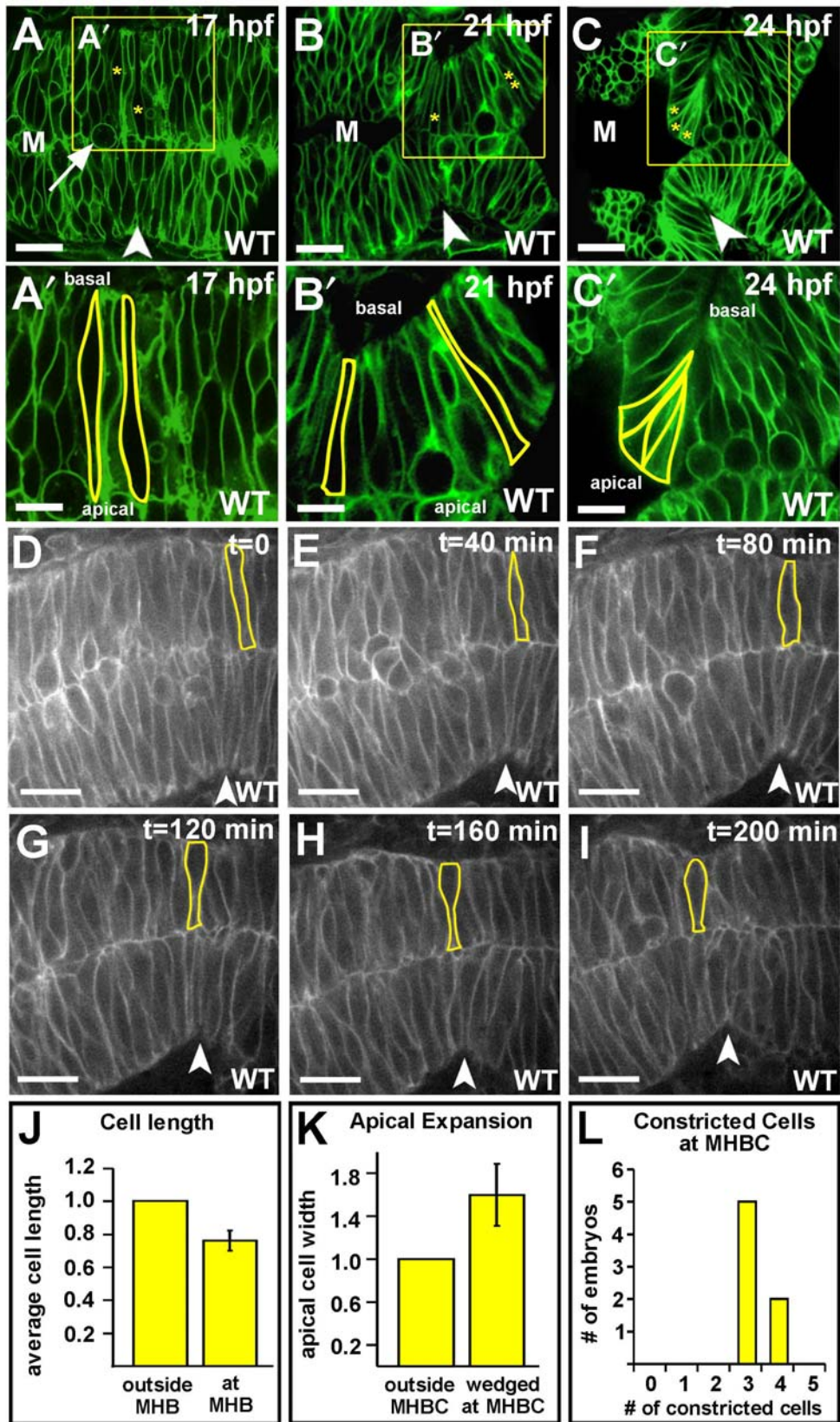






**Figure A2.3 Basal constriction at the MHBC is laminin-dependent and not dependent on ventricle inflation.**

(A-C') Live laser-confocal imaging of wild type, *snk* and *nok* embryos at 24 hpf, after injection with memGFP. Boxed regions in A-C are enlarged in panels A'-C'. Cells at the MHBC in (A-A') wild type, (B-B') *snk* and (C-C') *nok* undergo basal constriction (see cell outlines). (D-F') Imaging of *sly* mutants injected with memGFP mRNA at the one cell stage and imaged at 17, 21, and 24 hpf. Boxed regions in D-F are enlarged for panels D'-F'. (D') At 17 hpf, MHB and surrounding cells are similar in length (see outlined cells). (E') At 21 hpf, cells at the MHB are shorter than those surrounding. One cell at and one cell outside the MHB are outlined in yellow. Some cells are visible outside the neural tube. (F') At 24 hpf, cells at the MHBC fail to basally constrict. For panels A-C and D-F asterisks indicate the cell that is outlined in the image below. Cells with two asterisks are outside MHB. Arrowheads indicate the MHBC. Dotted lines delineate the outside of the neural tube. Some green fluorescence is apparent within outlined cells since the plane of section contains the surface of the cell membrane. Anterior is to the left in all images. Scale bars: A-C = 22  $\mu$ M, A'-C' = 12  $\mu$ M, D-F = 18  $\mu$ M, D'-F' = 9  $\mu$ M.

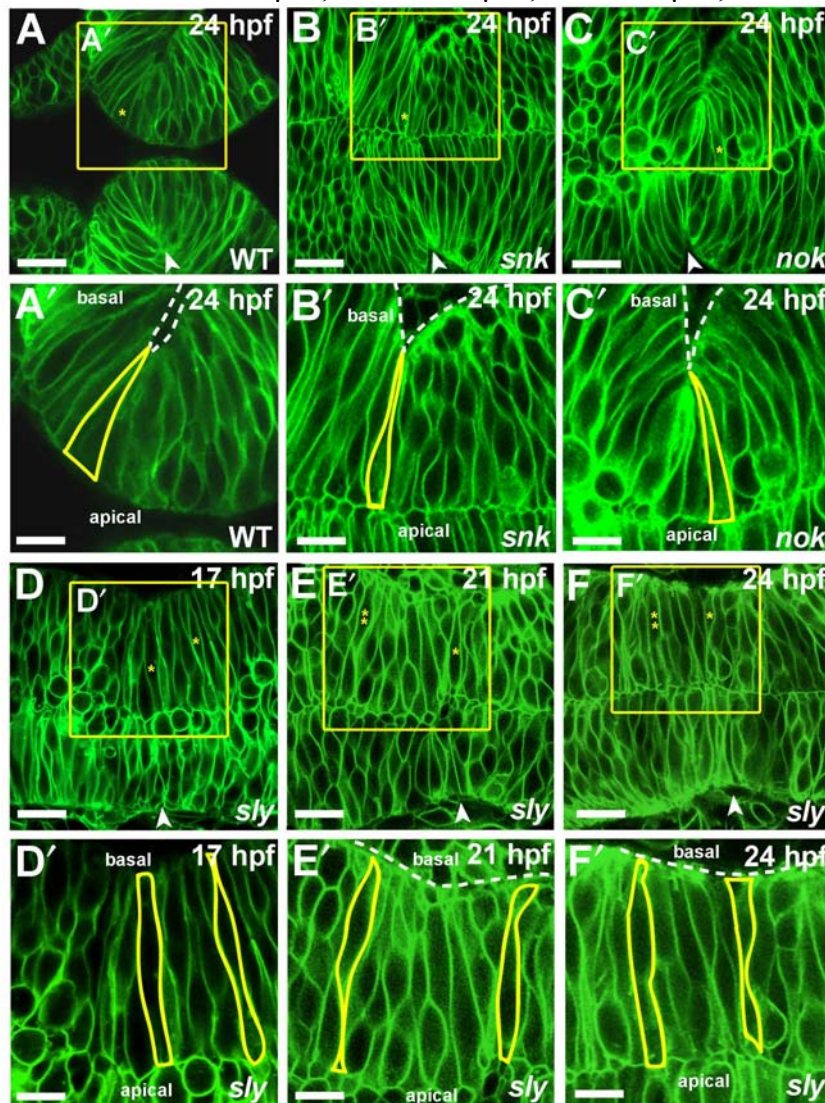




**Figure A2.4 Apical expansion does not correspond to basal constriction in lumen inflation mutants; cells are shorter at MHBC in *sly* mutants as in WT.**

(A) Graph compares the apical width of unwedged cells (outside MHBC) to basally constricted cells (wedged at MHBC) in *snk*, and *nok* embryos at 24 hpf. Basally constricted cells at the MHBC do not apparently show corresponding apical expansion *snk* and *nok* (n = 3 embryos each mutant, 2 cells at MHBC, 3 cells outside MHBC were measure per embryo). (B) Length of cells at the MHB relative to those outside the MHB in WT and *sly* mutants. At 21 hpf, cells at the MHB (at MHB) in *sly* mutants are 0.76 (+/- 0.094 s.d.) the length of those outside the MHB (outside MHB), as in WT embryos (n = 6).

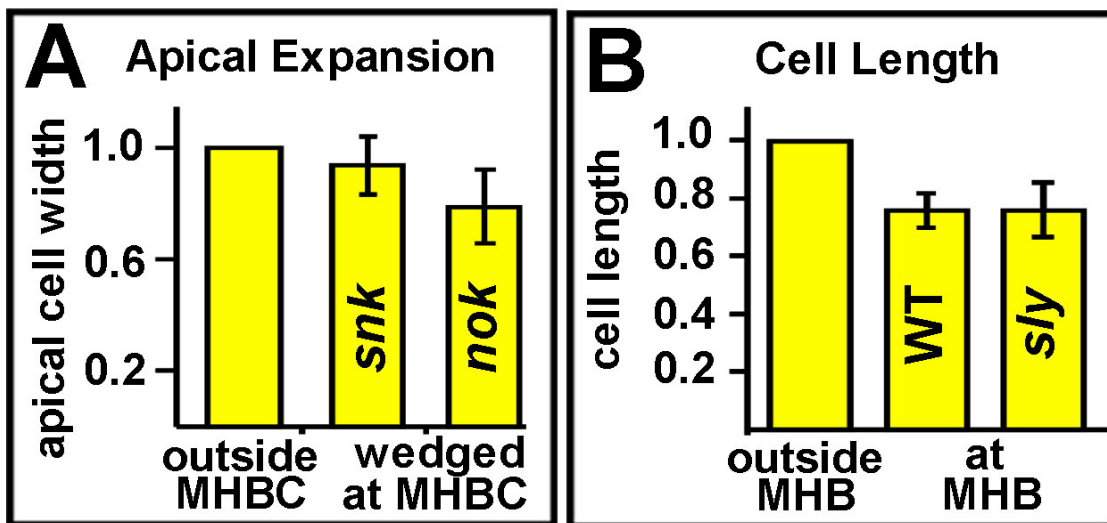
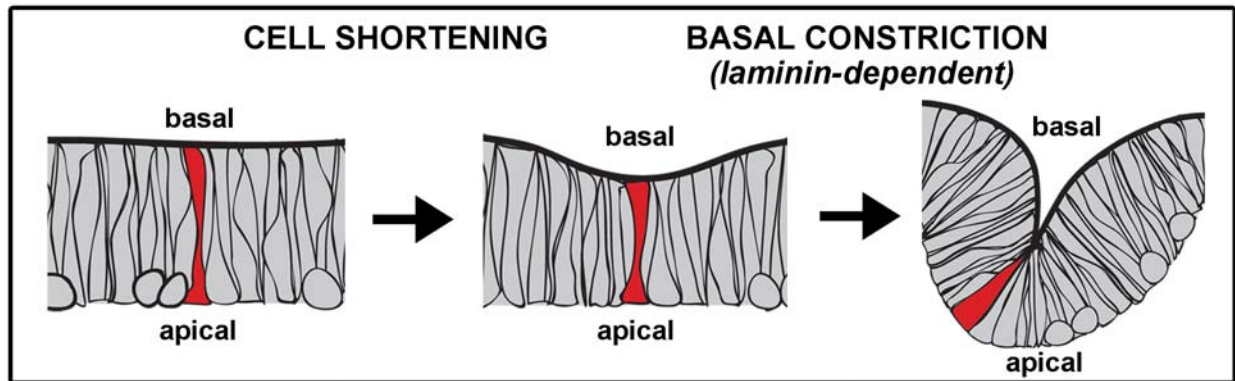




**Figure A2.5 Schematic of the two steps required in MHBC formation.**

In step one, cells shorten at the MHB. In step two, 3 to 4 cells (in a plane of section) basally constrict, and expand apically, to allow an acute bend angle to form. This second step is laminin dependent.





## References

- Amsterdam, A., R. M. Nissen, Z. Sun, E. C. Swindell, S. Farrington and N. Hopkins (2004). Identification of 315 genes essential for early zebrafish development. *Proc Natl Acad Sci U S A* 101(35): 12792-7.
- Berdougo, E., H. Coleman, D. H. Lee, D. Y. Stainier and D. Yelon (2003). Mutation of weak atrium/atrial myosin heavy chain disrupts atrial function and influences ventricular morphogenesis in zebrafish. *Development* 130(24): 6121-9.
- Bernfield, M., S. D. Banerjee, J. E. Koda and A. C. Rapraeger (1984). Remodelling of the basement membrane: morphogenesis and maturation. *Ciba Found Symp* 108: 179-96.
- Brand, M., C. P. Heisenberg, Y. J. Jiang, D. Beuchle, K. Lun, M. Furutani-Seiki, M. Granato, P. Haffter, M. Hammerschmidt, D. A. Kane, R. N. Kelsh, M. C. Mullins, J. Odenthal, F. J. van Eeden and C. Nusslein-Volhard (1996). Mutations in zebrafish genes affecting the formation of the boundary between midbrain and hindbrain. *Development* 123: 179-90.
- Desmond, M. E. and M. L. Levitan (2002). Brain expansion in the chick embryo initiated by experimentally produced occlusion of the spinal neurocoel. *Anat Rec* 268(2): 147-59.
- Fristrom, D. (1988). The cellular basis of epithelial morphogenesis. A review. *Tissue Cell* 20(5): 645-90.
- Garcia-Alonso, L., R. D. Fetter, and C. S. Goodman. (1996). Genetic analysis of Laminin A in *Drosophila*: extracellular matrix containing laminin A is required for ocellar axon pathfinding. *Development* 122: 2611-21.
- Hove, J. R., R. W. Koster, A. S. Forouhar, G. Acevedo-Bolton, S. E. Fraser and M. Gharib (2003). Intracardiac fluid forces are an essential epigenetic factor for embryonic cardiogenesis. *Nature* 421(6919): 172-7.
- Hynes, R. O. (2002). Integrins: bidirectional, allosteric signaling machines. *Cell* 110(6): 673-87.
- Jiang, Y. J., M. Brand, C. P. Heisenberg, D. Beuchle, M. Furutani-Seiki, R. N. Kelsh, R. M. Warga, M. Granato, P. Haffter, M. Hammerschmidt, D. A. Kane, M. C. Mullins, J. Odenthal, F. J. van Eeden and C. Nusslein-Volhard (1996). Mutations affecting neurogenesis and brain morphology in the zebrafish, *Danio rerio*. *Development* 123: 205-16.
- Joyner, A. L. (1996). Engrailed, Wnt and Pax genes regulate midbrain--hindbrain development. *Trends Genet* 12(1): 15-20.
- Karlstrom, R. O., T. Trowe, S. Klostermann, H. Baier, M. Brand, A. D. Crawford, B. Grunewald, P. Haffter, H. Hoffmann, S. U. Meyer, B. K. Muller, S. Richter, F. J. van Eeden, C. Nusslein-Volhard and F. Bonhoeffer (1996). Zebrafish mutations affecting retinotectal axon pathfinding. *Development* 123: 427-38.

- Kimmel, C. B., W. W. Ballard, S. R. Kimmel, B. Ullmann and T. F. Schilling (1995). Stages of embryonic development of the zebrafish. *Dev Dyn* 203(3): 253-310.
- Lee, C., H. M. Scherr, and J. B. Wallingford. (2007). Shroom family proteins regulate gamma-tubulin distribution and microtubule architecture during epithelial cell shape change. *Development* 134: 1431-41.
- Louvi, A., P. Alexandre, C. Metin, W. Wurst and M. Wassef (2003). The isthmic neuroepithelium is essential for cerebellar midline fusion. *Development* 130(22): 5319-30.
- Lowery, L. A. and H. Sive (2005). Initial formation of zebrafish brain ventricles occurs independently of circulation and requires the *nagie oko* and *snakehead/atp1a1a.1* gene products. *Development* 132(9): 2057-67.
- Malicki, J., S. C. Neuhauss, A. F. Schier, L. Solnica-Krezel, D. L. Stemple, D. Y. Stainier, S. Abdelilah, F. Zwartkruis, Z. Rangini, W. and Driever. (1996). Mutations affecting development of the zebrafish retina. *Development* 123: 263-73.
- Miner, J. H. and P. D. Yurchenco (2004). Laminin functions in tissue morphogenesis. *Annu Rev Cell Dev Biol* 20: 255-84.
- Parsons, M. J., S. M. Pollard, L. Saude, B. Feldman, P. Coutinho, E. M. Hirst and D. L. Stemple (2002). Zebrafish mutants identify an essential role for laminins in notochord formation. *Development* 129(13): 3137-46.
- Paulus, J. D. and M. C. Halloran (2006). Zebrafish *bashful/laminin-alpha 1* mutants exhibit multiple axon guidance defects. *Dev Dyn* 235(1): 213-24.
- Puelles, L. and M. Martinez-de-la-Torre (1987). Autoradiographic and Golgi study on the early development of n. isthmi principalis and adjacent grisea in the chick embryo: a tridimensional viewpoint. *Anat Embryol (Berl)* 176(1): 19-34.
- Rhinn, M. and M. Brand. (2001). The midbrain--hindbrain boundary organizer. *Curr Opin Neurobiol* 11, 34-42.
- Sato, T., A. L. Joyner and H. Nakamura (2004). How does Fgf signaling from the isthmic organizer induce midbrain and cerebellum development? *Dev Growth Differ* 46(6): 487-94.
- Schier, A. F., S. C. Neuhauss, M. Harvey, J. Malicki, L. Solnica-Krezel, D. Y. Stainier, F. Zwartkruis, S. Abdelilah, D. L. Stemple, Z. Rangini, H. Yang and W. Driever (1996). Mutations affecting the development of the embryonic zebrafish brain. *Development* 123: 165-78.
- Seidman, J. G. and C. Seidman (2001). The genetic basis for cardiomyopathy: from mutation identification to mechanistic paradigms. *Cell* 104(4): 557-67.



- Smith, J. L., G. C. Schoenwolf and J. Quan (1994). Quantitative analyses of neuroepithelial cell shapes during bending of the mouse neural plate. *J Comp Neurol* 342(1): 144-51.
- Svoboda, K. K. and K. S. O'Shea. (1987). An analysis of cell shape and the neuroepithelial basal lamina during optic vesicle formation in the mouse embryo. *Development* 100: 185-200.
- Sweeton, D., S. Parks, M. Costa and E. Wieschaus. (1991). Gastrulation in *Drosophila*: the formation of the ventral furrow and posterior midgut invaginations. *Development* 112: 775-89.
- Wang, N. and D. E. Ingber. (1994). Control of cytoskeletal mechanics by extracellular matrix, cell shape, and mechanical tension. *Biophys J* 66: 2181-9.
- Wei, X. and J. Malicki (2002). *nagie oko*, encoding a MAGUK-family protein, is essential for cellular patterning of the retina. *Nat Genet* 31(2): 150-7.
- Westerfield, M. (1995). *The Zebrafish Book: A guide for the laboratory use of zebrafish.*, University of Oregon Press.